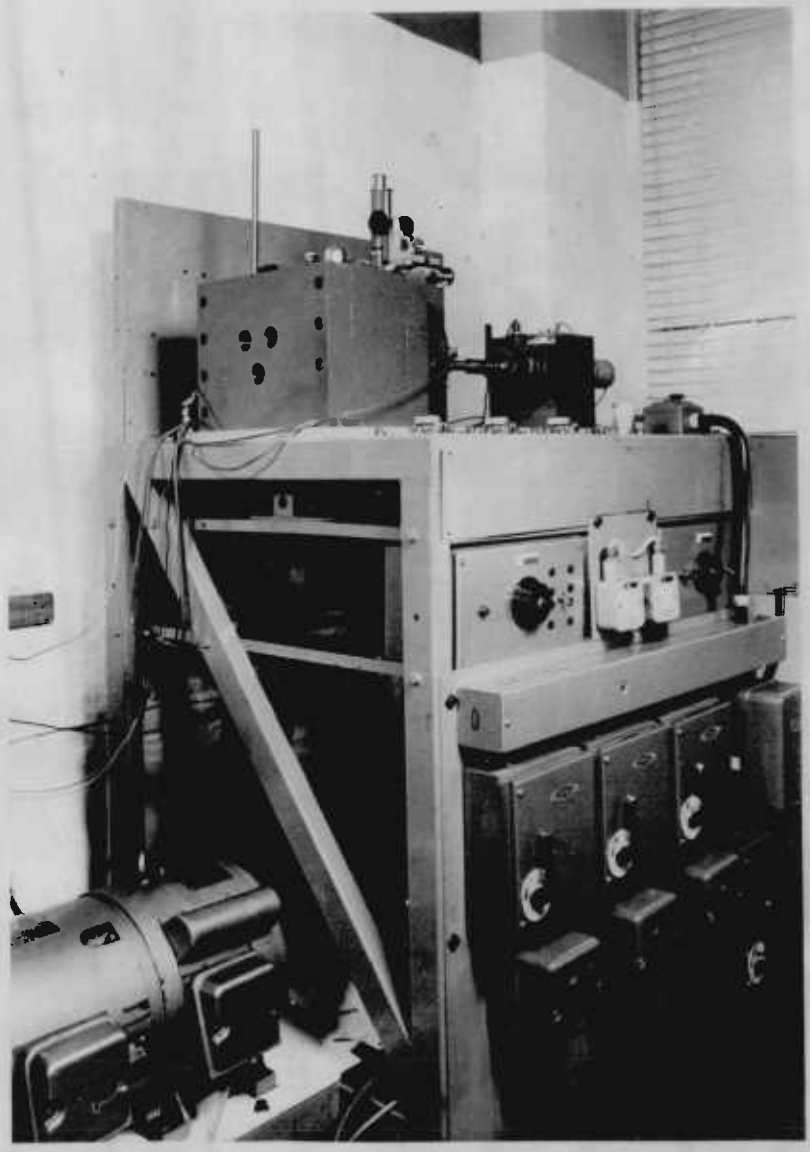

FRONTISPIECE. THE EXPERIMENTAL APPARATUS

FILM THICKNESSES IN A ROLLING SLIDING ELASTOHYDRODYNAMIC LINE CONTACT

BY

CHRISTOPHER JOHN HEDLEY

A THESIS SUBMITTED FOR THE DEGREES OF

DOCTOR OF PHILOSOPHY OF THE UNIVERSITY OF LONDON

AND

DIPLOMA OF IMPERIAL COLLEGE

DECEMBER 1977

LUBRICATION LABORATORY
IMPERIAL COLLEGE
EXHIBITION ROAD
LONDON, S.W.7

A B S T R A C T

A four disc machine has been designed and constructed to measure elastohydrodynamic oil film thickness and traction in a line contact. A range of temperatures and loads were used together with varying amounts of sliding and rolling. In preliminary experiments, traction curves were obtained using an x-y plotter, but later this quantity was only monitored when film thicknesses were measured. The technique of optical interferometry was used to obtain oil film thickness.

Comparison of traction curves with values obtained from other machines showed the agreement to be good, except for the lack of traction peak. It is suggested that this lack of a peak is due to the greater cooling effect in the contact due to submergence in oil.

The optical measurements in the higher ranges showed good agreement of behavioural trends with those of other workers. However, for lower values of film thickness, anomalies were encountered. It is suggested that these anomalies can be attributed to surface roughness effects which result in an enhancement of film thickness at higher values. At lower values of film thickness the enhancement is reduced and this reduction is magnified by the presence of sliding.

ACKNOWLEDGEMENTS

The following are gratefully acknowledged for their assistance in the production of this thesis.

- Professor A. Cameron for providing the opportunity to do this work and his supervision throughout the years.
- Mr. R. Dobson for his valuable advice and help on technical matters in the laboratory.
- The British Petroleum Company for their financial support and Mr. W.C. Pike for his help as industrial supervisor.
- Members of the Lubrication Laboratory, Imperial College for advice and assistance at all times.
- Rose Baldwin for typing.
- Friends and relations for putting up with me when I was in a bad mood.

TABLE OF CONTENTS

LIST OF FIGURES

LIST OF TABLES

GENERAL COMMENTS

References will be found at the end of the Chapter in which they are mentioned. All Tables and Figures will also be at the end of their respective Chapters.

S.I. units are used throughout the text, although other customary units are often additionally given for Chapters 1 to 5. However the apparatus used instrumentation which was calibrated in British units, therefore some of the preliminary calibrations were also made in these units. For this reason three Figures in Chapter 4 utilise British instead of S.I. units.

CHAPTER 1

INTRODUCTION AND LITERATURE SURVEY

1.1 INTRODUCTION

Basically the subject of lubrication stems from a practical study of the control of friction and the prevention of failure in machine elements. In both these aspects, the film thickness of the hydrodynamic lubricant film formed between the bearing surfaces is a very important consideration. This is particularly true for elastohydrodynamic (EHD) conditions where film thickness and surface irregularities are often of the same order of magnitude.

The present knowledge of EHD lubrication is such that the formation of an EHD film between smooth surfaces is understood more or less fully, and that in most cases the predicted values of film thickness from theory agree well with experimental measurements. Moreover several semi-empirical relationships have been propounded which further increase the accuracy with which film thicknesses can be estimated. However there is considerable doubt as to the validity of these predictions when the surfaces are rough, especially when the combined surface roughnesses are of the same magnitude as the EHD film thickness. This is further complicated by the presence of sliding when the thermal effects are more complex and difficult to assess.

This combination of operating factors is experienced in the Kopp variator and the Perbury gear and other such devices which rely on traction transmitted through the lubricant film. These EHD conditions already give rise to an anomalous behaviour in that the lubricant does not behave in

a Newtonian manner at higher sliding speeds, i.e. traction force is not proportional to the amount of slip. It is not known if this also gives rise to an anomalous behaviour in film thickness, especially at low values.

A test apparatus was designed and constructed to allow an EHD line contact to be viewed interferometrically whilst operating under typical traction conditions. In this way the film thickness could be measured and its behaviour noted. A line contact was chosen because, although it is more difficult to build the apparatus, it gives less complicated EHD conditions than point contact.

The remainder of this chapter is concerned with describing the current "state of the art" in EHD lubrication and traction as well as a literature survey. Chapters 2 and 3 describe the mechanical and optical design respectively whilst Chapters 4 and 5 deal with the experimental preliminaries and test procedure. The results are presented and briefly discussed in Chapter 6 with a more detailed analysis in Chapter 7.

1.2 ELASTOHYDRODYNAMIC LUBRICATION THEORY

1.2.1 The Hertz Equations

The equations developed by HERTZ (1) were for a dry static curved body with elastic properties loaded against a semi-infinite flat rigid surface. The curved surface is either cylindrical for line contact or spherical for point contact. The pressure distribution is found to be semi-elliptic over the contact area.

Two elastic cylinders in nominal line contact can be represented by a single cylinder in contact with a rigid plane by making the following substitution:-

$$\frac{1}{R} = \frac{1}{R_1} + \frac{1}{R_2} \tag{1.1}$$

$$\frac{1}{E'} = \frac{1}{2}\left(\frac{1-\nu_1^2}{E_1} + \frac{1-\nu_2^2}{E_2}\right) \tag{1.2}$$

where R_1 and R_2 are the radii of curvature, E_1 and E_2 are the elastic moduli, and ν_1 and ν_2 are the Poisson's ratios of the two bodies. (The same treatment also applies to two spheres in contact).

The half width of the line contact, a, and the maximum Hertzian pressure, p_{Hz}, are given by the following relationships:-

$$a = \left(\frac{8WR}{\pi LE'}\right)^{\frac{1}{2}} \tag{1.3}$$

$$p_{Hz} = \frac{2W}{\pi La} \tag{1.4}$$

where W = total load

L = length of contact of the two surfaces.

Although this treatment was derived for static surfaces its usage can be extended to moving surfaces with commendable accuracy. Thus when maximum Hertzian pressure and Hertzian half width are quoted for conditions when an EHD film is present the figures are those calculated for the equivalent static case.

1.2.2 Reynolds' Equation

Reynolds' equation forms the basis of hydrodynamic lubrication theory and describes the pressure in a lubricating film between two moving surfaces. For an incompressible fluid in two dimensions the equation is:-

$$\frac{\partial}{\partial x}\left(\frac{h^3}{\eta} \cdot \frac{\partial p}{\partial x}\right) + \frac{\partial}{\partial y}\left(\frac{h^3}{\eta}\frac{\partial p}{\partial y}\right) = 12 \cdot U \cdot \frac{\partial h}{\partial x} \qquad (1.5)$$

where U is the mean surface speed in the x-direction, p is the pressure generated in a film thickness h with viscosity η. The geometry is shown in Fig. 1.1.

The derivation of this equation relies on several simplifying assumptions as explained by CAMERON (2) or PINKUS and STERNLICHT (3). The assumptions are:-

1. No body forces.
2. Pressure and viscosity constant through film thickness.
3. No curvature of the oil film.
4. No slip at the boundaries.
5. The lubricant is Newtonian.
6. The flow is laminar.
7. Fluid inertia can be neglected.

If the two moving surfaces can be considered infinitely long (i.e. no side leakage) with no change in film thickness in the y-direction, all derivatives with respect to y disappear. By integrating with respect to x, Reynolds' equation becomes:-

$$\frac{dp}{dx} = 12\ U\ \eta\left(\frac{h-\bar{h}}{h^3}\right) \qquad (1.6)$$

where $\bar{h}$ is the film thickness at the point of maximum pressure. The assumption of an infinitely long bearing comes quite close to practical applications in most cases.

1.2.3 Classical Hydrodynamic Theory

In 1916 MARTIN (4) attempted to apply Reynolds' equa-

tion to the case of metal surfaces rolling over one another. Martin was trying to explain the lack of appreciable wear on gear teeth and approximated the situation to rigid cylinders lubricated by an isoviscous liquid to obtain the following expression:-

$$\frac{h_o}{R} = 4.896 \frac{U\eta_o}{W/L} \qquad (1.7)$$

where h_o is the film thickness on the line of centres of the cylinders.

This equation gave film thicknesses which were smaller than the surface roughnesses known to exist on the gears, and consequently wear should have been apparent. Obviously Martin's treatment contained some inherent inaccuracy or some other mechanism caused the lack of wear.

The assumption of rigid cylinders was modified to include the effects of elastic distortion by PEPPLER in 1936 (5) and 1938 (6) and MELDAHL in 1941 (7). A small increase in film thickness was obtained but the absolute values predicted were still too low.

The effect of pressure on viscosity was considered by GATCOMBE in 1945 (8) for his work on rigid cylinder lubrication. Again the effect on film thickness was beneficial but still the values were too low. The use of alternative pressure/viscosity relationships brought no further improvement either.

It was not until the effects of elastic deformation and pressure/viscosity dependence were combined that a more accurate value of film thickness could be predicted.

1.2.4 The First Solution to the Elastohydrodynamic Problem

The solution of the hydrodynamic equation involving elastic deformation and a viscosity dependence on pressure (these two conditions are now known as elastohydrodynamic conditions) is a very complex procedure. The first attempt to achieve any success was an approximation to the real situation. This major advance was made by ERTEL, whose work was published by GRUBIN (9) in 1949 and consequently has become known as Grubin's theory. The approximations that were made were largely justified and hence gave a quite good equation for film thickness in the line contact EHD problem.

He assumed that the viscosity dependence on pressure could be predicted by the following relationship:-

$$\eta = \eta_o \, e^{\alpha p} \qquad (1.8)$$

where η = viscosity at pressure p

α = pressure/viscosity coefficient

η_o = viscosity at atmospheric pressure

This exponential relationship is often known as the Barus relationship and is a good simple, representation for many lubricants. (A paper by CHU and CAMERON (10) discusses the accuracy of this equation).

He also made the close approximation that the pressure distribution and deformation of the lubricated rolling contact could be assumed the same as that of the dry, static Hertzian contact. This can be justified by the fact that the reduced pressure term (see later) is fairly constant for large pressures thus giving rise to an almost constant film thickness over most of the contact, moreover the thickness of the lub-

ricant film is significantly smaller than the elastic deformation. The shape of the contact is given in Fig. 1.2 where the Hertzian deformation has been combined with a parallel film thickness h_o.

Hydrodynamic pressure can only be generated between converging surfaces, and as the surfaces in the contact (deformed) area are assumed parallel this pressure generation must take place in the (converging) inlet region. The geometry of this region is assumed to be known and so this facilitates solution of Reynolds' equation which, including the pressure/viscosity relation, is now:-

$$e^{-\alpha p} \frac{dp}{dx} = 12\ U.\eta_o \left(\frac{h-\bar{h}}{h^3}\right) \qquad (1.9)$$

A reduced pressure, q, was defined such that

$$\frac{dq}{dx} = e^{-\alpha p} \frac{dp}{dx} \qquad (1.10)$$

thus equation (1.9) becomes

$$\frac{dq}{dx} = 12\ U.\eta_o \left(\frac{h-\bar{h}}{h^3}\right) \qquad (1.11)$$

This is similar to the isoviscous Reynolds' equation (equation (1.6)) and may be solved relatively straightforwardly.

By integration of equation (1.10) the following expression can be obtained

$$q = \frac{1}{\alpha}\left(1 - e^{-\alpha p}\right) \qquad (1.12)$$

By assuming that the pressure at the edge of the contact is large (which is true for heavily loaded contacts) the $e^{-\alpha p}$ term tends to zero and

$q \rightarrow 1/\alpha$

For a line contact Grubin's solution gives:-

$$\frac{h_o}{R} = 1.95 \left(\frac{\alpha \eta_o U}{R}\right)^{0.73} \left(\frac{W}{LE'R}\right)^{-0.091} \qquad (1.13)$$

This equation gives film thicknesses which are one or two orders of magnitude greater than those predicted by the rigid cylinder, isoviscous theories and so at last it seemed possible to theoretically predict hydrodynamic films of a sufficient magnitude to avoid surface contact.

1.2.5 More Refined Solutions to the Elastohydrodynamic Problem

Ertel went on to discuss how the film shape and pressure distribution might be expected to differ in practice from that given by his simple model. He predicted that the pressure distribution in the inlet region builds up to approach the Hertzian pressure smoothly at the contact edge. This has the effect of slightly deforming the inlet surfaces which in turn assists the pressure generation and film formation.

Moreover he predicted that the falling pressure distribution at the exit region implied the existence of a constriction. This restriction causes a pressure spike to be present at the exit region and has been the subject of much discussion.

Ertel's predictions were verified theoretically by PETRUSEVICH (11) in 1951 who obtained numerical solutions to the governing equations. The main characteristics of these solutions, which are now recognised as general of most EHD contacts, were (a) an almost parallel oil film over the majority of the contact with a restriction near the outlet,

(b) a near Hertzian pressure curve over most of the contact and (c) a significant pressure spike near the outlet region. Unfortunately this solution must be viewed suspiciously as it predicts a rise in film thickness with load.

WEBER and SAALFELD (12) showed how the film shape changed with increasing load using a numerical solution in 1954, but unfortunately this work was restricted to small elastic deformations and so the features of fully developed EHD contacts did not emerge.

In 1959 a new approach to elastohydrodynamic analysis was presented by DOWSON and HIGGINSON (13). Most computer solutions using an iterative procedure were very slow to converge for the contact zone and outlet region; the inlet region was less complicated. Dowson and Higginson overcame this by solving the inverse hydrodynamic problem.

Normally a solution of Reynolds' equation attempts to predict the pressure distribution for a given film shape; in the inverse problem the film shape to give a required pressure distribution is calculated. This is then compared against the film shape obtained from the elastic deformation of the surface due to the pressure. In the light of this comparison the pressure distribution is modified until good agreement is reached. This method converges quite rapidly but needs judgement in the modification of the pressure curve.

This early work of Dowson and Higginson did not show the presence of a pressure spike although the results were as expected in general. However in 1960 (14) they extended their work to include conditions of greater severity using a digital computer, the pressure spike was now clearly visible. The same authors later analysed their results (15) and came up

with a simple formula for minimum film thickness which can be written in a non-dimensional form as:-

$$\frac{h_{min}}{R} = 1.6\ G^{*0.6}\ U^{*0.7}\ W^{*-0.13} \qquad (1.14)$$

where $G^* = \alpha E'$

$$U^* = \frac{U\eta_o}{E'R}$$

$$W^* = \frac{W}{LE'R}$$

In 1962 DOWSON, HIGGINSON and WHITAKER (16) considered the effect of lubricant compressibility and found that it introduced a slight modification to the film shape just before the restriction, but only had a small effect on the restriction itself. They concluded that equation (1.14) could be applied to the compressible and incompressible lubricant problems.

ARCHARD, GAIR and HIRST (17) presented solutions, again using the inverse procedure of solving the hydrodynamic problem, in 1961 which illuminated the effect of speed, load, elasticity and pressure/viscosity coefficient in greater depth than before. They split the pressure zone into four parts and considered each one separately. Their results were in close agreement with those of Dowson and Higginson, although the height of the pressure peak was slightly smaller.

Once the solution of the isothermal EHD problem had reached a reasonably satisfactory state attention was turned to the effect of heating in an EHD contact, especially that due to sliding.

1.2.6 Thermal Considerations

A solution to the thermal elastohydrodynamic problem in which the energy equation is also satisfied, was first presented by STERNLICHT, LEWIS and FLYNN (18). They assumed that all the heat produced by viscous effects was convected away by the lubricant (the adiabatic solution). This form of solution is satisfactory for some hydrodynamic bearing problems but invalid for typical EHD conditions. In 1964 CHENG and STERNLICHT (19) included the conduction of heat to the surfaces. They showed that thermal effects in the film had little effect on its thickness under quite severe conditions of sliding, and that there was negligible effect in pure rolling. This agreed with experimental observations of CROOK (20) using varying amounts of sliding in a disc machine. Thus Dowson and Higginson's isothermal theory was considered to be still essentially correct, including the presence of a pressure spike. The analysis of Cheng and Sternlicht employed expressions for the mean viscosity across the film, this restriction was later removed by CHENG (21) and DOWSON and WHITAKER (22)in 1965, but this did not significantly affect the predicted behaviour and was only a refinement.

The shape of the EHD film and the pressure distribution are illustrated in Fig. 1.3 and compared with the situation considered by Martin, together with the dry, static Hertzian condition.

1.3 ELASTOHYDRODYNAMIC LUBRICATION EXPERIMENT

1.3.1 Measurement of Film Thickness

Techniques for measuring elastohydrodynamic film thickness can be subdivided into three basic categories:-

mechanical, electrical and optical.

The mechanical methods, although tending to be relatively simple in concept, are often subject to gross limitations. Two typical examples of mechanical systems are those developed by MEYER and WILSON (23) and JOHNSON and ROBERTS (24). Meyer and Wilson used strain gauges on a bearing to measure strain variations as the balls rotated. By applying thin ring bending theory and the Hertz equations they were eventually able to deduce the mean film thickness. Some good results were obtained, however some equally bad results were also present. This approach was based on assumptions about uniformity of film thickness at all points on the bearing, and the applicability of thin ring bending theory - both are suspect.

Johnson and Roberts' apparatus consisted of three equispaced balls nipped between two contrarotating steel plates. The load between these two plates was provided by a compressive spring dynamometer which had previously been calibrated for load against displacement. As the plates rotated and an EHD film built up, a change in load on the spring was detected and from this the film thickness could be deduced. This method was subject to large scatter in the results, mainly due to inherent errors present in any system that tries to measure small gaps using mechanical components.

Electrical methods of measuring EHD film thicknesses really started with LANE and HUGHES (25) in 1952. Although they did not measure the actual film thickness, they used electrical resistance methods to confirm that a substantial oil film was present in counterformal concentrated contacts when classical theory predicted little more than boundary lubri-

cation. The method consisted of measuring the electrical resistance between two moving surfaces; when there was contact the resistance was low and when there was a film present the resistance was high. This work was later confirmed by CAMERON (26) in 1954, LEWICKI (27) in 1955, CROOK (28) in 1957 and EL-SISI and SHAWKI (29) in 1958. Attempts to measure the film thickness itself by resistance methods were largely unsuccessful until El-SISI and SHAWKI (30) in 1960. They lowered and stabilised the resistivity of the oil somewhat by adding sodium petroleum sulphonate, however this still did not give dependable results. Probably the main objection to this technique is the fact that no allowance was made for any effect of the pressure and temperature experienced in the contact on the resistivity of the oil. Thus its main use nowadays is in lubrication of rough surfaces where the amount of asperity interaction is investigated.

One interesting aspect of Lewicki's work in 1955 was his attempt at measuring film thickness by capacitance methods. Although he did not meet with much success, he at least demonstrated the method was feasible. This approach was later taken up by CROOK (31) in 1958 who used pads riding on the surface films attached to the discs. These pads measured the film thicknesses on each of the discs after leaving the contact; from these the volume flow rate of oil through the contact could be deduced and hence the film thickness calculated. This method avoided the problem of having to assume the deformed shape of the specimens, which is necessary when interpreting capacitance measurements between the two moving surfaces themselves. This latter approach was used by ARCHARD and KIRK (32) in 1961 for point contacts. They showed that

their measurements of inter-specimen capacitance were consistent with the assumption of the Hertzian shape forecast by EHD theory. In 1961 CROOK (20) showed that the values of film thickness obtained from the pad-disc and disc-disc capacitance measurements agreed well with each other. In this paper and later in 1963 CROOK (33) describes the first ever measurement of film thickness shape. This involved depositing a chromium electrode on a glass disc and measuring the rate of change of capacitance as a steel disc rolled over it. He found an essentially flat region with a constriction at the exit region, thus confirming the basic characteristics predicted by theory. A similar technique was used by CHENG and ORCUTT (34) in 1965.

The capacitance technique of measuring film thickness was also used by DYSON, NAYLOR and WILSON (35) who published an extensive series of tests in 1965, and by several workers since.

In 1958 an attempt to measure film thickness was made by SIBLEY et al (36) by measuring the dielectric breakdown voltage. The results were largely dependent on the moisture content of the oil (as for the resistance method) and the technique was not followed up.

However, an extension of this approach was found to have more success later in that year. SIRIPONGSE, ROGERS and CAMERON (37, 38) showed that if sufficient voltage was applied across an oil film to cause dielectric breakdown, the subsequent voltage drop at currents above half an ampere depended only on the thickness of the film. They used this method to measure film thickness in a four ball machine, and in 1960 MacCONOCHIE and CAMERON (39) applied this technique to

gear teeth. However this method later fell into disuse following doubts as to its validity and the introduction of better methods. The main grounds for criticism were that the relatively high currents used (up to five amperes) were suspected of causing drastic changes in the contact region. These doubts prompted DYSON (40) in 1967 to examine the technique by making direct comparisons with capacitance measurements. He found the agreement was not good.

In 1961, SIBLEY and ORCUTT (41) passed a collimated beam of X-rays through the elliptical contact between two lubricated crowned discs in the direction of rolling. By measuring the intensity of the transmitted radiation they were able to estimate the minimum film thickness in the contact. This method gave good agreement with theory although the calculation of film thickness from transmitted intensity data needed considerable manipulation. This method used a beam width of 0.76 mm (0.030 in.). In 1965 KANNEL, BELL and ALLEN (42), using a beam width of 0.076 mm (0.003 in.), examined the contact from a direction perpendicular to the direction of rolling. By utilising collimation of this degree they were able to measure the shape of the contact and they observed the characteristic EHD shape.

The relative merits of X-ray measurement of film thickness were argued by KANNEL and BELL (43) in 1971 and they concluded that the method was accurate. However, the results of PARKER and KANNEL (44), who used this technique showed a large load dependence of film thickness at the higher Hertzian pressures. GENTLE et al (45)have argued that this is due to mismeasurement of film thickness, and results from an X-ray shadow cast by the surface roughnesses on the disc. Moreover,

to ensure measurement of film thickness, it is extremely important that the beam of X-rays is perfectly aligned with the EHD film in the contact, this calls for considerable experimental expertise. Thus some doubt must remain as to the validity of this technique when absolute values of film thickness are being measured. However, as the major source of any error is likely to result in a fixed discrepancy in film thickness at all values, this technique is very suitable for detecting small changes in film thickness.

The optical technique of interferometry has been one of the most widely used to study the EHD lubrication regime in experimental research; most of which work has been concentrated on the point contact configuration. This technique provides detailed information about both film thickness and shape. The first application of this method was by KIRK (46) and ARCHARD and KIRK (47) who observed white light interference fringes between crossed cylinders of perspex. Owing to the use of perspex they were restricted to low contact pressures. Also the extremely low reflectivity of this material in oil meant that the interference colours produced with white light were very faint. Nevertheless, evidence of a constriction at each side of the contact was seen and the general feasibility of the interferometric method demonstrated.

Using more realistic bearing materials of glass and steel in a sliding contact, CAMERON and GOHAR (48) in 1966 showed clearly the characteristic horse-shoe shaped constriction along the rear and lateral edges of a point contact. A wide range of other material combinations such as sapphire/steel and diamond/steel used by GOHAR and CAMERON (49) and rubber/glass used by ROBERTS and TABOR (50) also showed this

characteristic horse-shoe shaped constriction.

The results of GOHAR and CAMERON (49) were concerned with sliding contacts, while FOORD et al (51), using an improved interferometric system, presented more elegant results for rolling contacts in 1969. The first measurements of line contact film thicknesses were made by GOHAR (52) in 1967, although they were rather few in number and experimental difficulties were encountered. However this was remedied by WYMER (53) in 1972, who, using a tapered roller in contact with a circular flat plate, produced results for line contact for a large variety of operating parameters.

The technique of interferometry has been refined over the years, mostly by Cameron and co-workers, and now enables the measurement of ultra-thin films (WESTLAKE and CAMERON (54)) and film thicknesses in a real bearing (PEMBERTON (55)). This technique has also been adapted by PAUL and CAMERON (56), who, using a gas laser and photographing the interference fringes due to oil trapped between a fixed ball and a plate at successive time intervals, have deduced the viscosity of the oil at high pressures.

Recently WILLIS and SETH (57, 58) have been developing a technique for measuring oil film thickness by laser-beam diffraction methods. They have demonstrated the feasibility of this approach but more work needs to be done, the main problem being that more powerful (more expensive) lasers are needed the lower the film thickness that is to be measured. It will be interesting to note any significant advantages of this technique over others when it is fully developed.

The results of DYSON et al (35) showed good agreement between the theoretical predictions and experimental measurements (Fig. 1.4). However they measured average values and compared them with a theoretical prediction for minimum film thickness; WYMER (53) has shown that these measured values should be 20% higher than the predicted values. Nevertheless it is interesting to note that their excellent agreement deteriorates at the higher film thicknesses and that the presence of sliding further aggravates the situation. These authors suggest that this effect is due to shear heating in the inlet region and that this heating will be more significant when sliding is present. A similar effect was noted by WYMER (53), WESTLAKE and CAMERON (54) and FOORD et al (51) for their optical studies of rolling point contact. These authors also suggest that the cause is probably shear heating.

For low to medium Hertzian pressures, most other experimental observations also appear to agree with theory, at least as far as the basic behaviour pattern is concerned. Unfortunately empirical formulas for predicting film thickness seem to vary considerably, possibly due to the difficulty in placing an accurate and universally accepted value on the pressure/viscosity coefficient (the exponential pressure/viscosity relation is only an approximation and deviations are encountered); moreover any effect of surface roughness is ignored.

However this happy state of affairs is not applicable to the region of higher Hertzian pressures (in the order of 1.5 GN/m^2 (218,000 p.s.i.)) where there is considerable disagreement about the effect of load on film thickness. The results of PARKER and KANNEL (44) show that film thickness

falls with increasing rapidity as load increases (Fig. 1.5). As mentioned previously, the validity of these results has been questioned by GENTLE et al (45) who argued that this is a result of the use of X-rays as a method of determining film thickness. However work of LEE, SANBORN and WINER (59) using optical methods (albeit for a sliding contact) support the results of Parker and Kannel. Conversely work of SIBLEY and ORCUTT (41) using X-ray methods support the view of Gentle et al. This contradictory state of affairs has not been satisfactorily resolved as yet.

1.3.2 Measurement of Pressure and Temperature in the Contact

The measurement of pressure and temperature in an elastohydrodynamic contact has always proved to be a difficult task because of the small size of the contact normally encountered. Two basic methods of overcoming this problem have emerged. The first is to scale up the size of the contact, and the second is to use miniature transducers in the form of evaporated metal strips.

One method of scaling up the size of the contact is to use materials of a low elastic modulus. This method was used by HIGGINSON (60) in 1962 who measured pressure distribution in a contact between a rubber pad and bronze disc using a 0.508 mm (0.020 in.) diameter pressure-tap. The results agreed with theoretical predictions although the pressures were low:- 0.207 MN/m^2 (30 p.s.i.), and so the effect of the pressure viscosity coefficient was absent.

Another method is to arrange for the contact to have a large effective radius, usually by having conforming (sliding) contacts. This approach was used by DOWSON and LONGFIELD (61,

62, 63) who obtained pressures of up to 82.7 MN/m^2 (12,000 p.s.i.) using a bronze/bronze contact configuration. In addition they also made temperature measurements using embedded thermocouples and showed a rise in temperature in the inlet zone, reaching a maximum just before the outlet. In 1965, LONGFIELD (64) attained pressures of over 0.207 GN/m^2 (30,000 p.s.i.) using a bronze/steel contact configuration. The pressure spike was still not observed although he reported the appearance of a crude peak near the exit region under certain conditions. The pressure distribution in a counterformal contact was measured by NIEMANN and GARTNER (65) who used a pressure-tap of .0254 mm (0.001 in.) width, the results occasionally showed a maximum pressure in excess of the Hertzian value, but the relatively large size of the pressure-tap marred the readings.

A new means of pressure measurement was introduced in 1965 by KANNEL, BELL and ALLEN (42). They used a miniature manganin transducer which was evaporated onto one of two quartz discs in a disc machine. This transducer was aligned axially with the discs and the pressure was measured by its change in electrical resistance as it passed through the contact. This method gave pressure curves which were similar to those theoretically predicted although there was no pressure peak in the exit region, however its existence would probably have been masked by the finite width of the manganin strip.

A manganin strip was also used by CHENG and ORCUTT (66, 34) in 1965 in a glass/steel disc machine; in addition they measured the temperature distribution by using a similar strip of platinum. This knowledge of the temperature distri-

bution enabled the measurement of pressure distribution to be corrected for temperature effects. (The electrical resistance of manganin varies with temperature as well as pressure, thus an error was present in Kannel, Bell and Allen's uncorrected results). Again the pressure profile was similar to that predicted by theory although some discrepancies were still present, including the lack of a pressure spike; nevertheless some discontinuity was evident. The temperature measurements gave absolute values which were significantly less than those predicted theoretically, although CHENG and ORCUTT (34) suggested that this could be improved by accounting for the viscoelastic properties of the lubricant.

The first experimental verification of the existence of a secondary pressure peak was provided in 1965 by KANNEL (67). The quartz discs used in earlier experiments were replaced by steel ones, allowing higher pressures to be generated, and the manganin strip was insulated from the steel by a layer of silica. Under certain conditions a truncated spike was clearly visible on the oscilloscope traces (this truncation was to be expected due to the finite width of the manganin strip).

In 1967 HAMILTON and MOORE (68) confirmed the existence of a secondary pressure peak. They also used a nickel gauge for temperature measurement and, utilising a technique of ORCUTT'S (66), made measurements of film thickness from the variation of capacitance between the gauges and another steel disc. Thus it was possible to interrelate all three parameters.

A recent development by TURCHINA, SANBORN and WINER (69) has allowed measurement of contact temperatures using infra-red techniques. This method not only facilitates meas-

urement of absolute values but also the distribution of temperature can be obtained. However some manipulation of the experimental results is needed to allow for variations due to pressure effects. Nevertheless this method should prove to be a powerful tool in EHD research.

Another major measurement that is to be made in EHD contacts is that of traction due to relative motion between two surfaces.

1.4 TRACTION EXPERIMENTAL

The first investigations into sliding friction (traction) were performed by CROOK (33) and SMITH (70, 71, 72) and to a lesser extent by SASAKI, OKAMURA and ISOGAI (73) and ROUVEROL and TANNER (74). Crook's results were limited to pressures of 0.69 GN/m^2 (100,000 p.s.i.) which is much less than the pressures usually encountered in practical situations. Smith achieved much higher pressures of up to 2.76 GN/m^2 (400,000 p.s.i.) but unfortunately this was for a point contact arrangement which is much harder to analyse theoretically than Crook's line contact. Sasaki, Okamura and Isogai concentrated their attention on rolling friction and only a minor investigation of sliding friction was attempted; while the work of Rouverol and Tanner was mainly confined to high rolling speeds and high pressures in point contacts.

From these first few major investigations into sliding friction it was soon apparent that there was considerable difference between the experimental results and the theoretical expectations. Many explanations were pro-

pounded and it soon became clear that further data was needed in order that objective conclusions could be drawn. This data was subsequently provided by persons such as PLINT (75,76), POON and HAINES (77), BELL, KANNEL and ALLEN (78), JEFFERIS and JOHNSON (79), DOWSON and WHOMES (80) and JOHNSON and CAMERON (81), and by many workers since.

From the data which was then available it was soon apparent that there was a general behaviour pattern as demonstrated by Fig. 1.6. If the coefficient of traction, defined as sliding friction/normal load is plotted against sliding speed, a family of curves is obtained which for high pressures and low rolling speeds rise to a peak and then fall to a plateau region. These curves are bounded by what might be called a traction ceiling. For lower pressures and higher rolling speeds there tends to be no peak; the curve rises slowly to a plateau region which is bounded by the same traction ceiling. The dependence of this traction curve on rolling speed is of secondary importance when compared to pressure. These curves also exhibit a temperature dependence; for higher temperatures the curve tends to be lowered and the appearance of the traction peak is delayed. However this effect is not as well defined as that of pressure and rolling speed.

It has been suggested that a traction curve can be divided into three regions as shown in Fig. 1.7.

The first region from the origin to point A exhibits a linear response of shear stress (traction) against shear rate (sliding). This is commonly called the Newtonian region although work by JOHNSON and ROBERTS (82) shows that this may not be a linear viscous region but a linear elastic region.

They used the apparatus of POON and HAINES (77, 83) and examined the case of rolling with spin. If the lubricant response is viscous there should be no transverse force, but if the response is elastic there should be a force. Johnson and Roberts detected a force (in fact this was also noticed by Poon and Haines but without realising its significance) and they proceeded to demonstrate that the force, and its behaviour under varying conditions of temperature and pressure, was consistent with a viscoelastic behaviour pattern and that a transition from a viscous to an elastic response could be noticed.

The second region from point A to point B exhibits a non-linear response of shear stress against shear rate. There are several theories to explain this behaviour, but these will be discussed later.

The third region is commonly called the thermal region. It is generally accepted that the thermal effects from shear heating predominate here, although this does not preclude the fact that other phenomena may be contributive factors.

Traction curves are often replotted with the slide/roll ratio, Σ, in place of sliding speed.

$$\Sigma \equiv \frac{2(U_1 - U_2)}{(U_1 + U_2)} \qquad (1.15)$$

where U_1, U_2 are the speeds of the two surfaces. Plotting in this manner tends to reduce the results for different rolling speeds (but otherwise identical conditions) to a single curve, especially at the origin.

PLINT (76) attempted to demonstrate the nature of

the traction peak more clearly by using a semi-logarithmic plot (Fig. 1.8). At high pressures he has found that his results can be represented by two straight lines characterised by a sharp transition point. However it appears that this is not general as the results of JOHNSON and CAMERON (81), when tried on a similar plot, range from sharp to broad transitions.

CROOK (33) and Johnson and Cameron have used their results to determine the effective viscosity of the fluid. This is defined as the viscosity which would be obtained from the values of traction, sliding speed and film thickness if they were considered invariant across the contact and that the fluid was Newtonian. Crook found that the effective viscosity fell with rolling speed but that the pressure/viscosity relationship was approximately exponential. Johnson and Cameron confirmed Crook's work but showed that at pressures greater than those used by Crook the effective viscosity tailed off (Fig. 1.9). BELL, KANNEL and ALLEN (78) have produced results which indicate that viscosity obtains a fairly constant value above a limiting pressure although their quantitative values have been questioned by Johnson in the discussion of their paper.

More recent work by ADAMS and HIRST (84) has attempted to show that the shape of the traction curve can be attributed to a non-Newtonian behaviour of the lubricant. Using the results of HAMILTON and MOORE (68) they hypothesize that the oil is non-Newtonian above a critical shear stress and that this modifies the pressure curve and hence the traction curve. Unfortunately the pressure profile results of Hamilton and Moore were made for a glass/steel disc combination, whereas

the traction results of Adams and Hirst utilised a steel/steel disc configuration, this limited the range over which comparisons could be made. Moreover Hamilton and Moore's results were made for pure rolling and yet have been applied to rolling plus sliding. This traction work has been further extended to include the effects of molecular size of the lubricant by HIRST and MOORE (85).

GENTLE (86) and GENTLE and CAMERON (87, 88) have produced traction data for a variety of lubricants for a point contact configuration. They also drew attention to the remarkable similarity of the traction curve to that obtained by shearing a granular bed, and show that by treating traction in a similar manner a good fit to the traction curve can be obtained. However they are unable to justify this comparison theoretically although they list some possible causes of granularity.

1.5 TRACTION THEORY

1.5.1 Newtonian

The simplest approach to the problem of sliding friction (traction) is to consider that the lubricant behaves in a Newtonian manner i.e. for a small fluid element

$$\tau = \eta \cdot \frac{\partial u}{\partial z} \tag{1.16}$$

where τ is the frictional resistance of the element, η is the viscosity, and $\frac{\partial u}{\partial z}$ is the velocity gradient. The total friction force F can be obtained by integrating over the surface

$$F_{o,h} = \iint \tau_{o,h} \, dx.dy = \int\int \eta \left(\frac{\partial u}{\partial z}\right)_{o,h} \cdot dx.dy \tag{1.17}$$

It is now assumed that the viscosity is constant through the thickness of the oil film, this assumption is incorrect as will be shown later, however

$$\frac{\partial u}{\partial z} = \frac{U}{h} + \frac{1}{\eta} \cdot \frac{\partial p}{\partial x} (z - h/2) \tag{1.18}$$

can be used where U is the sliding velocity, h is the film thickness and $\frac{\partial p}{\partial x}$ is the pressure gradient. The friction is now

$$F_{o,h} = \int\int \left(\eta \cdot \frac{U}{h} + \frac{\partial p}{\partial x} (z - h/2) \right) dx.dy \tag{1.19}$$

A line contact situation is now assumed and the pressure curve is defined as extending from x = +a to x = -a, an assumption which is not exactly true as the pressure field extends into the inlet region. (The origin of the axes is at the centre of the Hertzian contact of width 2a).

Hence

$$F_{o,h} = L \int_{-a}^{+a} \left(\frac{U\eta}{h} \pm \frac{dp}{dx} \cdot \frac{h}{2} \right) dx \tag{1.20}$$

where L is the length in the y-direction. By assuming that the contact can be represented by two parallel surfaces separated by a distance h_o, then

$$F_{o,h} = \frac{LU}{h_o} \int_{-a}^{+a} \eta.dx \pm \frac{Lh_o}{2} \int_{-a}^{+a} \frac{dp}{dx}.dx \tag{1.21}$$

The second integral is zero as, by definition, p is zero at +a and -a. Thus

$$F = \frac{LU}{h_o} \int_{-a}^{+a} \eta \, dx \tag{1.22}$$

A function must now be inserted to represent the variation of η with x. The expression

$$\eta = \eta_o \, e^{\alpha p} \tag{1.23}$$

can be used to relate viscosity to the pressure, where η_o is the viscosity at atmospheric pressure for a given temperature and α is the pressure/viscosity coefficient. If it is assumed that the pressure distribution is Hertzian i.e.

$$\eta = \eta_o \, e^{\alpha p_{HZ}(1-x^2/a^2)^{\frac{1}{2}}} \tag{1.24}$$

where p_{HZ} is the maximum Hertzian pressure; then an expression is obtained which needs to be evaluated numerically. However if the simplifying assumption is made that the pressure distribution is parabolic i.e.

$$\eta = \eta_o \, e^{\alpha . p_{HZ} \, (1-x^2/a^2)} \tag{1.25}$$

then an analytical solution can be obtained, as shown by CAMERON (2). At high pressures

$$\mu \equiv \frac{F}{W} \rightarrow \frac{U.L.\eta_o}{h_o.W} . e^{\alpha . p_{HZ}} . a.\sqrt{\frac{\pi}{(\alpha . p_{HZ})}} \tag{1.26}$$

where μ is the coefficient of friction and W is the normal load.

By substituting typical values of the parameters into this expression, values of friction which are approximately one hundred times too large are obtained. An error of this magnitude cannot be attributed to the simplifying assumption of a parabolic pressure distribution, nor does an alternative pressure/viscosity relationship improve matters.

This problem can only be resolved by assuming the viscosity to vary across the film thickness. This behaviour is attributed to a temperature variation across the film due to heating of the lubricant.

1.5.2 Newtonian Plus Heating

The inclusion of thermal effects in Newtonian theory has been adopted by several authors such as CROOK (89), GRUBIN (90), HINGLEY (91), CHENG (21), and KANNEL and WALOWIT (92). The basic approach to the problem is to consider the dissipation of energy inside the contact. It has been shown by ARCHARD (93) and CROOK (89) that heat transmission is mainly by conduction to the surfaces, hence

$$\eta \left(\frac{\partial u}{\partial z}\right)^2 = - k\frac{d^2T}{dz^2} \qquad (1.27)$$

as explained by CAMERON (2), where T is the temperature of the oil and k is its thermal conductivity. It should be noted that in this expression terms involving compressibility have been neglected - this is a common assumption.

Combining this equation with equation (1.16) gives

$$\frac{d^2T}{dz^2} = - \frac{\tau^2}{\eta.k} \qquad (1.28)$$

If a suitable relationship between η and T can be found then this expression can be integrated twice to give T as a function of τ (and k). The first integration of this expression was by GRUBIN (90) who used a specialisation of the Slotte viscosity equation

$$\eta = \frac{s}{(t+c)^m} \qquad (1.29)$$

where t is the temperature of the oil in any scale and s, c, m are constants. This specialisation limited Grubin's work to one type of oil.

CROOK (89) used Reynolds' viscosity relation

$$\eta = \eta_o \, e^{-\alpha T} \tag{1.30}$$

where α is a constant, but this has been shown to be very inaccurate. Also, difficulty in the mathematical manipulation of the exponential term is encountered in the use of the more accurate Vogel's equation

$$\eta = k \, e^{b/t+\Theta} \tag{1.31}$$

where k, b, Θ are constants.

On the other hand Slotte's equation is fairly accurate and its use has been justified by CAMERON (94) who showed it to be very suitable for problems dealing with temperature variations across an oil film.

As t can be in any scale it is possible to define one with an origin at -c degrees centigrade i.e. T = (t+c), then

$$\eta = \frac{s}{T^m} \tag{1.32}$$

and equation (1.28) becomes

$$\frac{d^2T}{dz^2} = -\frac{\tau^2 . T^m}{s.k} \tag{1.33}$$

This can be integrated quite easily if τ is constant with respect to z i.e. $\frac{\partial \tau}{\partial z} = 0$. The basic relation for equilibrium of an element is

$$\frac{\partial \tau}{\partial z} = \frac{\partial p}{\partial x} \tag{1.34}$$

thus τ is constant when $\frac{\partial p}{\partial x} = 0$, this condition is satisfied at the point of maximum pressure. Strictly speaking equation (1.33) can only be integrated at this point, however $\frac{\partial p}{\partial x}$ is the term which controls rolling friction and, as this is small compared with the sliding friction, it is argued that there is some justification to the approximation that $\tau \neq f(z)$. Nevertheless it should be noted that typical values of $\frac{\partial p}{\partial x}$ away from the centre of contact are in the order of 2.71×10^{12} N/m^3 (10^7 lbf./in^3.), thus it seems hard to believe that τ is invariant across the thickness of the film.

In spite of the doubt surrounding the validity of the assumption this approach has been used by the authors mentioned at the beginning of this section. In addition, all have assumed that the temperatures of the two surfaces are equal ($T_1 = T_2$) and that the temperature distribution is symmetrical about the central plane of the oil film i.e. where $z_c = \frac{h}{2}$ (subscript c refers to conditions at the central plane, and subscripts 1, 2 refer to conditions at each of the two moving surfaces). The first estimate of the central plane temperature and viscosity was given by Grubin as

$$\frac{T_c}{\eta_c} = (U_2 - U_1)^2 \frac{(m+1)}{8k} + \frac{T_1}{\eta_1} \tag{1.35}$$

Using the measured values of s, m, and k it is possible to calculate T_c and η_c from this equation since

$$\frac{T^m}{s} = \frac{1}{\eta} \tag{1.36}$$

The use of these values of T_c and η_c enables a cal-

culation of an overall value for traction which includes thermal effects. It should be pointed out however that it is assumed that s, m, and k are constant. This may not be true for s and m, and is certainly not true for k as the pressure increases. (See reference to Naylor in JOHNSON and CAMERON (81)). This increase in k with pressure is of greater significance than the fall of k with temperature described by CRAGOE (95). Thus the effect of pressure decreases the temperature rise and hence reduces the fall in viscosity predicted by this method.

However using the values obtained from this type of analysis it is possible to obtain a qualitative fit of theory with experiment. CROOK (89) managed to obtain a peak in the traction curve but the values obtained were too large compared with his later experiments (33). He concluded that the discrepancy was due to the uncertainty in the values of the fluid properties at high pressures. Other workers have managed to obtain qualitative fits but quantitative fits have only been obtained by adjusting some of the values of the fluid properties.

The predictions of HINGLEY (91) give a better fit with experiment than Crook's as they used a more accurate form of viscosity/temperature relation. However there is a lack of data at low slips (the results are confined to the falling part of the traction curve). Even the more sophisticated techniques of CHENG (21) and KANNEL and WALOWIT (92) only give good quantitative fits if abnormal fluid properties are used (i.e. high pressure/viscosity coefficients).

The point of greatest disagreement between a Newtonian plus heating analysis and experimental results is on

the rising linear part of the traction curve, yet this is where agreement should be at its best.

In this region the traction force, F, can be expressed in the empirical relation

$$F \propto \frac{U_1 - U_2}{\bar{U}} \tag{1.37}$$

where U_1, U_2 are the two surface velocities and $\bar{U}$ is the mean velocity. Newtonian theory gives

$$F \propto \eta_a \cdot \frac{U_1 - U_2}{h_o} \tag{1.38}$$

where η_a is the apparent viscosity of the whole contact and h_o the gap. Using the close approximation

$$h_o \propto \bar{U}^{0.7} \tag{1.39}$$

the following result is obtained by combining equations (1.37), (1.38) and (1.39)

$$\eta_a \propto \bar{U}^{-0.3} \tag{1.40}$$

As the viscosity of a classical fluid is not affected by rolling speed it must be concluded that Newtonian theory, even including thermal effects, is not applicable in this region. This conclusion was reached by CROOK (33) and SMITH (71, 72) and later by JOHNSON and CAMERON (81) who treated the analysis more fully.

Thus this approach is not feasible. However it is generally accepted that thermal effects do play an important part in the traction response of a lubricant especially in the high slip region (falling or plateau section of the traction curve - see Fig. 1.7). The major reason for the dis-

crepancy appears to be the assumption of Newtonian behaviour. In the following section other theories for lubricant response are outlined and their projected behaviour in terms of traction are described.

1.5.3 The Plastic Solid Hypothesis

This behavioural model was first proposed by SMITH (71, 72) and later adopted by PLINT (75, 76). It adopts an approach different from that usually associated with liquid behaviour. Both Smith and Plint argued that, under the severe conditions encountered in an EHD contact, the fluid would behave more like a solid than a liquid. Instead of the shear stress being able to increase indefinitely with shear rate under equilibrium conditions, the (solid) lubricant would exhibit a "yield stress" above which there would be plastic flow. This has been highlighted by Plint with his semi-logarithmic plotting of the traction curve, the transition point being the onset of plastic flow (Fig. 1.8).

The traction peak depends on rolling speed, temperature and pressure, so the critical plastic shearing stress can be assumed to be dependent on shear rate, temperature and pressure. Shear rate and temperature are related as an increase in shear rate obviously creates more frictional heating. Hence there is a choice of two models:-

(a) Critical shear stress dependent on pressure and shear rate only.

(b) Critical shear stress dependent on pressure and temperature only.

These two models are considered in an excellent

review by JOHNSON and CAMERON (81) in which they also go on to compare the theory with experimental results. The first model is discarded as the maximum tractions observed at higher rolling speeds and disc temperatures lie appreciably below the traction ceiling. It is therefore concluded that traction must be limited by some other mechanism than that suggested by model (a).

Model (b) was first proposed by Smith and is more in line with experimental results. For a given pressure the critical shear stress is assumed dependent on temperature, which will be highest at the central plane of the contact. Therefore the critical shear stress will first be reached at this plane and it is here that shearing will take place. Thus for constant pressure the stress should be only dependent on the central plane temperature, no matter what combination of disc temperature, rolling speed, and sliding speed caused it.

Johnson and Cameron used the work of ARCHARD (93) to calculate this temperature and compared it with their results. They obtained good correlation for all but the highest temperatures. Johnson and Cameron pointed out that at these temperatures the oil film is very thin and that the shear plane temperature is not very different from the disc temperature, however they were unable to explain the discrepancy. Because of this and other variations from theory, they suggested that it would be wise to interpret with caution Smith's hypothesis that critical shear stress depends only on pressure and temperature.

It must be noted that this hypothesis is only used to try and explain the results to the right of the peak in

the traction curve, and therefore offers no explanation of the fall in effective viscosity with rolling speed or the "plateau" viscosity at high pressure.

More recent work by JOHNSON and ROBERTS (82) and DUCKWORTH (96) suggests that the linear part of the traction curve is not necessarily a Newtonian liquid response but may be an elastic response, depending on conditions. They do not attempt to relate these findings to any other part of the traction curve, but it is tempting to assume that if the fluid can respond elastically at low shear rates, then a plastic response at higher shear rates seems quite plausible.

As mentioned previously ADAMS and HIRST (84) and HIRST and MOORE (85) have also proposed a critical shear stress model to explain their results at low sliding speeds. However they do not assume that the lubricant behaves in a plastic manner, instead they suggest that the liquid is still viscous but that at high pressures its viscosity decreases with shear stress above a critical shear stress. Hirst and Moore attempted to relate this critical shear stress to the average molecular size of the lubricant. They concluded that this stress was approximately inversely proportional to the molecular volume and so tends to add support to the Ree-Eyring model for fluid behaviour.

1.5.4 The Ree-Eyring Model

This model attempts to explain the fluid behaviour in terms of molecular behaviour. It is known as the significant structures theory and was developed by EYRING et al (97, 98). For a lubricant this theory has the simplified form

$$\tau = \frac{x}{\alpha} \sinh^{-1} (\beta \dot{s}) \tag{1.41}$$

where $\dot{s}$ is the shear rate, $1/\alpha$ is a shear modulus, x is the fraction of the liquid flowing in a non-Newtonian manner and β is a factor which is proportional to the relaxation time of the fluid.

In addition the following definitions are used

$$x = x_o \, e^{\gamma_1 p} \tag{1.42}$$

$$\beta = \beta_o \, e^{\gamma_2 p} \tag{1.43}$$

For a given fluid at constant temperature; α, x_o, β_o, γ_1 and γ_2 are all considered constant. It can be seen that for $\beta.\dot{s} << 1$ (i.e. low shear rate) $\sinh^{-1} \beta\dot{s} \simeq \beta\dot{s}$, hence

$$\tau = \frac{x_o \beta_o}{\alpha} \, e^{(\gamma_1+\gamma_2)p} \, . \, \dot{s} \tag{1.44}$$

This represents Newtonian behaviour of a fluid whose viscosity dependence on pressure is governed by an exponential law i.e.

$$\tau = \eta_o \, e^{\gamma p} \, . \, \dot{s} \tag{1.45}$$

where $\eta = \frac{x_o \beta_o}{\alpha}$ and $\gamma = \gamma_1 + \gamma_2$

Thus it can be seen that at low shear rates the Ree-Eyring model predicts Newtonian behaviour in accordance with experimental findings.

This model has been applied to EHD contacts by BELL (99), BELL, KANNEL and ALLEN (78), and BELL and KANNEL (100). They have achieved reasonable success in describing the film thickness using certain approximations but the fit with the

traction curve is only qualitative.

The main problems with the model can be summarised as follows:-

(a) There is a lack of information about the material parameters and these can only be obtained from continuous shear experiments under the appropriate conditions. However EHD conditions are virtually unique and as such it is almost impossible to simulate them elsewhere, therefore any quantitative fit is suspect.

(b) The model is very difficult to use mathematically, even in its simplified form.

(c) At the moment the theory can only be applied to isothermal conditions as most, if not all, of the material parameters are temperature dependent.

(d) The theory suggests a much weaker influence of rolling speed on film thickness and traction than that observed experimentally, especially at high shear rates.

1.5.5 Shear Viscoelasticity

One possible explanation of the non-Newtonian behaviour of a lubricant is shear viscoelasticity i.e. the oil deforms in an elastic manner as well as the more usual Newtonian (viscous) manner. Hence the apparent viscosity of the oil is reduced due to this additional deformation although its true viscosity is unimpaired. Examples of viscoelastic materials are pitch, glass and plastic which over short periods of time appear elastic solids but over (much) longer periods flow in a liquid manner.

The simplest model to represent this kind of behaviour is the Maxwell model which supposes the lubricant response to be represented by an elastic response and viscous response in series. This leads to an expression of the form

$$\dot{\gamma} = \frac{\tau}{\eta} + \frac{1}{G} \cdot \frac{d\tau}{dt} \qquad (1.46)$$

where $\dot{\gamma}$ is the shear rate, τ is the shear stress, η is the viscosity (for low shear rates), G is the shear modulus (for high shear rates) and t is the time.

It has been shown by BARLOW and LAMB (101), using a piezoelectric crystal, that this expression does give a fair representation of a viscous oil under their laboratory conditions. However these involved very small strains and very high frequencies, the complete opposite of the EHD condition of steady shear and very large strains.

If equation (1.46) is applied in a system of reference axes which maintains its orientation relative to the planes of shear, viscoelastic effects become important when the transit time of the oil through the contact (2a/U) is of the order of the relaxation time (η/G) - where a is the Hertzian half width of the contact and U the velocity - as found by MILNE (102) and CROUCH and CAMERON (103). Unfortunately the conditions necessary to achieve such a state are very rarely found in an EHD contact.

DYSON (104) has shown that equation (1.46) cannot be applied to a system of axes as described above as rotation of the shear planes has to be considered. This was pointed out by OLDROYD (105) and other workers and later

followed up by TANNER (106). However even taking this shear plane rotation into account was still unsatisfactory and Dyson went on to show that this model has serious objections when trying to relate oscillatory shear results to EHD conditions.

In 1970 DYSON (107) suggested that the Barlow-Lamb model for viscoelastic behaviour would be better. This model is similar to the Maxwell model but it combines the admittances of the viscous and elastic components instead of the compliances. The justification for this is based on the fact that for a liquid to behave as a Maxwell fluid the viscosity should show an Arrhenuis relation to temperature

$$\eta = A + \frac{B}{T} \tag{1.47}$$

where T is the absolute temperature and A, B are constants. This is rarely true for liquids having viscosities above 0.01 Ns/m^2 (0.1 poise). However it has been shown by BARLOW, ERGINSAV and LAMB (108) that liquids above 0.01 Ns/m^2 can be described by the Doolittle free volume equation, and that liquids obeying this relation should also obey the Barlow-Lamb model. If it is assumed that density is a linear function of temperature then the Doolittle free volume equation can be written

$$\text{Ln } \eta = C + \frac{D}{T-T_o} \tag{1.48}$$

where C, D are constants, η is the viscosity at temperature T, and T_o is a fundamental reference temperature. HUTTON (109) has produced some evidence to show that mineral oils can be described quite accurately by the Barlow-Lamb model.

DYSON (107) used this model, with the simplifying assumption of constant pressure instantaneously applied over the contact, to try and explain the general shape of the traction curve. He showed that the Barlow-Lamb model gave better agreement with experimental results than the Maxwell model,but the quantitative fit was dubious due to the lack of data and the constant pressure assumption. Moreover the fit was poor for the linear part of the traction curve.

1.5.6 Compressional Viscoelasticity

It was suggested by FEIN (110) that the reason for the low values of effective viscosity which are observed could be the inability of the lubricant to respond to the rapid pressure changes involved in passing through the contact. His analysis shows that, under certain conditions, the passage time of the lubricant through could be short compared with the time necessary for the fluid to reach its equilibrium viscosity after an applied pressure step.

A compressional viscoelastic model can be represented by the spring and dashpot system shown in Fig. 1.10. It is assumed that the response of a liquid to a rapid change in pressure consists of an instantaneous volume change (represented by K_∞) followed by a time dependent volume change (represented by K_f with damping η_f). The instantaneous change is attributed to compression of the crystal "lattice", while the time dependent response is attributed to molecular rearrangements.

This type of model was used by Fein and also by HARRISON and TRACHMAN (111), TRACHMAN (112), and TRACHMAN and CHENG (113). Fein's analysis only showed compressional visco-

elasticity could be significant and no attempt was made to demonstrate an accurate correlation. He used an exponential dependence of viscosity variations from the equilibrium to density variations from the equilibrium and assumed values of the liquid parameters crudely approximated from oscillatory shear experiments.

HARRISON and TRACHMAN (111) obtained a qualitative fit of theory with experiment using the Doolittle free volume equation and a shear model which consists of a visco-elastic liquid and a limiting shear stress. They also attempted to obtain more accurate estimates of the liquid parameters from oscillatory shear experiments. This work was continued by TRACHMAN and CHENG (112, 113) who used a hyperbolic liquid model to obtain a smooth transition from shear viscoelasticity to a limiting shear stress. They concluded that compressional viscoelasticity is only significant at low sliding speeds and that at high sliding speeds it is suppressed by the limiting shear stress.

One interesting feature of Harrison and Trachman's work is that they suggest that the "levelling off" of effective viscosity with pressure (as found by JOHNSON and CAMERON (81) is not a liquid property, but is in fact a consequence of the false extrapolation of effective viscosity to its value at zero rolling speed.

1.5.7 Granular Theory

This theory was first outlined by GENTLE and CAMERON (86, 87) after noticing some remarkable similarities between shearing a bed of sand and an EHD traction curve. Loose packed granules (which predominate at low pressure)

give an arrangement which is broken down gradually by shear until a steady traction force is produced by randomly colliding granules (see Fig. 1.11). At high pressures, the granules are hexagonally packed and offer more resistance to shear owing to the more rigid configuration. However once the order is broken down by shearing, this force is once again caused by collisions of random granules.

Gentle and Cameron suggest that one possible cause of granularity is that the region of constant viscosity of lubricants at high pressures corresponds to solidification or glassing of the fluids. In a sliding contact the nucleation centers (around which molecular aggregates grow) are prevented from uniting to form a continuous medium by shearing. The result is that the lubricant would behave as a granular solid if the temperature in the contact was below the pour point corresponding to the pressure of the Hertzian region. Unfortunately there is little data on the raising of pour point with pressure and so this concept must remain pure supposition. Nevertheless it is an interesting hypothesis.

1.6 SUMMARY

There is considerable argument over the behaviour of film thickness at high Hertzian pressures under rolling conditions and mostly centres around the choice of experimental technique. As yet measurement of film thicknesses in EHD line contact at these pressures has not been made using optical interferometric methods. However this technique has been used for the point contact configuration where a normal load dependence of film thickness was observed (86). Conversely an X-ray method of measuring film thickness in

line contact has produced results which show a greater load dependence than expected (44).

Otherwise the behaviour of film thickness in the EHD contacts appears to be as predicted for the more common lubricating oils although some anomalous trends are sometimes exhibited for the specialist fluids (e.g. DYSON et al (35)). There is however a discrepancy which is occasionally apparent even for mineral oils. This occurs at the higher film thicknesses where the measured film thickness falls below the predicted value, a trend which is further aggravated by the presence of sliding (35, 51, 53, 54). All these authors attribute this effect to shear heating but their justification is vague.

There are many theories which have been proposed to explain the shape of the traction curve, most of which are more concerned with the low slip region. In the high slip region it is generally recognised that thermal effects predominate although this does not preclude other effects also being present. Most of these theories are concerned with the contact itself and so should not affect film thickness as this is considered to be determined by the inlet conditions. The only possibilities appear to be a viscosity dependence on shear stress modifying the film build up in the inlet region or significant heat flow back out of the contact lowering the oil viscosity. The experimental work to date does not show any unusual trends in film thickness under traction conditions which are not present in pure rolling. However the (more) accurate technique of optical interferometry has not been applied to EHD line contact as yet, only to the point contact configuration which is more complex.

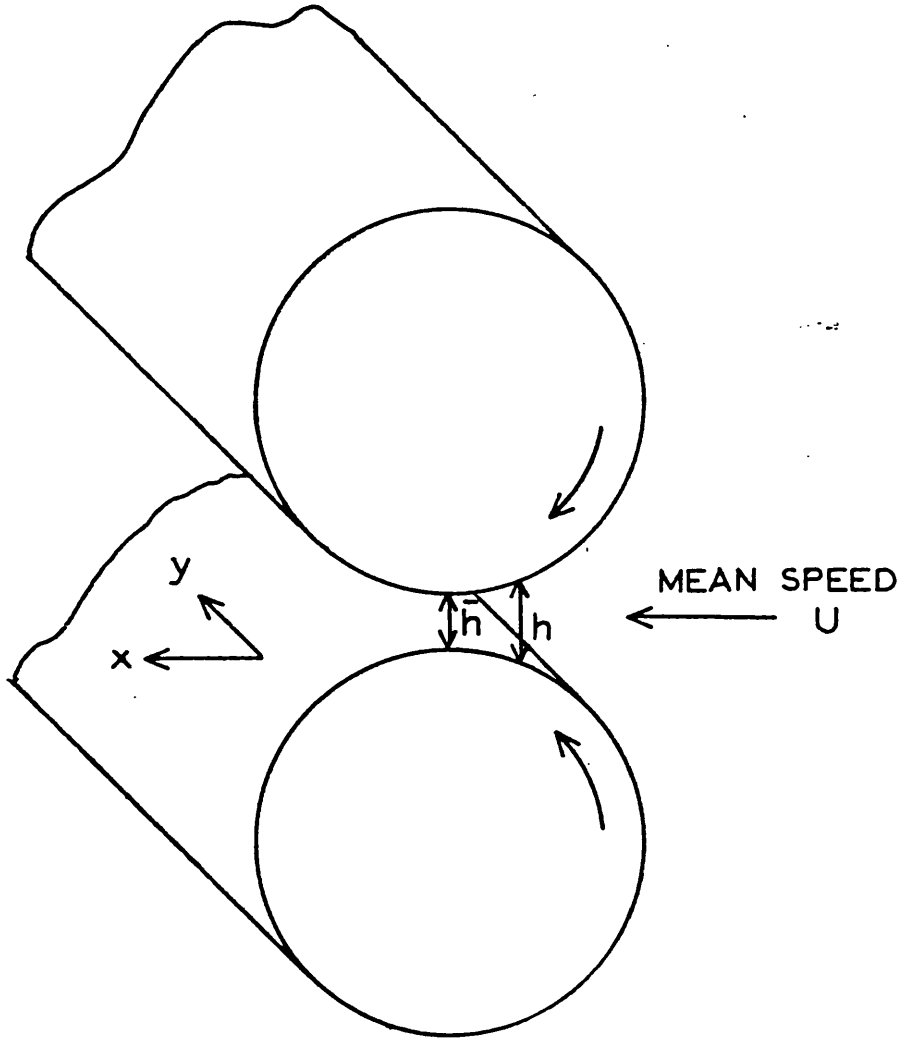

FIG. 1.1. CONTACT GEOMETRY FOR REYNOLDS' EQUATION

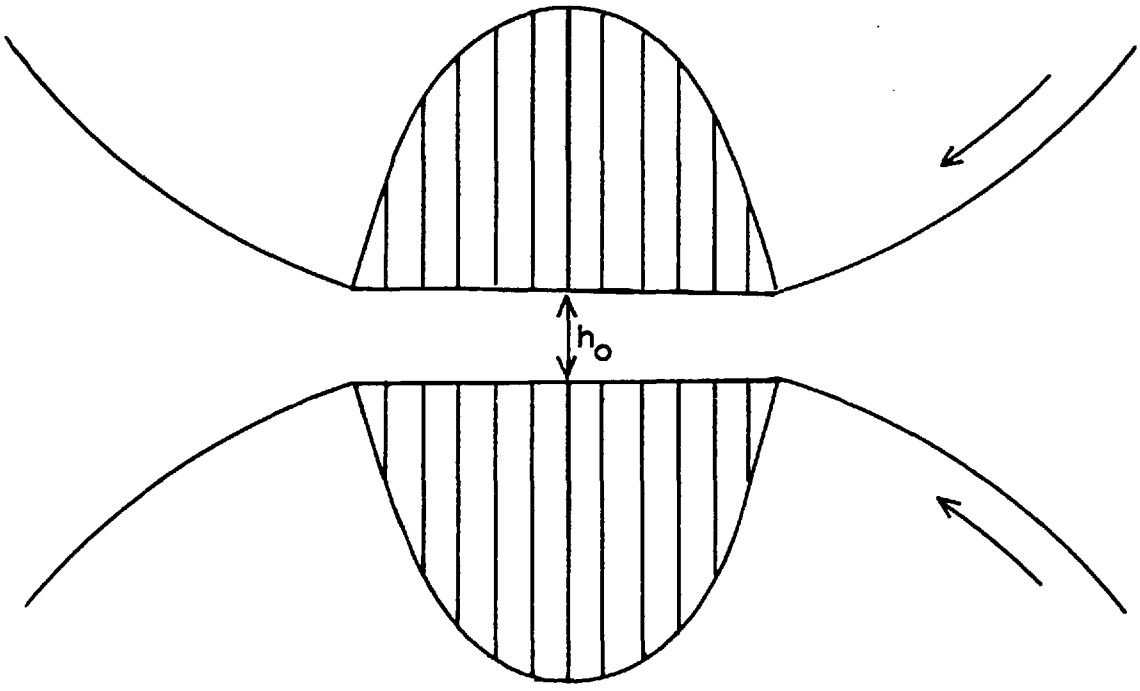

FIG. 1.2. THE ASSUMED CONTACT CONDITIONS IN GRUBIN'S THEORY

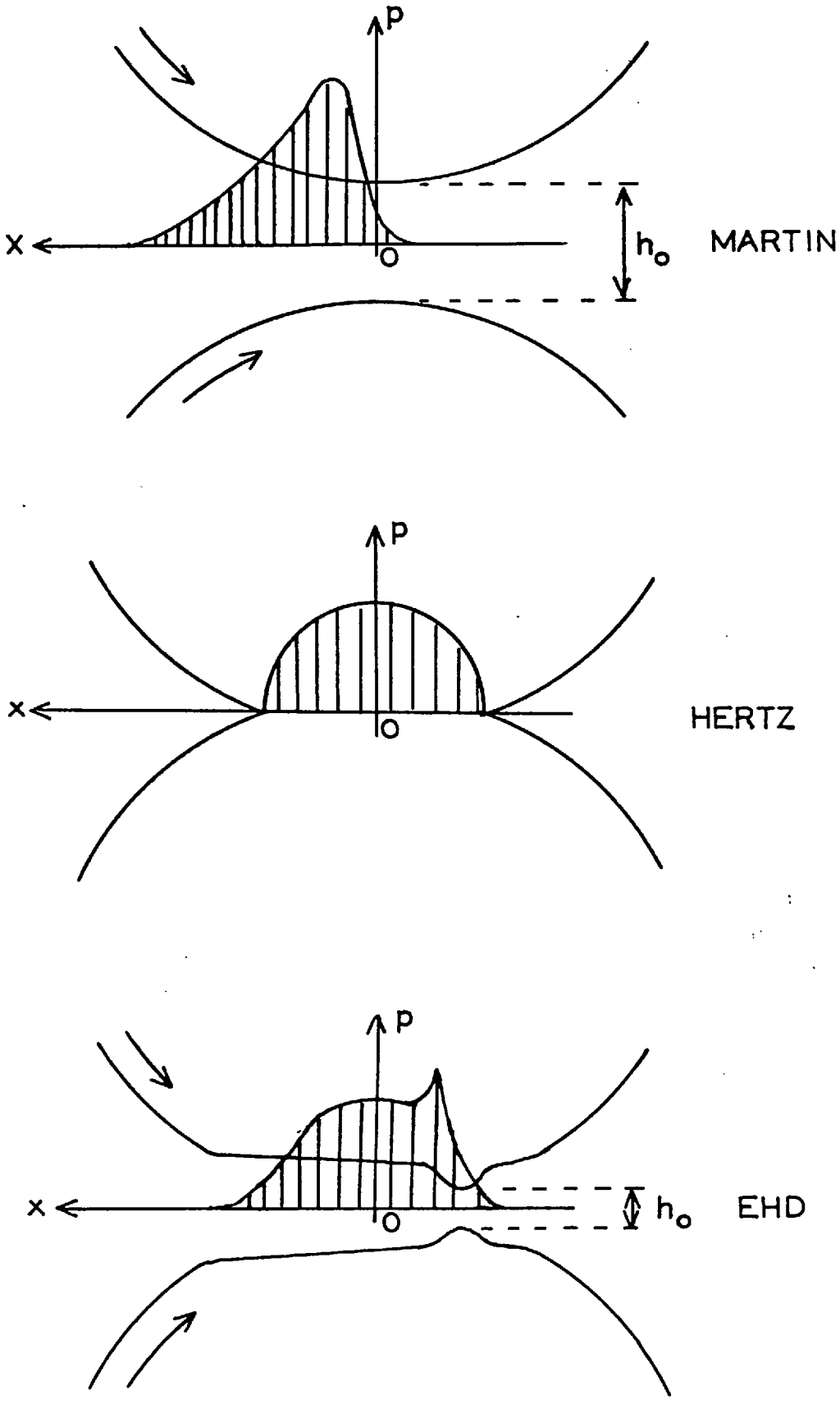

FIG. 1.3. COMPARISON OF PRESSURE DISTRIBUTIONS FOR MARTIN, HERTZ, AND EHD CONDITIONS

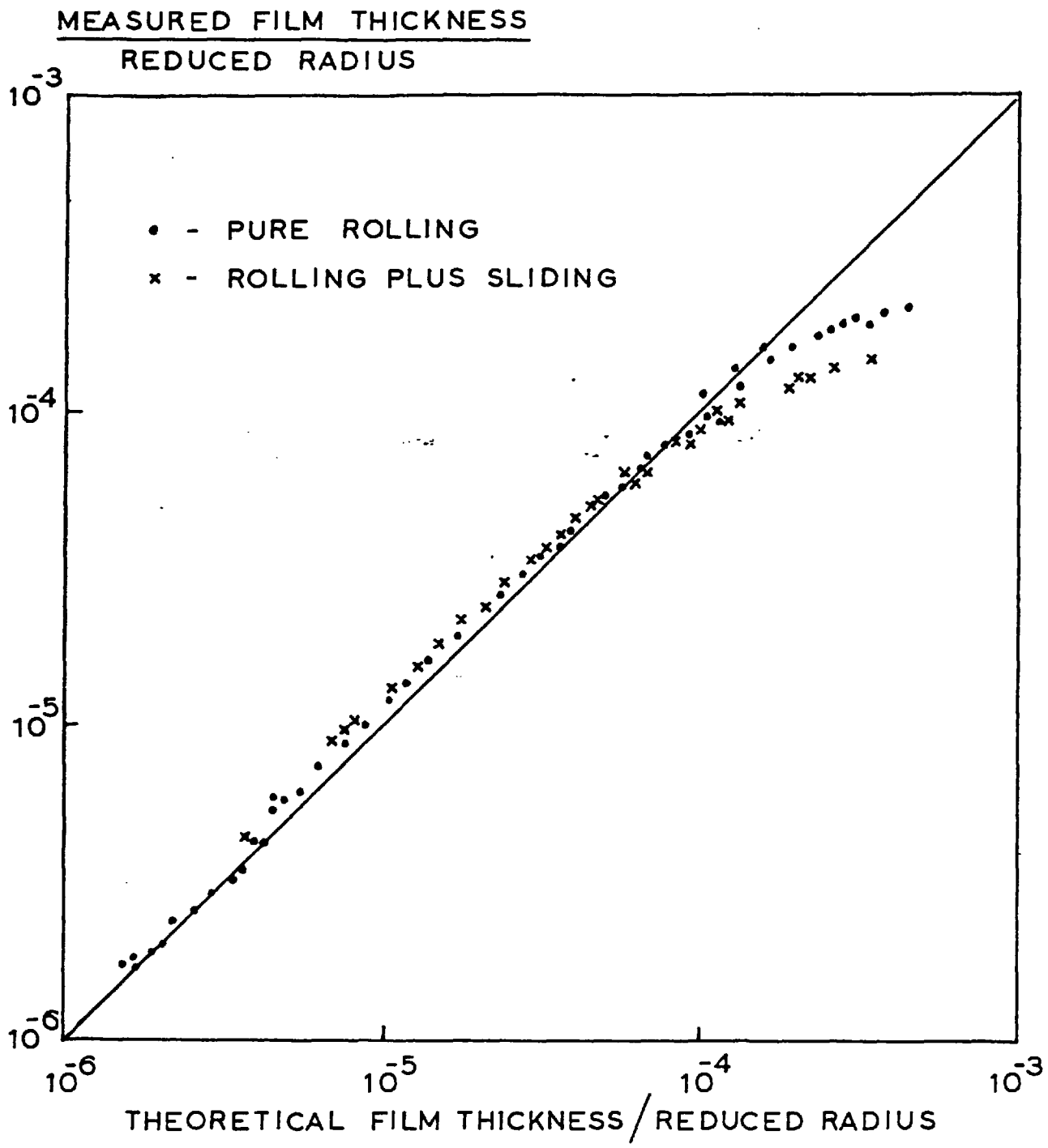

FIG. 1.4. THE FALL OF FILM THICKNESS AT HIGHER VALUES (TAKEN FROM DYSON, NAYLOR AND WILSON (35))

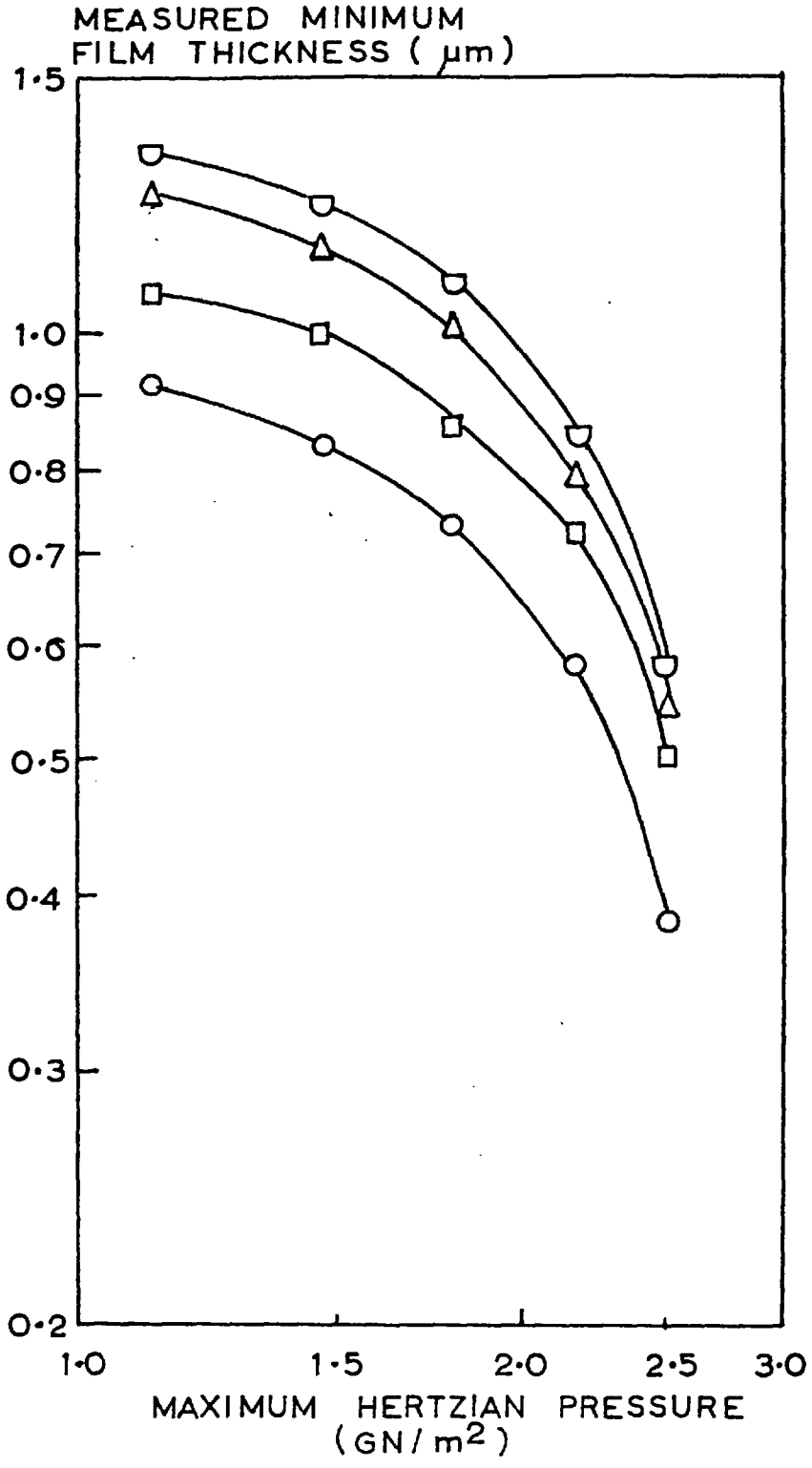

FIG. 1.5. THE INCREASE IN SENSITIVITY OF FILM THICKNESS TO LOAD AT HIGHER HERTZIAN PRESSURES (TAKEN FROM PARKER AND KANNEL (44)

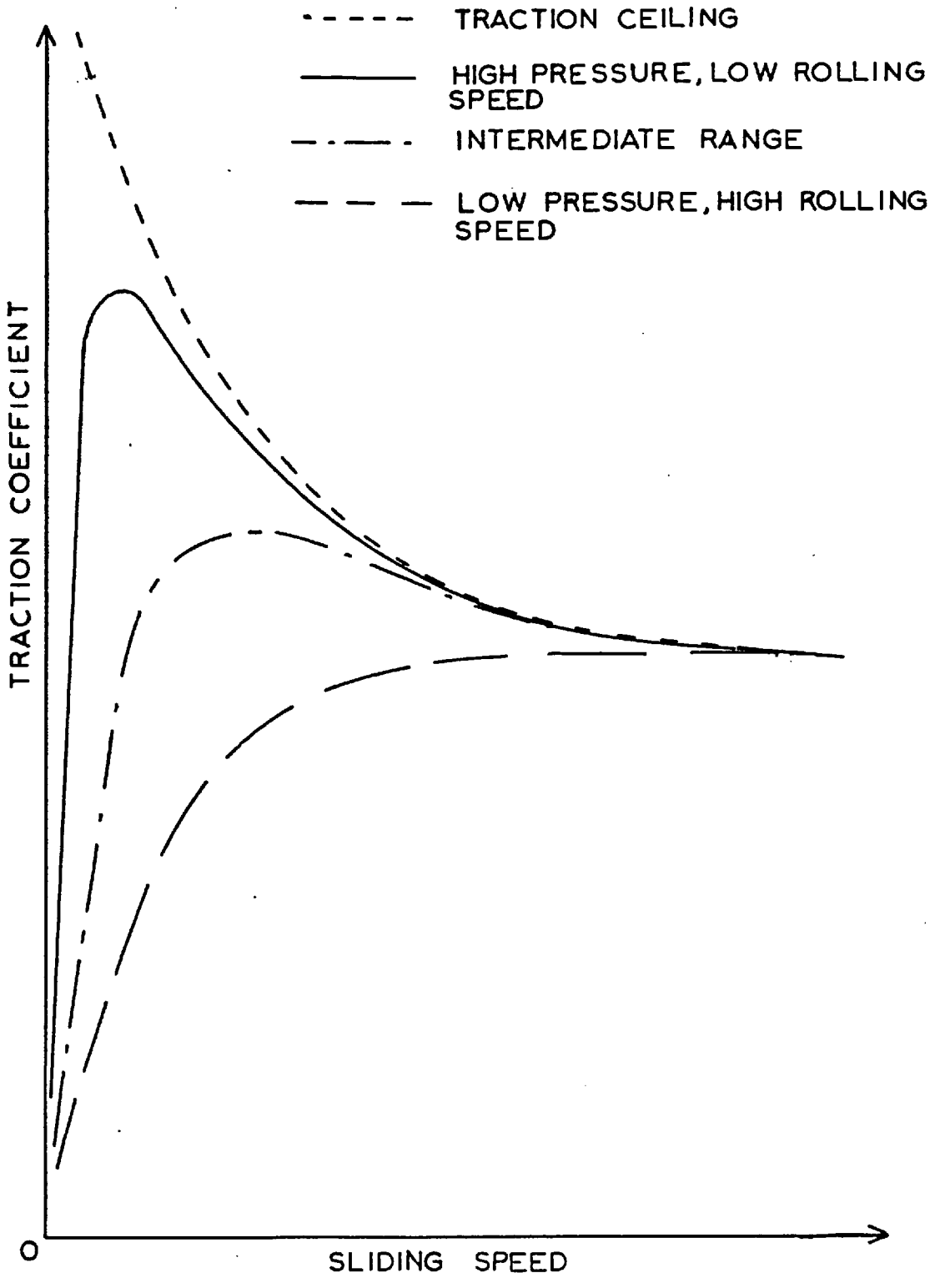

FIG. 1.6. GENERAL BEHAVIOUR PATTERN OF TRACTION RESPONSE

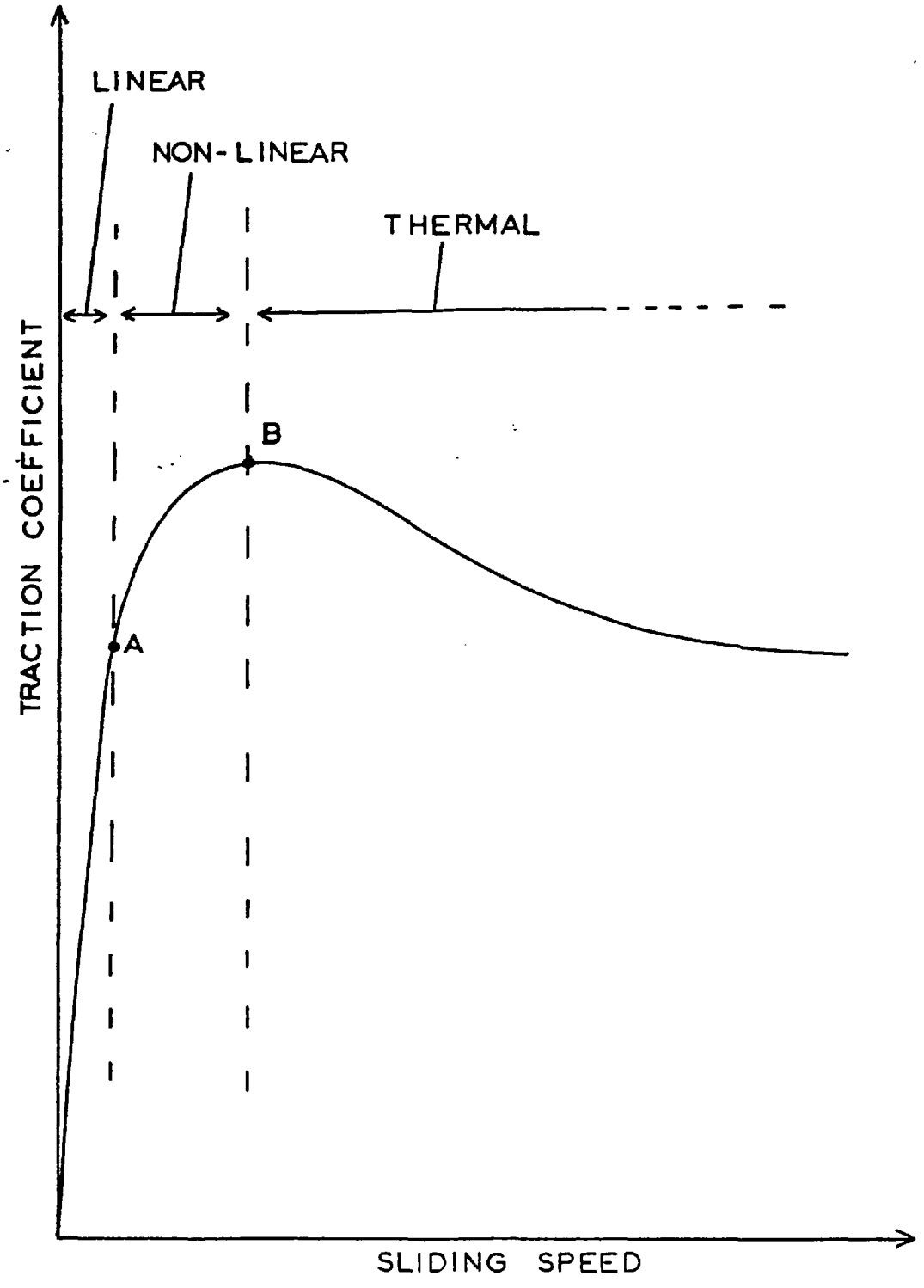

FIG. 1.7. THE THREE REGIONS OF A TYPICAL TRACTION CURVE

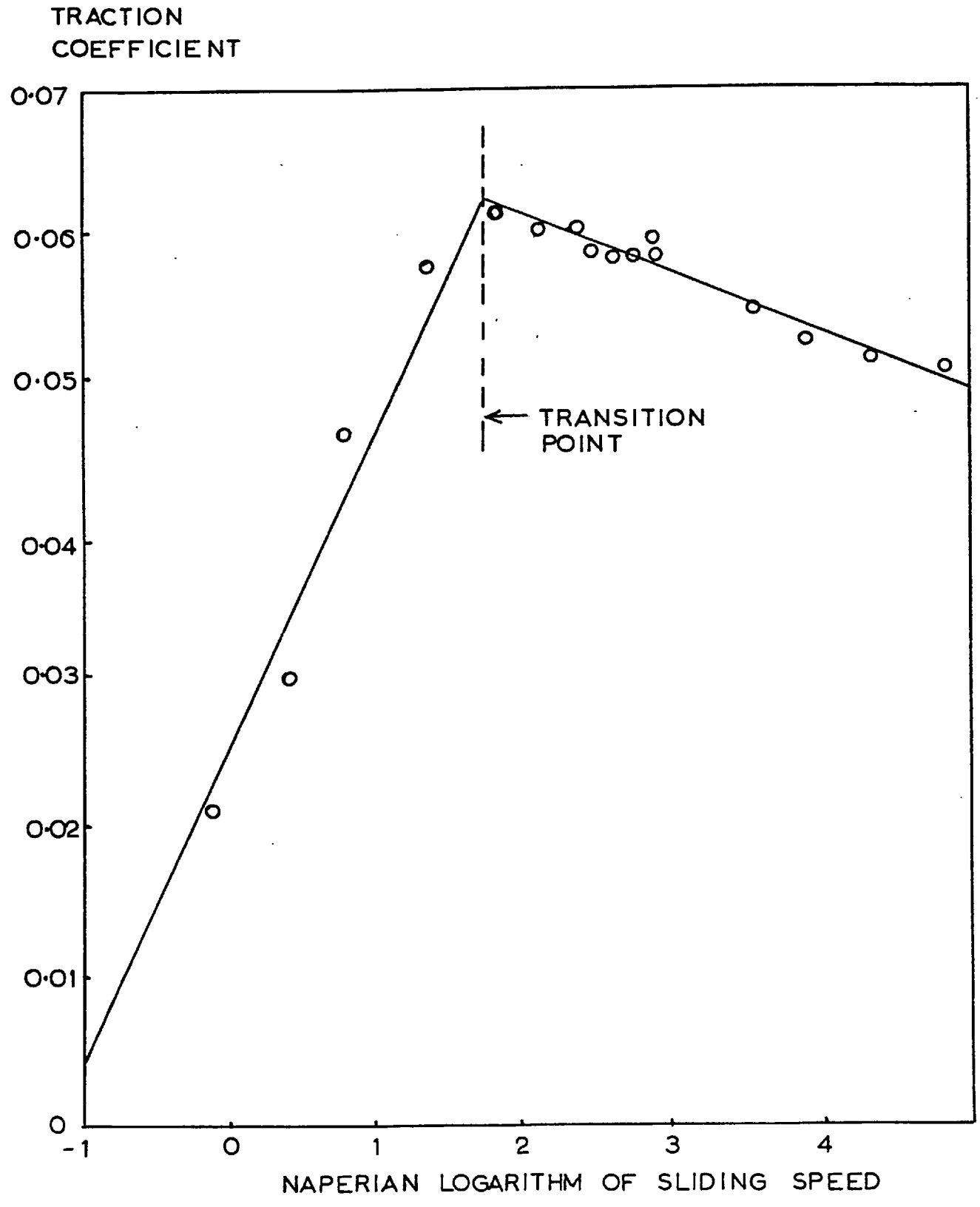

FIG. 1.8. A SEMI-LOGARITHMIC METHOD OF PLOTTING TRACTION (TAKEN FROM PLINT (76))

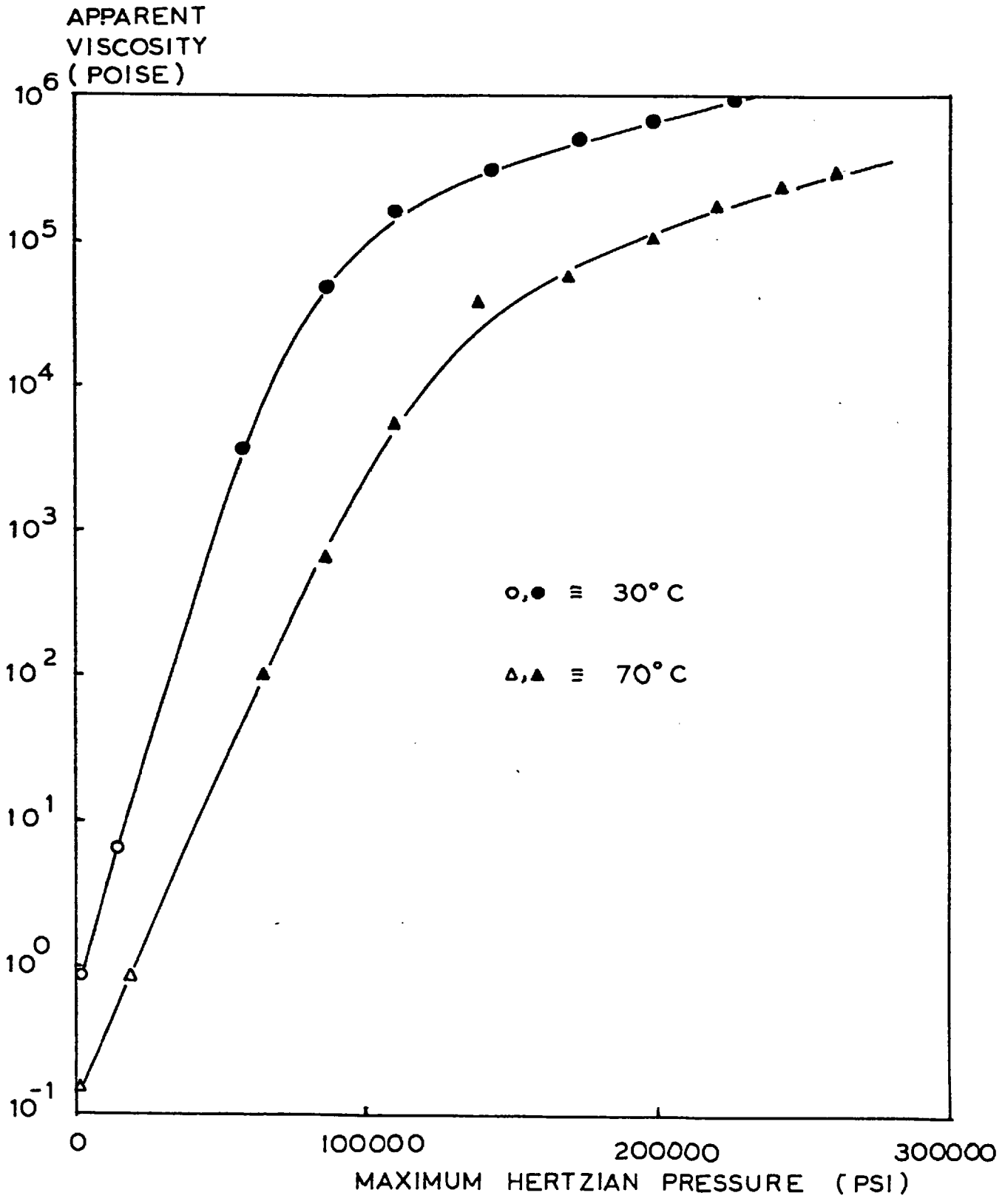

FIG. 1.9. THE BEHAVIOUR OF EFFECTIVE VISCOSITY
(TAKEN FROM JOHNSON AND CAMERON (81))

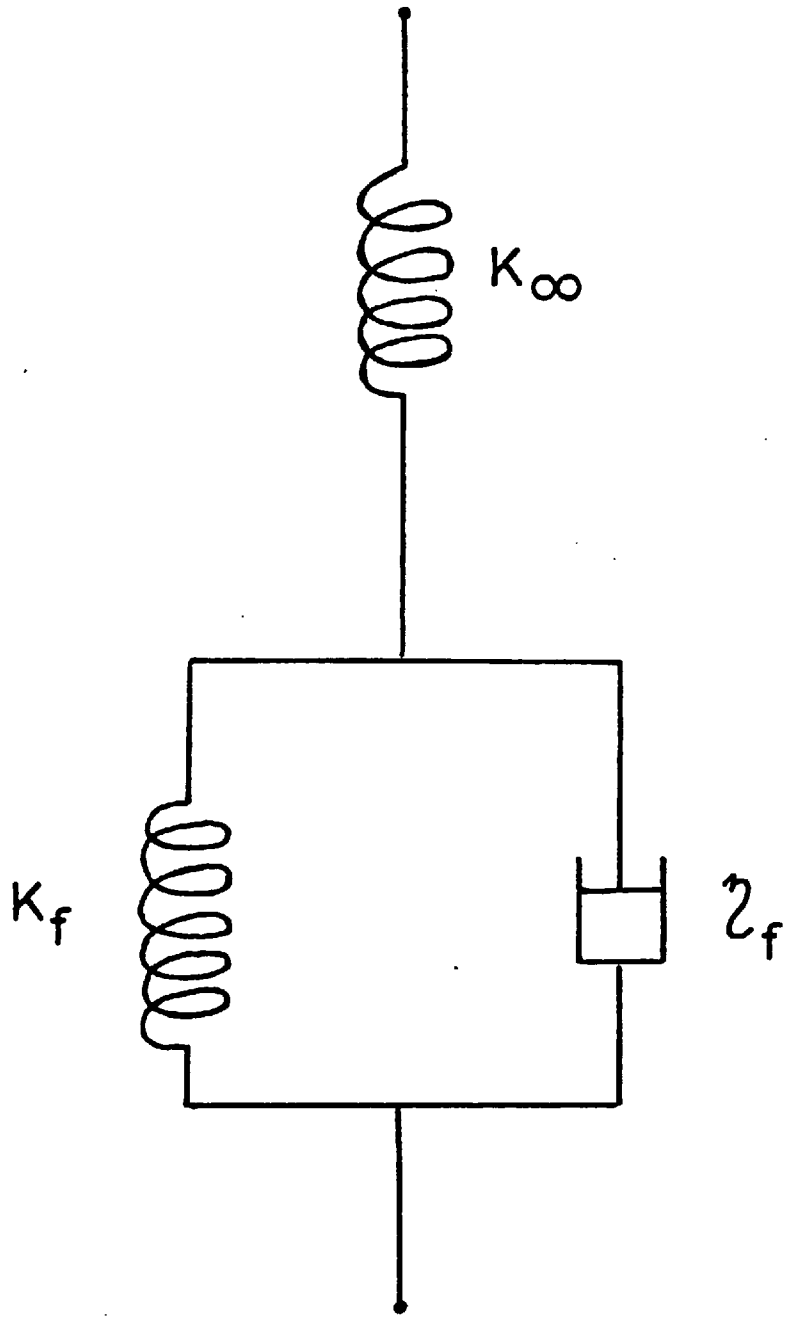

FIG. 1.10. SPRING AND DASHPOT REPRESENTATION OF COMPRESSIONAL VISCOELASTICITY

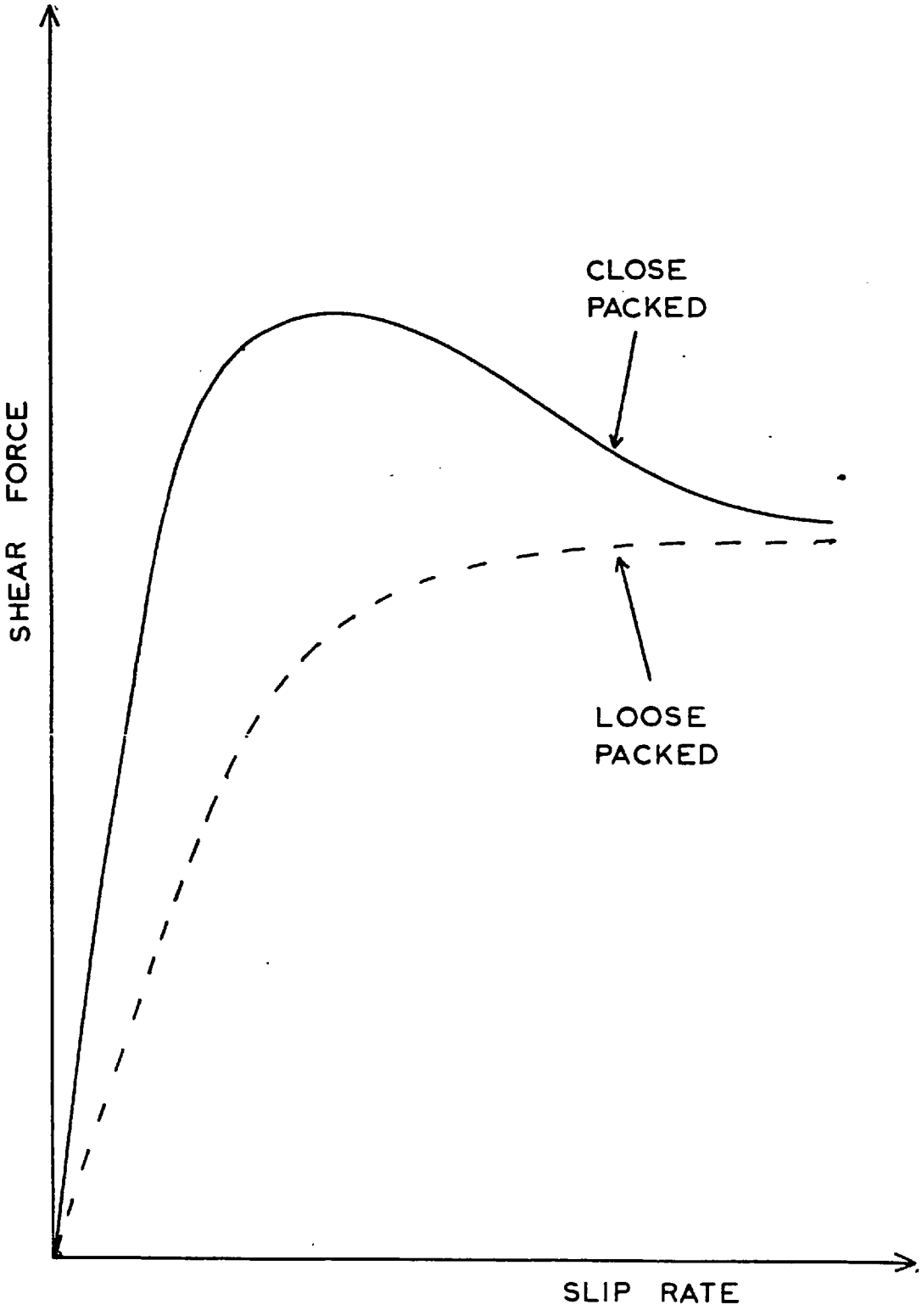

FIG. 1.11. SHEARING OF A BED OF SAND (TAKEN FROM GENTLE AND CAMERON (87))

CHAPTER 1: REFERENCES

1. HERTZ H. - "On the Contact of Elastic Solids", and "On the Contact of Rigid Elastic Solids and on Hardness", reprinted in "Miscellaneous Papers", translated by Jones D.E. and Schott G.A., Macmillan Co. Ltd., London, 1896, pp. 146-183.
2. CAMERON A. - Principles of Lubrication, Longmans, 1966.
3. PINKUS O. and STERNLICHT B. - Theory of Hydrodynamic Lubrication, McGraw-Hill Book Co., 1961.
4. MARTIN - "The Lubrication of Gear Teeth", Engineering, Aug. 11, 1916, Vol. 102.
5. PEPPLER W. - "Untersuchungen über die Druckübertragung bei Belasteten und Geschmierten Umlaufenden Achsparallelen Zylindern", Maschinenelemente-Tagung, Auchen 1935. VDI Verlag 1936 (Berlin), p. 42.
6. PEPPLER W. - "Druckübertragung und Geschmiert Zylindrischen Gleit und Wälzglächen", VDI Forschrift 1938, p. 391.
7. MELDAHL A. - "Contribution to the Theory of the Lubrication of Gears and the Stressing of the Lubricated Flanks of Gear Teeth", Brown Boveri Rev., 1941, Vol. 28 (No. 11), p. 374.
8. GATCOMBE E.K. - "Lubrication Characteristics of Involute Spur Gears - a Theoretical Investigation", Trans. ASME, 1945, Vol. 67, p. 177.
9. GRUBIN A.N. - "Fundamentals of the Hydrodynamic Theory of Lubrication of Heavily Loaded Cylindrical Surfaces", Symposium: Investigation of the Contact of Machine Components, Central Scientific Institute for Technology and Mechanical Engineering TsNIITMASh, Book No. 30, Moscow, 1949, pp. 115 - 166, (D.S.I.R. Translation).
10. CHU P.S.Y. and CAMERON A. - "Pressure Viscosity Characteristics of Lubricating Oils", J. Inst. Petrol., 1962, Vol. 48, pp. 147 - 155.
11. PETRUSEVICH A.I. - "Fundamental Conclusions from the Contact - Hydrodynamic Theory of Lubrication",

Izvestia Uzbekist. Fil. Akad. Nauk SSSR (OTN), 1951, Vol. 2, p. 209, (Ministry of Defence translation No. 293).

12. WEBER C. and SAALFELD K. - "Schmierfilm bei Walzen mit Verformung", Zeits. ang. Math. Mech., 1954, Vol. 34, p. 54.

13. DOWSON D. and HIGGINSON G.R. - "A Numerical Solution to the EHD Problem", J. Mech. Eng. Sci., 1959, Vol. 1, No. 1, pp. 6 - 15.

14. DOWSON D. and HIGGINSON G.R. - "The Effect of Materials Properties on the Lubrication of Elastic Rollers", J. Mech. Eng. Sci., 1960, Vol. 2, No. 3, pp. 188 - 194.

15. DOWSON D. and HIGGINSON G.R. - "A New Roller-Bearing Lubrication Formula", Engineering, London, 1961, Vol. 192, p. 158.

16. DOWSON D., HIGGINSON G.R. and WHITAKER, A.V. - "Elastohydrodynamic Lubrication: A Survey of Isothermal Solutions", J. Mech. Eng. Sci., 1962, Vol. 4, No. 2, p. 121.

17. ARCHARD G.D., GAIR F.C. and HIRST W. - "The EHD Lubrication of Rollers", Proc. Roy. Soc. (A), 1961, Vol. 51, pp. 51 - 72.

18. STERNLICHT B., LEWIS P. and FLYNN P. - "Theory of Lubrication and Failure of Rolling Contacts", J. Basic Eng., Trans. ASME, 1961, Vol. 83, Series D, No. 2, p. 213.

19. CHENG H.S. and STERNLICHT B. - "A Numerical Solution for the Pressure, Temperature and Film Thickness Between Two Infinitely Long, Lubricated Rolling and Sliding Cylinders under Heavy Loads", J. Mech. Eng. Sci., 1965, Vol. 87, pp. 695 - 707.

20. CROOK A.W. - "The Lubrication of Rollers II. Film Thickness with Relation to Viscosity and Speed", Phil. Trans. Roy. Soc. (A), 1961, Vol. 254, pp. 223 - 236.

21. CHENG H.S. - "A Refined Solution to the Thermal EHD Lubrication of Rolling and Sliding Cylinders", ASLE Trans. 1965, Vol. 8, pp. 397 - 410.

22. DOWSON D. and WHITAKER A.V. - "A Numerical Procedure for the Solution of the EHD Problem of Rolling and Sliding Contacts Lubricated by a Newtonian Fluid", Proc. Inst. Mech. Eng., 1965-66, Vol. 180, Part 3B, p. 57.

23. MEYER D.R. and WILSON C.C. - "Measurement of Elasto-hydrodynamic Oil Film Thickness and Wear in Ball Bearing by the Strain Gauge Method", Jnl. Lub. Tech., Trans. ASME, Vol. 93, Series F, 1971, p. 224.

24. JOHNSON K.L. and ROBERTS A.D. - "Film Thickness Variation with Load in EHL Contacts", Wear, Vol. 27, No. 3, 1974, p. 391.

25. LANE T.B. and HUGHES J.R. - "A Study of the Oil Film Formation in Gears by Electrical Resistance Measurements", Brit. J. Appl. Phys., 1952, Vol. 3, pp. 315 - 318.

26. CAMERON A. - "Surface Failure in Gears", J. Inst. Petrol. 1954, Vol. 40, p. 191.

27. LEWICKI W. - "Some Physical Aspects of Lubrication in Rolling Bearings and Gears", Engineer, 1955, Vol. 200, pp. 176 - 178 and 212 - 215.

28. CROOK A.W. - "Simulated Gear Tooth Contacts", Proc. Inst. Mech. Eng., 1957, Vol. 171, pp. 187 - 214.

29. EL-SISI S.I. and SHAWKI G.S.A. - "Measurement of Oil-Film Thickness on Gear Teeth", J. Basic Eng., Trans. ASME, 1958, Vol. 80, Series D, No. 1, p. 12.

30. EL-SISI S.I. and SHAWKI G.S.A. - "Measurement of Oil-Film Thickness Between Disks by Electrical Conductivity", J. Basic Eng., Trans. ASME, 1960, Vol. 82, Series D, No. 1, p. 12.

31. CROOK A.W. - "The Lubrication of Rollers", Phil. Trans. Roy. Soc. (A), 1958, Vol. 250, pp. 387 - 409.

32. ARCHARD J.F. and KIRK M.T. - "Lubrication at Point Contacts", Proc. Roy. Soc. (A), 1961, Vol. 261, pp. 532 - 550.

33. CROOK A.W. - "The Lubrication of Rollers IV. Measurements of Friction and Effective Viscosity", Phil. Trans. Roy. Soc. (A), 1963, Vol. 49, pp. 295 - 307.

34. CHENG H.S. and ORCUTT F.K. - "A Correlation Between the Theoretical and Experimental Results on the EHD Lubrication of Rolling Sliding Contacts", Proc. Inst. Mech. Eng., 1965-66, Vol. 180, Part 3B.

35. DYSON A., NAYLOR H. and WILSON A.R. - "The Measurement of Oil Film Thickness in Elastohydrodynamic Contacts", Proc. Inst. Mech. Eng., 1965-66, Vol. 180, Part 3B, p. 119.

36. SIBLEY L.B., BELL J.C., ORCUTT F.K., ALLEN C.M., and GOLDTHWAITE W.H. - "A Study of the Influence of Lubricant Properties on the Performance of Aircraft Gas Turbine Engine Rolling Contact Bearings", W.A.D.C. Tech. Rep., 1958, No. 58-565.

37. SIRIPONGSE C., ROGERS P.R., and CAMERON A. - "Thin Film Lubrication: 1 - Discharge Through Thin Oil Films", Engineering, 1958, Vol. 186, pp. 146 - 147.

38. SIRIPONGSE C. and CAMERON A. - "Thin Film Lubrication: 2 - Lubrication of the Four Ball Machine", Engineering, 1958, Vol. 186, pp. 147 - 149.

39. MacCONOCHIE I.O. and CAMERON A. - "The Measurement of Oil Film Thickness on Gear Teeth", J. Basic Eng., Trans.ASME, 1960, Vol. 82, Series D, p. 29.

40. DYSON A. - "Investigation of the Discharge-Voltage Method of Measuring the Thickness of Oil Films Formed in a Disc Machine under Conditions of Elastohydrodynamic Lubrication", Proc. Inst. Mech. Eng., 1966-67, Vol. 181, Part 1, pp. 633 - 646.

41. SIBLEY L.B. and ORCUTT F.K. - "Elastohydrodynamic Lubrication of Rolling Contact Surfaces", Trans. ASLE, 1961, Vol. 4, No. 2, pp. 234 - 249.

42. KANNEL J.W., BELL J.C. and ALLEN C.M. - "Methods for Determining Pressure Distributions in Lubricated Rolling Contact", Trans. ASLE, 1965, Vol. 8, pp. 250 - 270.

43. KANNEL J.W. and BELL J.C. - "Interpretations of the Thickness of Lubricant Films in Rolling Contact. 1. Examination of Measurements Obtained by X-rays", Trans. ASME, Oct. 1971, pp. 478 - 497.

44. PARKER R.J. and KANNEL J.W. - "Elastohydrodynamic Film Thickness Between Rolling Disks with a Synthetic Paraffinic Oil to 589K", NASA Tech. Note, TND-6411.

45. GENTLE C.R., DUCKWORTH R.R., and CAMERON A.- "Elastohydrodynamic Film Thicknesses at Extreme Pressures", ASME Pub. No. 74-LUB-27, 1974.

46. KIRK M.T. - "Hydrodynamic Lubrication of Perspex", Nature, 1962, Vol. 194, p. 965.

47. ARCHARD J.F. and KIRK M.T. - "Influence of Elastic Modulus on the Lubrication of Point Contacts", Inst. Mech. Eng., 1963, Lubrication and Wear Convention, Paper 15.

48. CAMERON A. and GOHAR R. - "Theoretical and Experimental Studies of the Oil Film in Lubricated Point Contacts", Proc. Roy. Soc. (A), 1966, Vol. 291, pp. 520 - 536.

49. GOHAR R. and CAMERON A. - "The Mapping of Elastohydrodynamic Contacts", Trans. ASLE, 1967, Vol. 10, pp. 215 - 225.

50. ROBERTS A.D. and TABOR D. - "Short Communication; Fluid Film Lubrication of Rubber - An Interferometric Study", Wear, 1968, Vol. 11, pp. 163 - 166.

51. FOORD C.A., WEDEVEN L.D., WESTLAKE F.J., and CAMERON A. - "Optical Elastohydrodynamics", Proc. Inst. Mech. Eng., 1969-70, Vol. 184, Part 1, pp. 487 - 503.

52. GOHAR R. - "A Ball-and-Plate Machine for Measuring Elastohydrodynamic Oil Films", Proc. Inst. Mech. Eng., 1967 - 68, Vol. 182, Part 3G, pp. 43 - 45.

53. WYMER D. - Ph.D. Thesis, University of London, 1972, and "Elastohydrodynamic Lubrication of a Line Contact", Proc. Inst. Mech. Eng., 1974, Vol. 188, Paper 19/74, pp. 221 - 238.

54. WESTLAKE F.J. and CAMERON A. - "A Study of Ultra-Thin Lubricant Films using an Optical Technique", Proc. Inst. Mech. Eng., 1967 - 68, Vol. 182, Part 3G, pp. 75 - 78.

55. PEMBERTON J.C. - Ph.D. Thesis, University of London, 1976.

56. PAUL G.R. and CAMERON A. - "Time Dependence Viscosity Following a Pressure Rise Measured on an Impact Viscometer", Trans. ASLE, Vol. 19, No. 1, 1976, pp. 17-22.

57. WILLIS T. and SETH B. - "Gap Geometry Measurements in Oil-Filled Gaps using Laser Diffraction Techniques", 30th Annual Meeting of ASLE, Paper No. 75, AM-8A-1, 1975.

58. WILLIS T. and SETH B. - "Optical Measurement of Oil Film Thickness Between Rollers", ASME, Paper No. 76-LUB-10, 1976.

59. LEE D., SANBORN D.M. and WINER W.O. - "Some Observations of the Relationship Between Film Thickness and Load in High Hertz Pressure Sliding Elastohydrodynamic Contacts", Jnl. Lub. Tech., Trans. ASME, Vol. 95G, 1973, pp. 386 - 390.

60. HIGGINSON G.R. - "A Model Experiment in Elastohydrodynamic Lubrication", Int. J. Mech. Sci., 1962, Vol. 4, p. 205.

61. DOWSON D. and LONGFIELD M.D. - "An Elastohydrodynamic Lubrication Experiment", Nature, 1963, Vol. 197, p. 586.

62. DOWSON D. and LONGFIELD M.D. - "The Distribution of Pressure and Temperature in a Highly Loaded Lubricated Contact", Proc. Lub. and Wear Conv. (Bournemouth), 1963, Paper No. 3, pp. 27-33, (Inst. Mech. Eng.).

63. DOWSON D. and LONGFIELD M.D. - "The Lubrication of Rolls of Finite Width: An Investigation of Oil Film Characteristics", 3rd Annual Meeting of the Lub. and Wear Group (Cardiff), 1964, paper No. 7, (Inst. Mech. Eng.).

64. LONGFIELD M.D. - "Pressure Distributions in a Highly Loaded Lubricated Contact", Proc. Inst. Mech. Eng., 1965-66, Vol. 180, Part 3B, pp. 113-118.

65. NIEMANN G. and GARTNER F. - "Distribution of Hydrodynamic Pressure on Counterformal Line Contacts", Trans. ASLE, 1965, Vol. 8, No. 3, pp. 235 - 249.

66. ORCUTT F.K. - "Experimental Study of Elastohydrodynamic Lubrication", Trans. ASLE, 1965, Vol. 8, pp. 381-396.

67. KANNEL J.W. - "The Measurement of Pressure in Rolling Contacts", Proc. Inst. Mech. Eng., Vol. 180, Part 3B, 1966.

68. HAMILTON G.M. and MOORE S.L. - "A Modified Gauge for Investigating an Elastohydrodynamic Contact", Proc. Inst. Mech. Eng., 1967-68, Vol. 182, Part 3A, p. 251.

69. TURCHINA V., SANBORN D.M. and WINER W.O. - "Temperature Measurements in Sliding Elastohydrodynamic Point Contacts", ASME, Paper No. 73-LUB-23, 1973.

70. SMITH F.W. - "Lubricant Behaviour in Concentrated Contact Systems - The Castor Oil-Steel System", Wear, Vol. 2, 1958 - 59, pp. 250 - 263.

71. SMITH F.W. - Rep. Nat. Res. Labs. Ottowa, Canada, MP-17, 1960.

72. SMITH F.W. - "Effect of Temperature in Concentrated Contact Lubrication", Trans. ASLE, Vol. 5, No. 1, Apr. 1962, pp. 142 - 148.

73. SASAKI T., OKAMURA K., and ISOGAI R. - "Fundamental Research on Gear Lubrication", Bull. Jap. Soc. Mech. Eng., 1961, Vol. 4, pp. 382 - 394.

74. ROUVEROL W.S. and TANNER R.I. - "A Brief Examination of Factors Affecting Tractive Friction Coefficients of Spheres Rolling on Flat Plates", Trans. ASLE, Vol. 3, No. 1, Apr. 1960.

75. PLINT M.A. - "Some Recent Research on the Perbury Variable-Speed Gear", Elastohydrodynamic Lubrication, Proc. Inst. Mech. Eng., 1965 - 66, Vol. 180, Part 3B, p. 225.

76. PLINT M.A. - "Traction in Elastohydrodynamic Contacts", Proc. Inst. Mech. Eng., 1967 - 68, Vol. 182, Part 1, No. 14.

77. POON S.Y. and HAINES D.J. - "Frictional Behaviour of Lubricated Rolling Contact Elements", Proc. Inst. Mech. Eng., 1966-67, Vol. 181, Part 1, p. 363.

78. BELL J.C., KANNEL J.W. and ALLEN C.M. - "The Rheological Behaviour of the Lubricant in the Contact Zone of a Rolling Contact System", Trans. ASME, J. Basic Eng., Vol. 86, Part D, 1964, p. 423.

79. JEFFERIS J.A. and JOHNSON K.L. - "Sliding Friction Between Lubricated Rollers", Proc. Inst. Mech. Eng., 1967-68, Vol. 182, Part 1, No. 14, p. 281.

80. DOWSON D. and WHOMES T.L. - "Effect of Surface Quality upon the Traction Characteristics of Lubricated Cylindrical Contacts", Proc. Inst. Mech. Eng., 1967-68, Vol. 182, Part 1, No. 14, Paper 2.

81. JOHNSON K.L. and CAMERON R. - "Shear Behaviour of Elastohydrodynamic Oil Films at High Rolling Contact Pressures", Proc. Inst. Mech. Eng., 1967-68, Vol. 182, Part 1, No. 14, Paper 4.

82. JOHNSON K.L. and ROBERTS A.D. - "Observations of Viscoelastic Behaviour of an Elastohydrodynamic Lubricant Film", Proc. Roy. Soc. (A), Vol. 337, 1974, pp. 217-242.

83. POON S.Y. - "An Experimental Study of the Shear Traction Distribution in Rolling with Spin", Wear, Vol. 10, 1967, p. 61.

84. ADAMS D.R. and HIRST W. - "Friction Traction in Elastohydrodynamic Lubrication", Proc. Roy. Soc. (A), Vol. 332, 1973, pp. 505 - 525.

85. HIRST W. and MOORE A.J. - "Non-Newtonian Behaviour in Elastohydrodynamic Lubrication", Proc. Roy. Soc. (A), Vol. 337, 1974, pp. 101 - 121.

86. GENTLE C.R. - Ph.D. Thesis, Univ. of London, 1971.

87. GENTLE C.R. and CAMERON A. - "Some Granular Aspects of E.H.L. Traction", Wear, Vol. 27, 1974, pp. 71 - 81.

88. GENTLE C.R. and CAMERON A. - "An Investigation of Traction in Elastohydrodynamic Point Contacts Using Optical Interferometry", ASLE, Paper No. 74LC-A1-1, 1974.

89. CROOK A.W. - "The Lubrication of Rollers III. A Theoretical Discussion of Friction and Temperature in the Oil Film", Phil. Trans. Roy. Soc. (A), Vol. 254, 1961, pp. 237 - 258.

90. GRUBIN A.N. - "Contact Stresses in Toothed Gears and Worm Gears", Cen. Sci. Res. Inst. for Tech. and Mech. Eng., 1949, Book 30.

91. HINGLEY C.G. - Ph.D. Thesis, Univ. of London, 1964.

92. KANNEL J.W. and WALOWIT J.A. - "Simplified Analysis for Tractions Between Rolling Sliding EHD Contacts", Trans. ASME, Vol. 93, Series F, No. 1, 1971, pp. 39 - 46.

93. ARCHARD J.F. - "The Temperature of Rubbing Surfaces", Wear, Vol. 2, 1958, pp. 438 - 455.

94. CAMERON A. - "Hydrodynamic Lubrication of Rotating Discs in Pure Sliding - A New Type of Oil Film Formation", J. Inst. Pet., Vol. 37, 1951, p. 471.

95. CRAGOE C.S. - Miscellaneous Publications No. 97, U.S. Bureau of Standards.

96. DUCKWORTH R.R. - Ph.D. Thesis, Univ. of London, 1977.

97. EYRING H., REE T., and HIRAI N. - "Significant Structures in the Liquid State", Proc. Nat. Acad. Sci., Vol. 44, 1958, p. 683.

98. EYRING H. and JHON M.S. - "Significant Structures of Liquids", Wiley and Sons Inc., 1969.

99. BELL J.C. - "Lubrication of Rolling Surfaces by a Ree-Eyring Fluid", Trans. ASLE, Vol. 5, No. 1, Apr. 1962, pp. 160 - 171.

100. BELL J.C. and KANNEL J.W. - "Interpretations of the Thickness of Lubricant Films in Rolling Contacts. 2. Influence of Possible Rheological Factors", Trans. ASME, Jnl. Lub. Tech., Oct. 1971, pp. 485 - 497.

101. BARLOW A.J. and LAMB J. - "The Visco-Elastic Behaviour of Lubricating Oils under Cyclic Shearing Stress", Proc. Roy. Soc. (A), Vol. 253, 1959, pp. 52 - 69.

102. MILNE A.A. - "Theory of Rheodynamic Lubrication for a Maxwell Liquid", Proc. Conf. Lub. Wear, Inst. Mech. Eng., 1957, Paper 41, p. 66.

103. CROUCH R.F. and CAMERON A. - "Graphical Integration of the Maxwell Fluid Equation and its Application", Jnl. Inst. Petrol., Vol. 46, 1960, pp. 119 - 125.

104. DYSON A. - "Flow Properties of Mineral Oils in EHD Lubrication", Phil. Trans. Roy. Soc., 1965, Vol. 258, pp. 529 - 564.

105. OLDROYD J.G. - "Non-Newtonian Effects in Steady Motion of some Elastico-Viscous Liquids", Proc. Roy. Soc. (A), Vol. 245, 1958, p. 278.

106. TANNER R.I. - "Full Film Lubrication Theory for a Maxwell Fluid", Int. Jnl. Mech. Sci., Vol. 1, 1960, pp. 206 - 215.

107. DYSON A. - "Frictional Tractional and Lubricant Rheology in Elastohydrodynamic Lubrication", Phil. Trans. Roy. Soc. (A), Vol. 266, 1970, p. 1 - 33.

108. BARLOW A.J., ERGINSAV A., and LAMB J. - "Viscoelastic Relaxation of supercooled Liquids, II", Proc. Roy. Soc. (A), Vol. 298, pp. 481 - 494.

109. HUTTON J.F. - "Viscoelastic Relaxation Spectra of Lubricating Oils and Their Component Fractions", Proc. Roy. Soc. (A), Vol. 304, 1968, p. 65.

110. FEIN R.S. - "Possible Role of Compressional Viscoelasticity in Concentrated Contact Lubrication", Jnl. of Lub. Tech., Trans. ASME, Series F, Vol. 89, pp. 127 - 131.

111. HARRISON G. and TRACHMAN E.G. - "The Role of Compressional Viscoelasticity in the Lubrication of Rolling Contacts", Jnl. of Lub. Tech., Trans. ASME, Series F, Vol. 94, No. 4, 1972, pp. 306 - 312.

112. TRACHMAN E.G. - "The Short-Time Viscosity Behaviour of a Lubricant in a Hertzian Pressure Zone", ASME Paper No. 74-Lub-8, 1974.

113. TRACHMAN E.G. and CHENG H.S. - "Rheological Effects on Friction in Elastohydrodynamic Lubrication", NASA Report CR-2206, March 1973, p. 213.

CHAPTER 2

THE MECHANICAL SYSTEM

2.1 INTRODUCTION

The basic design criterion of the apparatus was the application of the technique of optical interferometry in a study of the lubrication of an EHD line contact under traction conditions. It was decided that a four roller configuration should be used in order to give a stable three-point loading system (Fig. 2.1).

The central roller was chosen as the optical member of the system, the transparent material being sapphire. This was selected in order to achieve realistically high loads (and hence Hertzian pressures) as the compressive strength of sapphire at 2 GN/m^2 (290,000 p.s.i.) is approximately three times that of glass. For certain preliminary traction tests this central sapphire roller was replaced by one made from steel. The shaft that was attached to the central roller will often be referred to as the output shaft.

Means were provided to control the temperature of the oil, the load on the rollers and also the amount of sliding between the outer rollers and the sapphire roller, together with the resulting traction force. To obtain accurate measurement of traction, strain gauges were mounted on a coupling connected to the central roller via two universal joints.

2.2 ADVANTAGES OF A FOUR ROLLER HYDROSTATIC SYSTEM

The advantages of such a system can ~~be~~ most easily be shown by outlining the problems associated with other possible systems.

2.2.1 The Two Roller System

In a two roller system it is difficult to ensure that full alignment is maintained i.e. that the rollers are square to each other. They must not skew, nor run at an angle (Fig. 2.2). These restrictions are critical as a small misalignment can invalidate the results. Case (a) would give an elliptical contact with oil shear perpendicular to the direction of rolling; whereas case (b) would give an uneven pressure loading in the EHD contact, thus making it impossible to draw any conclusions about the effect of load (and hence Hertzian pressure) on the film thickness under traction conditions.

No mechanical two roller system yet advanced has completely overcome the alignment problems. The most successful rig to date is the Caterpillar device (1) which uses crowned rollers. Unfortunately a crowned sapphire roller would not be suitable for optical interferometry, as the lens effect from looking through the sapphire would be extremely difficult to correct; this gives an overriding disadvantage. Moreover this system would give an elongated elliptical contact and not a line contact, though an ellipse of about 10 : 1 major : minor axis ratio can be treated as a line with acceptable accuracy.

There is also the problem of high shear forces on the shafts which are attached to the rollers. As it must be possible to view through the sapphire the shaft cannot project into the sapphire but must be attached to one of the flat faces. In a conventional disc machine the rollers are loaded together via their shafts, giving rise to high shear stresses at the interface between roller and shaft (Fig. 2.3). No

known method of bonding sapphire to steel (or any other suitable material) can withstand stresses of this magnitude and it would be prohibitively expensive to make the whole assembly out of sapphire itself.

This problem of shear stress could be eliminated by using back-up rollers (Fig. 2.4). However these would tend to obstruct the optical path through the sapphire roller, and they would each have to be accurately aligned with the working rollers.

2.2.2 The Three Roller System

The three roller system (Fig. 2.5) has two major disadvantages: the first is that the central roller would tend to be squeezed sideways when the load was applied and secondly the optical path through the central (sapphire) roller is completely obstructed. (If one of the outer rollers was the transparent member of the system the problem of bonding the sapphire to the shaft would then be present, as for the two roller system).

These problems would be extremely difficult, if not impossible, to overcome.

The four roller system perfectly locates and supports the central roller, so eliminating high shear stresses at the interface between the sapphire roller and its shaft. It also permits a clear optical path.

An increase in the number of rollers over four does not give any added advantage and only tends to restrict the working area. Thus the four roller system is the optimum choice.

Having adopted the four roller system, it was decided that a self-aligning system of supporting the three outer rollers was needed. Rolling element bearings were considered but necessitated a complex system with very tight manufacturing tolerances. Hydrostatic bearings were chosen because their basic configuration is simple, they are sufficiently self-aligning, and, by proper design, they can be made to act as a loading system as well.

2.3 THE HYDROSTATIC BEARINGS AND LOADING SYSTEM

The hydrostatic bearings consisted of hard steel rings mounted on steel spigots onto which were shrunk phosphor bronze sleeves (Figs. 2.6 and 2.7). These rings acted as the outer (driven) discs and will often be referred to as such.

Phosphor bronze sleeves were chosen as this material has good "embedability" (i.e. any hard foreign matter can embed itself into the surface rather than cause scoring) and being relatively soft the risk of damage to the steel rings in case of malfunction of the apparatus is reduced.

High pressure oil was fed to the hydrostatic recess via internal drillings. This pressure gradually decays as the oil spreads outwards from the hydrostatic recess until it eventually reaches ambient pressure at the edges of the bearing surface. Hence by machining pressure relieving sides in the sleeve it was arranged that the oil pressure acted on just under half the ring circumference and so gave a nett thrust in one direction. This thrust constituted the applied load between the discs and it was ensured that its resultant direction acted through the centre of the sapphire disc. The pressure relieving sides did not significantly affect the

stability of the bearing and consequently the ring was accurately supported and located.

In order to keep the oil flow rate through the hydrostatic bearing down to a reasonable level the radial clearance between the ring and the sleeve was designed to be 0.0254 mm (.001 in.). This was thought to be the lowest practicable value as a smaller clearance would make the machining of the components unnecessarily difficult. However this clearance would undoubtedly lead to a large hydrodynamic effect at the spigot face opposite the hydrostatic recess. To avoid this unwanted effect the surface of the phosphor bronze sleeve was machined at the back such that its radius was reduced by approximately 0.254 mm (.010 in.) i.e. the gap was increased by 0.254 mm , a figure which was found to be suitable by MacPHERSON (2).

In addition a small annular undercut was machined in the phosphor bronze sleeve, this allowed low pressure oil at the exit from the main bearing area to leak between the sleeve and the inner face of the ring. This gave a slight hydrostatic thrust bearing effect at this point which reduced the risk of metal to metal contact and hence surface damage.

Each ring was made of an EN30B steel and had a Vickers Hardness of 330. It had dimensions of 50.8 mm (2.0 in.) outside diameter, 34.9 mm (1.375 in.) inside diameter, and a face width of 20.6 mm (0.812 in.). This face was chamfered to give an offset track width of 9.5 mm (0.375 in.). As the ring overhung the spigot by 1.6 mm (0.062 in.) for clearance purposes, this offset track was arranged to be exactly in line with the hydrostatic bearing recess and hence give an even loading. The central sapphire disc had a dia-

meter of 25.4 mm (1.0 in.) and a face width of 12.7 mm (0.5 in.). By making the face width of the sapphire disc greater than the track width of the outer rings it was ensured that the edge conditions of the elastohydrodynamic contact would be visible.

The spigots were then mounted in a faceplate (Fig. 2.7) which was accurately bored so that the spigots were square to this plate. At this point the sapphire disc had not been ordered as it had been realised that it would be extremely difficult to ensure that the correct clearance was achieved between the steel rings and the spigot. (This clearance depended on the sizes of the steel rings, the sapphire disc and the location of the spigot centres). Instead the spigot centres were located such that a disc of approximately 25 mm (1.0 in.) diameter would just fit between the rings when the unit was assembled. The actual diameter of the disc that just fitted was then measured and found to be 25.44 mm (1.0015 in.). As a clearance of 0.0254 mm (0.001 in.) was required between each steel ring and the working face of the spigot, a sapphire disc of 25.39 mm (0.9995 in.) diameter was ordered. This method of ensuring the correct clearance was much easier than trying to accurately locate the spigot centres.

The basic choice of dimensions of the rings and disc was not critical but was influenced by the following factors:-

(1) A Hertzian pressure of approximately 1.38 GN/m^2 (200,000 p.s.i.) was required. This gives a safety factor of about 1.5 on the compressive strength of sapphire at approximately 2.0 GN/m^2 (290,000 p.s.i.).

(2) The hydrostatic oil pressure should preferably not exceed 20.7 MN/m^2 (3,000 p.s.i.) so that hydraulic equipment would be readily available.

(3) There must be sufficient room to allow the close approach of a microscope.

(4) The diameter of the sapphire should not be too large as this increases the working distance requirements of the microscope, and also costs a lot.

These conditions have been fulfilled in the present system. Using the Hertz equations

$$p_{Hz} = \frac{2.W}{\pi L a} \tag{2.1}$$

$$a = \left(\left(\frac{1-\nu_1^2}{E_1} + \frac{1-\nu_2^2}{E_2} \right) \frac{4}{\pi} \cdot \frac{W.R}{L} \right)^{1/2} \tag{2.2}$$

where p_{Hz} = maximum Hertzian pressure,

W = load,

L = contact length

a = half contact width

ν = Poisson's ratio,

E = Young's Modulus,

R = reduced radius $= \frac{R_1 R_2}{R_1 + R_2}$,

(subscripts 1, 2 denote the two contact materials) and a manual on hydrostatic bearings (3) it was calculated that 1.38 GN/m^2 (200,000 p.s.i.) maximum Hertz pressure could be obtained with a hydrostatic bearing pressure of approximately 8.62 MN/m^2 (1250 p.s.i.). Moreover 25.4 mm (1.0 in.) sapphire is optically equivalent to approximately 14.2 mm (0.56 in.) in air which meant that commercially available

microscope objectives (which can operate with working distances in excess of this figure) could be utilised.

The hydraulic system is shown schematically in Fig. 2.8. The oil supply to each bearing was part of a recirculating system capable of giving approximately 2.27 x 10^{-4} m^3/s (3.0 gall./min.) at a maximum pressure of 20.7 MN/m^2 (3,000 p.s.i.). Initial calculations for the expected flow rate of a 0.01 Ns/m^2 (0.1 poise) viscosity oil had produced a figure of 7.57 x 10^{-5} m^3/s (1.0 gall./min.) at 10.3 MN/m^2 (1500 p.s.i.) for the whole system. This meant that the majority of the oil flow would be directed via a pressure relief valve through an oil cooler and back to the oil reservoir. The pressure of the oil supply to the hydrostatic bearings was regulated by an in-line pressure control valve immediately after the pressure relief valve.

The bearing oil supply then passed through an oil filter with a 5 μm (197 μin.) mesh and into a manifold from which were taken three separate lines to flow control valves and finally to the hydrostatic bearings themselves. Flow control valves were the most convenient form of restrictors for the bearings as they could be adjusted to suit the different operating conditions which would arise when the hydrostatic bearing pressure was changed, (the load was varied by altering this pressure); they also allowed for an actual performance different from that predicted due to construction tolerances. For a discussion on the need for and usage of restrictors see reference (3).

After the oil had passed through the bearings it collected in the working chamber and by suitably arranging the level of an overflow pipe it was ensured that the central disc

would remain fully flooded with lubricant. This oil then passed into a header tank which constituted the suction reservoir for the pump. The tank was located a sufficient height above the pump inlet to ensure that a positive pressure was maintained on the inlet, thus avoiding cavitation problems in the pump.

When this system was operational it was discovered that the pump was not able to supply more than about 11.0 MN/m^2 (1600 p.s.i.) at the higher temperatures used in the experiment. This was attributed to two factors. The first was that the rings tended to run in and after a short time the gap between the hydrostatic bearings and the rings had increased to approximately 0.0381 mm (0.0015 in.); the second was that there was considerable "slippage" in the gear pump for the lower viscosity (higher temperature) fluid thus decreasing its efficiency. These two factors meant that the maximum pressure of the pump of 20.7 MN/m^2 (3,000 p.s.i.) could not be utilised. It was thought that this problem could be alleviated by decreasing the clearance between the bearings and the rings, but this would mean new rings or a new sapphire disc, both of which would have been costly and time consuming. Therefore, as calculations had shown that a maximum Hertzian pressure of 1.5 GN/m^2 (217,000 p.s.i.) could be obtained with 10.3 MN/m^2 (1,500 p.s.i.) oil pressure from the pump, this modification was not attempted.

2.4 THE BRAKE AND DRIVE SYSTEM

"Dynadrive" motors were chosen for both the drive and brake. The "Dynadrive" system consisted of an A.C. motor continuously running at full speed which provided drive to the

output via an induction coupling device. The selected speed was stabilised by an electronic tachometer feedback circuit which controlled the induction coupling and provided a torque sufficient to maintain the speed desired. Hence if the speed was below that selected, a torque was provided to increase it to the required value. However if the speed was above that selected, no torque was applied and the speed dropped only from frictional losses.

This mode of operation was correct for the drive motor but was obviously unsuitable for the brake motor. Fortunately it was found that a relatively simple modification enabled the motor to act as a brake. The signal from the tachometer feedback was altered such that the torque would only be provided if the speed was above that selected. Obviously this required the rotation of the A.C. motor to oppose the rotation of the brake shaft, otherwise the brake section would try to run at full speed in the direction of rotation of the brake shaft. This was easily achieved by interchanging two of the 3-phase supply lines.

The mode of operation was such that if the speed was above that selected, a torque was provided to decrease it to the desired value; whereas if the speed was below that selected no torque was applied, i.e. there was no braking until the output shaft was driven at the "braking" speed.

By using this type of system the slip between the outer rings and the central disc, and the rolling speed could be set to desired values which would remain steady under varying conditions. In practice there was a slight variation when the load was altered by a large amount,but this was easily corrected. Also there was some drift of the speed

settings as the rig got hotter. This increase in temperature affected many of the electronic components in the motor controller and it was for this reason that the settings needed occasional readjustment.

However this method of braking was preferable to other possible systems as can be seen in Fig. 2.9. For gear braking the slip between the driving and driven members is maintained constant, the value depending on the gear ratios chosen. (The two sets of discs are both driven by the same motor but their speeds are altered by changing the gear ratio between the motor and each set). This method has the disadvantage that the slip speeds are not easily changed and in practice are usually limited in choice. This was not considered desirable for this experiment as it was anticipated that the rig would need to be as flexible in its settings as possible.

Another method is to use a friction disc brake. Unfortunately this has two distinct drawbacks, the first being that the brake would tend to suffer from fade and hence would be difficult to keep constant. The second drawback is that at certain points on a typical traction slip speed curve this method of braking would be unstable. This can be seen by considering operationg point B in Fig. 2.9. If the slip speed increases the driving traction decreases. As the braking force is now greater than the driving force the slip speed continues to increase and eventually the system stalls (i.e. the driven disc stops completely). On the other hand, if the slip speed falls the driving traction increases, and so the slip speed falls even more until the stable operating point A is reached. Therefore it is impossible to investigate

the falling part of the traction curve using this method of braking.

The system that was chosen for the current apparatus suffered from neither of these faults. The speed range was zero to 2,200 r.p.m. (giving a maximum disc velocity of 2.93 m/s (115 in./s.) for the present configuration) and the rated maximum torque (which was available at all speeds) 16.3 Nm (12.0 ft. lbf.). This torque could be exceeded for short periods but care had to be taken to avoid overheating in the motor/induction coupling device.

As the outer (driving) discs were twice the diameter of the central (driven) disc, this central disc rotated at twice the angular velocity of the outer discs. To compensate for this the drive motor was geared down by a factor of two. This was done using a toothed flexible timing belt and matching pulleys to drive a separate lay shaft at half the motor speed. This shaft carried three timing belt pulleys which in turn drove the three input shafts of the machine, again via suitable flexible belts. (Figs. 2.10 and 2.11). Each of these input shafts was connected to a corresponding outer ring by a form of Oldham coupling which incorporated shear pins (Figs. 2.12 and 2.13). This coupling served the dual purpose of allowing for any small misalignment of the shaft and the centre of its corresponding ring, and protecting the apparatus in case of sudden seizure. The shear pins were made from 1.59 mm (0.063 ins.) diameter sintered bronze welding rods. Simple shear tests had shown that these pins should shear at approximately twice the rated torque of the apparatus.

The central driven disc, which was bonded to a steel

shaft with adhesive (see Chapter 4), was connected to a separate lay shaft via two Hooke's joints and a torque measuring device (Fig. 2.14).

These joints allowed for any axial and angular misalignment of the driven shaft and its lay-shaft. This lay-shaft was then connected to the brake motor using a flexible timing belt and pulleys as before, however unlike the drive section there was no gearing effect present.

2.5 TORQUE MEASUREMENT

The torque on the central disc was measured by the device mentioned in the previous section. This consisted of a blade held in a boss which mated with slots in a cup-like receptacle (Fig. 2.15). The torque transmitted from the boss to the cup-like receptacle caused the blade to deflect. Under normal operating conditions this deflection would be small and insufficient to cause damage to the blade, however in the case of a possible seizing of the apparatus whilst running this might not have been the case. To avoid any damage to this blade the boss was machined such that stops prevented excess movement.

A matched set of four strain gauges of 120 ohms resistance were mounted on the blade to form a resistance bridge (Fig. 2.16). Any applied torque to the device caused a strain in the blade. This strain could be detected in the form of a change in potential difference across two opposite corners of this bridge if a voltage was applied to the other two corners. By suitably calibrating this change in potential difference the torque could be calculated. It was confirmed that temperature effects on this calibration were negligible

for the range covered in the experiments.

The voltage applied to the strain gauge bridge was 4½ volts which was supplied by a stabilised power pack, and the output from the bridge was monitored on either a milli-voltmeter or one channel of an x-y plotter. Facility was provided for balancing this resistance bridge before operation.

2.6 SPEED MEASUREMENT

The speeds of both the driving and driven shafts were measured using a digital counter. A small spur gear with one hundred teeth was mounted on one of the three main input shafts, whilst a similar gear was mounted on the layshaft which held the torque measuring device. A magnetic transducer was mounted near each gear with its tip as close to the circumferential tooth crests as possible. As the shaft plus the gear rotated, small voltage pulses were produced in the transducer as the gear tooth crests passed. These voltage pulses were fed into a digital counter. By selecting a suitable time base for the pulse count it was possible to obtain a direct read-out of speed. The same digital counter was used for both the driving and driven shafts thus it was not possible to obtain both speeds at exactly the same instant. However it required only a few seconds to select and read one channel after the first had been read, and so it was thought that no appreciable change in speed would have occurred in this time and that the values obtained would be valid.

The magnitude of these pulses was proportional to the rotational speed of the toothed gear wheel, hence at low speeds the signal from the transducer was insufficient to trigger the digital counter. For the model of digital

counter used for the experiment the minimum voltage was quoted as 100 millivolts. By tracing the voltage pulses on an oscilloscope this threshold voltage was found to be reached at a speed of approximately 65 r.p.m. for the input shaft. It was confirmed that a steady reading on the digital counter was obtained at this speed. The lowest speed used in the experiment was well above this value and so the reading on the digital counter could be taken with confidence for all the test conditions.

A secondary form of speed measurement was used for the output (driven) shaft. A tacho-generator giving a D.C. voltage output of 7v/1,000 r.p.m. was driven by a gear which meshed with the gear used for the magnetic transducer. Thus a D.C. voltage was obtained which was directly proportional to the output speed of the apparatus. By feeding this voltage signal into one channel of an x-y plotter and the output from the torque measuring device into the other channel, a direct plot of torque versus output speed could be obtained.

2.7 TEMPERATURE CONTROL AND MEASUREMENT

It was not possible to effect a great deal of control over the temperature, it was necessary to wait until the required temperature was attained. Some slight control could be obtained, however, by varying the water supply to the oil cooler. There was a large amount of heat injected into the oil from the oil pump and this caused the oil temperature to rise steadily. However, for the majority of the operating conditions the larger proportion of the flow was by-passed back to the oil reservoir through the pressure relief valve. This flow, which was at a low pressure, was passed through an oil

cooler; the cooling medium being water. The bulk temperature of the oil in the reservoir could thus be controlled by varying the supply of water to this oil cooler. (Additional cooling was also obtained from natural convection currents). The temperature of the oil in the reservoir was monitored using a thermocouple.

The remainder of the oil flow from the pump (which passed through the hydrostatic bearings) had not passed through an oil cooler and thus was at a higher temperature than the oil reservoir. This meant that the working area enclosing the discs was always slightly hotter than the bulk of the oil. The skin temperature on the surface of the discs is the important value in determining EHD film thickness, and so the temperature of the sapphire disc and one of the steel rings was monitored using trailing thermocouples. The thermocouples were placed such that the beads were as close as possible to the inlet of the contact being viewed optically. The trailing thermocouple has been shown to be capable of giving accurate readings of inlet temperature by O'DONOGHUE and CAMERON (4), however it must be ensured that no frictional heating is present between the bead of the thermocouple and the moving surface. In the case of the thermocouple on the sapphire this was achieved by moving the thermocouple very gradually towards the sapphire whilst the rig was running in the pure rolling mode, until a temperature rise was detected. As the temperature of the disc was similar to the temperature of the oil in the working area,this temperature rise could only be due to frictional heating. The thermocouple was then backed off slightly and the rig speed was varied. Any further frictional heating would have caused a temperature change as this

heating is proportional to speed; it was ensured that no temperature change was present.

In the case of the thermocouple on the steel disc a slightly different method was employed. As the steel ring was electrically conducting an Avo-meter was connected between the steel ring (via the main bulk of the apparatus) and the thermocouple. The thermocouple was moved towards the ring until electrical contact was just made. The speed of the rig was again varied to check for frictional heating; no temperature change was detected.

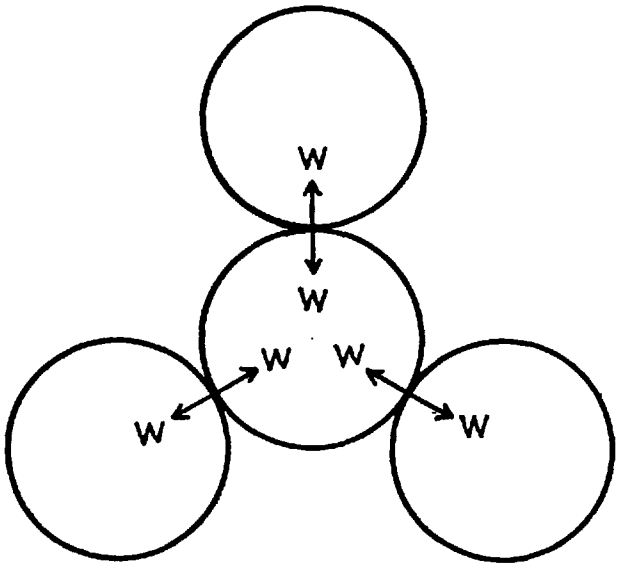

FIG. 2.1. THE FOUR DISC CONFIGURATION

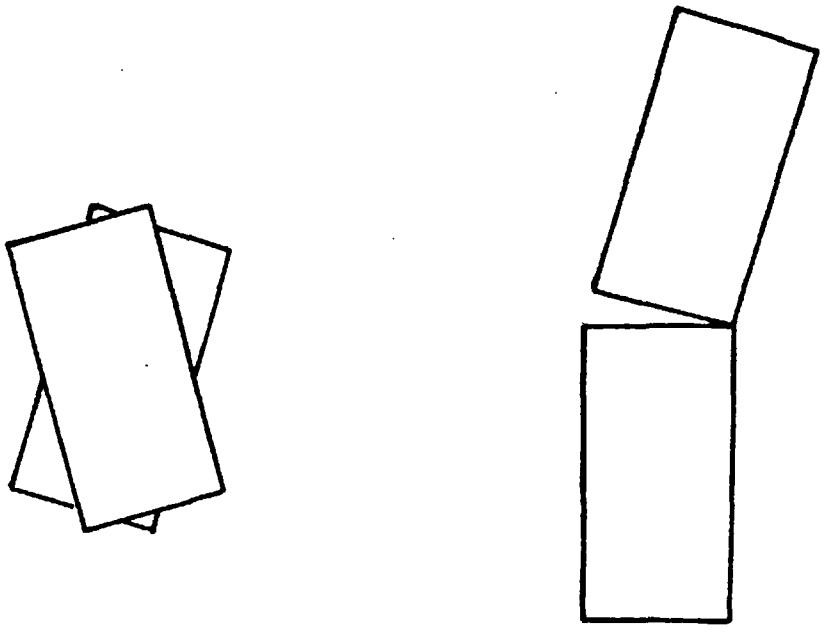

(a) EXAGGERATED SKEW CONDITIONS

(b) EXAGGERATED AXIAL MISALIGNMENT

FIG. 2.2. POSSIBLE ALIGNMENT PROBLEMS

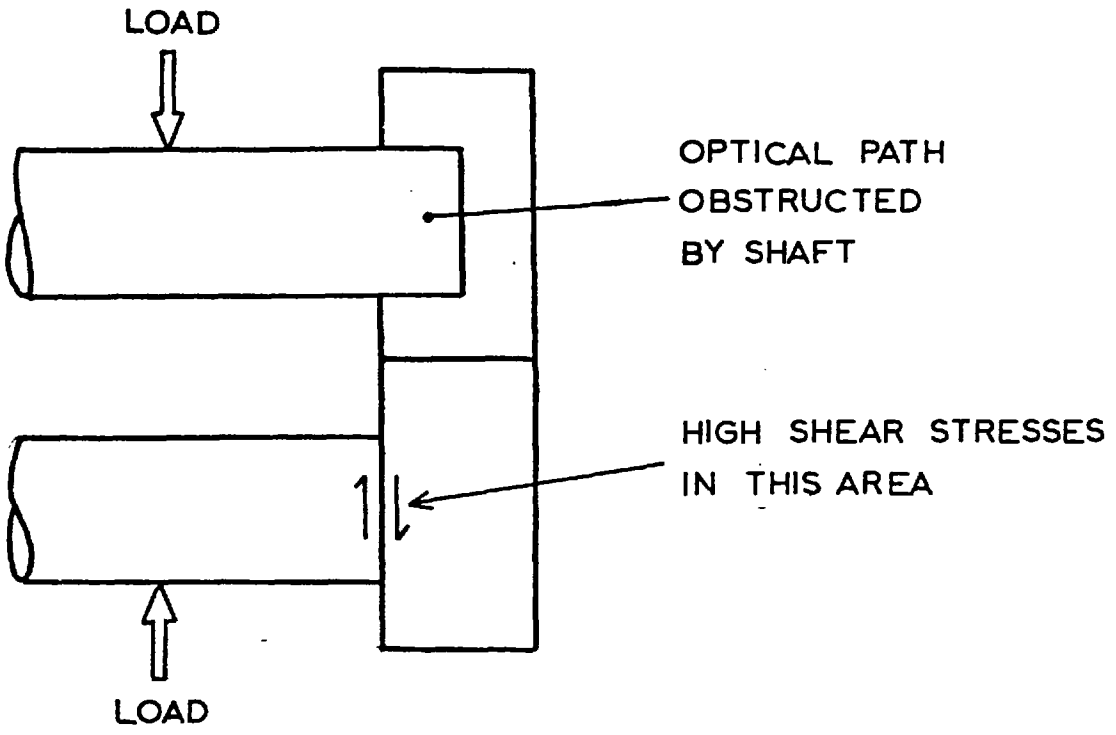

FIG. 2.3. PROBLEMS WITH THE ATTATCHMENT OF THE TRANSPARENT DISC TO ITS SHAFT

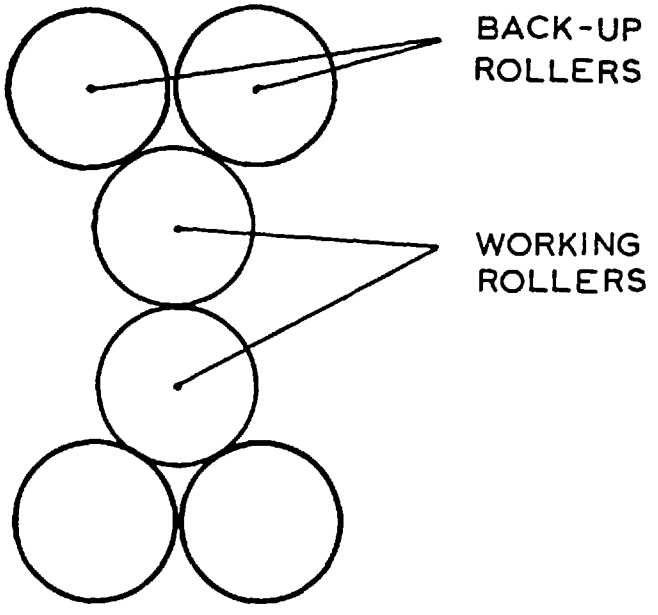

FIG. 2.4. THE BACK-UP ROLLER SYSTEM

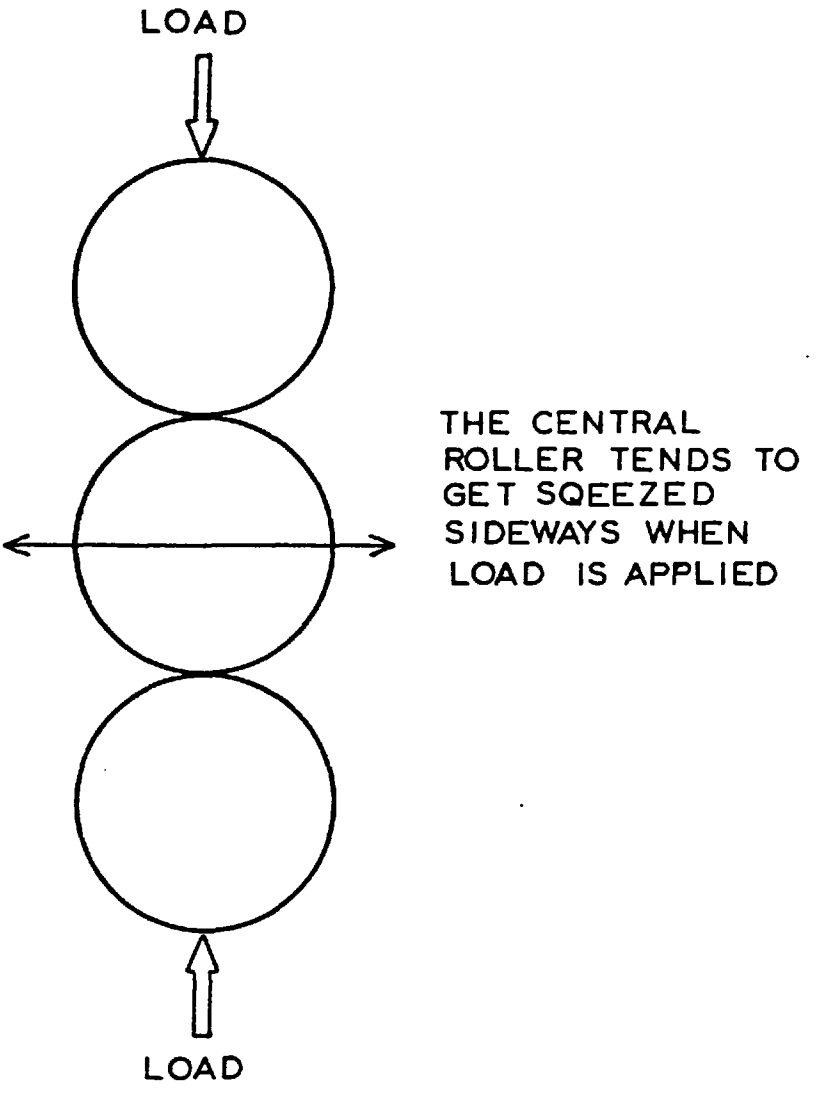

FIG. 2.5. THE THREE ROLLER SYSTEM

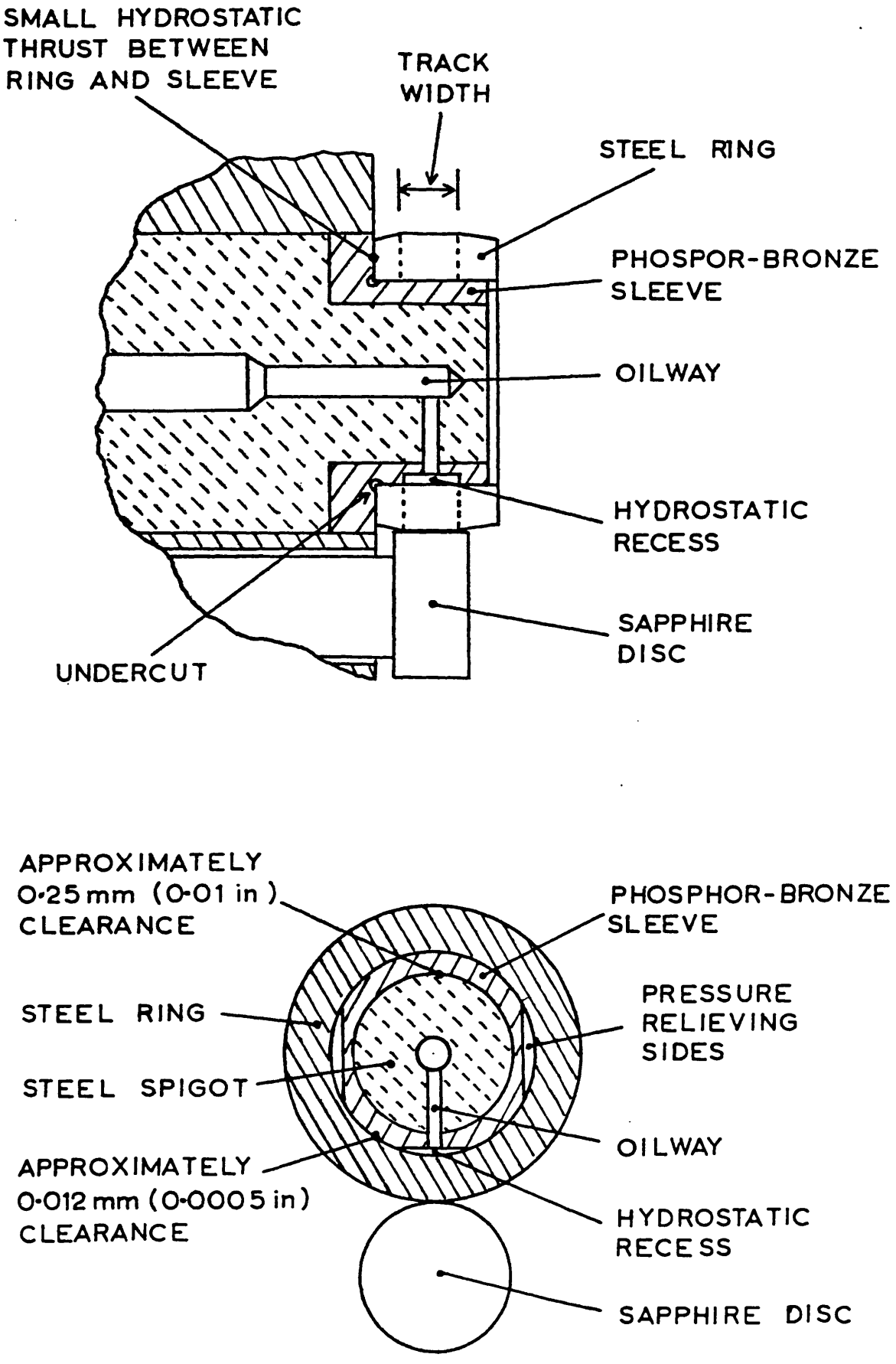

FIG. 2.6. CUTAWAY OF THE HYDROSTATIC BEARINGS

FIG. 2.7. THE HYDROSTATIC BEARINGS

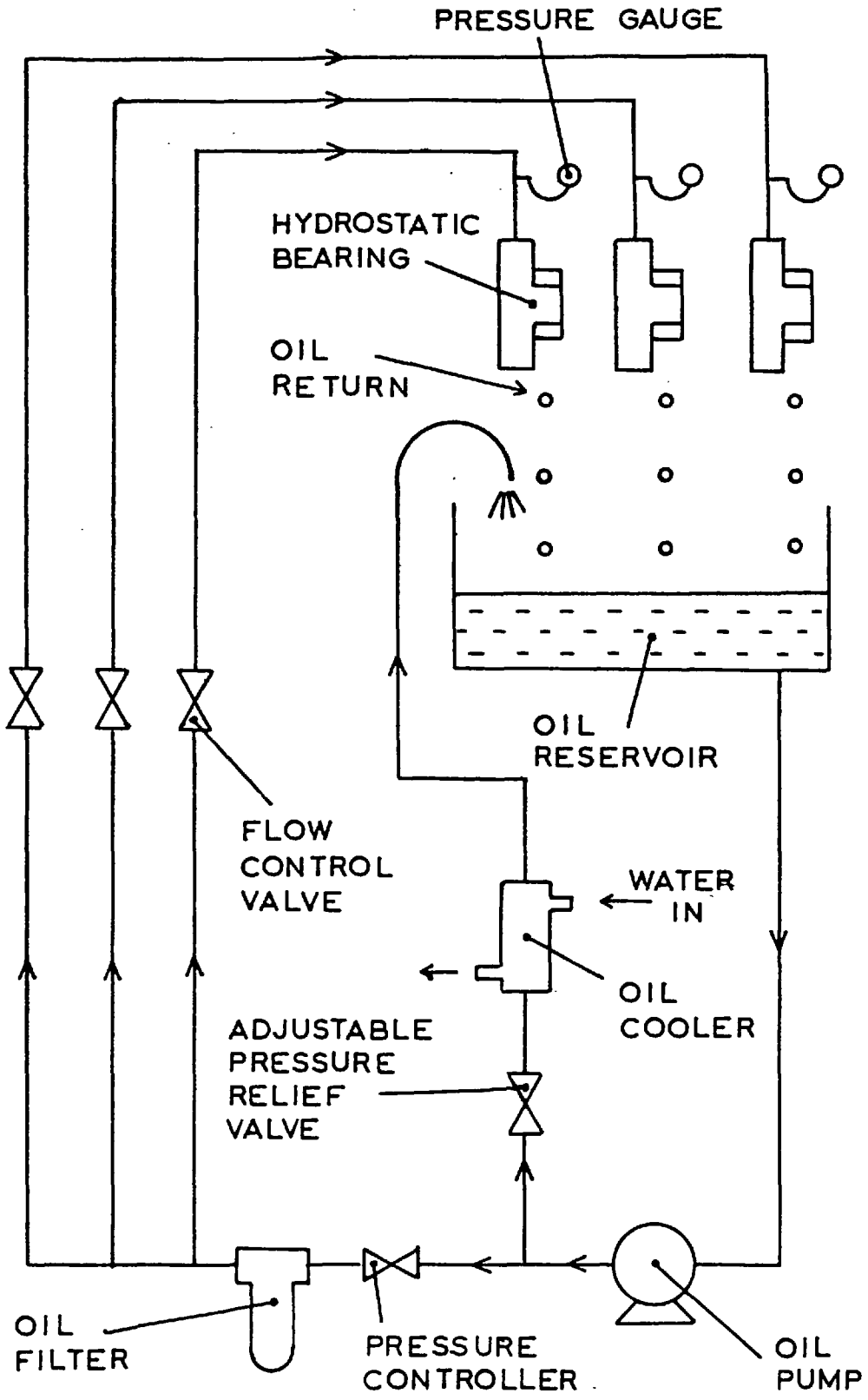

FIG. 2.8. THE HYDRAULIC CIRCUIT FOR THE HYDROSTATIC BEARINGS

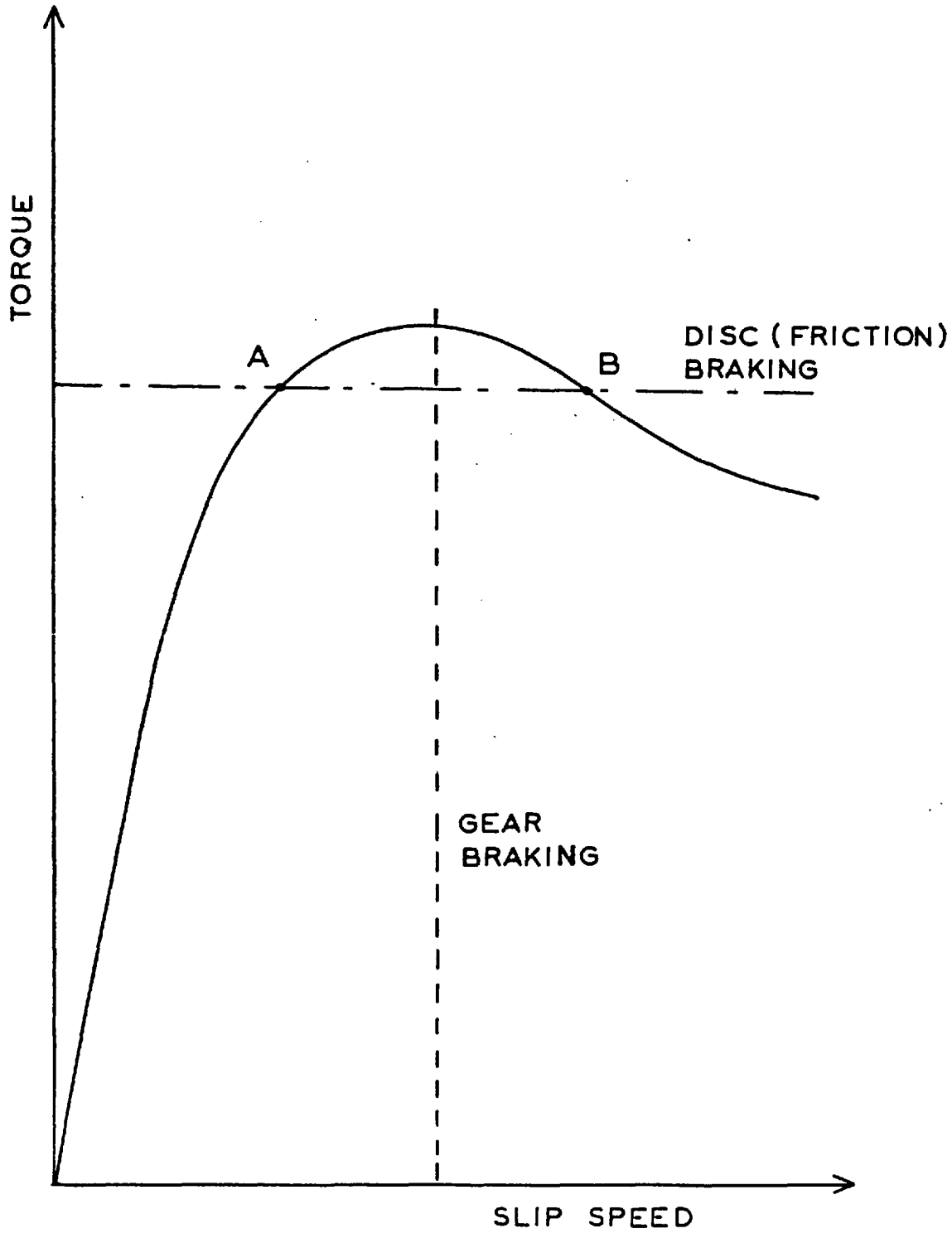

FIG. 2.9. THE EFFECT OF TRACTION RESPONSE ON GEAR AND DISC BRAKING

FIG. 2.10. THE DRIVE MOTOR AND LAYSHAFT

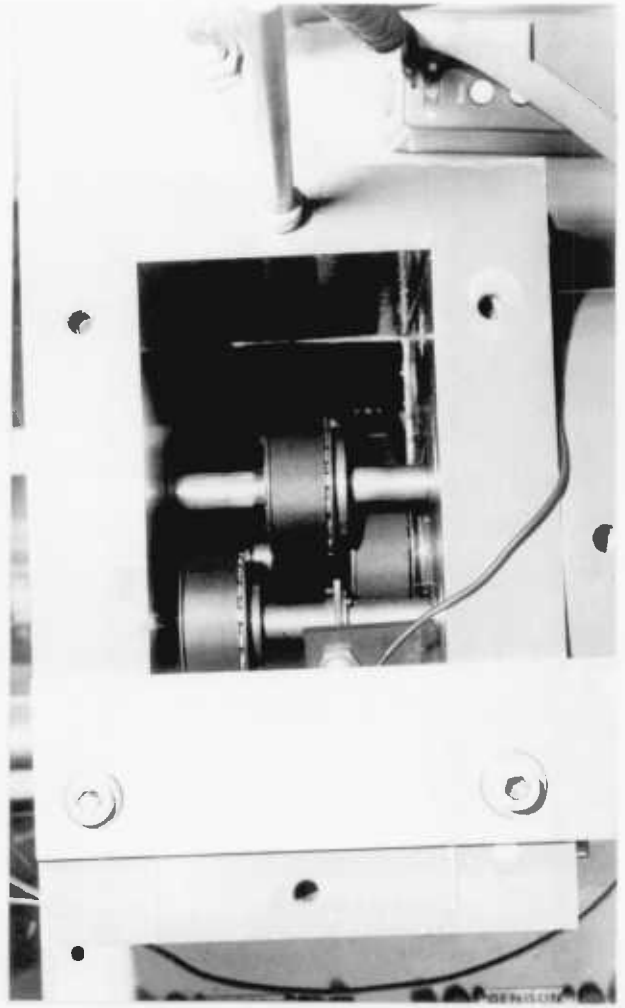

FIG. 2.11. THE THREE INPUT SHAFTS

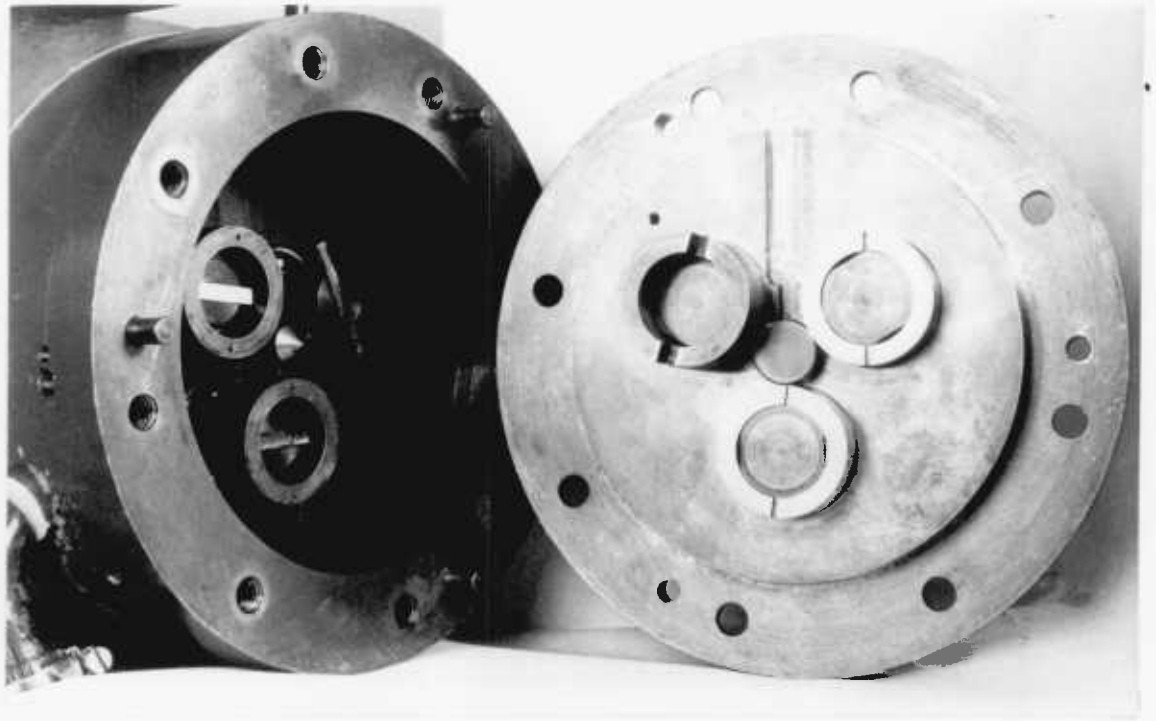

FIG. 2.12. THE WORKING AREA

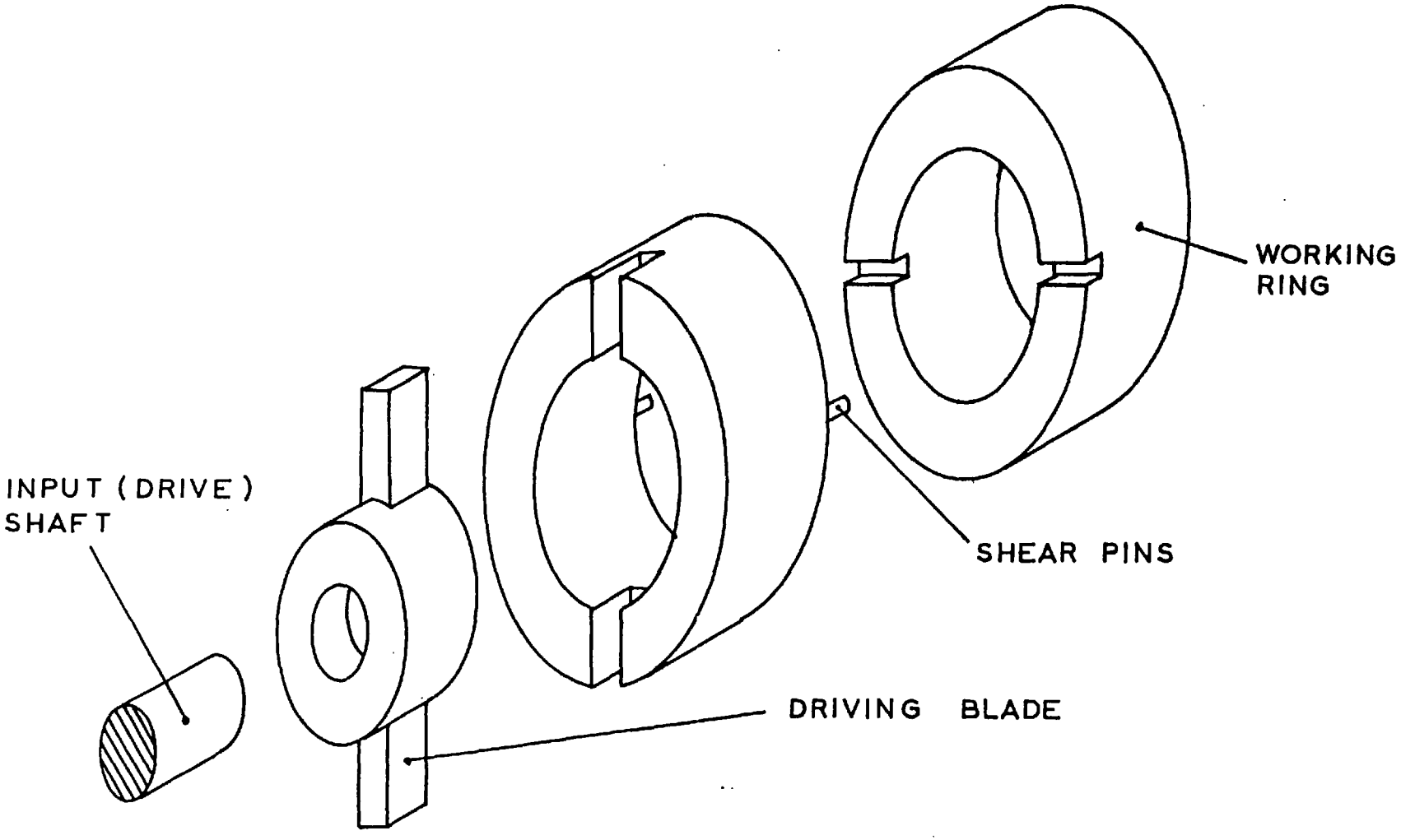

FIG. 2.13. THE OLDHAM COUPLING AND SHEAR PINS

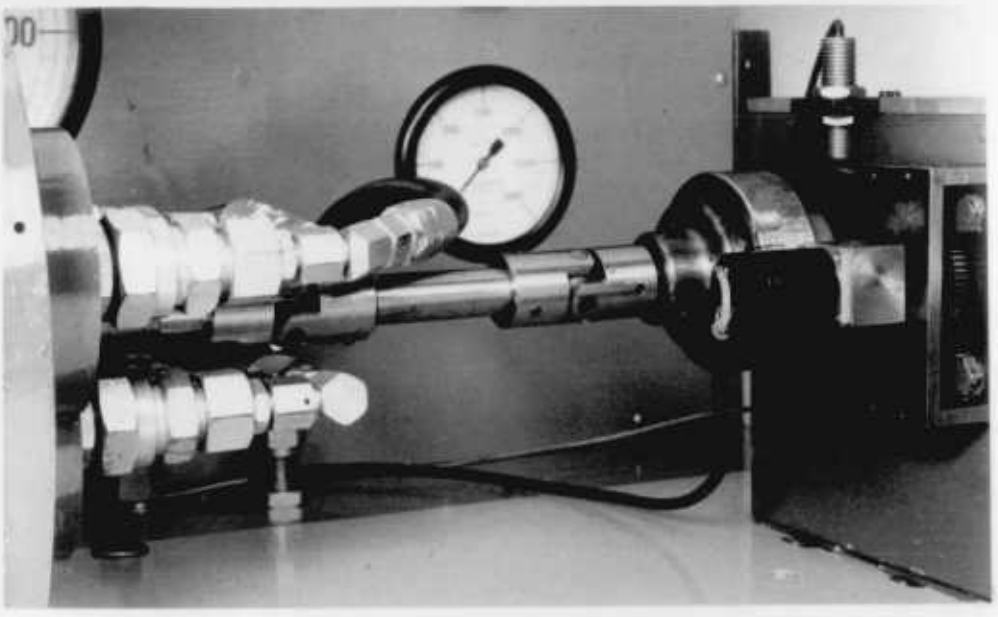

FIG. 2.14. THE OUTPUT SECTION

FIG. 2.15. THE TORQUE MEASURING DEVICE

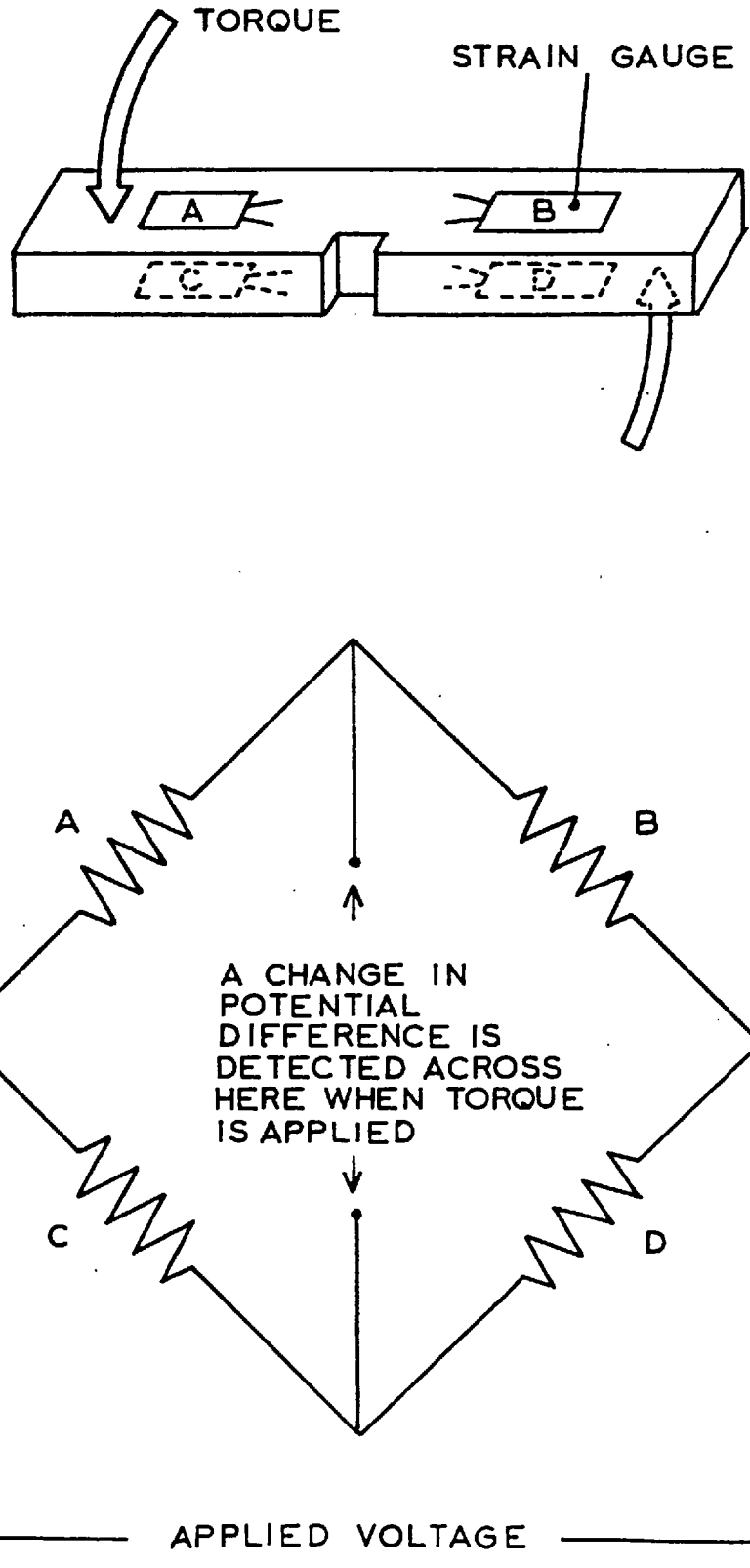

FIG. 2.16. THE TORQUE BLADE AND STRAIN GAUGE BRIDGE

CHAPTER 2 - REFERENCES

1. BENEDICT G.H. and KELLEY B.W. - "Instantaneous Coefficients of Gear Tooth Friction", Trans. ASLE, Vol. 4, 1961, pp. 59 - 70.
2. MacPHERSON P.B. - Ph.D. Thesis, University of London, 1972.
3. CAST BRONZE HYDROSTATIC BEARING DESIGN MANUAL - Prepared by Harry C. Rippel, Published by the Cast Bronze Bearing Institute, Inc., Cleveland, Ohio.
4. O'DONOGHUE J.P. and CAMERON A. - "Friction and Temperature in Rolling Sliding Contacts", Trans. ASLE, Vol. 9, 1966, pp. 186 - 194.

CHAPTER 3

THE OPTICAL SYSTEM

3.1 INTRODUCTION

The use of optical interferometry as a method of evaluating film thickness has been developed to a fine art in recent years. The pioneering work of CAMERON and GOHAR (1) has been improved and refined to a point where there are several specialised systems available to suit a wide range of measurements required. These techniques are described fully by FOORD, WEDEVEN, WESTLAKE and CAMERON (2) and range from some sophistications of the original method to the use of spacer layers and of stroboscopic illumination.

In the present work the requirements were for a system capable of measuring EHD lubricant film thicknesses from 0.1 μm to 0.75 μm (3.94 μin. to 29.5 μin.), approximately equivalent to optical film thicknesses of 0.15 μm to 1.1 μm (5.91 μin. to 43.3 μin.). This system had to be capable of being illuminated by an extermally triggered stroboscopic system. (This is also an essential requirement in order to take photomicrographs). As a high sensitivity of film thickness measurement was required a "white light" or chromatic interferometric system was designed and used.

For the loads and slip speeds envisaged for the experiment it was necessary to use a transparent material of high strength and an optical coating of good durability. Sapphire was chosen as the transparent material even though it had the undesirable optical property of birefringence (sapphire has a slightly different refractive index along one axis, the c-axis, compared with an axis at right angles to the

first); however this problem was circumvented quite easily in the event. The technique of sputtering was used to deposit a thin semi-reflecting optical coating onto the surface. This gives a good bond strength between the coating and substrate, with corresponding long life when compared against the more conventional vacuum deposition method.

3.2 THE BASIC INTERFEROMETRIC SYSTEM

A detailed account of the principles of interferometry may be found in many optical textbooks; TOLANSKY (3) is a very good example. In the present arrangement the situation is similar to that depicted in Fig. 3.1, although this has been simplified to a large extent.

A beam of light incident upon the contact between two lubricated elements is split into two parts by the semi-reflecting optical layer deposited on the sapphire. One part is reflected from this layer while the other passes through this and the oil to be reflected at the surface of the disc, and hence to re-enter the sapphire. These two parts of the beam then recombine in the sapphire and can be observed using a microscope.

As light has a waveform these two light beams interfere with each other and the resultant is determined by their relative amplitudes and phase angles. If the two beams are in phase they reinforce each other, whereas if they are of equal magnitude but opposite phase they can completely cancel each other out. This gives the familiar fringe pattern associated with interferometry.

The amplitudes are determined by the relative reflectivities, absorptivities and transmissivities of the semi-

reflecting layer, the oil and the steel surface. The phase angle is determined by the difference in the optical path lengths of the two beams and the phase changes experienced by the beams. (There is a phase change of 180 degrees when a beam passing from one medium to a denser medium is reflected at the interface; this includes the reflection at the oil/steel interface).

The difference in optical path lengths is proportional to the separation between the sapphire and the steel. Thus, knowing the phase changes and the refractive index of the oil, the film thickness can be calculated for a given interferometric fringe.

This is a very simple example, actual systems are more complicated than is suggested here.

3.3 THE CHOICE OF A CHROMATIC SYSTEM

For monochromatic light of wavelength λ there is constructive interference (i.e. the two rays reinforce each other) if the optical path difference between the beam reflected from the semi-reflecting layer and the beam reflected from the steel is some integral multiple of λ, i.e. $N\lambda$ where N is an integer. The optical path difference includes the effect of any phase change on reflection. There is destructive interference (i.e. the two rays tend to cancel each other out) if the path difference is equal to $(N + \frac{1}{2})\lambda$. This integer N is known as the "order" of interference.

White light can be approximated by a large number of wavelengths each corresponding to a different colour. For each of these wavelengths the interference process just described is valid. Hence the fringe patterns of each colour are

superimposed giving a pattern of varying coloured fringes but no dark ones.

Although the number of coloured fringe patterns is actually unlimited, in practice it is only possible to identify a few fixed shades; namely yellow, red, blue and green. These appear alternatively as the optical path difference is increased i.e. as the film thickness increases. This sequence repeats itself and corresponds to an increase in the order of interference. Hence, for a nominal change of one fringe order in a monochromatic system, a series of distinct shades can be obtained in the chromatic (white light) system. Thus the chromatic system is more accurate, especially when the range of film thicknesses is small.

The second reason for the choice of a chromatic system was to avoid any possible problems with the visibility of the fringes. If a monochromatic system were used in the experimental situation the visibility of the fringes would not be high even in the ideal case; and with the random scattering of the light that is bound to occur the visibility of the fringes will be reduced even further. This meant that difficulty might be experienced in clearly distinguishing light and dark fringes. However the overall high background light level would not significantly affect the ability to distinguish coloured fringes.

3.4 THE OPTICAL SEMI-REFLECTING COATING

The semi-reflecting coating that was used for the experimental interferometric system was Chromic Oxide (Cr_2O_3), a dielectric material. This is a tough transparent substance which absorbs very little light i.e. all light associated with

this material can be accounted for in terms of transmissivity and reflectivity.

The coating was deposited onto the sapphire by a technique known as sputtering. A full description of this method of attaching thin coatings to materials can be found in several publications (for example (4), (5)) and a section of a thesis by LEATHER (6) draws special attention to its use in optical interferometry.

3.4.1 The Sputtering Process

A simplified explanation of the process is as follows:-

The system consists of two plates known as the target and the substrate (or more usually the substrate table). The target is a metal base plate onto which is attached the material that is being sputtered (i.e. the coating material that is to be deposited), and the substrate is the object that is to be coated. The substrate table or the substrate itself is connected to earth (see Fig. 3.2).

The target and substrate are enclosed in an air tight chamber and the whole volume is evacuated to a pressure of approximately 4×10^{-4} N/m^2 (3×10^{-6} torr.). A gas is then introduced (usually an inert gas such as Argon) giving a controlled atmosphere for the process.

In D.C. sputtering, a high direct voltage is applied to the target and the intervening space becomes ionised. Particles of the target are carried into this ionised region and begin to deposit themselves on the earthed substrate. This works quite well if the target material is a conductor but not so well if it is an insulator (such as Chromic Oxide). When

this is the case there is a large potential drop across this material and the gas in the intervening space does not become ionised sufficiently, hence very low deposition rates result.

This problem can be circumvented if the target is excited by a high voltage radio frequency (approximately 13 MHz.) instead of a direct voltage. Any potential difference which tries to build up across the target material in one half of the radio frequency cycle is quickly neutralised in the other half. However the gas in the intervening space is still ionised, so particles of the target will still get carried over and deposited on the substrate.

A reversal of this technique is called "sputter etching" and is often used as a preliminary to sputtering. In this case the table is excited by the radio frequency, and consequently any surface film is driven off the substrate leaving a very clean surface ready to be coated in the normal manner. (To avoid contamination of the target, a grounded plate is interposed between the table and the target during this process).

This combination of sputtering and sputter etching produces a very good bond between the substrate and the coating. Consequently it gives a longer life under the severe operating conditions encountered in a rolling/sliding EHD contact than the more conventional vacuum deposition method.

3.4.2 The Coating

The actual interferometric process is not as simple as previously described; multiple reflections are taking place, and consequently multiple interference of the light beams also. Fig. 3.3 shows a diagramatic representation of

the major components of this process although the actual components are theoretically limitless.

It is desirable that beams (1) and (2) are as much in phase with each other as possible so that any interference in the system is mainly due to the oil film thickness, and is not unduly affected by the interaction between these two beams. For this reason the semi-reflecting coating thickness is arranged to be one quarter the wave length of green light ($\lambda/4$). Thus the path difference between the beams (1) and (2) is twice this value ($\lambda/2$) and, for green light, is equivalent to the phase change experienced by beam (1) at the sapphire/chromic oxide interface.

Although the two beams are only in phase for one specific wavelength of light, the selection of green light as the reference wavelength tends to make most of the other major colours in phase to a certain extent, and has been found to be the best choice in practice.

The selection of the thickness of the semi-reflecting film is not critical to the basic operation of the system (although it will have an effect), but is made in an attempt to improve the quality of the interference fringes. It is not necessary to know this film thickness as its effect can be accounted for when the system is calibrated (Chapter 4).

3.5 THE EXPERIMENTAL OPTICAL ARRANGEMENT

Most optical interferometric studies of an EHD contact have involved the use of a flat plate as the transparent body and consequently have had a relatively unobstructed view. In the present arrangement the transparent body was not flat as a line contact was wanted between the discs. This meant

that it was necessary to look through the curved portion of the disc to view the contact.

One consequence of this was that only half the circumference of the sapphire disc could be optically coated, otherwise a major part of the incident light ray would be reflected before it reached the EHD contact. It was intended that the contact would be viewed using a stroboscopic device. This would be triggered externally such that a clear optical path would be assured; however it later proved unnecessary to use this device. A further consequence was that a lens effect would be experienced by the light passing through the curved surface.

Moreover the four disc configuration gave a rather congested working area for the optical study. Thus a custom built optical system had to be designed and used. The selected experimental arrangement is shown both schematically and pictorially in Figs. 3.4 and 3.5.

A correction lens was used to counteract the distortion of the optical path due to the sapphire. This distortion is high as there is a large difference in the refractive indices of the sapphire (R.I. = 1.77) and the surrounding medium (oil, of R.I. ≈ 1.5), also the curvature of the sapphire is quite large. If the central disc had been made of crown glass (R.I. ≈ 1.5) the lens effect would have been greatly reduced and the necessary optical correction could have been relatively easily applied. Unfortunately crown glass does not have the required mechanical properties and hence could not be used.

As the correction lens was not to be loaded in any manner, the mechanical properties of the lens material were un-

important. Thus, although sapphire was preferred for the lens, it was not in fact chosen due to its high cost and the difficulty in machining it. Two possibilities presented themselves; either to use a common optical glass and machine the surface to a sufficiently small radius of curvature to give the desired lens effect; or to try and match the refractive index of the sapphire with another glass and machine the surface to the same radius of curvature as that of the sapphire. The latter solution was chosen as this had the added advantages of (a) reducing the possibility of cavitation of the oil between the correction lens and the sapphire disc (as the gap between these two was to be small a hydrodynamic effect would be unavoidable) and so minimising the distortion of the optical path, and (b) enabling the two surfaces to be more easily aligned.

The correction lens was made of double extra dense flint glass (R.I. ≈ 1.73) and had an anti-reflection coating of magnesium fluoride deposited on its upper (flat) surface (see Fig. 3.6). The outer edges of the lens were ground flat in an attempt to ensure the build-up of a uniform hydrodynamic film between the lens and sapphire disc (these edges were outside the optical path). As the refractive indices were not exactly matched there was a small magnification effect. Using simple optical theory a magnification factor of 1.022 was calculated (see Chapter 4). This factor only applies to the circumferential direction, there is no magnification in the axial direction. There is also no effect on the optical film thickness measurements.

With the lens in situ on the rig and resting on the sapphire disc, a rectangular tube (made from brass sheet) was

pushed through a machined slot in the outer casing and partially over the lens. This was then firmly attached to the lens using packing pieces and "Araldite". Hence the lens was in line with the sapphire disc and only needed to be raised slightly to give a suitable clearance. The lens and tube assembly was then made leak proof to keep out the oil when the working area was flooded, and hence acted as an inspection tube. This meant that the objective lens of the microscope could be brought closer to the sapphire disc, thus reducing the working distance requirement of the microscope and the amount of oil distorting the optical path.

It was physically impossible to bring a standard, commercially available microscope plus side illuminator close to the correction lens, nor was a sufficiently long working distance objective lens available for the microscope. The problem was solved by re-mounting the objective lens in an extension tube (Fig. 3.7); this was easily done and involved minimal machining.

The modification allowed the objective lens just to touch the correction lens if required, and only reduced the working distance by approximately 15% (a figure which was acceptable). An increase in magnification of approximately 50% was obtained. No noticeable deterioration in viewing quality was observed.

The light source was either a continuous tungsten filament lamp or a high voltage Xenon discharge lamp triggered by an external source. This external trigger consisted of a mirror attached to the output shaft which reflected a small light source onto a phototransistor pick-up once per revolution. Collimation was achieved simply using adjustable diaphragm

irises in the side illuminator. Otherwise the experimental arrangement was similar to that used by many previous workers (2).

Early experiments showed that, using a continuous light source, the central film thickness colour could be easily distinguished even though for half the revolution the semi-reflecting coating was in the wrong position. For this reason the Xenon discharge lamp was only used for photomicrographs.

It was also noticed that there was a slight "double image" effect which varied with the relative rotation of the disc. This did not detract from the observation of the central fringe colour, but gave an unwanted superimposition of the fringe patterns for the photomicrographs. This phenomenon was attributed to the birefringence of the sapphire. It was found that, by inserting a piece of "POLAROID" plastic between the light source and the microscope side illuminator, this unwanted effect could be eliminated.

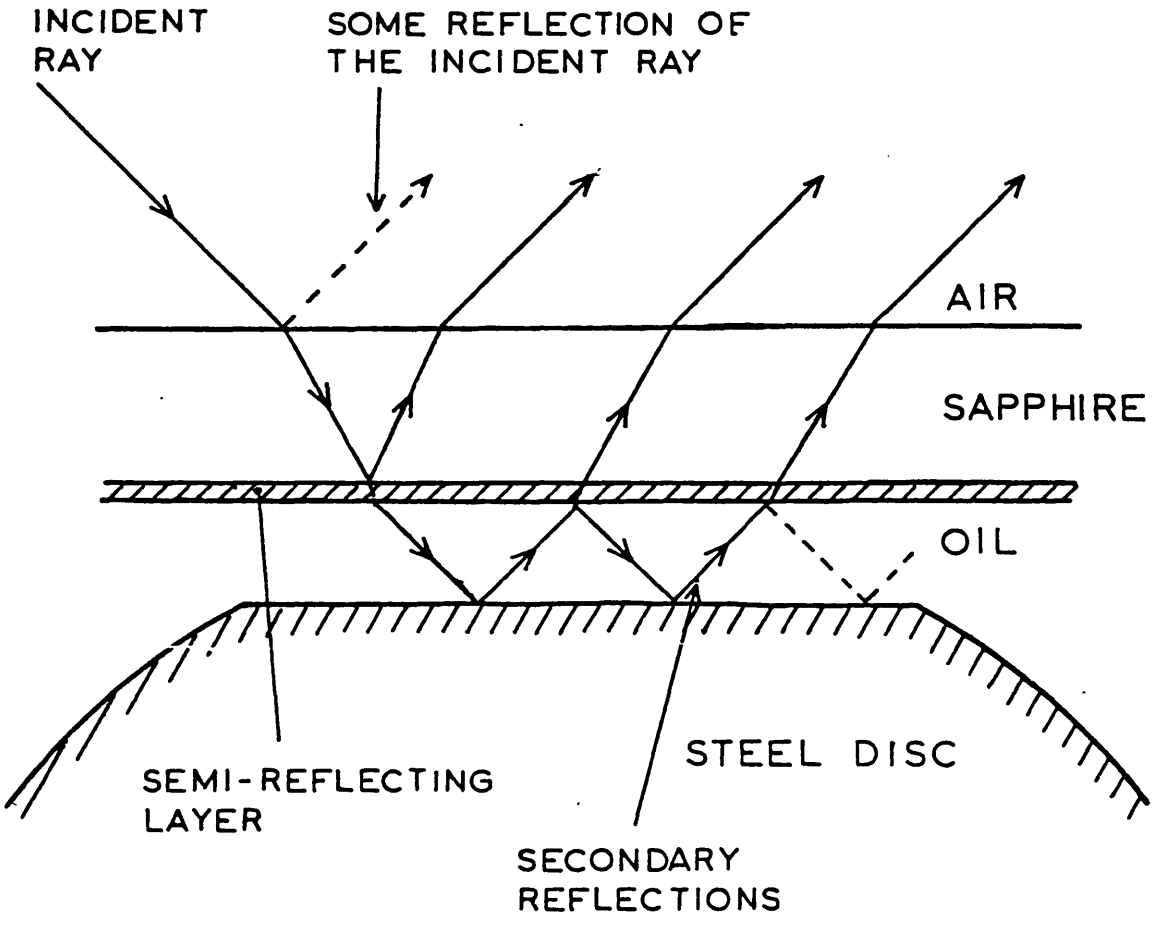

FIG. 3.1. THE SIMPLE INTERFEROMETRIC PROCESS

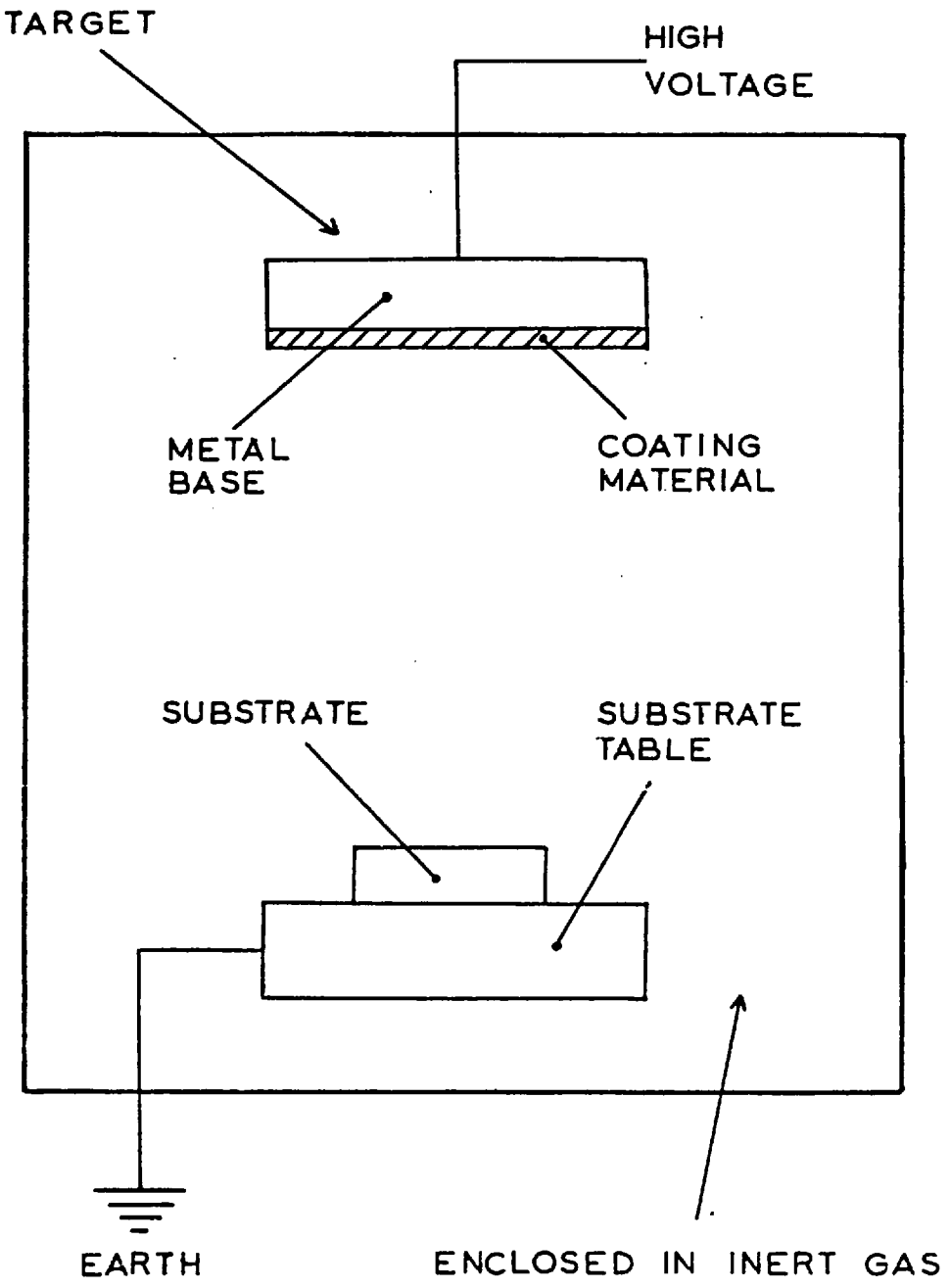

FIG. 3.2. THE SPUTTERING PROCESS

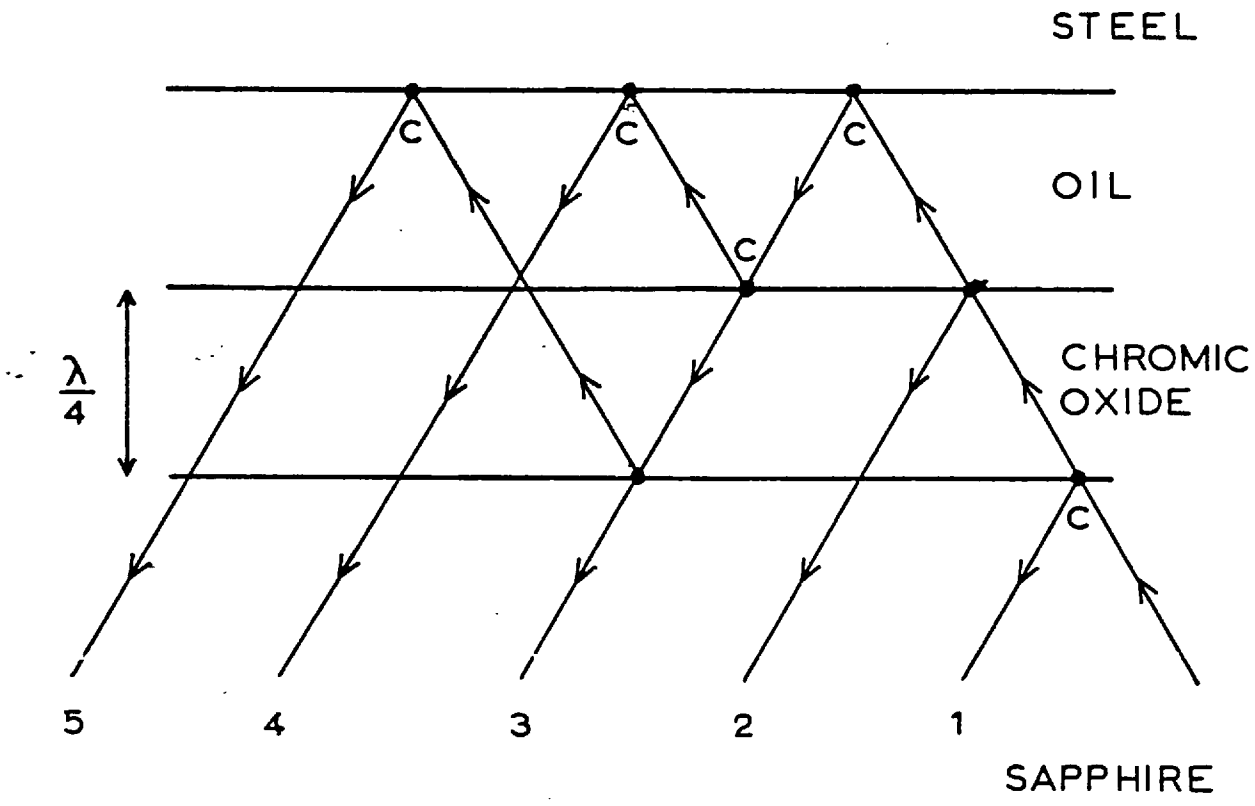

C - PHASE CHANGE OF 180°

λ - WAVELENGTH OF GREEN LIGHT

FIG. 3.3. THE SIMPLIFIED INTERFERENCE PROCESS IN THE EXPERIMENTAL SYSTEM

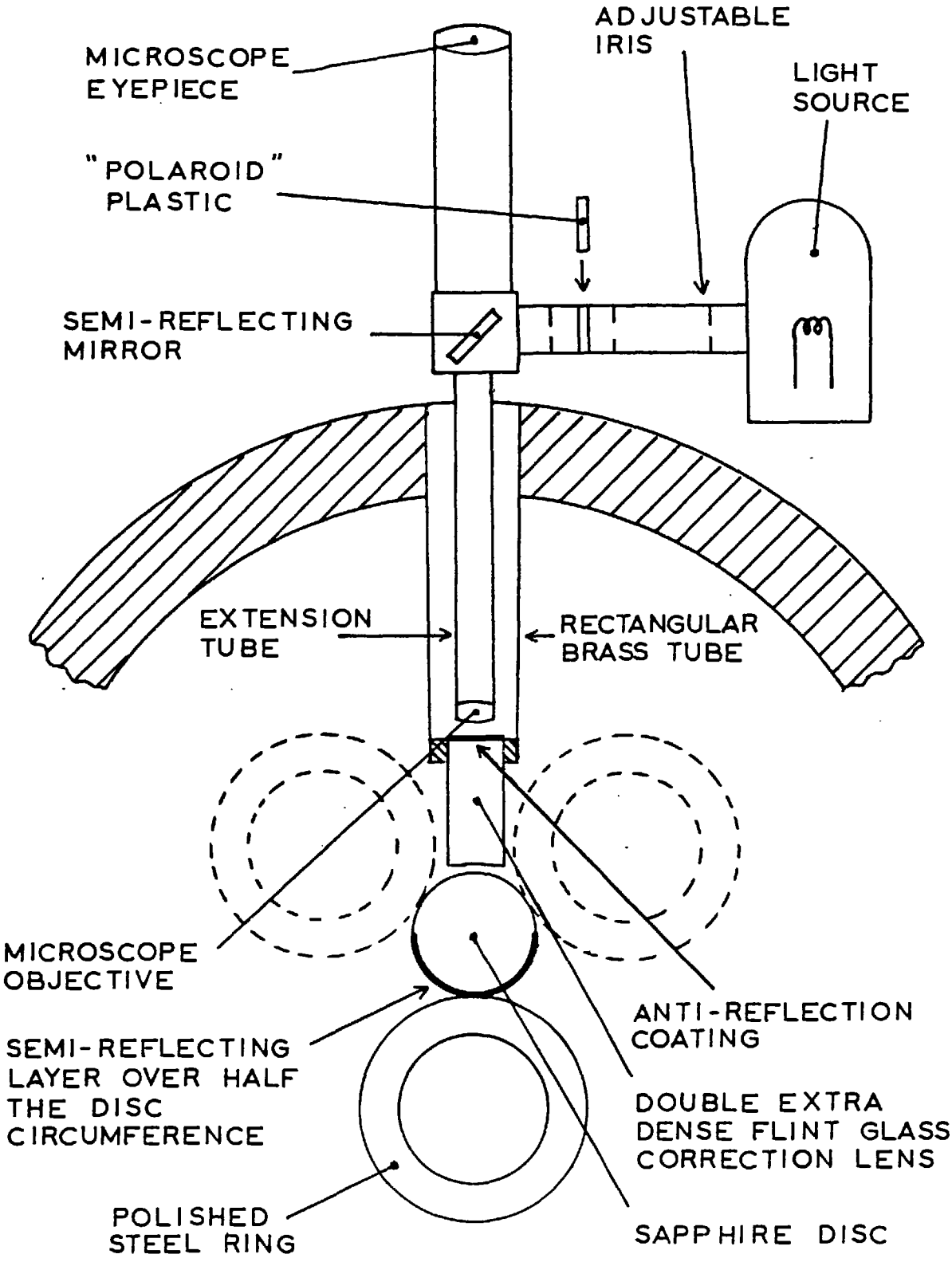

FIG. 3.4. SCHEMATIC DIAGRAM OF THE OPTICAL ARRANGEMENT

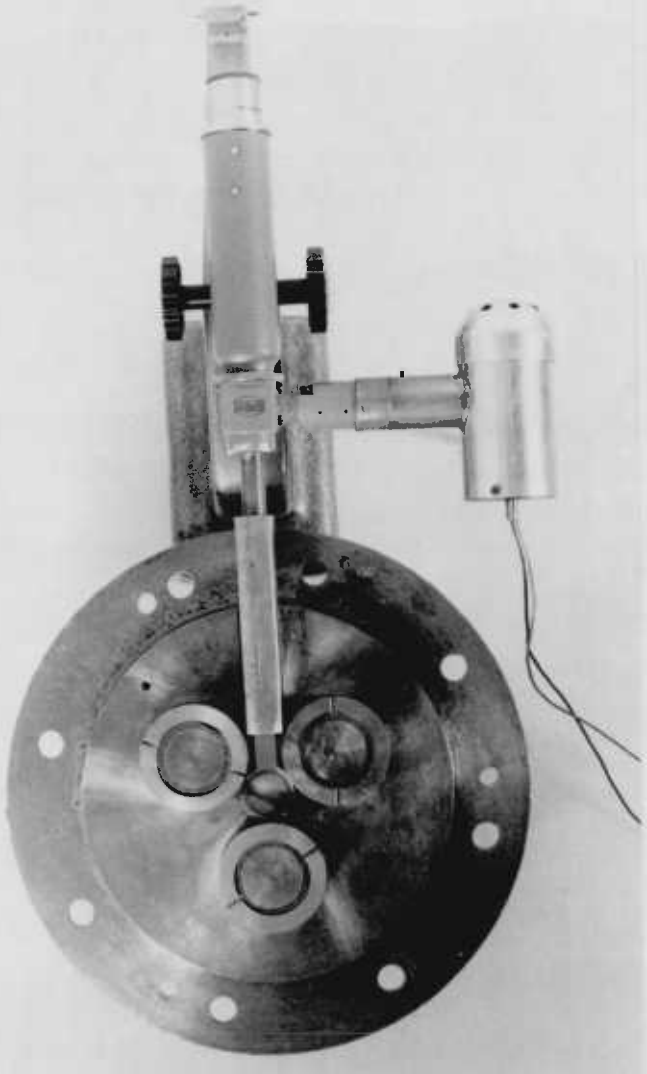

FIG. 3.5. THE OPTICAL ARRANGEMENT

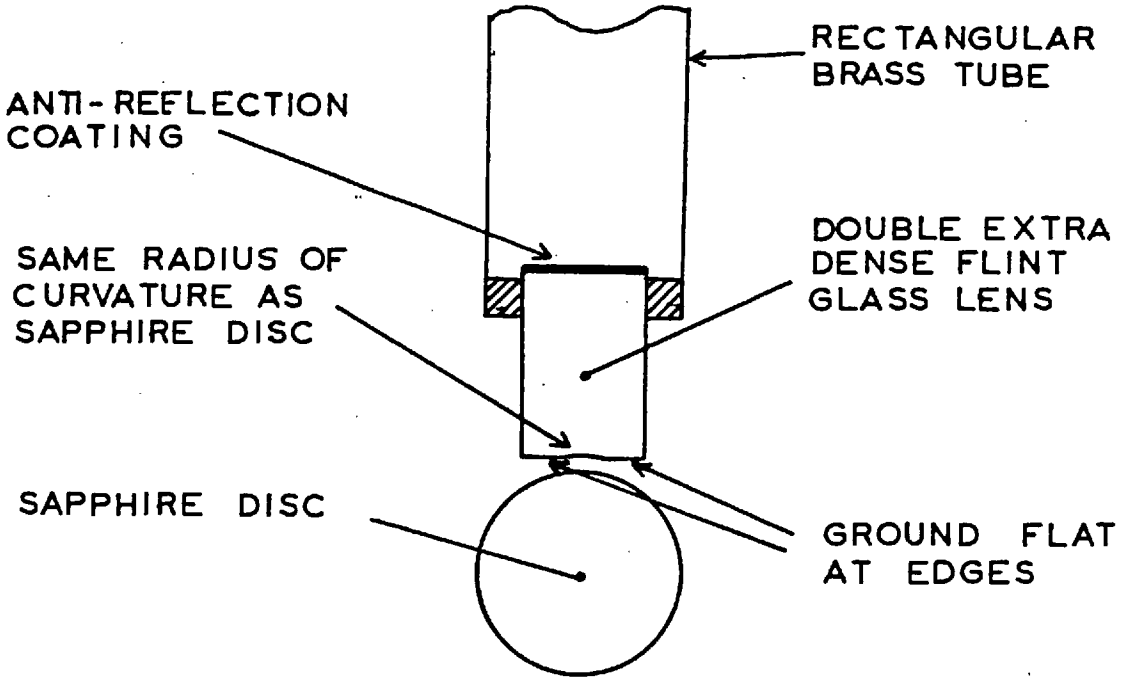

FIG. 3.6. THE CORRECTION LENS

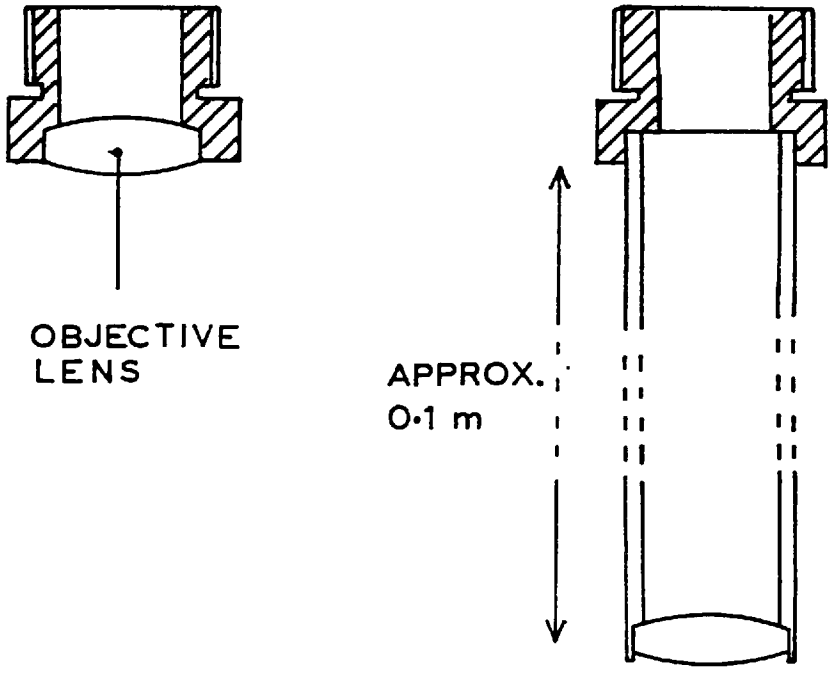

FIG. 3.7. THE MODIFIED OBJECTIVE LENS UNIT WITH EXTENSION TUBE

CHAPTER 3 - REFERENCES

1. CAMERON A. and GOHAR R. - "Theoretical and Experimental Studies of the Oil Film in Lubricated Point Contact", Proc. Roy. Soc. (A), 1966, Vol. 291, p. 520.
2. FOORD C.A., WEDEVEN L.D., WESTLAKE F.J. and CAMERON A. - "Optical Elastohydrodynamics", Proc. Inst. Mech. Eng., 1969-70, Vol. 184, Part 1.
3. TOLANSKY S. - An Introduction to Interferometry, Longmans, London, 1966.
4. DAVIDSE P.D. and MAISSEL L.I. - Journal Applied Physics, Vol. 37, 1966, p. 574.
5. BUTLER H.S. and KINO G.S. - "Plasma Sheath Formation by Radio Frequency Fields", Physical Fluids, Vol. 6, 1963, p. 1346.
6. LEATHER J.A. - Ph.D. Thesis, Univ. of London, 1977.

CHAPTER 4

EXPERIMENTAL PRELIMINARIES

4.1 SURFACE PREPARATION OF THE DISCS

The surface finish of the discs is an important factor in optical interferometrical studies of EHD contacts. If the surfaces are too rough the quality of the interference fringes will suffer and it will be difficult to measure the film thicknesses. Ideally the surfaces should be perfectly smooth, but this is impossible to achieve. The problem in getting an acceptable finish is that the polishing is always in the same circumferential direction and clogging of the polishing pads tends to occur, especially for steel surfaces.

Also to ensure an even contact the discs should be uniform in shape, with the outer surface being concentric with the inner surface and parallel to it. Any irregularities in form can produce local areas of higher Hertzian pressure and invalidate the results.

4.1.1 The Outer Discs

A mandrel was made to hold the discs firmly and accurately in place both for the initial machining operations and the final polishing. The main shaft of the mandrel was located by centre points at each end and its diameter was ground and lapped to 34.9 mm (1.375 in.). A cylindrical block of steel was then bored and honed to such a diameter that it just fitted the main shaft of the mandrel. This block of metal was then parted on a lathe to give three rings whose bores were all accurately fitted to the mandrel and whose side faces were perpendicular to their bores.

Using the same centre points as were used to grind the shaft of the mandrel, the outer surfaces of the rings were ground to a diameter of just over 50.8 mm (2.0 in.). Thus the inner bores and outer surfaces of the rings were concentric. The chamfer was then ground onto the rings (again using the mandrel) and the outer surfaces were fine lapped to 50.8 mm (2.0 in.).

The sharp edge between the track and the chamfer was blended using fine emery paper and hand lapping. This avoided any edge conditions which could give rise to above normal Hertzian pressures in the contact, as shown by WYMER (1).

Finally the outer track was polished using varying grades of diamond paste until a good reflective surface was obtained.

Surface profile traces of the rings showed good uniformity of shape and gave centre line average (C.L.A.) roughness values of 0.039, 0.042, and 0.043 μm (1.54, 1.65, and 1.69 μin.). (Samples of the traces are given in Fig. 7.23, Chapter 7).

A general assembly photograph and drawing of the ring and mandrel arrangement is shown in Fig. 4.1.

4.1.2 The Central Sapphire Disc

A rough machined sapphire disc with an outside diameter of 28.6 mm (1.125 in.), a width of 12.7 mm (0.5 in.) and a projecting "tongue" from one face was supplied by a manufacturer. This was attached to a steel shaft with a corresponding groove in it using an adhesive (see Fig. 4.2).

This adhesive was one of the cyanoacrylate variety

which combines a high shear strength with a certain amount of flexibility (it is often used as a strain gauge cement). This is superior to other adhesives such as "Araldite" which have little or no flexibility and which can shatter under an impulse load.

The shaft and sapphire were then returned to the manufacturer for final machining and polishing. By holding the assembly by the steel shaft it was possible to ensure that the sapphire was machined concentric with the shaft. The diameter of the sapphire was nominally 25.4 mm (1.0 in.). However the actual value was determined by assembling the steel discs on their spigots and measuring the size of the central disc necessary to give a tight fit and then subtracting 0.0508 mm (0.002 in.) from this value. This gave a nominal clearance of 0.0254 mm (0.001 in.) between the spigot and the ring when the hydrostatic bearing was in operation.

As sapphire is harder than steel it is easier to obtain a good, highly polished surface finish. This fact plus the professional, but unfortunately expensive, techniques employed by the supplier produced a uniform surface with a C.L.A. roughness value of 0.002 μm (0.079 μin.).

The disc was then sputtered with the optical coating as described in Chapter 3.

4.1.3 The Central Steel Disc

The disc and shaft were machined from one solid piece of steel and the surfaces of both were ground with the assembly held between centres, thus ensuring that the shaft and the disc were concentric. The surface of the disc was then lapped and polished in a similar manner to that used for the steel rings

and to the same diameter as for the sapphire disc.

The disc surface had a uniform shape and a C.L.A. surface roughness value of 0.034 μm (1.34 μin.).

4.2 CALIBRATION OF THE TORQUE MEASURING SYSTEM

The system of torque measurement utilised strain gauges mounted on a flexing metal blade as described in Chapter 2. Several commercial Wheatstone bridge systems are available to measure strain and from this, knowing the geometry and material of the strain gauge blade, the stress and hence the torque can be calculated. Unfortunately this method is susceptible to inaccuracies, especially when a small, non-uniform strain gauge blade is used, as local effects on the strain characteristic of the blade will be significant.

A far simpler and more accurate method is to calibrate the output from the strain gauge bridge against a known torque. This calibration was performed using a torque loading arm as shown in Fig. 4.3. The strain gauge assembly was left in position on the rig and one end of the torque shaft was clamped into this assembly using the grub screws already present for the output shaft (when in position). The other end of the torque shaft was supported in a block of metal into which a PTFE bush had been inserted, hence the friction offered by this support was minimal.

As the torque shaft was symmetrical about its centre it did not contribute any torque due to its weight, the only dead weight torque was produced by the torque arm. Knowing the weight of this arm and the dimensions of the arm and torque shaft, the deadweight torque could be easily calculated by assuming the centre of gravity of the arm to be

at its geometric centre. This was the minimum torque that could be produced. Further increases in torque were obtained by hanging known weights at a known distance from the centre of the torque shaft. Hence the total torque produced could easily be calculated and plotted against the measured output from the strain gauge bridge. It was confirmed by a simple test that, by having the strain gauge blade in a horizontal position, vertical loads on the torque shaft itself did not affect the output from the bridge. Hence, even though the strain gauge assembly also acted as a support in this configuration, the calibration was not invalidated.

The plots of torque against output voltage gave a straight line which, when extrapolated from the minimum torque value, passed through the origin, thus showing that there were no measurable spurious frictional torques in the system. Readings obtained when the torque arm was systematically unloaded also lay on this line, thus showing that there was no hysteresis effect.

This method of calibration was very quick and simple and it was quite easy to check the system periodically throughout the tests. When this was done, no variation from the initial calibration was found.

4.3 LOAD CALIBRATION

The loading produced by each hydrostatic bearing can be calculated by one of two methods. The first expresses the load as

$$W = a_r . p_r + a_\ell . \frac{p_r}{2} \qquad (4.1)$$

where W = load
a_r = projected recess area
a_ℓ = projected land area
p_r = recess pressure

See Fig. 4.4

This method assumes that, due to the symmetry of the bearing, the surface integral of the pressure in the y-direction is zero, leaving a nett force in the x-direction, i.e. the pressure can be considered to act over the projected area of the bearing. It also assumes that full recess pressure is maintained over the recess area and that an average pressure of $p_r/2$ exists over the land area (i.e. the pressure drops to ambient at the edges in a linear manner from full pressure at the recess).

From this can be obtained the relation

$$W = 3.74 \times 10^{-4} \, p_r \qquad (4.2)$$

for the bearing geometry of the experimental apparatus where W is in N and p_r is in N/m^2, or alternatively

$$W = 0.58 \, p_r \qquad (4.3)$$

if W is in lbf. and p_r is in p.s.i.

The second method is to use information found in the CAST BRONZE BEARING DESIGN MANUAL (2) which expresses the load as

$$W = a_f . A_p . p_r \qquad (4.4)$$

where A_p = total projected area of the bearing
a_f = load coefficient.

The load coefficients are found using an electric analogue technique and for the geometry used here a value of $a_f = 0.60$ is obtained, this gives a load/pressure relation of

(S.I. Units $W = 3.61 \times 10^{-4} p_r$ (4.5)

(British Units) $W = 0.56 p_r$ (4.6)

Both these methods give very similar results. However it was felt that the second method was more accurate and hence this relationship was adopted in the preliminary design calculations.

Prior to usage the three pressure gauges (one for each hydrostatic bearing) were checked using a deadweight pressure tester and found to be accurate.

The loads predicted by the preferred method were checked by comparing the calculated Hertzian contact width using these loads against the measured value for static conditions.

Hertzian theory for line contact gives

$$a = \sqrt{\frac{8WR}{\pi LE'}} \tag{4.7}$$

where a = Hertzian half width

R = Reduced radius

E' = Reduced Young's Modulus

W = Load

L = Length of contact

hence

$$W = \frac{\pi LE' a^2}{8R} \tag{4.8}$$

E', L, R are known and a can be measured, hence the load can be calculated.

To measure "a" the microscope system employed on the apparatus was fitted with a micrometer eyepiece. This consisted of a fine cross wire which was moved across the field of view by turning a calibrated dial. The microscope was focussed on a fine graticule in air which had a 1.0 mm (0.0394 in.) length in 100 divisions accurately etched upon it. The cross wire was traversed across this length and the difference in readings on the micrometer scale noted. Hence, by focussing on the Hertzian contact and traversing the cross wire from one edge of the contact to the opposite edge, it was possible to calculate this distance by noting the difference in micrometer readings and comparing it against the value for the graticule. However to obtain the real value of the Hertzian width (2a) it is necessary to apply a correction factor due to the distortion produced by the correction lens, oil film, and sapphire.

Referring to Fig. 4.5, for the first part of the light ray path simple optical theory gives

$$\frac{n_3}{u} + \frac{n_2}{v'} = \frac{n_3 - n_2}{R_B} \tag{4.9}$$

If the oil gap is small, then the second part of the light ray path can be approximated by

$$\frac{n_2}{-v'} + \frac{n_1}{v} = \frac{n_2 - n_1}{R_A} \tag{4.10}$$

Combining (4.9) and (4.10) and using $R_A = R_B = R$ gives

$$\frac{n_3}{u} + \frac{n_1}{v} = \frac{n_3 - n_1}{R} \tag{4.11}$$

(i.e. the same as for a curved surface with a sapphire/flint glass interface). The magnification is given as

$$m = \frac{|v|}{u} \qquad (4.12)$$

Using $n_3 = 1.765$, $n_2 = 1.728$, $u = 25.4$ mm (1.0 in.) and $R = 12.7$ mm (0.5 in.), a value of m of 1.022 is obtained.

Thus the real Hertzian width equals the apparent value divided by 1.022.

The Hertzian width was measured at five pressures and it was confirmed that these values did not change with temperature. The comparison of the values of load from hydrostatic bearing considerations and Hertzian width calculations is given in Fig. 4.6. It can be seen that the agreement between the two methods is not good, the value calculated from Hertzian width measurements being less than predicted.

It was clear that the hydrostatic bearings were not performing as predicted and that they would need to be calibrated directly against the oil supply pressure. However the experimental method of determining load just described is very sensitive to the half contact width (a), and so it was considered that this method of calibrating the hydrostatic bearing was not the most satisfactory. Therefore it was decided to construct a purpose-built load cell to measure the performance of the hydrostatic bearings.

This load cell was designed to replace the central disc and is shown in Figs. 4.7 and 4.8. As it was decided that the loads produced by the hydrostatic bearings were only to be measured for the static condition, (the practicalities of a rotating calibration were considered too complex and the performance of a hydrostatic bearing is the same for both

motion and no motion in any case) it was not necessary to design this load cell to close tolerances. Instead the fit between the bearings was obtained using various thicknesses of steel shims. Two "active" strain gauges were bonded to the load tube and two "dummy" strain gauges to the semi-cylindrical platform. These gauges were then wired up to form a resistance bridge.

In a similar manner to the torque measuring system this load cell was calibrated against a known compressive load in a "Denison" testing machine. The response was closely linear and the curves of voltage output against load were the same for loading and unloading.

The load cell was then located in the experimental apparatus such that the line of action of the resultant force produced by the hydrostatic bearing passed along the centre line of the load tube. The output from the load cell was noted for six hydrostatic bearing pressures and it was confirmed that this was consistent for all temperatures. From this the load could be calculated; the results are shown in Fig. 4.9.

It can be seen that the bearings are producing a load less than expected. The reasons for this are not clear but may be due to the presence of some scoring on the bearing faces. (Although the bearings were initially operated without the steel rings during construction to drive out any swarf etc., some metal debris must have still been present to cause this minor damage at a later date).

4.4 REFRACTIVE INDEX OF THE OIL

The calibration of film thickness in terms of fringe order or interference fringe colour is a measure of

the optical film thickness, not necessarily the actual film thickness. The two thicknesses are related as follows:-

$$h_{optical} = h_{actual} \times n(p,T) \qquad (4.13)$$

where $n(p,T)$ is the refractive index of the intervening medium which is a function of pressure and temperature; thus they are only the same if $n(p, T) = 1$ and for oil this is not the case.

Therefore to interpret the measured film thickness in terms of the real EHD film thickness it is necessary to know the refractive index of the oil at the contact pressures and temperatures. It is not possible to measure refractive indices at the pressures experienced in the contact of this apparatus and so they must be calculated.

The pressure and temperature chosen at which to determine the refractive index were the inlet temperature and the maximum Hertzian pressure. The refractive index does not change very rapidly with temperature so the assumption that the contact temperature is uniform and equal to the inlet temperature is adequate in this case. (To produce a 5% change in refractive index temperature rises in the order of 200°C are needed). The reason for choosing the maximum Hertzian pressure is that the film thickness is measured in this area (i.e. the centre of the contact) and so this pressure is the most applicable.

4.4.1 Refractive Index Measurements at Inlet Temperatures

Measurements of refractive index were performed for the lubricant at ambient pressure using an Abbé Refractometer. The temperature was controlled by circulating water

through the refractometer from a thermostatically regulated bath. The working area was allowed to reach a steady temperature over a period of one hour before the lubricant was applied to the working surface. A measurement of refractive index was then taken. The thermostatic water bath was set to a new temperature and the procedure was repeated.

A graph was plotted of refractive index against temperature; it was found that, for the range of temperatures used, there was a linear relationship between the two parameters.

4.4.2 Calculation of Refractive Index at Contact Pressures

Once the refractive index of the lubricant had been deduced for the required value of inlet temperature, it could be recalculated for the pressures at the centre of the contact using the Lorentz-Lorenz equation:-

$$n_p = \frac{(1 + 2A)^{\frac{1}{2}}}{(1 - A)} \qquad (4.14)$$

where n = refractive index

$$A = \frac{\rho_p}{\rho_o} \frac{(n_o^2 - 1)}{(n_o^2 + 2)}$$

ρ = density

subscripts p and o refer to pressure p and ambient pressure respectively.

The behaviour of density with pressure and temperature is given later in this chapter.

4.5 OPTICAL FILM THICKNESS CALIBRATION

It is impracticable to try and interpret the visual observations of fringe order and colour in terms of

optical film thickness by theoretical means. The reasons are threefold: firstly the coloured fringes which can be identified in the contact are largely the subjective impressions of the observer; for example, what may seem a "true green" to one person may seem a slightly "blue-green" to another. Secondly, there is a phase change when the beam is reflected from the steel surface; the value of this change cannot be accurately predicted. Thirdly, the semi-reflecting layer used in the present optical system is a dielectric material. This means that light is reflected from both the sapphire/chromic oxide interface and the chromic oxide/oil interface, and that the light reflected from the steel will interfere with both these beams. The relative phase of the beams will be dependent on the thickness of the chromic oxide layer which was optimised at approximately ¼ wavelength of green light. This thickness is not exact and cannot be easily measured thus causing more uncertainty.

The only way of accurately calibrating the optical film thickness is to match the observer's subjective opinion of fringe colour against a known film thickness. The calibration method adopted was similar to that used by WEDEVEN (3) and involved the use of a simple "Newton's Rings" type of interference pattern.

A small piece of optically flat crown glass was sputtered with chromic oxide at the same time as the sapphire disc was sputtered. It was ensured that this piece of glass was placed next to the sapphire and at the same distance from the target, thus it would have been coated with the same thickness of chromic oxide as the sapphire. In the optical interferometric system the material of the clear substrate does not

affect the measurements as long as it has a refractive index below that for the coating, as is the case for the sapphire. (The refractive indices for sapphire, crown glass and chromic oxide are approximately 1.8, 1.5 and 2.4 respectively).

This piece of glass was then lightly pressed against a piece of steel that had a convex surface of 9.144 m. (30.0 ft.) radius and which had been polished to a high optical finish. Oil was present between the glass and the steel. On releasing the pressure on the glass the two surfaces were held together such that they were just touching by the surface tension of the oil. This combination of light pressure then no pressure did two things. It firstly ensured that there were no dust particles etc. present between the two surfaces which could artificially raise the film thickness (Fig. 4.10), and secondly prevented any Hertzian distortion of the two surfaces i.e. although in contact they maintained their original shapes.

At any given distance r from the point of contact of the two surfaces the separation h can easily be calculated from geometric considerations (see Fig. 4.11). Assuming that the radius of the steel equals R then from the chordal rule for a circle

$$r^2 = (2R - h)h \tag{4.15}$$

or for small h

$$h = \frac{r^2}{2R} \tag{4.16}$$

Thus by measuring the diameter of the coloured fringe under observation, the separation that it corresponds to can be easily calculated using the above relation. By

multiplying this value of separation by the refractive index of the oil, the optical film thickness for a given fringe can be found.

The calibration obtained is given in Table 4.1. It can be seen that the blue fringe was only clearly distinguishable at the first order and the yellow fringe only to the third order.

4.6 TEMPERATURE CORRECTION TO THE MEASURED VALUES OF FILM THICKNESS WHEN SLIDING IS PRESENT

As mentioned in Chapter 2 the inlet temperature was measured by a trailing thermocouple on the steel disc which comprised one surface of the EHD contact being viewed through the microscope. Under conditions of pure rolling this measured temperature is the same as that of the sapphire, and hence can be assumed to represent the inlet temperature of the contact.

When sliding is introduced there is heat generated between the moving surfaces in each of the three contacts. Ignoring any differences in thermal conductivity and thermal diffusivity of the sapphire and steel (which are very small), it can be seen that three times as much heat is being injected into the sapphire as into the steel. (There are three heat generating contacts on the sapphire compared to one on each of the steel discs). Thus under sliding conditions the temperature of the sapphire disc will be higher than that of the steel discs, and hence the measured temperature of the steel disc cannot be equated to the inlet temperature.

Due to the relatively rapid change of temperature when sliding was introduced, it was found difficult to monitor

both the sapphire and steel temperatures as other readings also needed to be taken at the same time. As the inlet temperature is generally assumed to be the mean of the two disc temperatures a simple experiment was performed to see if, by joining the output of each thermocouple in parallel, the mean voltage and hence mean temperature could be obtained. Unfortunately this did not prove to be practicable and some large errors in measurement were found to occur using this technique. For this reason another method was used to determine the central disc temperature and thus the mean inlet temperature.

4.6.1. Prediction of the Sapphire Temperature

A series of tests were performed to find the variation of the temperature differential between the sapphire and steel discs with changes in speed, slide/roll ratio, temperature and hydrostatic bearing pressure (i.e. load).

As sliding was introduced the temperature differential rose sharply and, after a period of a few seconds, levelled off to a steady value. This steady value appeared to be independent of the temperature itself (as measured for the steel disc). The results of this preliminary experiment are presented in Fig. 4.12 and are valid for all temperatures, as long as sufficient time is allowed for the temperature differential to stabilise.

From theoretical considerations it is expected that the heat generated in each contact would be linearly proportional to load (or hydrostatic bearing pressure) and sliding speed (which can be expressed as a linear function of mean speed and slide/roll ratio)

i.e. $$Q \propto V_m \cdot \Sigma \cdot p \qquad (4.17)$$

where Q = rate of heat generation

V_m = mean velocity of the discs

Σ = slide/roll ratio

p = hydrostatic bearing pressure.

Equation (4.17) assumes that coefficient of traction is a constant, this is not always true. However at the higher values of slide/roll ratio and Hertzian pressure, it is a good approximation and greatly simplifies the following analysis.

Experimental work in heat dissipation from rotating bodies in a fluid gives relationships of the form:-

For the rim of a disc (4)

$$N_u = 0.18 \ (0.5 \ Re^2 \cdot Pr)^{0.315} \qquad (4.18)$$

For the side of a disc (5)

$$N_u = 0.62048 \ (Pr^{1/3}) \ (Re^{1/2}) \qquad (4.19)$$

where N_u = Nusselt Number = $\frac{\alpha . D}{k}$

Pr = Prandtl Number = $\frac{C_p \cdot \rho \cdot \eta}{k}$

Re = Reynolds Number = $\frac{\rho . V . D}{\eta}$

α = heat transfer coefficient

D = diameter

k = thermal conductivity of disc

ρ = density

V = velocity of the individual disc

η = dynamic viscosity

C_p = specific heat.

It can be seen that for both the rim and the sides that the heat transfer coefficient, α, is a function of the velocity and several other physical quantities. Of these latter quantities a change can only be brought about by a change of pressure or temperature of the bulk fluid. As the pressure in the experimental system used here remained at ambient there can be no change due to pressure. Thus:

$$\alpha \propto V^{A_1} \cdot f\{T\} \tag{4.20}$$

where A_1 is a constant, $f\{T\}$ is a function of temperature.
But

$$Q \propto \alpha \cdot \Delta T \tag{4.21}$$

where ΔT is the temperature differential between the disc and the surrounding fluid.
$\therefore$ combining equations (4.17), (4.20) and (4.21)

$$V^{A_1} \cdot f\{T\} \cdot \Delta T \propto V_m \cdot \Sigma \cdot p \tag{4.22}$$

$$\therefore \Delta T = A_2 \cdot \frac{V_m \cdot \Sigma \cdot p}{V^{A_1} \cdot f\{T\}} \tag{4.23}$$

where A_2 is a constant.
Thus the difference in temperature between the sapphire disc and the steel discs, $\Delta T'$, can be defined as:-

$$\begin{aligned} \Delta T' &= (\Delta T)_{\substack{\text{SAPPHIRE}\\\text{DISC}}} - (\Delta T)_{\substack{\text{STEEL}\\\text{DISC}}} \\ &= \left(\frac{A_2 \cdot V_m \cdot \Sigma \cdot p}{V^{A_1} \cdot f\{T\}}\right)_{\substack{\text{SAPPHIRE}\\\text{DISC}}} - \left(\frac{A_2 \cdot V_m \cdot \Sigma \cdot p}{V^{A_1} \cdot f\{T\}}\right)_{\substack{\text{STEEL}\\\text{DISC}}} \end{aligned} \tag{4.24}$$

As there are three heat generating contacts on the sapphire disc, the constant A_2 is different for the sapphire

and steel discs. If it is assumed that both $V_{\substack{\text{SAPPHIRE}\\\text{DISC}}}$ and $V_{\substack{\text{STEEL}\\\text{DISC}}}$ can be reasonably replaced by V_m then

$$\Delta T' = A_{2\ \substack{\text{SAPPHIRE}\\\text{DISC}}} \cdot V_m^{A_4} \cdot \Sigma \cdot p \left(\frac{1}{f\{T\}_{\substack{\text{SAPPHIRE}\\\text{DISC}}}} - \frac{A_3}{f\{T\}_{\substack{\text{STEEL}\\\text{DISC}}}} \right) \quad (4.25)$$

where A_3 $(= A_{2\ \substack{\text{STEEL}\\\text{DISC}}} / A_{2\ \substack{\text{SAPPHIRE}\\\text{DISC}}})$ and A_4 $(= 1-A_1)$ are constants.

However the experimental results show no dependence of the temperature difference on the temperature itself, so the effect of $f\{T\}$ appears to be negligible. Thus an expression of the form

$$\Delta T' = C.\ V^B.\ \Sigma\ .\ p \quad (4.26)$$

should fit the experimental results.

By trial and error the best fit was found to be

$$\Delta T' = 2.35 \times 10^{-4} \times p \times \Sigma \times V^{0.78} \quad (4.27)$$

where $\Delta T'$ is in ^{o}C

p is in p.s.i.

$\Sigma \equiv (U_1-U_2)/(\frac{1}{2}(U_1+U_2))$

$V \equiv \frac{1}{2}(U_1+U_2)$

U_1, U_2 are the respective disc speeds in terms of input r.p.m.

Thus knowing the operating conditions and the steel disc temperature the sapphire temperature can be predicted by the above relationship. The inlet temperature is then assumed to be the mean of these two temperatures.

The maximum error between the measured value and the predicted value of temperature differential is approximately

$2^{o}C$, giving a possible inlet temperature error of not more than $1^{o}C$. This prediction was found to be valid over the complete range of experimental conditions used, even for those conditions under which film thickness anomalies were later found to occur.

4.6.2 Modification to Film Thickness Measurements

Knowing the temperature correction which needed to be applied to the measured (steel disc) temperature to obtain the inlet temperature, two possible approaches presented themselves. Either the film thickness measurements could be related to this new temperature or, using a suitable film thickness/ temperature relation, the results could be modified to allow for this "mismeasurement" of temperature.

The second course was chosen as this enabled a direct comparison to be drawn against the rolling results for the same temperature. The disadvantage of this method is that it is assumed the behaviour of the film thickness is known in order to predict the modified film thickness; however any error will be small and certainly will not affect the qualitative picture of the results.

It was decided to use a film thickness/temperature relation based on experimental work carried out by WYMER (1) to modify the results. He investigated the behaviour of central film thickness to changes in various parameters and produced the following expression:-

$$h_o^* = 0.44\ U^{*0.64}\ W^{*-0.17}\ G^{*0.58} \qquad (4.28)$$

where $h_o^* = \frac{h_o}{R}$

$$U^* = \frac{U.\eta_o}{E'.R}$$

$$W^* = \frac{W}{L.E'.R}$$

$$G^* = \alpha.E'$$

h_o = central film thickness under rolling conditions

R = reduced radius

U = speed

η_o = inlet dynamic viscosity

E' = reduced Young's Modulus

W = load

L = contact length

α = pressure/viscosity coefficient.

In Chapter 7 it is shown that for the present purposes the experimental results agree very well with this relationship.

It can be seen that the only parameters on the right hand side of the relation that are affected by temperature are η_o and α. Thus

$$h_o \propto \eta_o^{0.64}\ \alpha^{0.58} \qquad (4.29)$$

The variation of η_o with temperature was found by using the Walther-A.S.T.M. formula for kinematic viscosity

$$\log_e (\log_e (\nu + 0.6)) = K - C.\log_e T \qquad (4.30)$$

where ν = kinematic viscosity in centistokes

C,K = constants to be determined

T = absolute temperature (^oF or ^oC).

The density of the lubricant and the pressure viscosity coefficient were calculated from information supplied by The British Petroleum Company Ltd. (further details are given

in Section 4.7).

Knowing the change in α and η_o with temperature the modification to the film thickness was easily calculated.

4.7 PHYSICAL VALUES FOR THE OIL, STEEL AND SAPPHIRE

4.7.1 The Steel

Young's Modulus = 207 GN/m^2

Poisson's Ratio = 0.3

Thermal conductivity = 46.1 $J/sec.m.^oC$

Thermal diffusivity = 0.12×10^{-4} m^2/sec

The thermal information was taken from CARSLAW and JAEGER (6).

4.7.2 The Sapphire

Young's Modulus = 432 GN/m^2

Poisson's Ratio = 0.265

Thermal conductivity = $42 \times e^{-.004T}$ $J/sec.m.^oC$

Thermal diffusivity = $1.4 \times 10^{-5} \times e^{-.004T}$ m^2/sec

$\Big\}$ T_o in ^oC

Refractive index = 1.765 (average).

The thermal data was extracted from a paper by FOORD et al (7) and the remaining data was obtained from the manufacturer - Industrie de Pierres Scientifiques Hrand Djevahirdjian S.A. of Switzerland.

4.7.3 The Oil

The oil that was used throughout the tests was a paraffinic type supplied by British Petroleum (Ref. L74/1113). The data given in Table 4.2 plus the following was also provided:-

$$\rho = \rho_o \frac{(1 + C_1 \cdot T + C_2 \cdot T^2)}{(1 + C_3 \cdot \sqrt{T} \cdot \log_e (p+p_o))} \qquad (4.31)$$

where ρ = density in kg/m^3

T = temperature in ^oC

p = pressure in MN/m^2

$C_1 = -0.00098$, $C_2 = 8 \times 10^{-8}$, $C_3 = -0.00344$, $p_o = 130$, $\rho_o = 876$.

From this data the constants in the Walther-A.S.T.M. formula for viscosity could be calculated. Moreover for each temperature the pressure/viscosity coefficient α was computed for the pressure range of ambient to 69 MN/m^2 (10,000 p.s.i.). An empirical relation was then derived which gave

$$\alpha = (2.710 - 0.0111T) \times 10^{-8} \ (N/m^2)^{-1} \qquad (4.32)$$

where T is in ^oC.

The results of the refractive index measurements (taken using the Abbé refractometer) were as follows:-

Temperature (^oC)	Refractive Index
22	1.487
42	1.480
64	1.473
79	1.467

giving

$$n_T = 1.495 \ (1 - 0.000235 \ T) \qquad (4.33)$$

where n_T = refractive index at temperature T^oC.

TABLE 4.1 CALIBRATION OF OPTICAL FILM THICKNESS

Fringe (Order and Colour)	Optical Film Thickness (μm)
1st Yellow	0.165
1st Red	0.260
1st Blue	0.340
1st Green	0.400
2nd Yellow	0.455
2nd Red	0.525
2nd Green	0.650
3rd Yellow	0.740
3rd Red	0.820
3rd Green	0.955
4th Red	1.100
4th Green	1.260

TABLE 4.2 PRESSURE/VISCOSITY DATA SUPPLIED BY THE BRITISH PETROLEUM CO. LTD. FOR THE TEST OIL L74/1113

Pressure (kg/cm^2)	Viscosity (Centipoise)	Temperature (^oF)
1	320.0	59
149.9	495.0	"
600.1	1444	"
981.7	3508	"
1367.7	9870	"
1	79.23	100
244.5	142.6	"
569.7	282.0	"
992.6	653.5	"
1655.3	2158	"
1954.2	3399	"
2219.6	5228	"
2643.5	10310	"
1	8.49	210
133.3	10.69	"
603.0	22.22	"
820.5	30.26	"
1698.5	94.5	"
2224.7	180.9	"
2806.6	349.0	"
3492.2	717.2	"
4414.8	1835	"
5512.4	5162	"
6390.7	11250	"
7279.6	24390	"
8425.9	60220	"

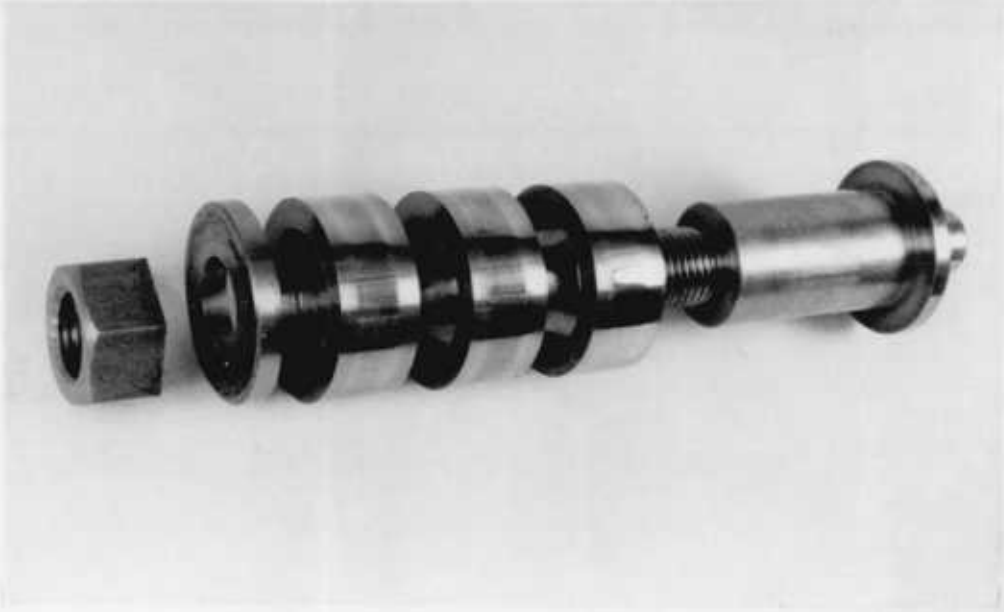

FIG. 4.1. THE STEEL RINGS AND MANDREL

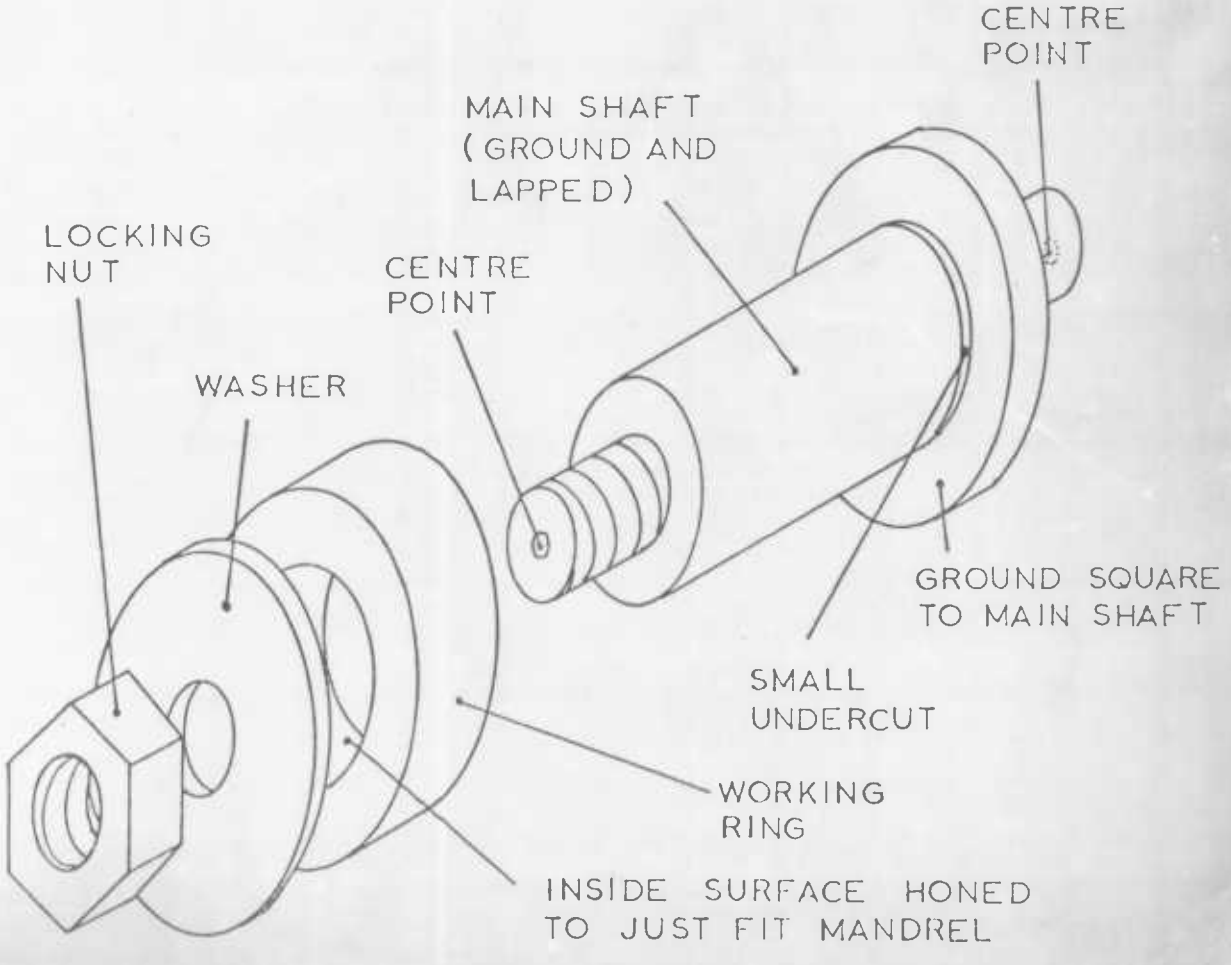

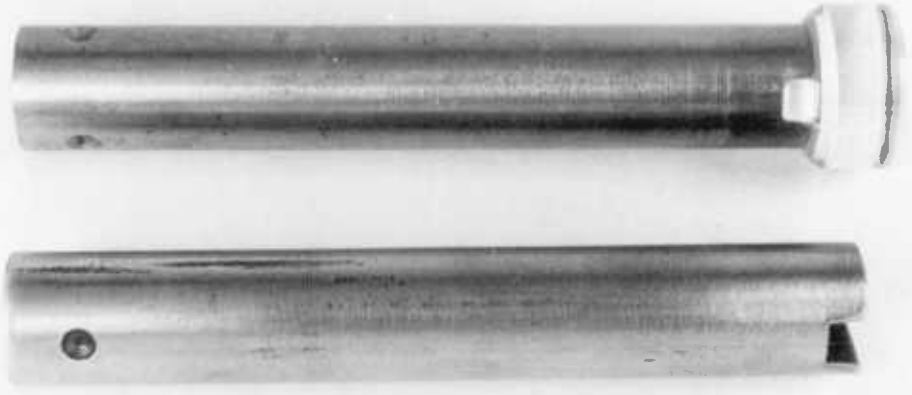

FIG . 4.2. THE CENTRAL DISC PLUS SHAFT

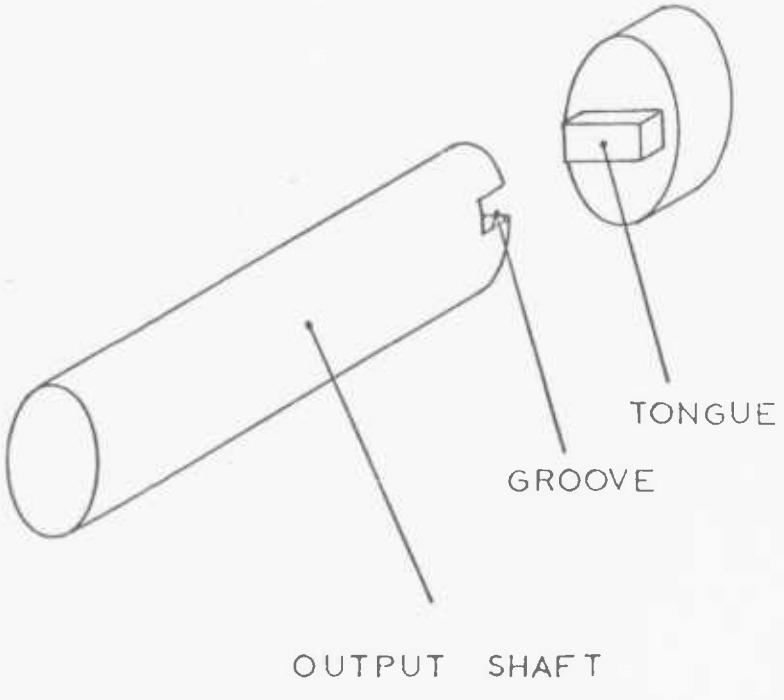

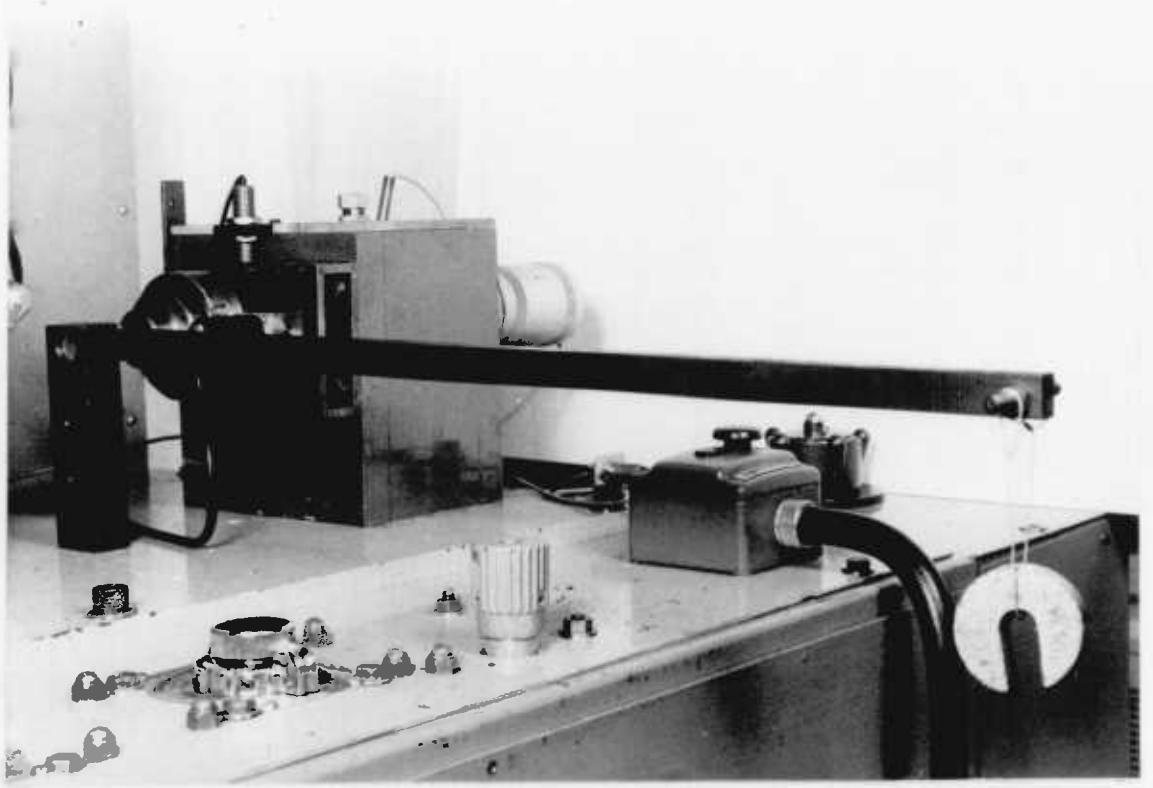

FIG. 4.3. ARRANGEMENT OF THE TORQUE CALIBRATION SYSTEM

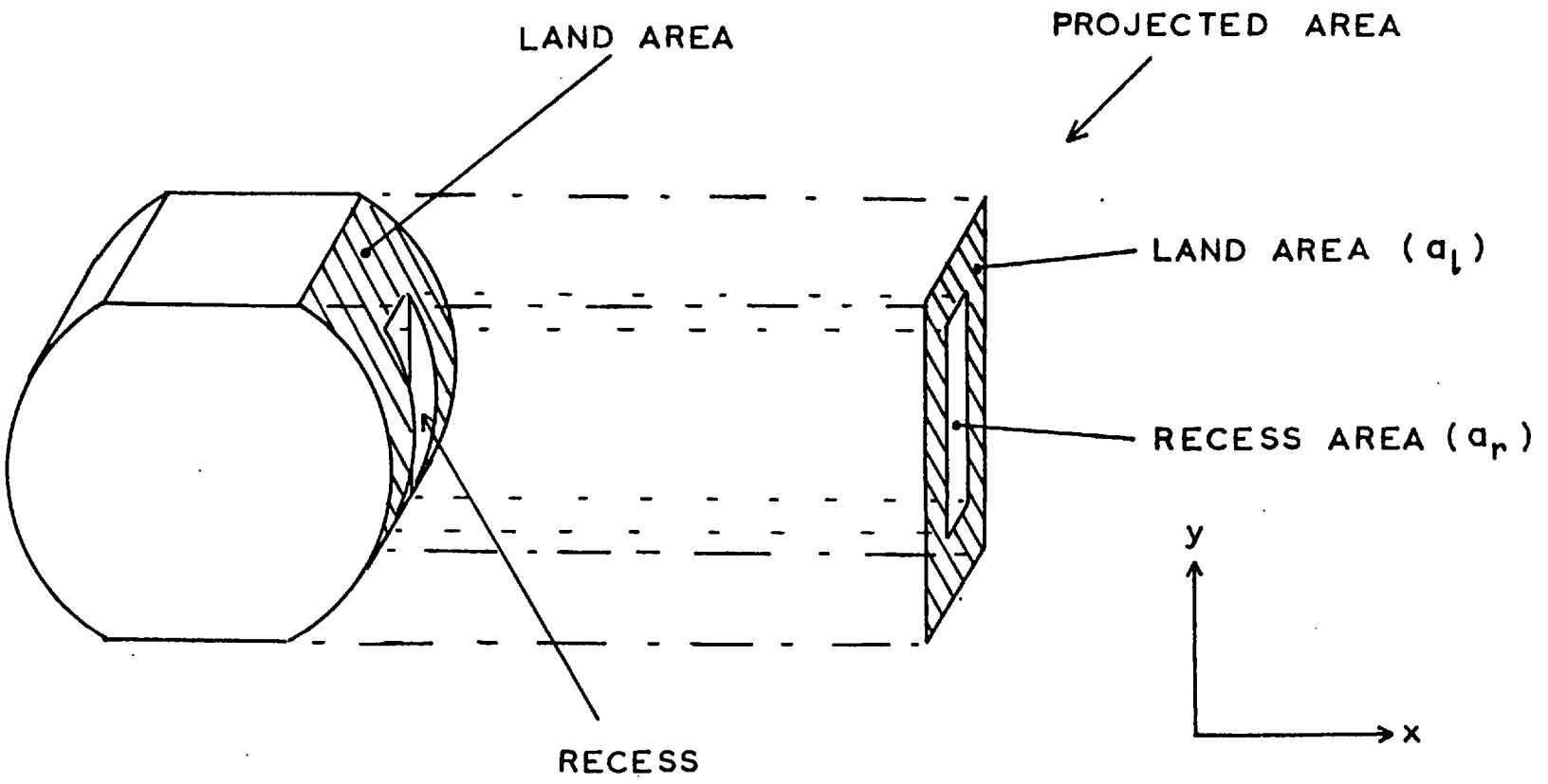

FIG. 4.4. SCHEMATIC DIAGRAM OF THE HYDROSTATIC BEARING

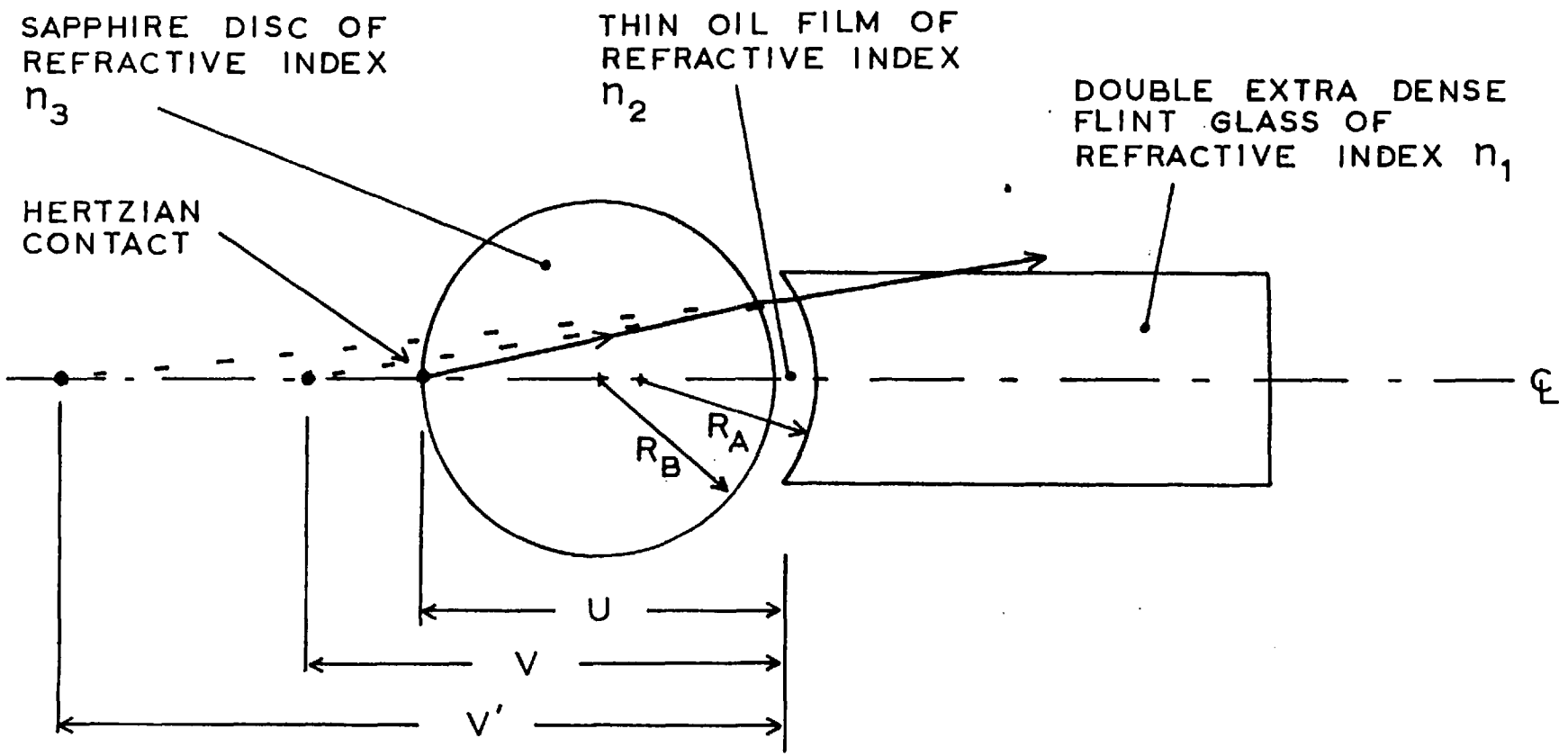

FIG. 4.5. SCHEMATIC DIAGRAM OF THE OPTICAL PATH

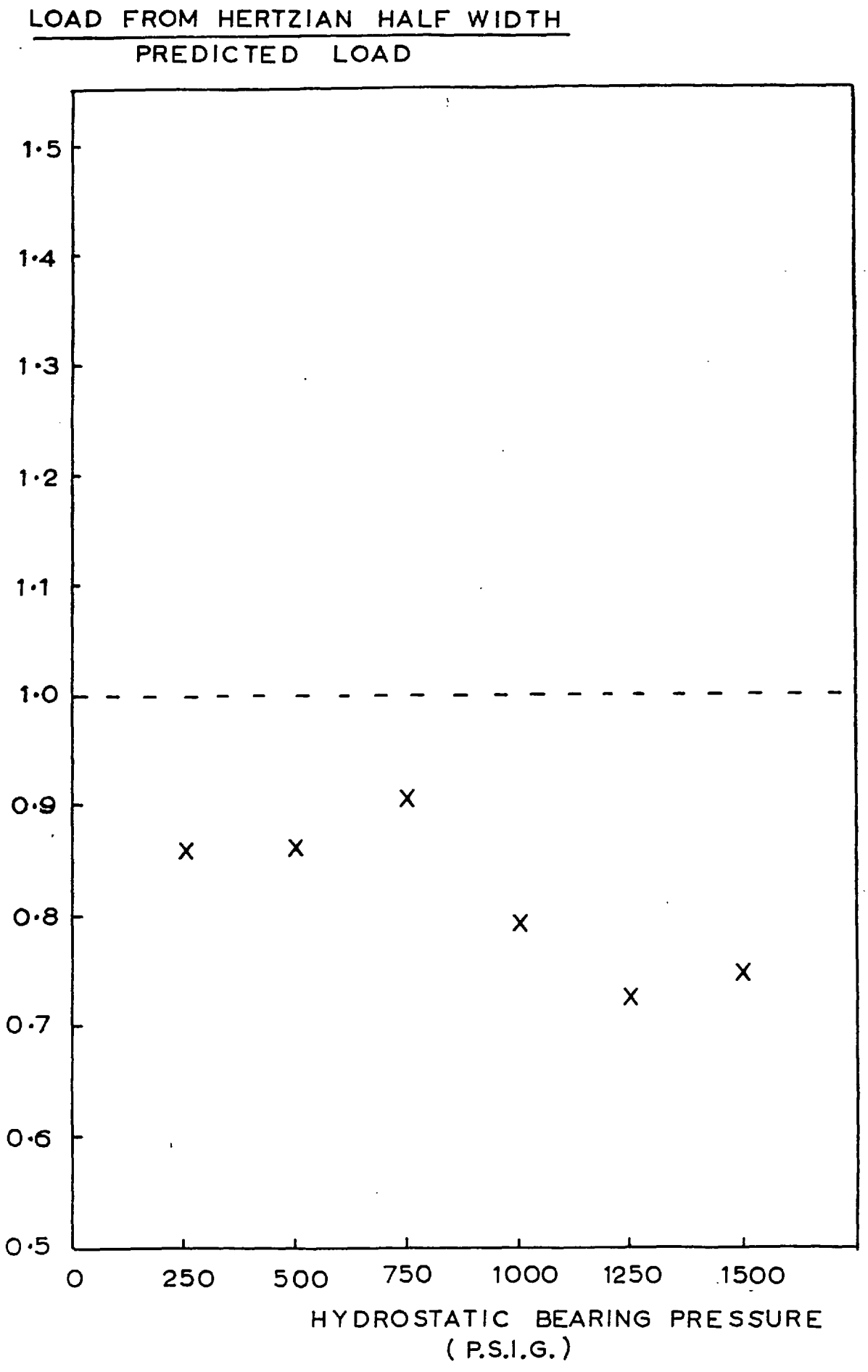

FIG. 4.6. CHECK OF HYDROSTATIC BEARING PERFORMANCE

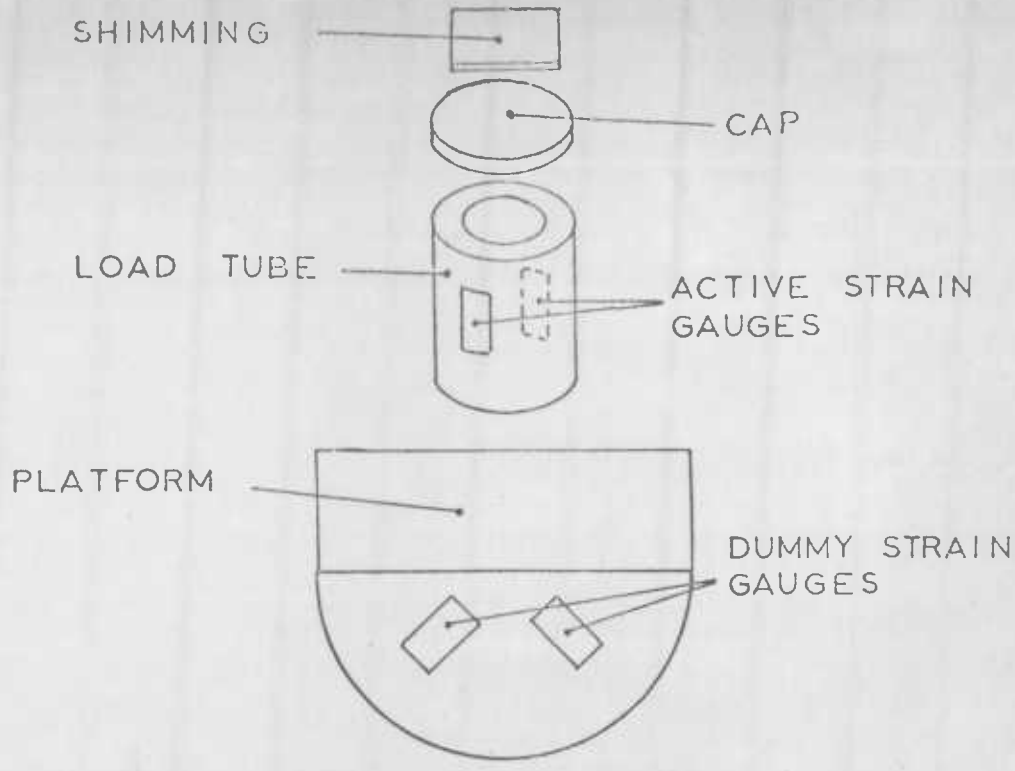

FIG. 4.7. LOAD CELL FOR HYDROSTATIC BEARING CALIBRATION

FIG. 4.8. LOAD CELL IN SITU

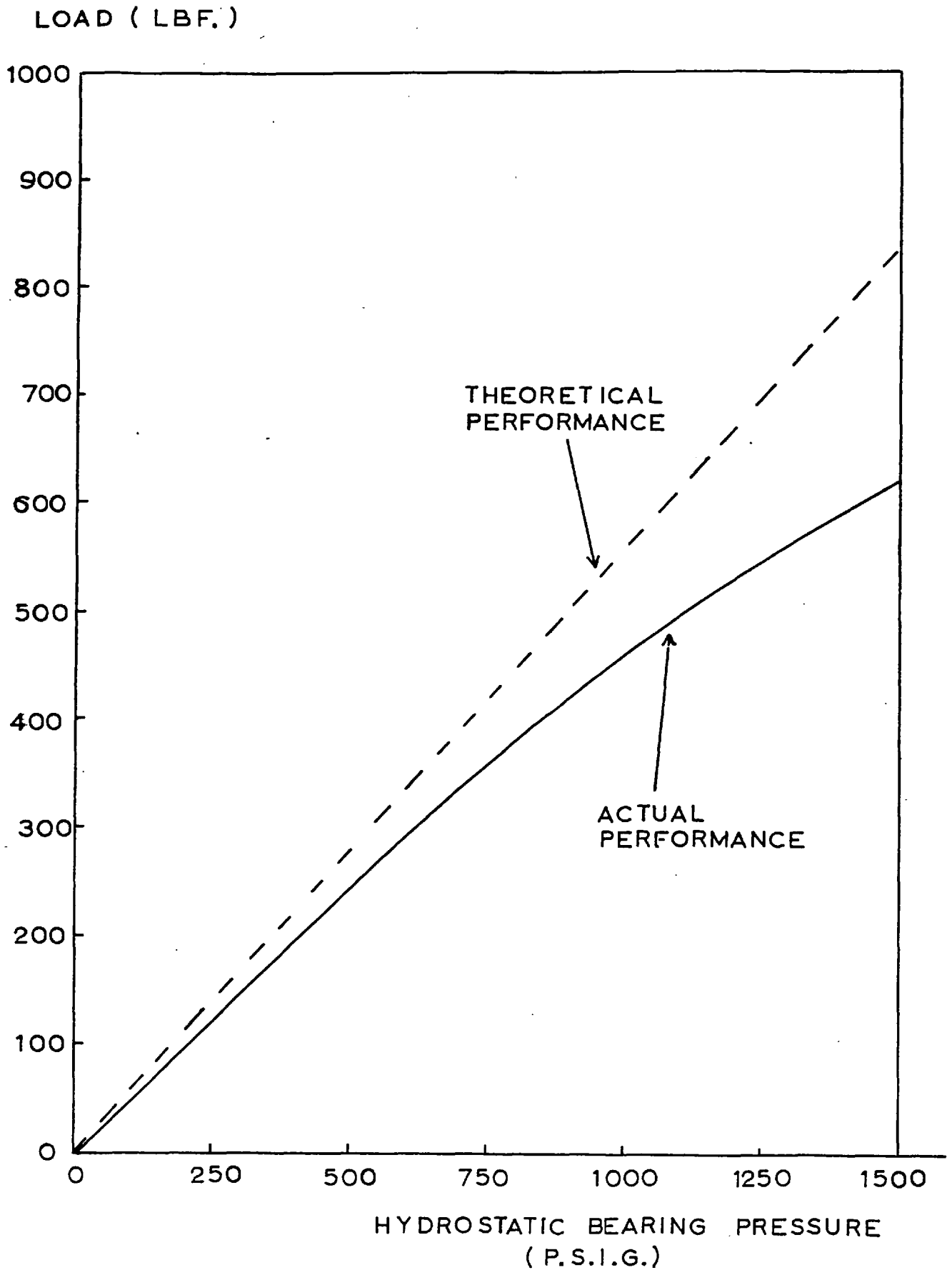

FIG. 4.9. CALIBRATION OF LOAD PRODUCED BY HYDROSTATIC BEARINGS

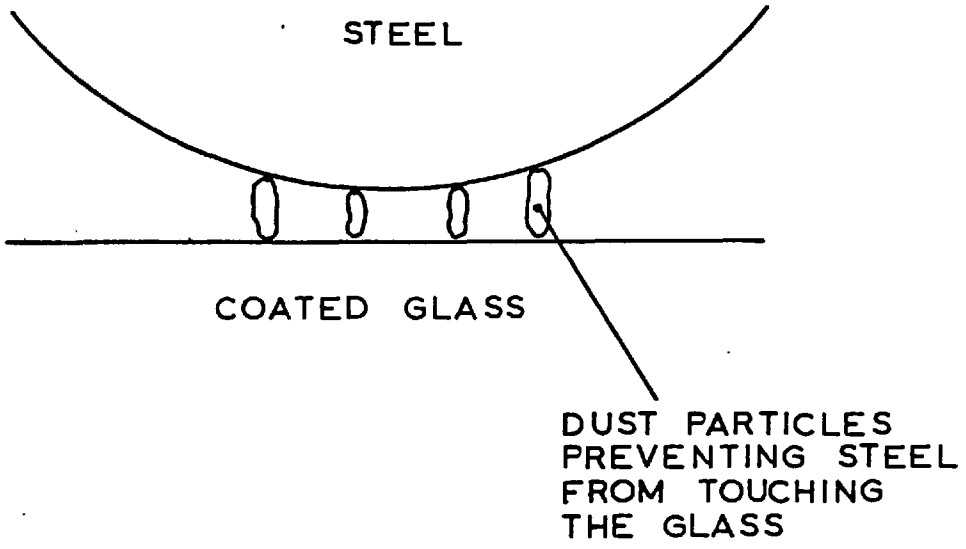

FIG. 4.10. RAISING OF FILM THICKNESS BY DUST PARTICLES

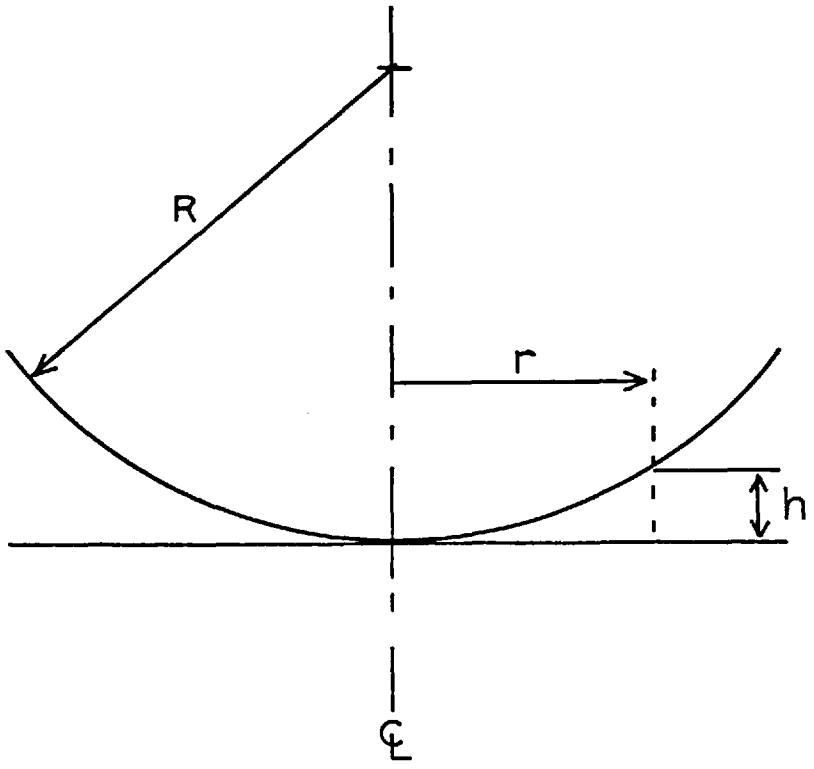

FIG. 4.11. GEOMETRY FOR FILM THICKNESS CALIBRATION

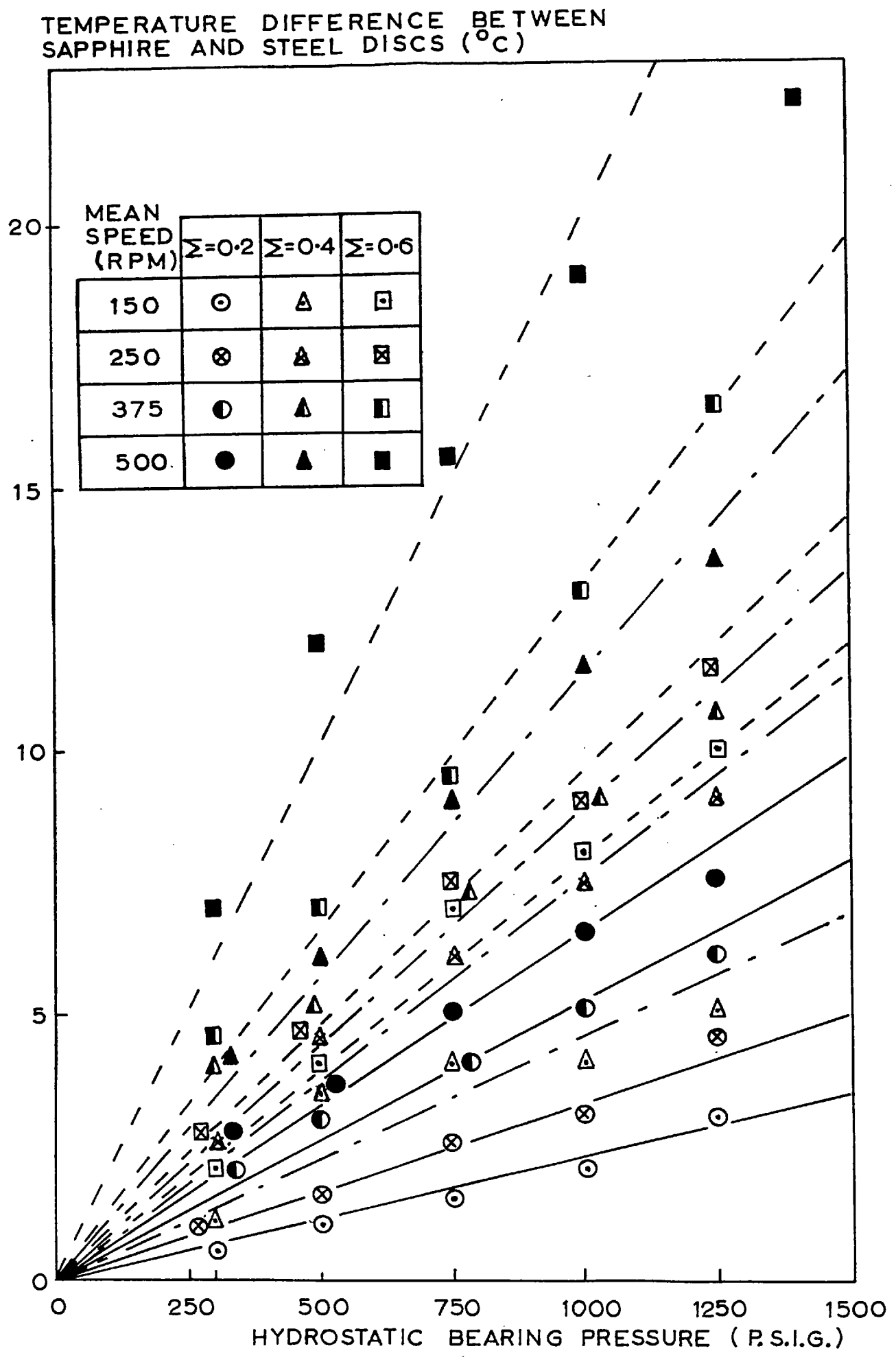

FIG. 4.12. CALIBRATION OF TEMPERATURE DIFFERENCE BETWEEN THE STEEL AND SAPPHIRE DISCS

CHAPTER 4: REFERENCES

1. WYMER D.G. - Ph.D. Thesis, Univ. of London, 1972, and "Elastohydrodynamic Lubrication of a Line Contact", Proc. Inst. Mech. Eng., 1974, Vol. 188, Paper 19/74, pp. 221 - 238.
2. CAST BRONZE HYDROSTATIC BEARING DESIGN MANUAL - Prepared by Harry C. Rippel, Published by the Cast Bronze Bearing Institute Inc., Cleveland, Ohio.
3. WEDEVEN L.D. - Ph.D. Thesis, Univ. of London, 1970.
4. KREITH F. - "Convection Heat Transfer in Rotating Systems", Advances in Heat Transfer, Vol. 5, 1968.
5. SPARROW E.M. and GREGG J.L. - "Heat Transfer From a Rotating Disk to Fluids of any Prandtl Number", Technical Brief, ASME, Journal of Heat Transfer.
6. CARSLAW H.S. and JAEGER J.C. - "Conduction of Heat in Solids", 2nd Edition, Oxford Univ. Press, 1959.
7. FOORD C.A., WEDEVEN L.D., WESTLAKE F.J. and CAMERON A. - "Optical Elastohydrodynamics", Proc. Inst. Mech. Eng., Vol. 184, Part 1, 1969 - 70.

CHAPTER 5

EXPERIMENTAL METHOD

5.1 TRACTION MEASUREMENTS

Prior to the optical investigation of EHD film thickness under varying conditions of rolling and sliding, a series of tests were carried out to determine the behaviour of the lubricant under traction conditions. For this test programme the central sapphire disc was replaced by one made of steel. This was done so that the optical coating on the sapphire was not subject to any premature wear before the measurement of the EHD film thickness was started, and to avoid damage in case of any malfunction of the test apparatus. These tests were considered part of the commissioning procedure for the rig.

5.1.1 Experimental Procedure

Water was circulated through the oil cooler, the pressure controller was set to limit the oil supply to the hydrostatic bearings to approximately 1.72 MN/m^2. (250 p.s.i.) and the oil pump was switched on. At times some hydraulic hammer was apparent but this was eliminated by increasing the setting of the pressure relief valve until the hammering stopped, and then backing off to a position corresponding to approximately 17.2 MN/m^2. (2500 p.s.i.). (As the pressure relief valve was spring loaded a simple resonance had been set up when the pump was first started).

The oil circulated through the hydrostatic bearings and collected in the disc chamber. Thus the oil level in the chamber rose until the oil flowed back to the reservoir via the

overflow pipe. This ensured that all three EHD contacts were completely submerged in oil, hence eliminating any problems due to starvation of the contacts.

The brake motor was switched on and the controller was set to apply a braking torque when the central disc had reached the maximum design speed i.e. under all conditions except that of maximum speed the brake motor was inoperative. The drive motor was then started and its controller adjusted to give the required speed for the outer discs for the particular test. It was very important that the brake motor was switched on before the drive motor because, due to the design of the motor controller circuit, the brake motor effectively locked solid for a fraction of a second when first started. If the outer discs were being driven and consequently driving the central disc, severe damage may have resulted from this instantaneous stoppage.

The system was allowed to settle down until the inlet temperature, as measured by the trailing thermocouple on one of the outer steel discs, had reached a reasonably steady value and the rig could be considered warmed up. The drive motor was then stopped and the inputs to the x-y plotter (from the strain gauges on the torque measuring device and the tachogenerator on the output shaft) were both zeroed. As a check for residual "locked in" torque in the system, the output shaft was rotated back and forth by hand to see if the zero point altered.

The drive motor was then switched on again and the input (driving) speed was read from the digital counter. The sensitivity of the ordinate of the x-y plotter was adjusted so that the signal from the tachogenerator gave a deflection

of the marker pen as close to full scale deflection as possible. The input speed was then marked opposite this point, thus effectively scaling the ordinate. (The output from the tachogenerator was linear and the zero point had also been marked). The abscissa was scaled by noting the sensitivity range of that channel (in mv/cm.); and hence, at a later date, the deflection could be measured, interpreted in terms of a voltage, and converted to a torque using the strain gauge calibration curve previously prepared.

The brake motor controller was then slowly adjusted until braking was just about to start for the selected driving speed. The pressure controller was set to give the required hydrostatic bearing pressure and hence load. By increasing the oil pressure the flow through the hydrostatic bearing was also increased and, as this oil was hotter than the previously stable rig temperature, the disc temperature started to rise - the oil gained heat from work done by the oil pump.

Braking was then initiated to bring the output speed down by approximately 30% in about three to four seconds. This braking rate was found to be the best by trial and error. If the braking was too rapid there might be some rotational inertia effects which would tend to give a temporarily high torque reading and hence a false traction peak. On the other hand, if the braking was too slow the temperature would have risen significantly over that time due to the hot oil through the hydrostatic bearings and the heat generated in the sliding contacts. Over three to four seconds the measured temperature of the steel disc never rose more than $6^{\circ}C$. However for the highest loads, when the temperature of the central disc was measured rises of $15^{\circ}C$ were recorded. As mentioned in Chapter 4 this

was due to more heat being injected into the central disc than the outer discs. This temperature differential between the discs increased even more with time but eventually levelled off to a steady value.

This meant that, at worst, a mean temperature rise of approximately 11°C was experienced, however this did not appear to affect the traction results significantly. A simple test was performed to check this fact. For one run the braking was held at a steady value when the output speed had dropped by approximately 10% (1 second time). After a further few seconds only a very small fall in traction had taken place although the outer disc temperature had risen about 4°C and the central disc temperature by about 14°C.

Several points were taken from the output trace from the x-y plotter and replotted on a different scale so that comparison could be made against other results. This method was chosen in preference to obtaining discrete measurements and then drawing the traction curve for two reasons. Firstly it was possible to ensure that the operating conditions were maintained the same for the whole traction curve (except for the relatively small temperature rise). This meant that the load, input speed and temperature did not have to be re-set for each individual point. Secondly, any traction peak was easily detectable and its shape could be redrawn from the x-y plotter trace.

Traction was also monitored when the optical investigation was being undertaken, but in this case the results were taken as discrete points for differing values of temperature, load, speed and slide/roll ratio.

5.2 ROLLING FILM THICKNESS MEASUREMENTS

A series of tests were carried out to determine the behaviour of the EHD film thickness under pure rolling conditions only. The reason for this was twofold; firstly the results could be plotted and compared against previous workers' results to make sure that there were no obvious anomalies in the behaviour of the experimental rig. Secondly, a set of measurements were then available against which the results for the rolling plus sliding situation could be compared. This is preferable to comparing these results against a theoretical prediction.

Unfortunately it was not possible to obtain conditions of pure rolling as there was a certain amount of friction in the output section. This friction was mainly due to the bearings on the pulley shaft, to which the torque measuring device and the slip ring pick-up were attached, the timing belt drive, and the brake motor itself. The magnitude of the braking effect due to these factors was small, but at low loads and hence low driving torques there was a difference of approximately 3% between the input (driving) speed and the output (driven) speed. At higher loads this difference fell to less than 0.5%.

To obtain pure rolling, both the input and the output shafts would have had to be driven by their respective motors. In this way the friction losses would have been eliminated. However to do this would have required modifications to the motor system; this would have raised doubts about the stability of such a configuration as the major driving torque would be alternating between one motor and the other. For these reasons, and the fact that it was thought that the small

speed differences would not significantly affect the validity of the results, this modification was not attempted. Thus the results obtained by the following experimental method were assumed to represent pure rolling.

5.2.1 Experimental Procedure

The start up procedure was the same as for the traction experiments with the exception that the brake motor was left switched off. The braking system was thus inoperative and free to rotate. Before the main series of tests a very crude test was carried out to get a "feel" for the results.

For a given hydrostatic bearing pressure the input speed was gradually increased until the first yellow fringe was visible through the microscope; the speed and the disc temperature were noted. This was repeated for all the coloured fringes up to the third green fringe.

In this way when a particular coloured fringe was seen during the main test (for example a red fringe) it was possible to know whether this was the first, second, or third red fringe by reference to this crude table, and not have to count the fringes from zero speed up to the measured speed. For the main series of tests the procedure was as follows.

It was always ensured that the steady state temperature of the rig before a measurement was taken was at least $10^{o}C$ below the temperature at which the measurement was wanted. This was done so that there was sufficient time to prepare to take a measurement after the controls were set - the influx of hot oil caused the temperature to rise. The input speed was adjusted to the desired value and the oil pressure controller set to give the required load. The tem-

perature was watched until it had reached the value at which the result was wanted. At this point the interference fringe was examined and its colour noted as well as the output speed and the small amount of torque due to friction losses on the output side. The last two readings were only taken as a check that the speeds were close to pure rolling. The interference fringe was not classed purely as one colour but was subjectively described as one colour with a proportion of another e.g. 75% of first blue with 25% of first red. A simple linear interpolation was then used to assign a film thickness to this measurement. In this way it was possible to give a more accurate description of film thickness.

The reason for this method, rather than the more usual practice of altering the test conditions (normally the speed) until a true colour is obtained for the interference fringe, was that future rolling plus sliding results could be directly compared against the pure rolling results for similar conditions of speed, load, and temperature. Hence a more accurate impression of the effect of sliding could be obtained by this method than by comparing the parameters necessary to produce the same interference fringe.

5.3 ROLLING PLUS SLIDING FILM THICKNESS MEASUREMENTS

It was decided to adopt three different slide/roll ratios for the rolling plus sliding measurements. For any given slide/roll ratio the input and output speeds were chosen such that their mean speed corresponded with one of the speeds used in the pure rolling experiments.

The outer disc temperatures that were used were the same as for the pure rolling case. However in this case the

mean inlet temperatures were not exactly the same, as the central sapphire disc was now hotter than the outer discs.

5.3.1 Experimental Procedure

The experimental method was the same as for the pure rolling measurements except that,as for the traction results, the brake motor was switched on before the drive motor. Now, however, before the hydrostatic bearing pressure was increased, the input and output speeds were set to the required value. This procedure was adopted because it took a finite time to set the motor controllers and, if the oil pressure was high, the combination of hot incoming oil and frictional heating would probably cause the temperature to overshoot the required value. When the speeds had been set the oil pressure was quickly increased.

As before it was ensured that initially the temperature was well below the required temperature for the measurement. In this case it was doubly important as sufficient time had to be allowed for the temperature differential between the central and outer discs to reach a steady value, otherwise the previously derived empirical relationship describing this differential would not be valid. The film thickness was then measured.

The input and output speeds were then re-checked as a change in the load (and hence torque) affected these settings slightly and they drifted from their original values. The torque was noted and was examined to ensure that there had been no rapid rise that might be associated with surface to surface contact.

5.4 TEST PROGRAMME

The aim of the investigation was to compare the EHD film thicknesses under pure rolling and rolling plus sliding for a broad spectrum of loads, speeds, slide/roll ratios and temperatures. Most analyses of the traction phenomenon have assumed that the EHD film thickness can be predicted by the same formulae as used for the pure rolling case. However there is a lack of accurate experimental evidence to back this assumption, especially at low film thicknesses.

The investigation was limited to one oil in order that most of the operating conditions encountered by other workers could be covered, albeit for different fluids. The oil used was a paraffinic oil as described in Chapter 4.

Accordingly tests were performed at four input speeds of 150 r.p.m., 250 r.p.m., 375 r.p.m., 500 r.p.m., six loads corresponding to hydrostatic bearing pressures of 1.72, 3.45, 5.17, 6.09, 8.62 and 10.3 MN/m^2 (250, 500, 750, 1000, 1250 and 1500 p.s.i.), three slide/roll ratios of 0.2, 0.4, 0.6 and generally thirteen temperatures ranging between 30°C and 60°C in 2½°C steps, although this varied occasionally.

The limiting factors placed on the tests were either EHD film thicknesses which were too low to be measured (corresponding to high temperature or low speed or both), or a tendency for the oil film between the correction lens and the sapphire disc to break up (this sometimes occurred as the viscosity decreased and the speed increased) hence obliterating the view of the interference fringe.

The whole test programme was a comprehensive one. In all some 1300 results were taken.

CHAPTER 6

RESULTS

The results are presented in two sections, the first contains traction data of which the majority refers to a steel/steel contact (i.e. the central sapphire disc was replaced by one made of steel). The second section contains the film thickness data for both the pure rolling and rolling plus sliding cases. In all cases the film thickness presented is the central film thickness.

6.1 TRACTION DATA

In general the rolling speeds used for the steel/steel disc configuration were higher than those used for the sapphire/steel disc configuration. The steel/steel tests were the first part of the investigation and at that time no data on the film thickness behaviour had been obtained other than theoretical predictions. For this reason the rolling speeds were kept high in order to ensure that a thick EHD film was present and hence to minimise the risk of damage to the surfaces. Although EHD theory predicts that the presence of sliding should not affect film thickness for the same values of mean speed, temperature and load as used for pure rolling, it was thought that the use of these higher speeds was a worthwhile precaution.

As mentioned previously, the traction data was taken from the output trace of an x-y plotter where one axis represented the torque and the other axis represented the speed of the central (braked) disc. A copy of a typical trace from the x-y plotter for a maximum Hertzian pressure of 1.117 GN/m^2

is shown in Fig. 6.1 and it can be seen that, although there are small signal oscillations present, the shape of the traction curve is easily discernible, and that a mean line representing traction can be drawn quite accurately. Point B represents a disc speed of approximately 60% of the initial speed at point A. This trace shows no sign of a traction peak and all the other traces that were obtained showed a similar lack of traction peak.

In Figs. 6.2 to 6.9 the traces from the x-y plotter have been redrawn on common axes of slide/roll ratio

$$\Sigma = \frac{\text{sliding speed}}{\text{mean rolling speed}} = \frac{(U_1 - U_2)}{\frac{1}{2}(U_1 + U_2)}$$

(where U_1, U_2 are the speeds of the outer and inner discs respectively) and coefficient of traction $f = \frac{\text{traction force}}{\text{normal force}}$. This enables an easier comparison of the effects of differing values of load, temperature and rolling speed.

When the central steel disc was replaced by one made of sapphire a similar lack of a traction peak was noticed and, rather than risk damage to the optical coating, a full series of traction tests was not attempted. Instead the traction data for the sapphire/steel disc configuration was taken as discrete points at predetermined values of slide/roll ratio in the course of the optical investigation. These discrete point readings were not taken on the rising part of the traction curve but were taken at slide/roll ratios which corresponded to what might be called the "plateau" region.

During early tests which were performed as a preliminary part of the optical investigation, it was realised that an anomalous behaviour in the EHD film thickness seemed to be

apparent at lower values of film thickness (Figs. 6.17 to 6.19), and so the majority of the optical investigation was concentrated in this region. A consequence of this is that the rolling speeds employed were of a lower value than those for the previous traction tests, this meant that only at one speed was traction data available for both the steel/steel and steel/sapphire disc configurations. A comparison of the two sets of data is given in Fig. 6.10 for a load of 2046 N (equivalent to a maximum Hertzian pressure of 0.956 GN/m^2 for the all steel configuration).

Although the mean speed stayed constant for the sapphire/steel disc configuration (as the central disc was braked the outer discs were speeded up), it was not constant for the all steel configuration. In this case the outer discs were maintained at the same speed while the central disc was braked, and so the mean speed dropped. Also, due to the difference in Young's Modulus between steel and sapphire the Hertzian pressures were approximately 15% higher for the sapphire/steel situation even though the loads were the same.

These factors meant that the steel/steel and sapphire/steel disc configurations did not experience exactly the same conditions for similar loads and nominally similar mean speeds. However it is thought that these differences do not significantly affect the results and that they may be compared against each other.

A plot of traction results for the sapphire/steel disc configuration is given in Fig. 6.11. It can be seen that, even for the conditions of a lower speed (0.399 m/sec) and a higher load (2780 N) which would help to promote a traction peak, one is not apparent.

Although traction data was available for a large range of operating conditions it is not all plotted here as the primary purpose of this investigation was to examine EHD film thickness behaviour.

In all cases the temperature that is quoted on the graphs is the temperature of the outer discs (and central disc) at the start of the test run. No allowance has been made for frictional heating and consequent increase in temperature.

6.2 FILM THICKNESS MEASUREMENTS

Prior to the optical investigation of film thickness under rolling and sliding conditions, measurements were taken for the "pure" rolling case. (This was not in fact pure rolling, but involved up to 3% slip for the lower loads but less than 0.5% slip for the higher loads due to bearing friction, as is explained in Chapter 5). A selection of photomicrographs can be seen in Fig. 6.12 and the full interpreted results are given in Figs. 6.13 to 6.16. These take the form of a double logarithmic plot of central film thickness against load for the four basic speeds and several temperatures. This method of plotting was chosen so that comparison could be made with the work of KANNEL and BELL (1) and PARKER and KANNEL (2). Kannel and Bell showed a greater dependence of film thickness on load than suggested previously for a mineral oil at Hertzian pressures between 0.55 GN/m^2 and 1.21 GN/m^2 and speeds up to 46.2 m/sec ; whereas Parker and Kannel showed that this greater load dependence was only apparent at pressures above approximately 1.5 GN/m^2 for a synthetic paraffinic oil at speeds up to 37.6 m/sec.

A selection of the experimental results is also

plotted in two other common forms. Figs. 6.17 and 6.18 show a double logarithmic plot of central film thickness against the parameter $U.\eta_o$ where U = disc surface velocity and η_o = inlet viscosity, this has been done for loads of 512 N and 2046 N respectively. Fig. 6.19 shows a double logarithmic plot of central film thickness against the parameter $U.\alpha.\eta_o$ (where α = pressure/viscosity coefficient) for a load of 2046 N.

After having taken these initial measurements for rolling, the procedure was repeated for values of slide/roll ratio of 0.2, 0.4, and 0.6; the mean rolling speed remaining constant. A selection of these results is presented in Figs. 6.20 to 6.23, again in the form of a double logarithmic plot of film thickness against load. These results are a representative selection but due to the large number of results available (nearly 1300) it was thought superfluous and possibly confusing to present them all in this form, although they are all used in the plots presented in Chapter 7.

In Chapter 4 it was mentioned that, knowing the temperature of the sapphire disc to be greater than that of the steel discs, a correction could be applied to the measured film thickness using a relationship given by WYMER (3). This has been done for all the results obtained in these experiments. Hence a theoretical allowance has been made for the fact that the mean temperature of the discs is greater than that measured for the steel discs alone. This enables a comparison to be made between the rolling results (also presented in Figs. 6.20 to 6.23) and the sliding results for a given set of conditions.

A double logarithmic plot of central film thickness

against the parameter $U.\eta_o$ is presented for two specific cases:-

(a) 0.665 m/sec mean rolling speed and 2046 N load.

(b) 0.399 m/sec mean rolling speed and 2402 N load.

Figs. 6.24 and 6.25 show plots of these results for pure rolling and slide/roll ratios of 0.2 and 0.6. For the sliding results a plot of film thickness against the parameter $U.\alpha.\eta_o$ is not shown as this method does not appear to give any further insight than does the plot of film thickness against the parameter $U.\eta_o$.

It is clear from these measurements of optical film thickness, especially those presented in Figs. 6.17, 6.18 and 6.19, that some sort of anomalous behaviour is taking place at low values of central film thickness. This will be discussed in the next chapter where an explanation for both the fall in film thickness at the lower values under pure rolling, and also the discrepancy between the rolling and rolling plus sliding results will be proposed.

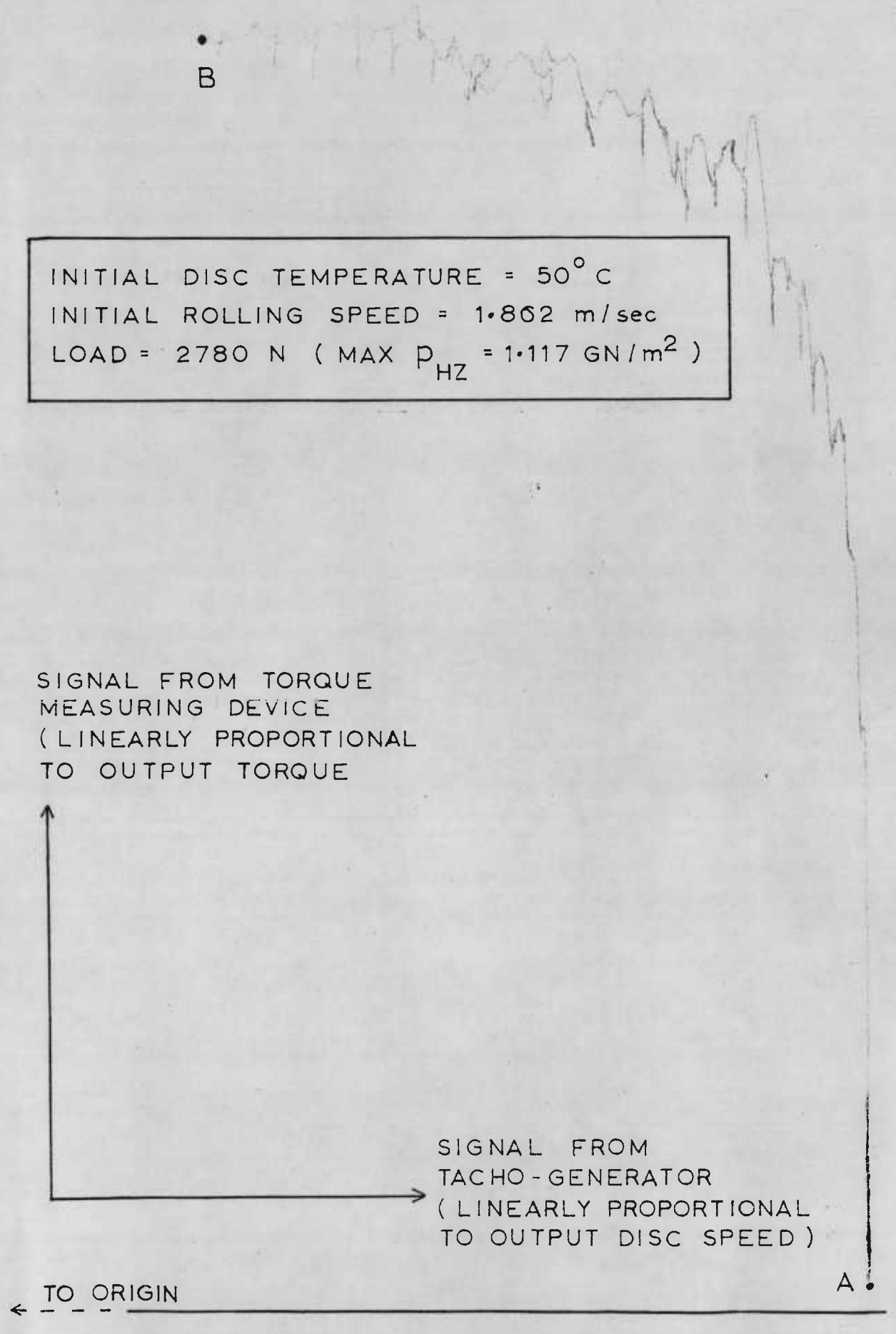

FIG. 6.1. A TYPICAL TRACTION TRACE FROM THE X-Y PLOTTER

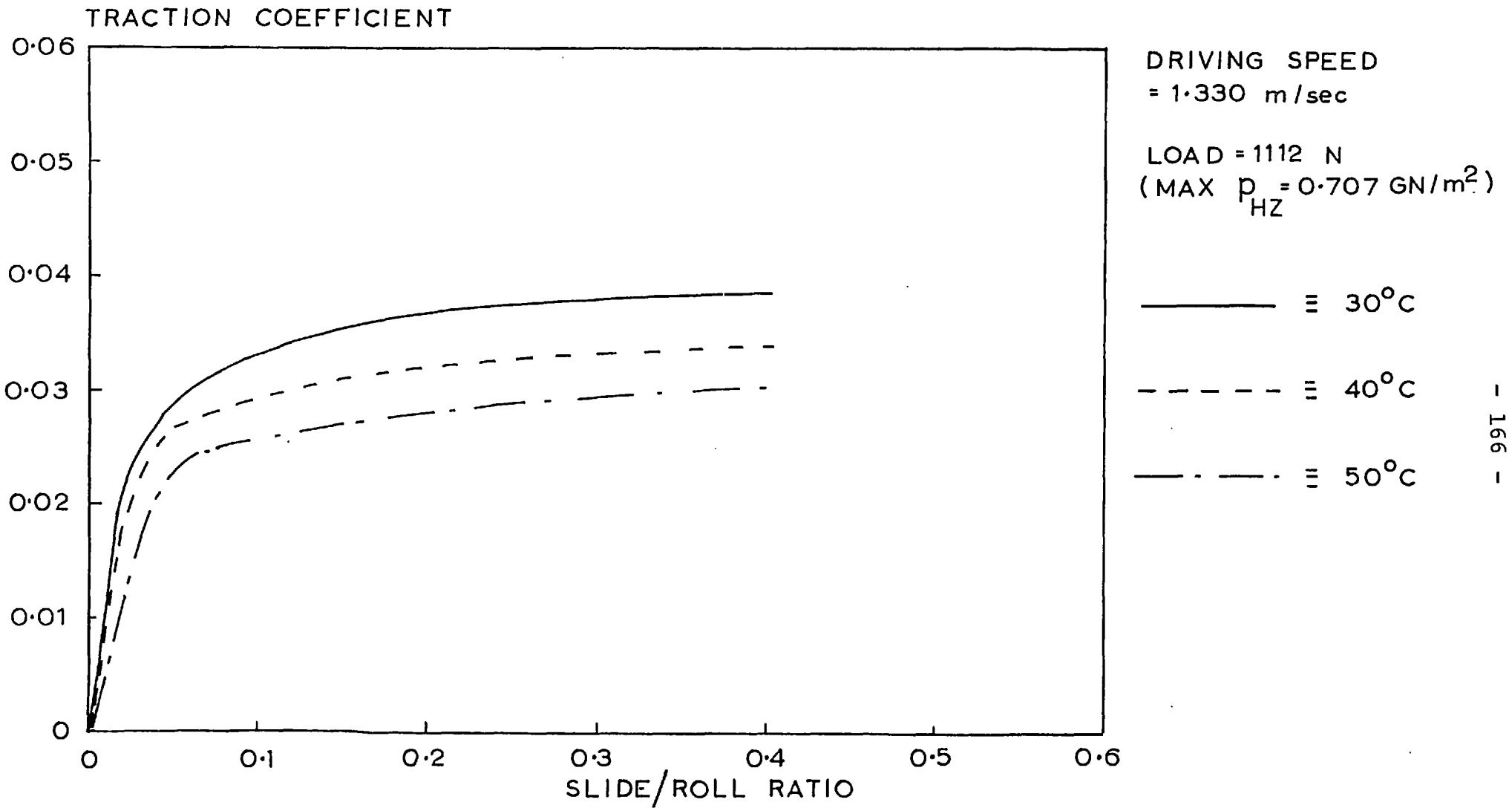

FIG. 6.2. TRACTION CURVES FOR A STEEL/STEEL DISC CONFIGURATION

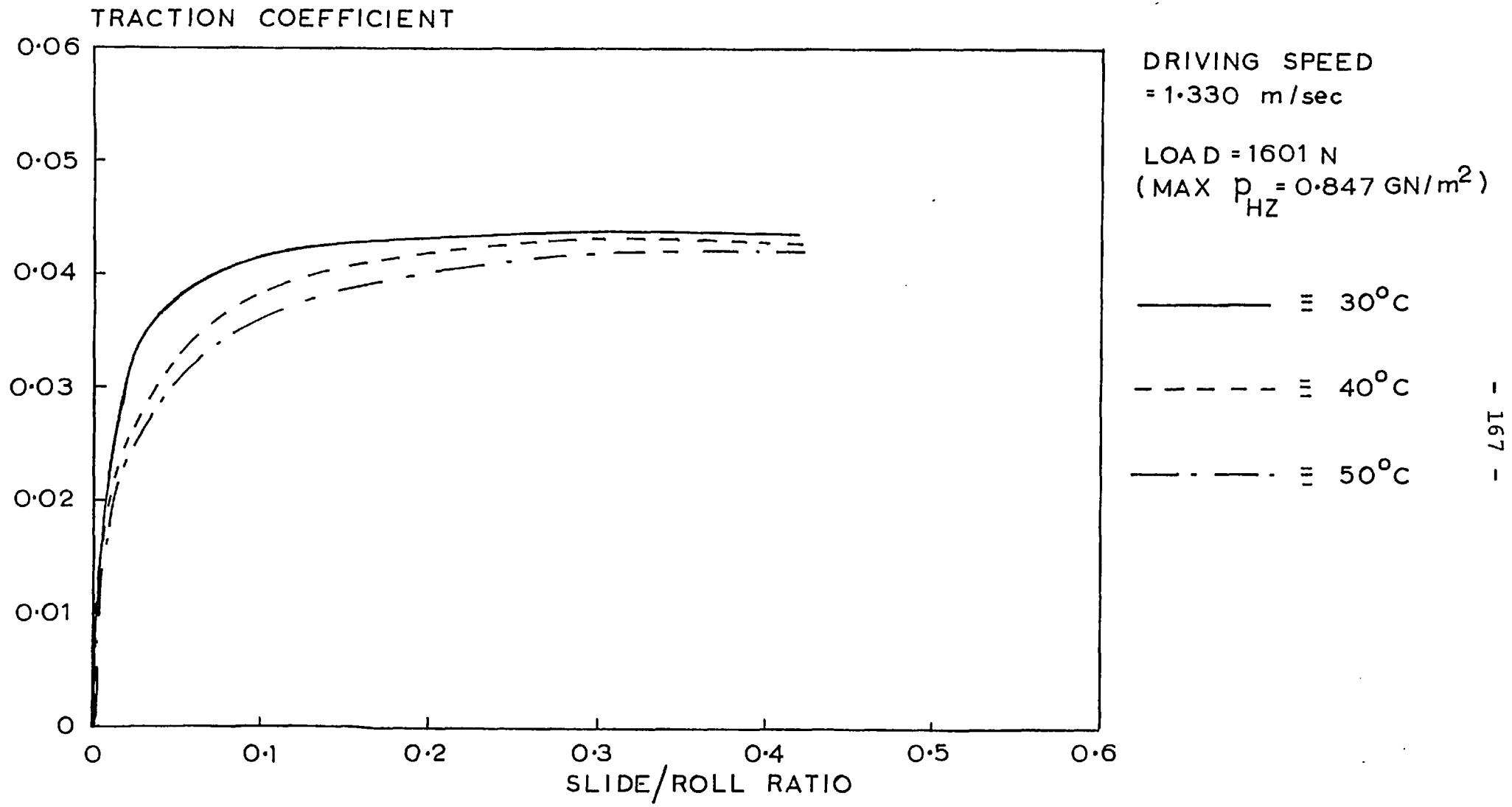

FIG. 6.3. TRACTION CURVES FOR A STEEL/STEEL DISC CONFIGURATION

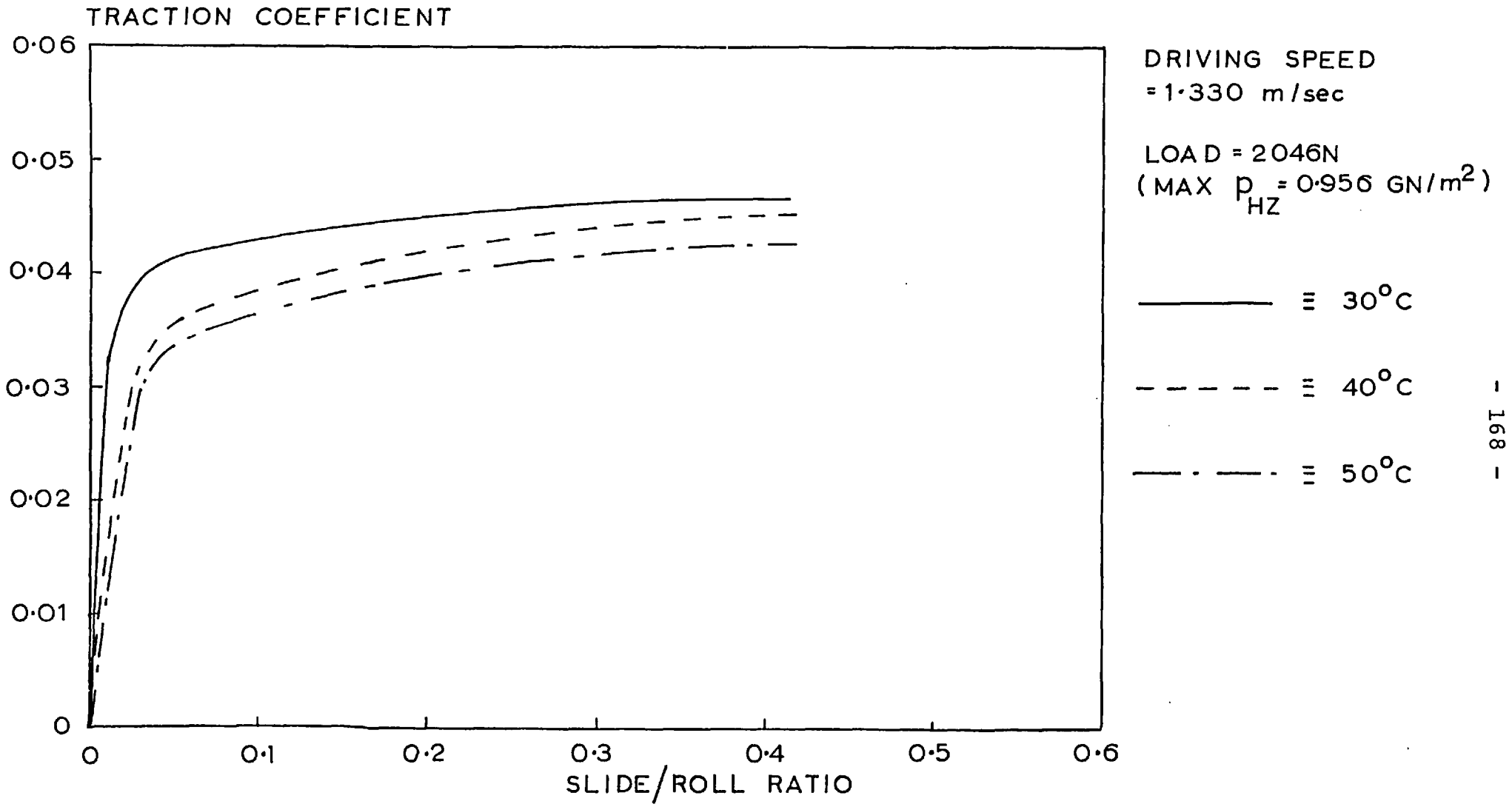

FIG. 6.4. TRACTION CURVES FOR A STEEL/STEEL DISC CONFIGURATION

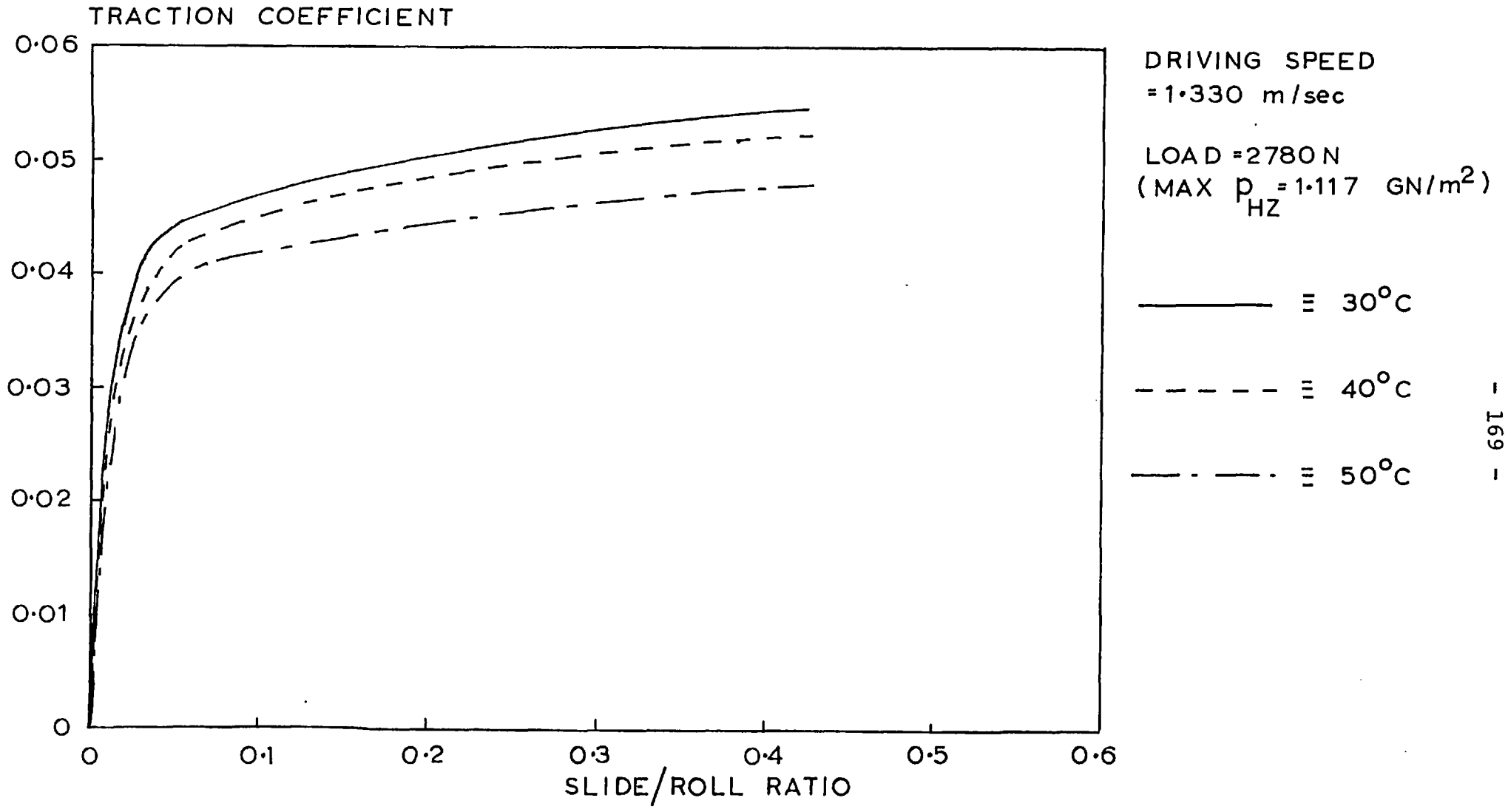

FIG. 6.5. TRACTION CURVES FOR A STEEL/STEEL DISC CONFIGURATION

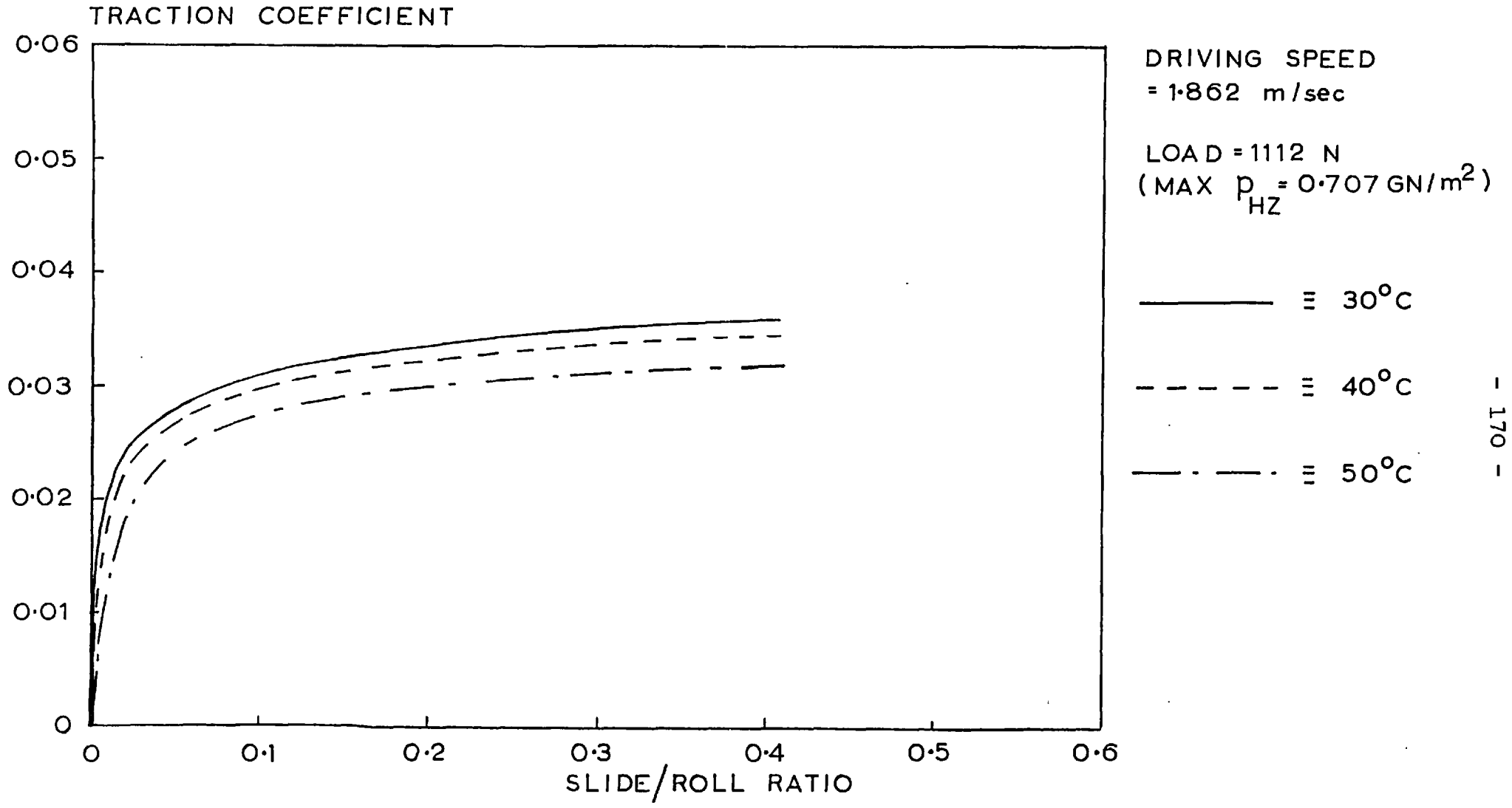

FIG. 6.6. TRACTION CURVES FOR A STEEL/STEEL DISC CONFIGURATION

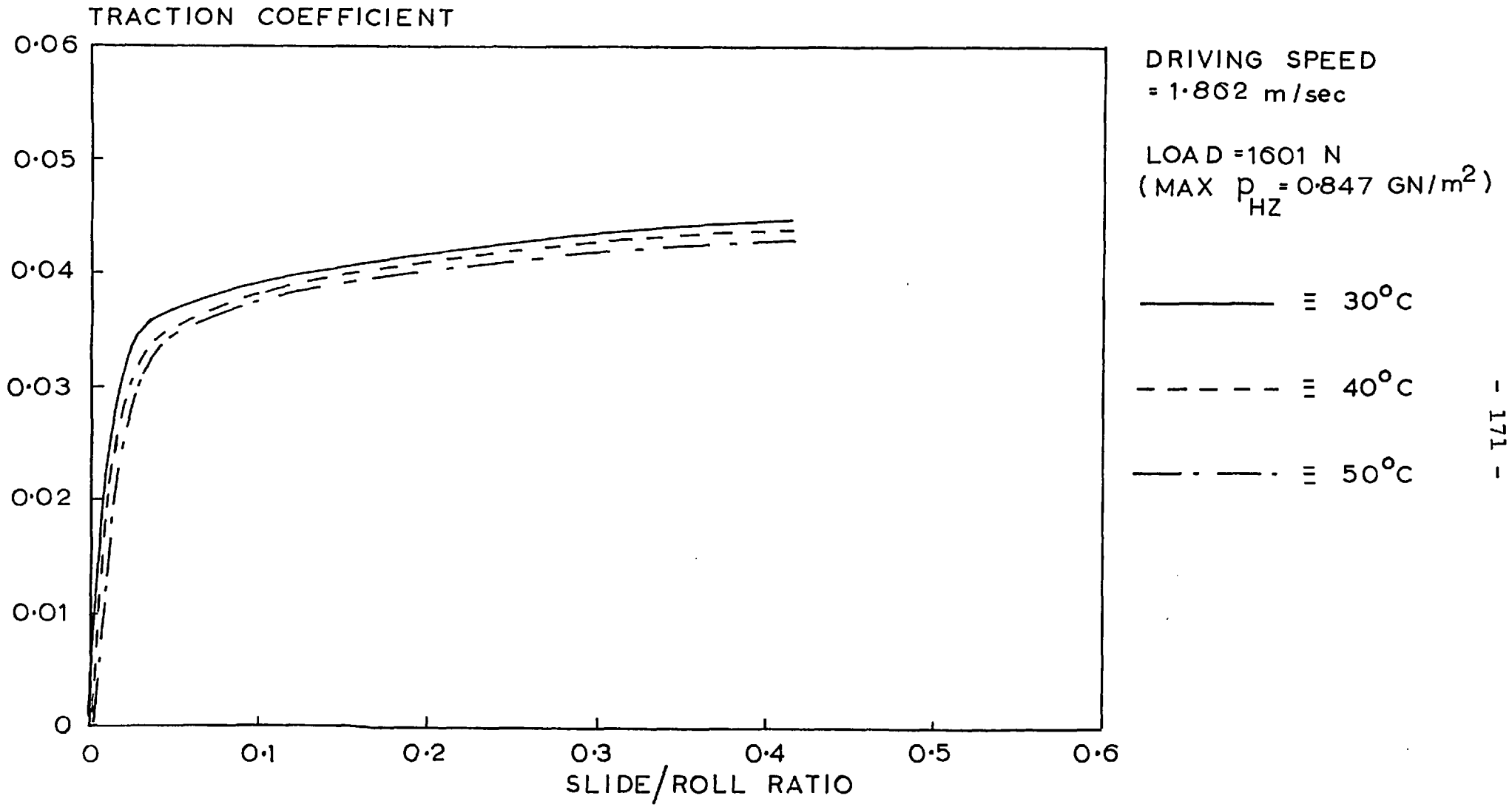

FIG. 6.7. TRACTION CURVES FOR A STEEL/STEEL DISC CONFIGURATION

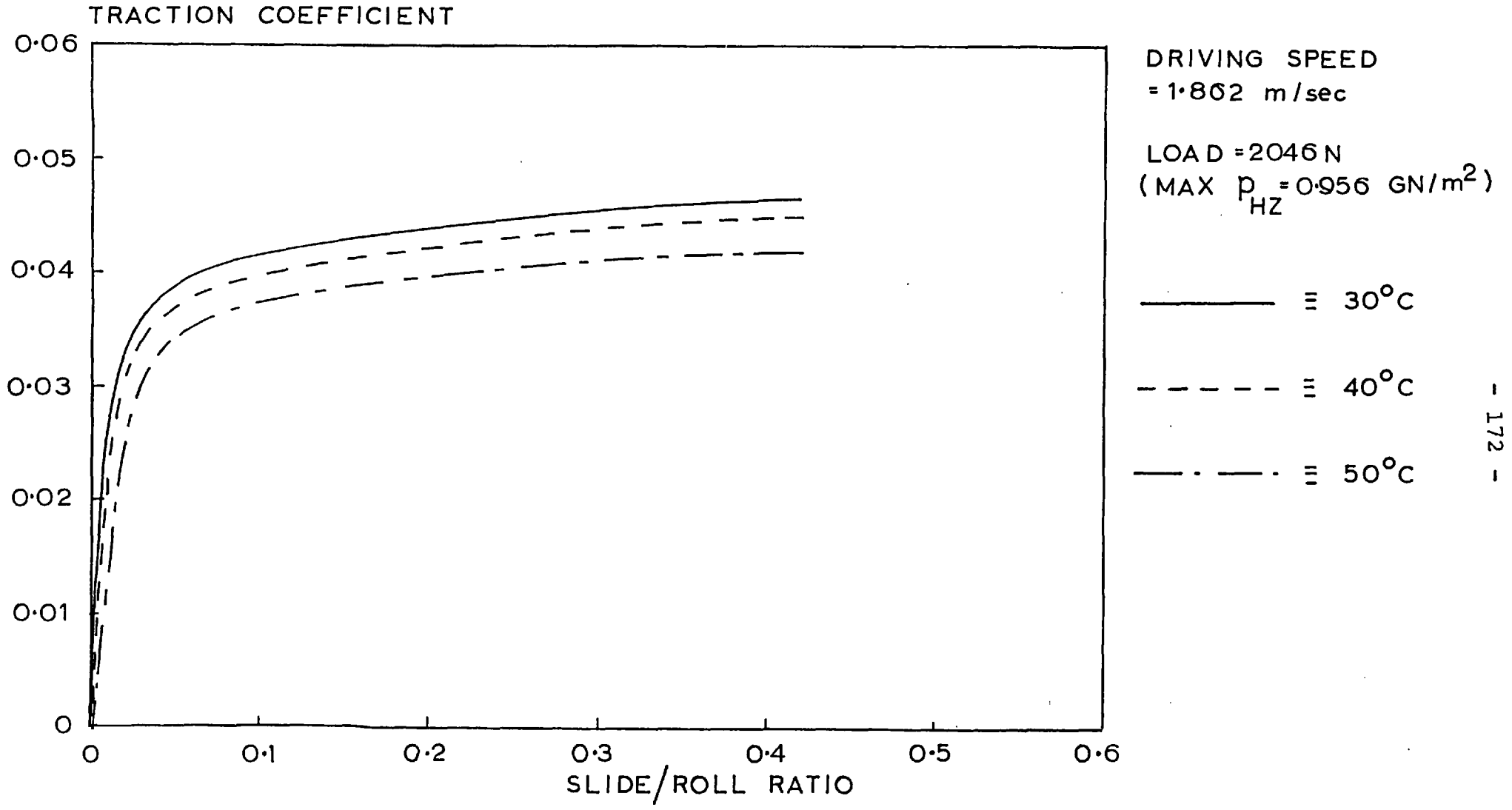

FIG. 6.8. TRACTION CURVES FOR A STEEL/STEEL DISC CONFIGURATION

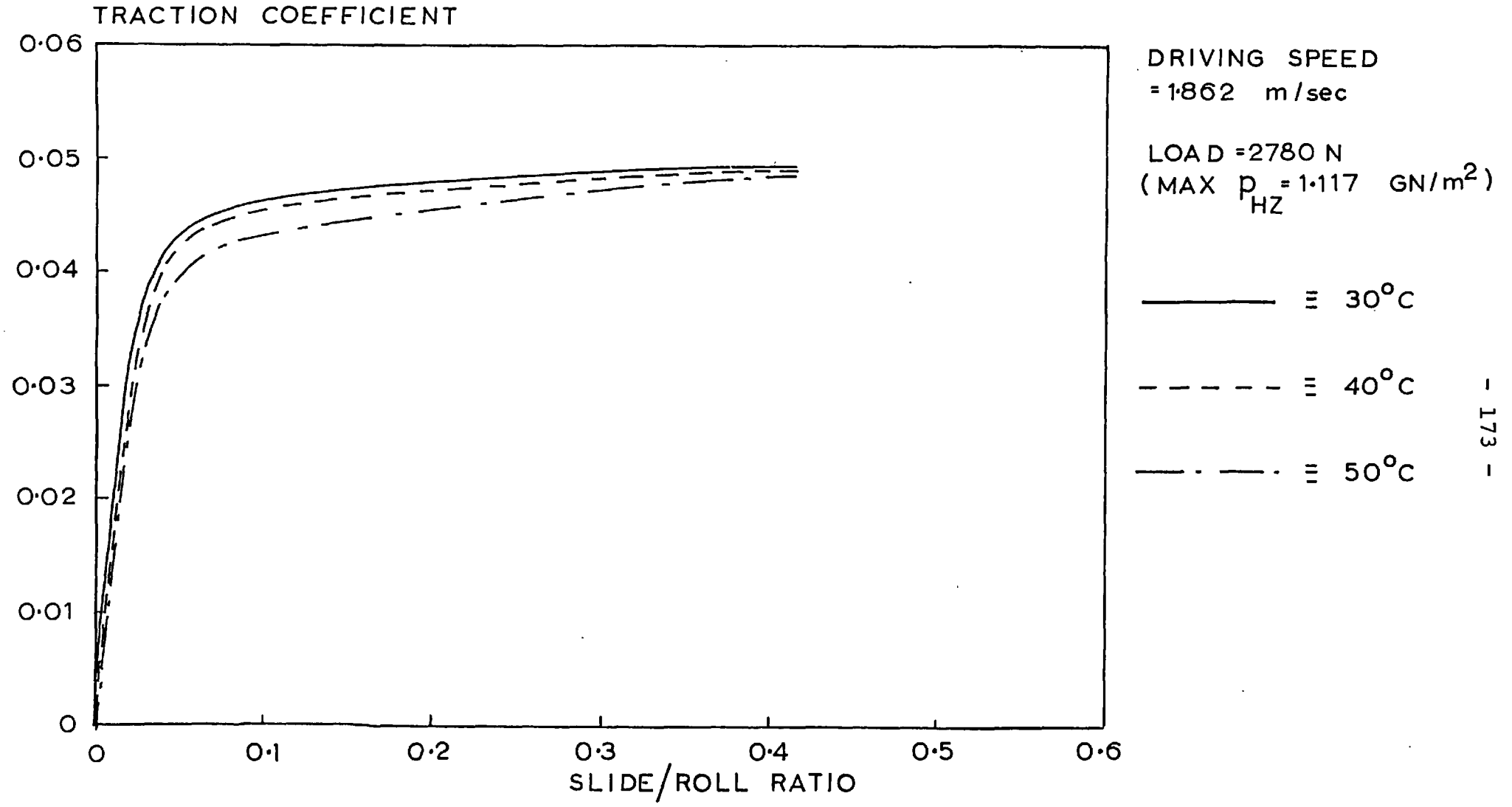

FIG. 6.9. TRACTION CURVES FOR A STEEL/STEEL DISC CONFIGURATION

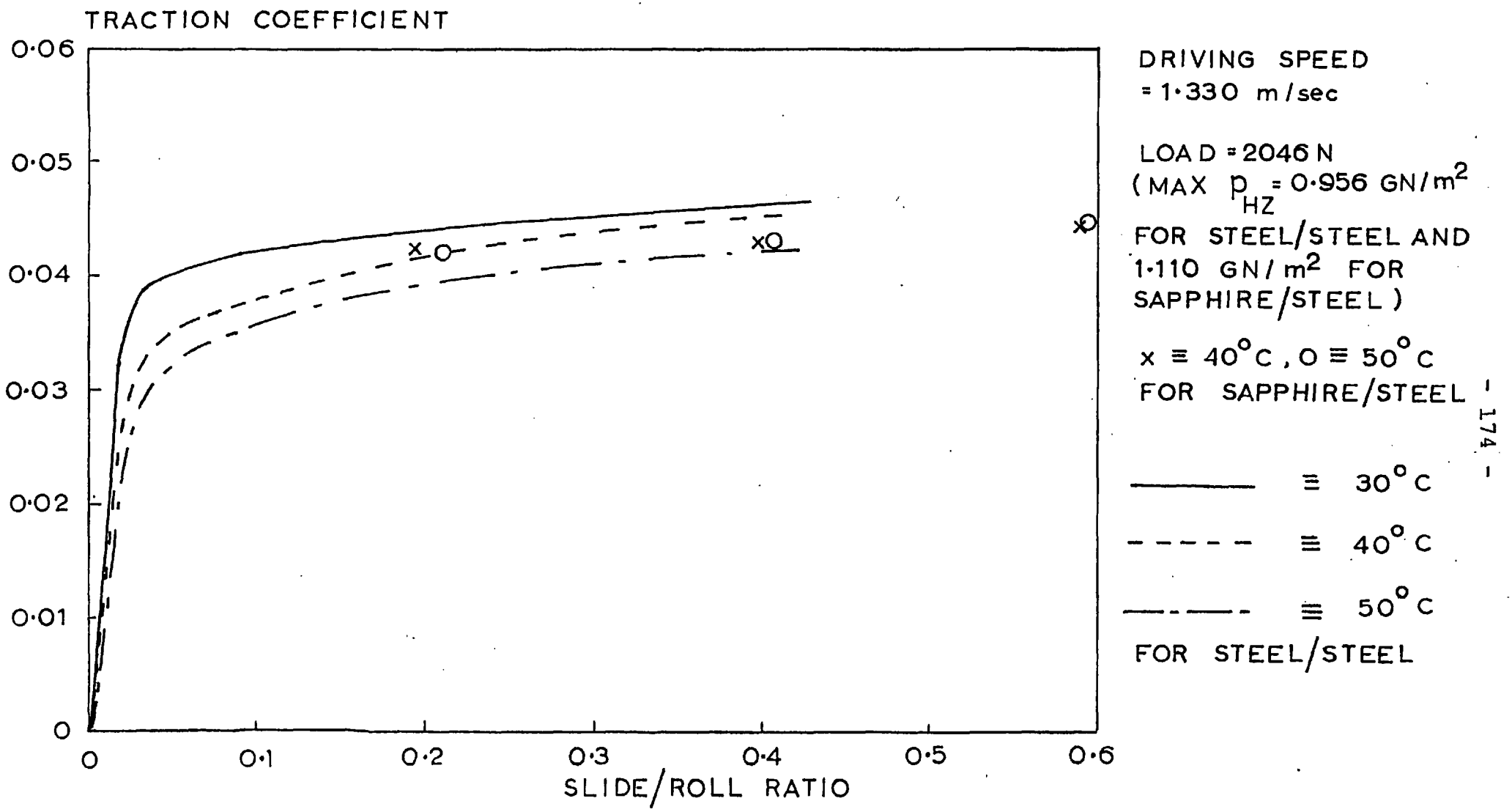

FIG. 6.10. COMPARISON OF TRACTION DATA FOR STEEL/STEEL AND SAPPHIRE/STEEL DISC CONFIGURATIONS

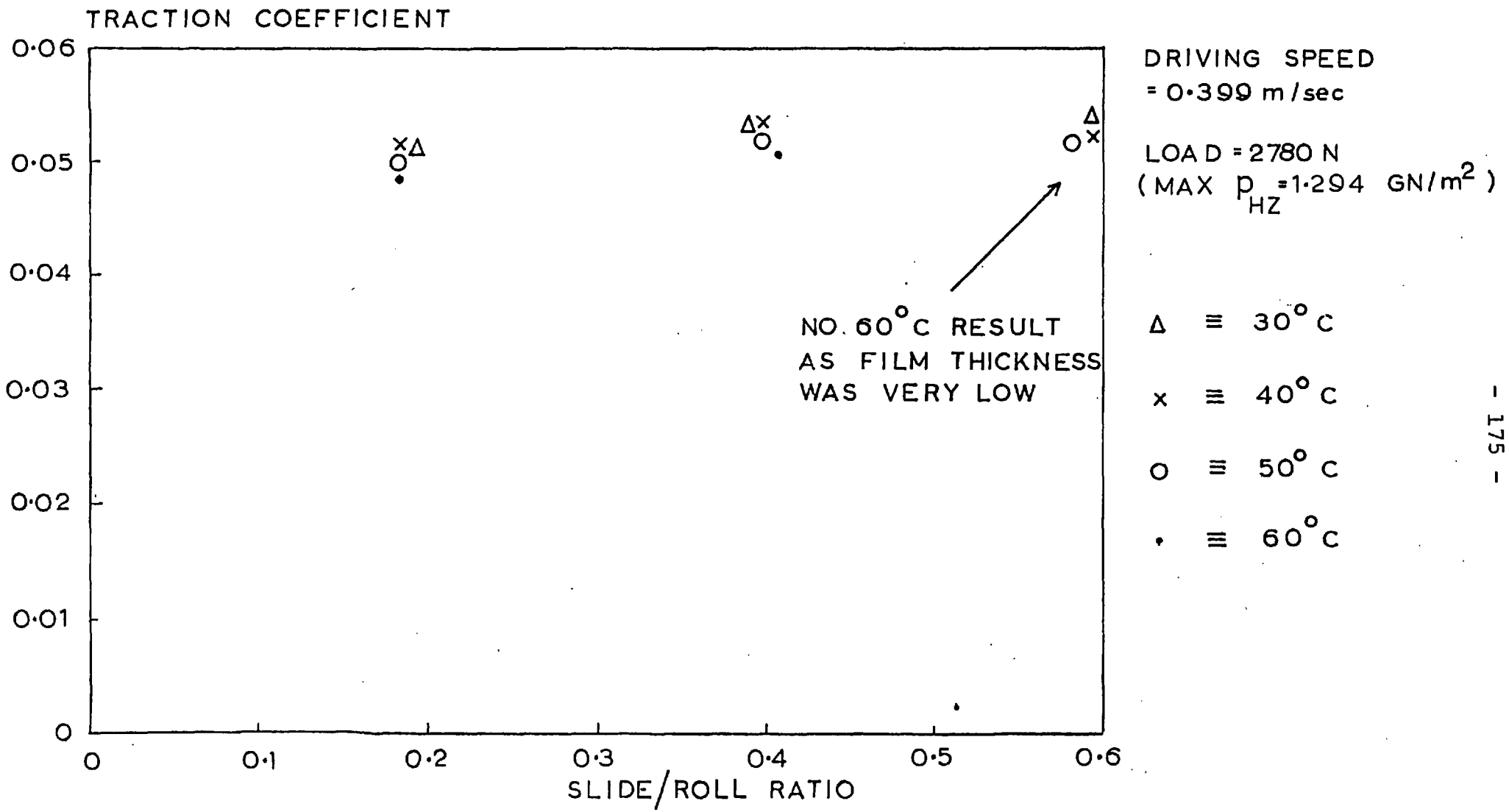

FIG. 6.11. TRACTION PLOTS FOR A SAPPHIRE/STEEL DISC CONFIGURATION

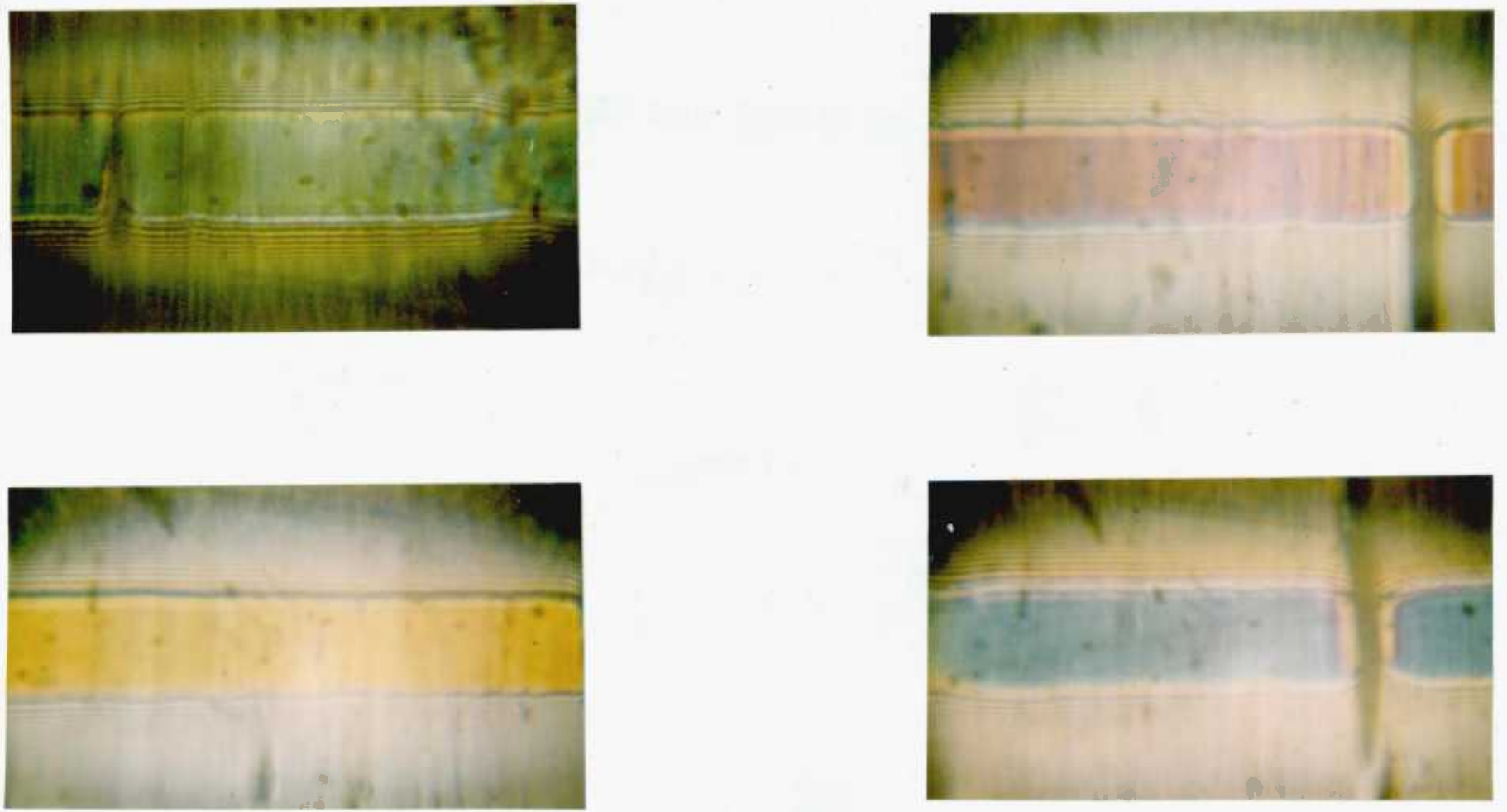

FIG. 6.12. TYPICAL PHOTOMICROGRAPHS OF THE EHD CONTACT

SPEED = 0·399 m/sec

• ≡ 25°C, 35°C, 45°C, 55°C x ≡ 27·5°C, 37·5°C, 47·5°C, 57·5°C

o ≡ 30°C, 40°C, 50°C, 60°C Δ ≡ 32·5°C, 42·5°C, 52·5°C

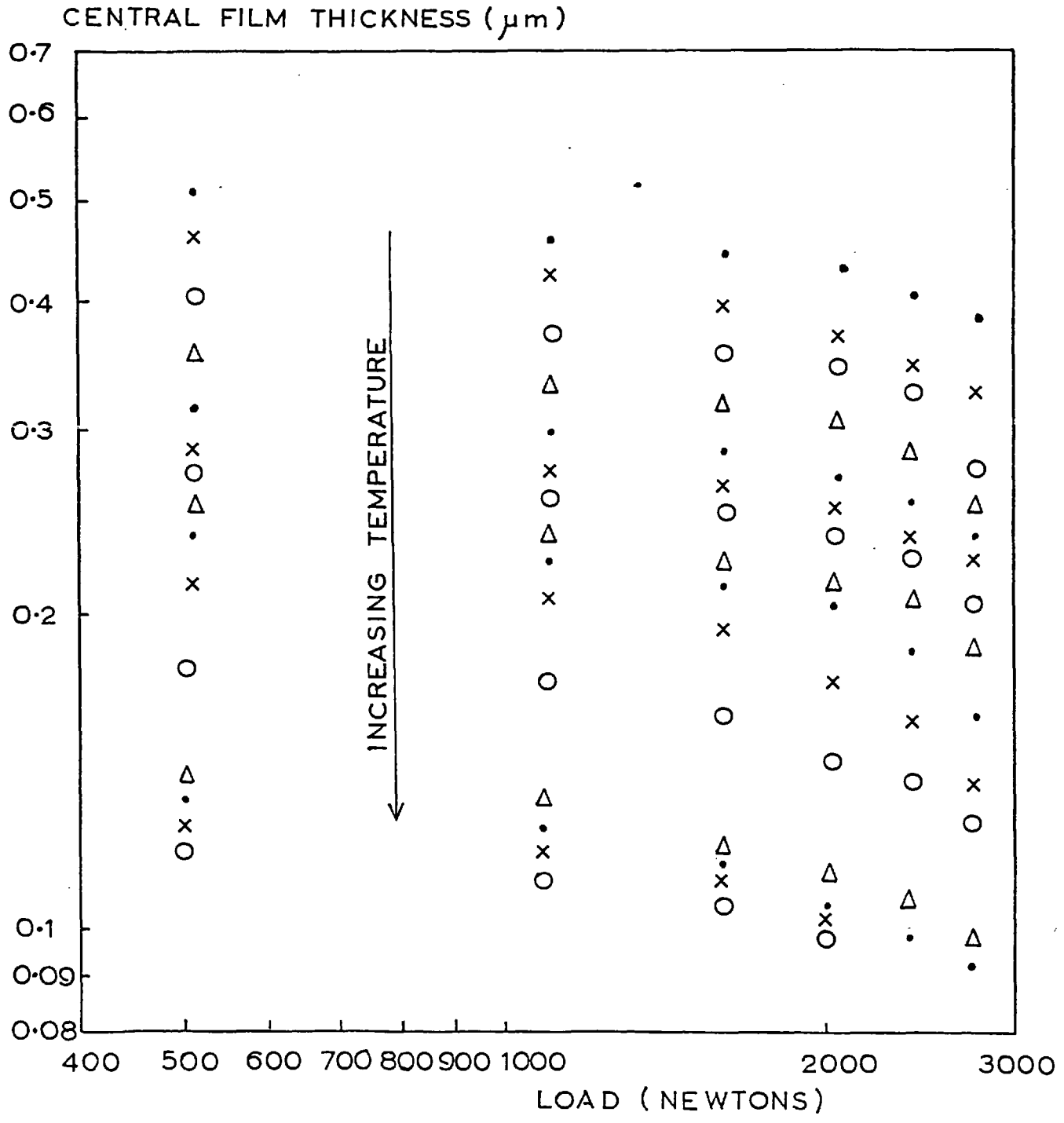

FIG. 6.13 FILM THICKNESS AGAINST LOAD FOR PURE ROLLING

SPEED = 0·665 m/sec

○ ≡ 30°C, 40°C, 50°C, 60°C Δ ≡ 32·5°C, 42·5°C, 52·5°C

• ≡ 35°C, 45°C, 55°C × ≡ 37·5°C, 47·5°C, 57·5°C

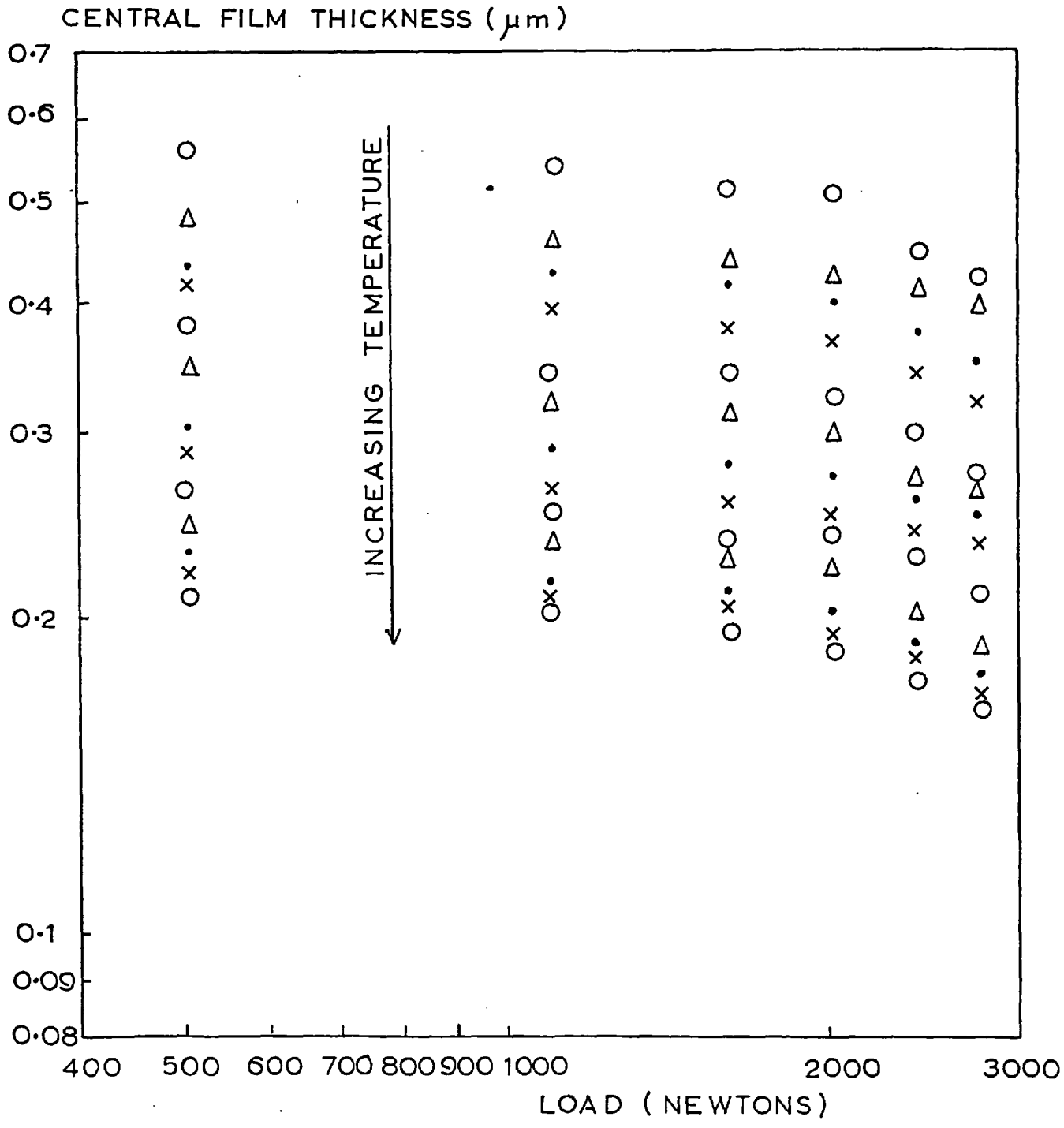

FIG. 6.14. FILM THICKNESS AGAINST LOAD FOR PURE ROLLING

SPEED = 0·997 m / sec

O ≡ 30°C, 40°C, 50°C, 60°C Δ ≡ 32·5°C, 42·5°C, 52·5°C

• ≡ 35°C, 45°C, 55°C × ≡ 37·5°C, 47·5°C, 57·5°C

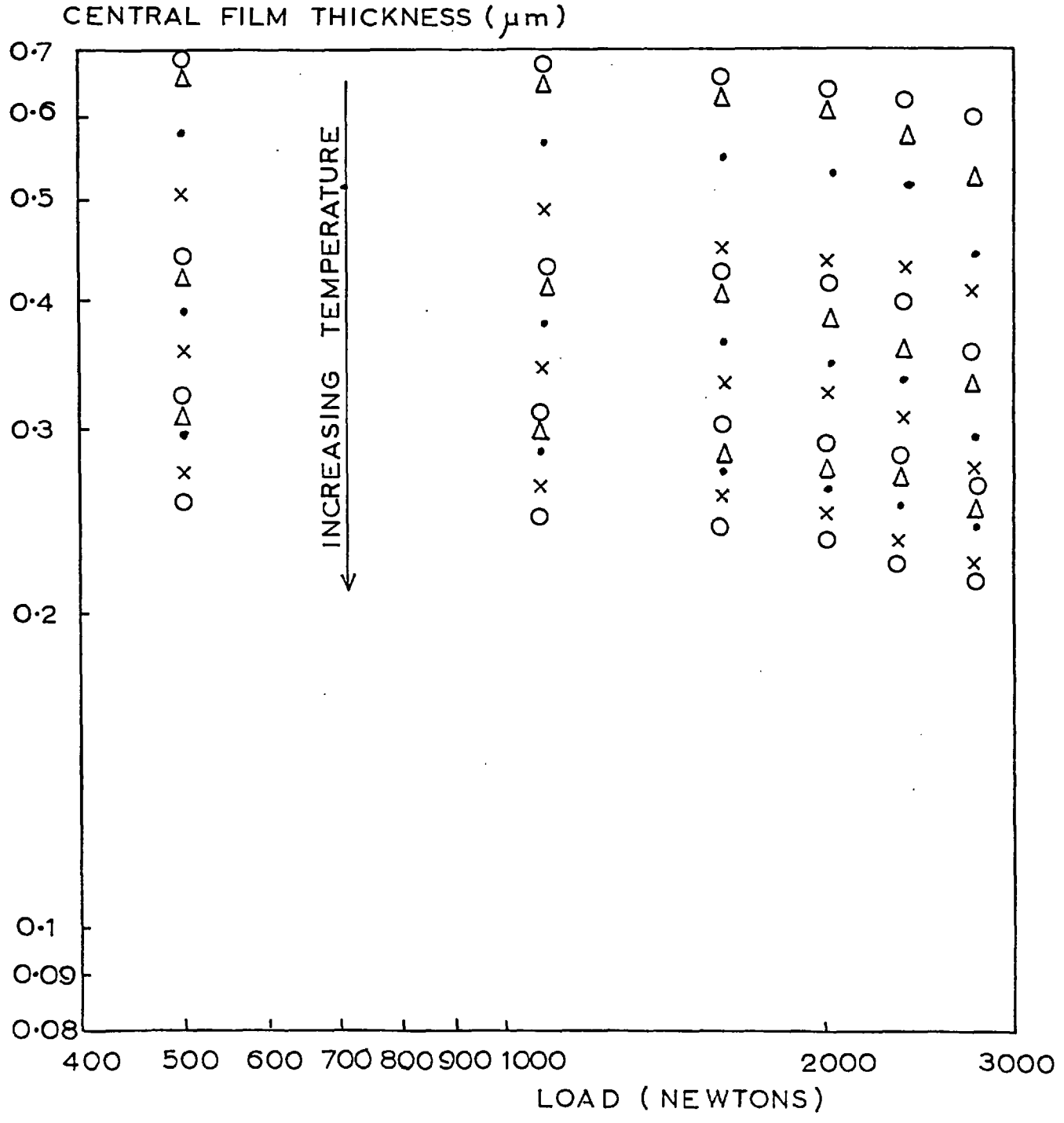

FIG. 6.15. FILM THICKNESS AGAINST LOAD FOR PURE ROLLING

SPEED = 1·330 m/sec

O ≡ 40°C, 50°C, 60°C Δ ≡ 42·5°C, 52·5°C, 62·5°C

• ≡ 45°C, 55°C, 65°C × ≡ 47·5°C, 57·5°C, 67·5°C

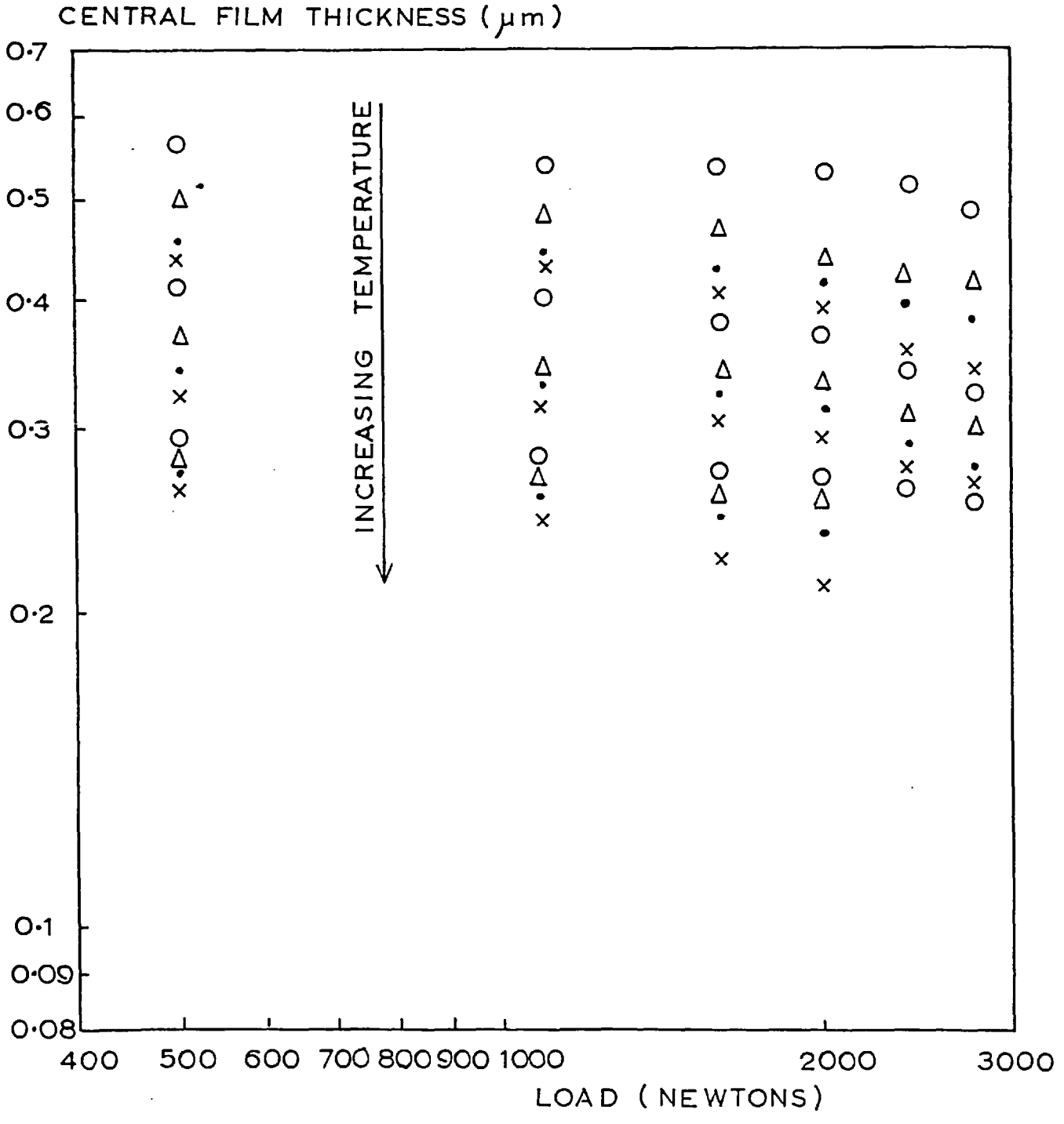

FIG. 6.16. FILM THICKNESS AGAINST LOAD FOR PURE ROLLING

LOAD = 512 N (MAX p_{HZ} = 0·556 GN/m^2)

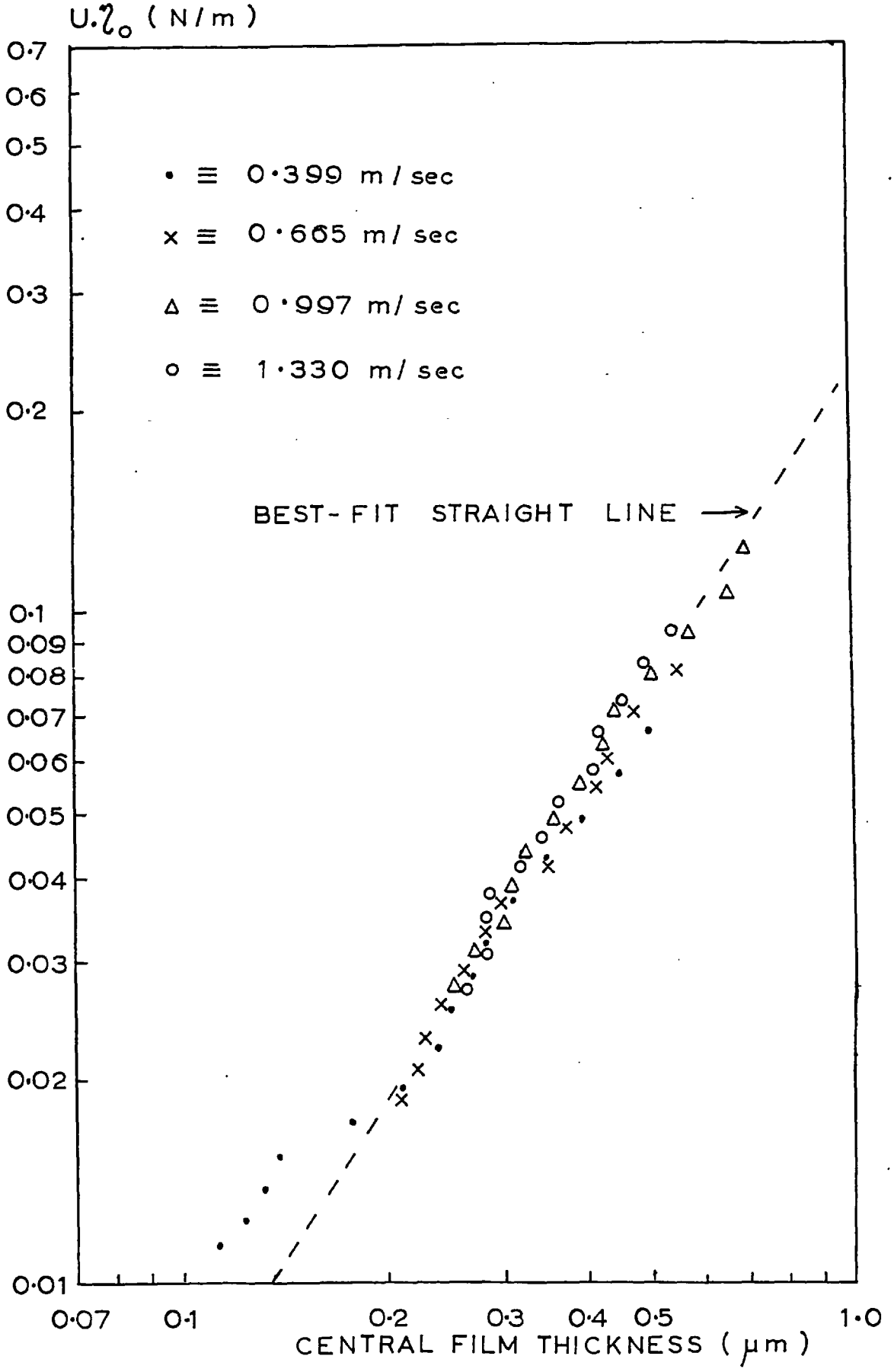

FIG. 6.17. FILM THICKNESS AGAINST U.η$_o$ FOR PURE ROLLING

LOAD = 2046 N (MAX p_{HZ} = 1·110 GN/m^2)

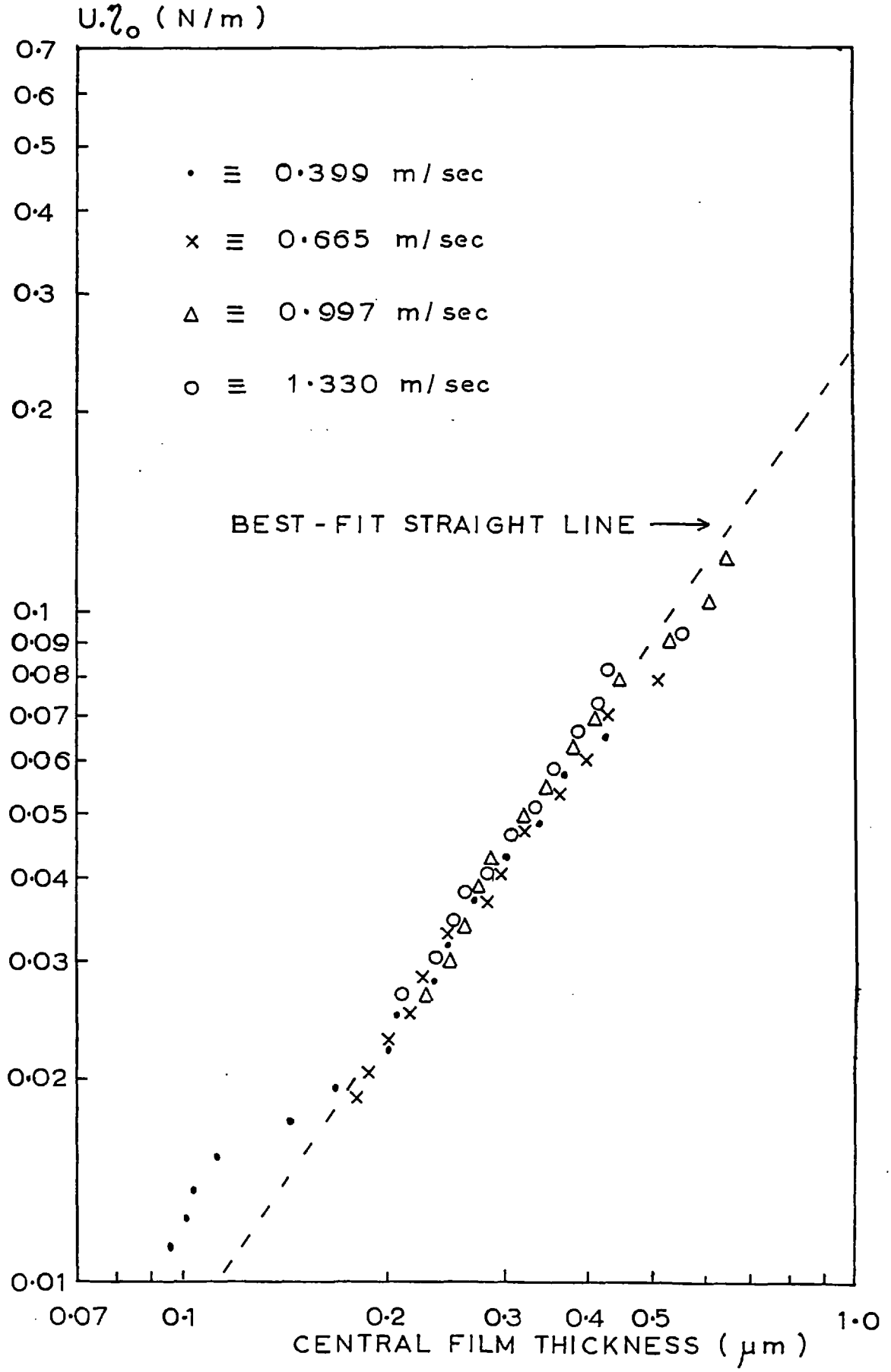

FIG. 6.18. FILM THICKNESS AGAINST U.η_o FOR PURE ROLLING

LOAD = 2046 N (MAX p_{HZ} = 1·110 GN/m^2)

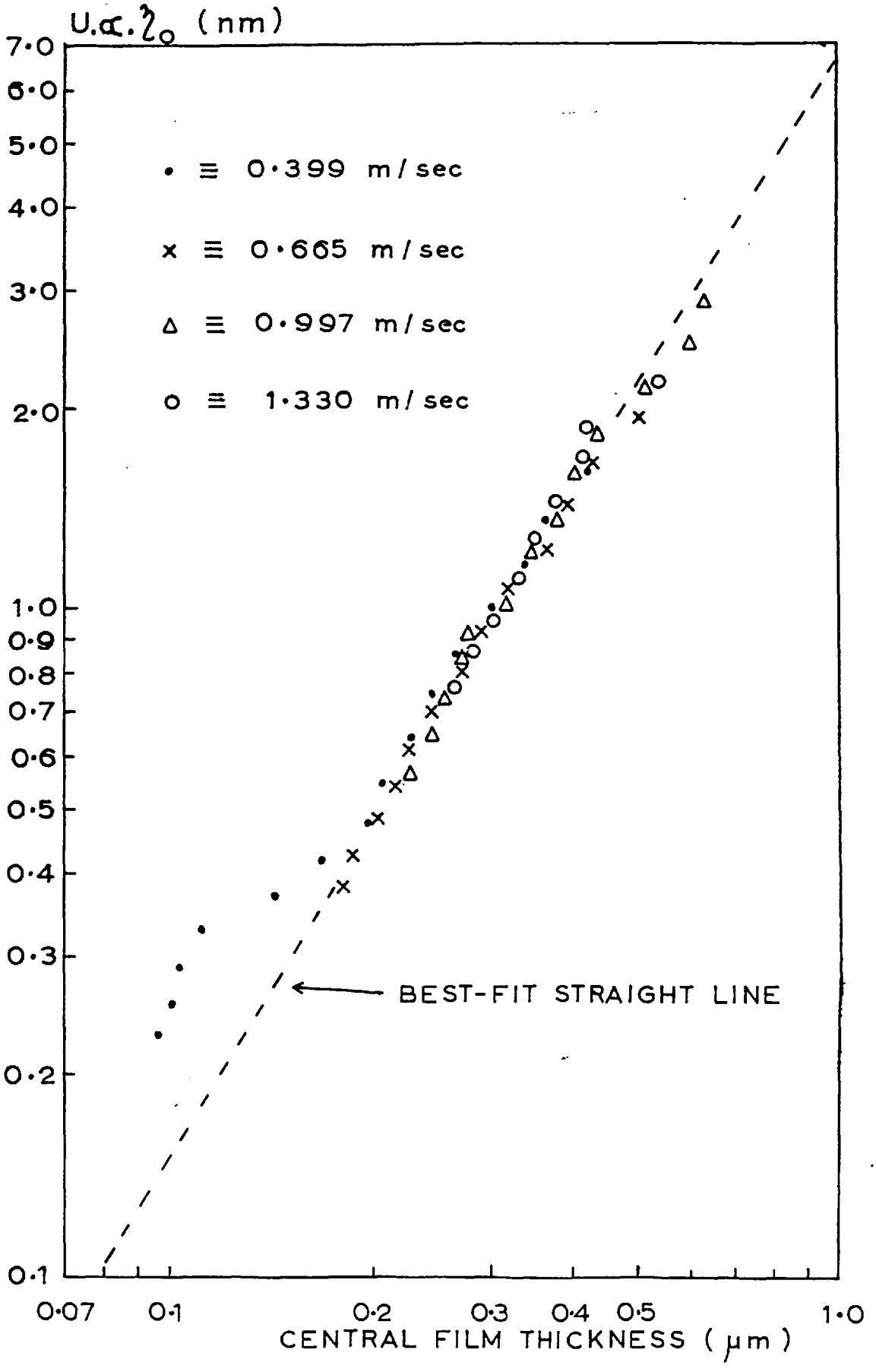

FIG. 6.19. FILM THICKNESS AGAINST U.α.η$_o$ FOR PURE ROLLING

MEAN SPEED = 0·399 m/sec

—•—• ≡ PURE ROLLING, O ≡ Σ = 0·2

× ≡ Σ = 0·4, Δ ≡ Σ = 0·6

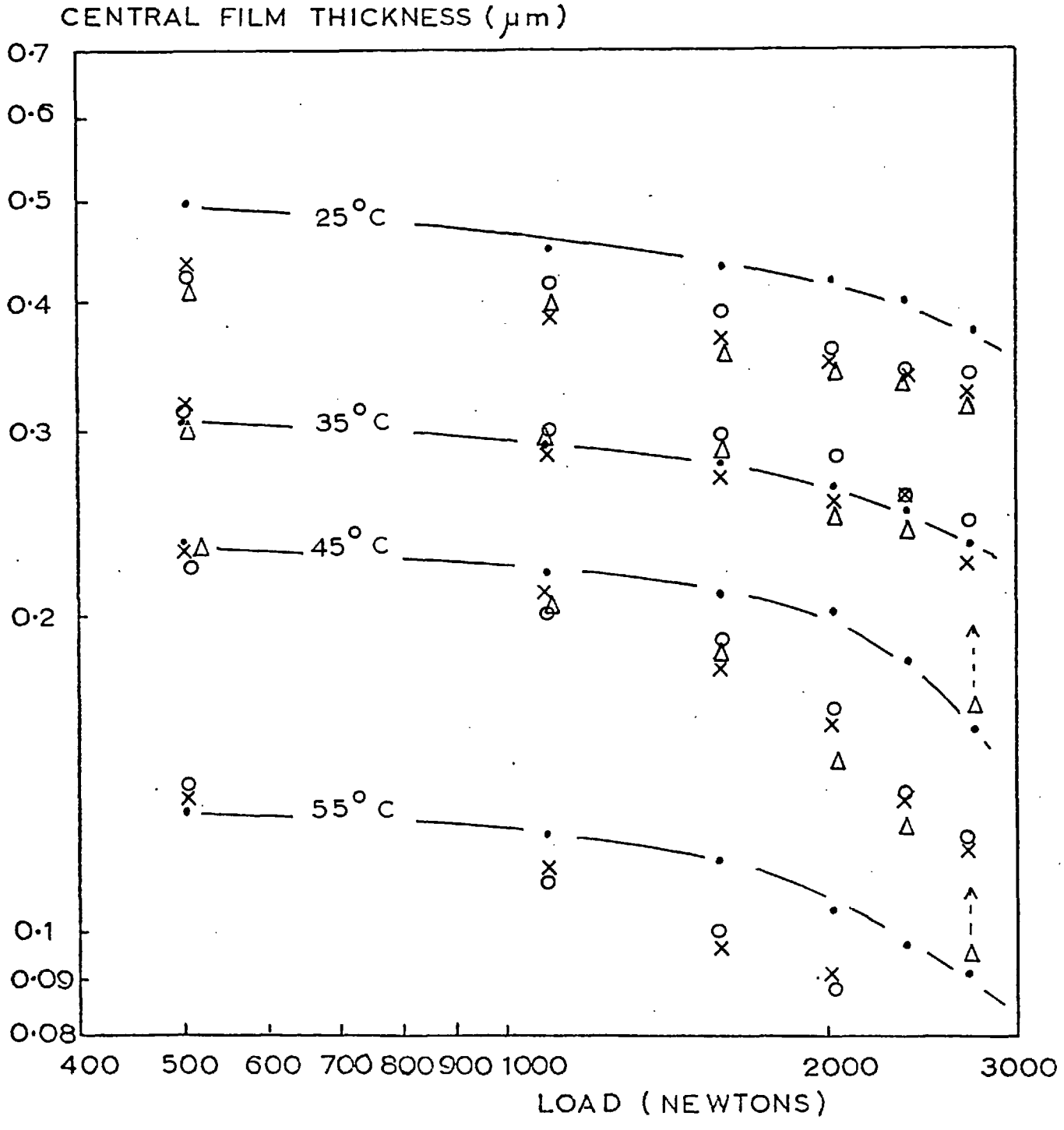

FIG. 6.20. FILM THICKNESS AGAINST LOAD FOR ROLLING AND ROLLING PLUS SLIDING

MEAN SPEED = 0·665 m/sec

—•—• ≡ PURE ROLLING, O ≡ Σ = 0·2

× ≡ Σ = 0·4, Δ ≡ Σ = 0·6

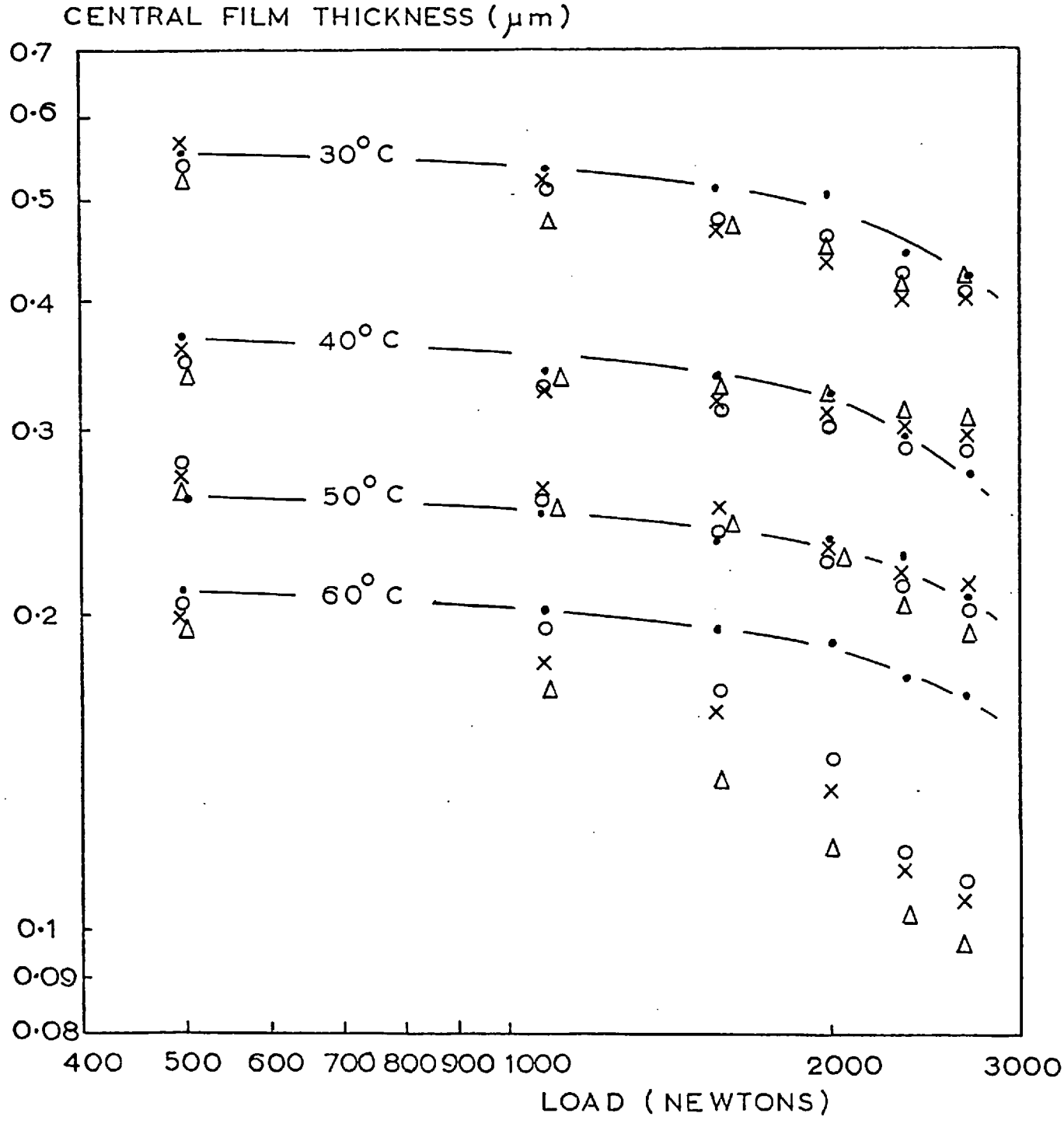

FIG. 6.21. FILM THICKNESS AGAINST LOAD FOR ROLLING AND ROLLING PLUS SLIDING

MEAN SPEED = 0·997 m/sec

—•—• ≡ PURE ROLLING, O ≡ Σ = 0·2

× ≡ Σ = 0·4, Δ ≡ Σ = 0·6

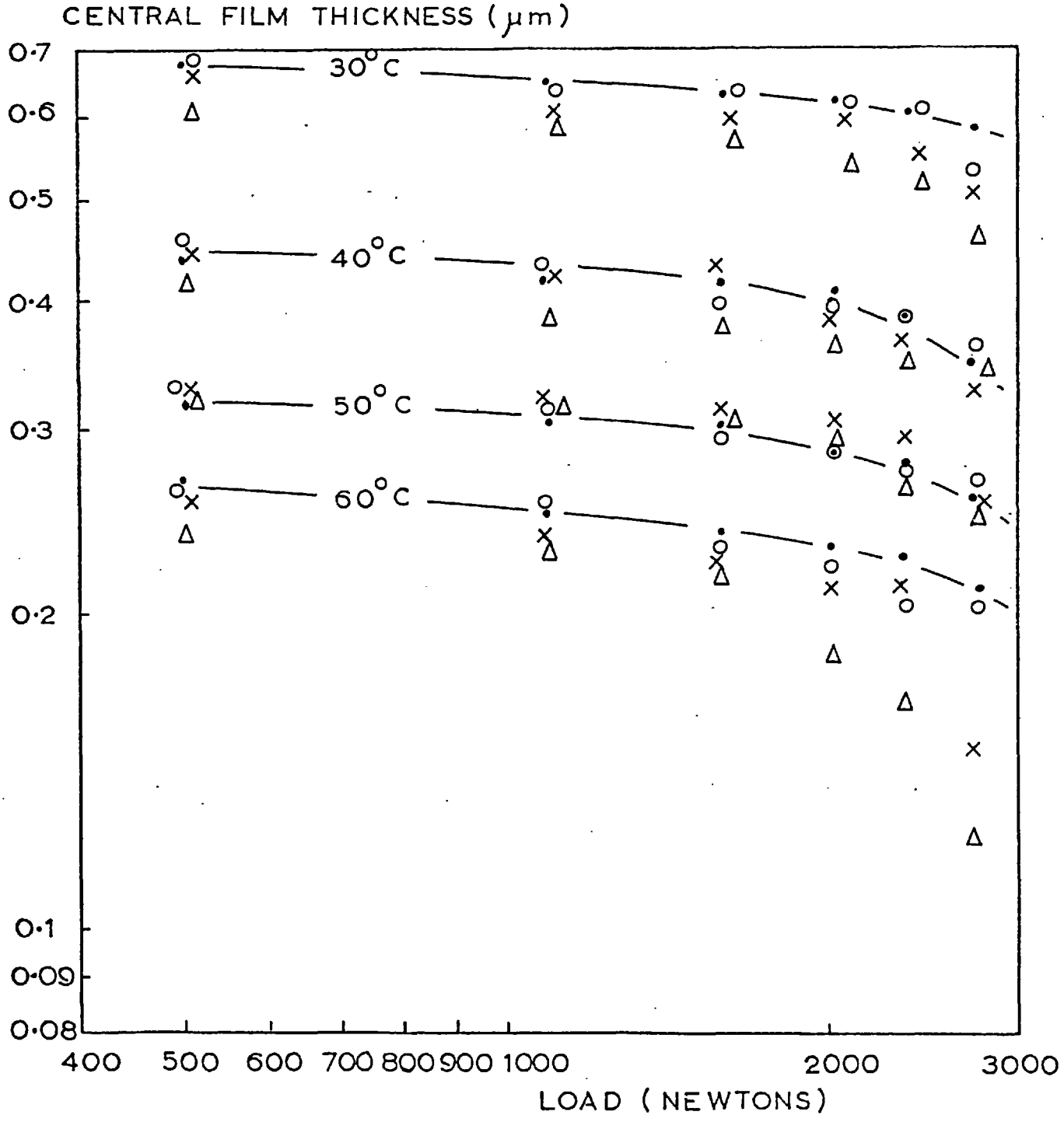

FIG. 6.22. FILM THICKNESS AGAINST LOAD FOR ROLLING AND ROLLING PLUS SLIDING

MEAN SPEED = 1·330 m/sec

—•—• ≡ PURE ROLLING, O ≡ Σ = 0·2

× ≡ Σ = 0·4, Δ ≡ Σ = 0·6

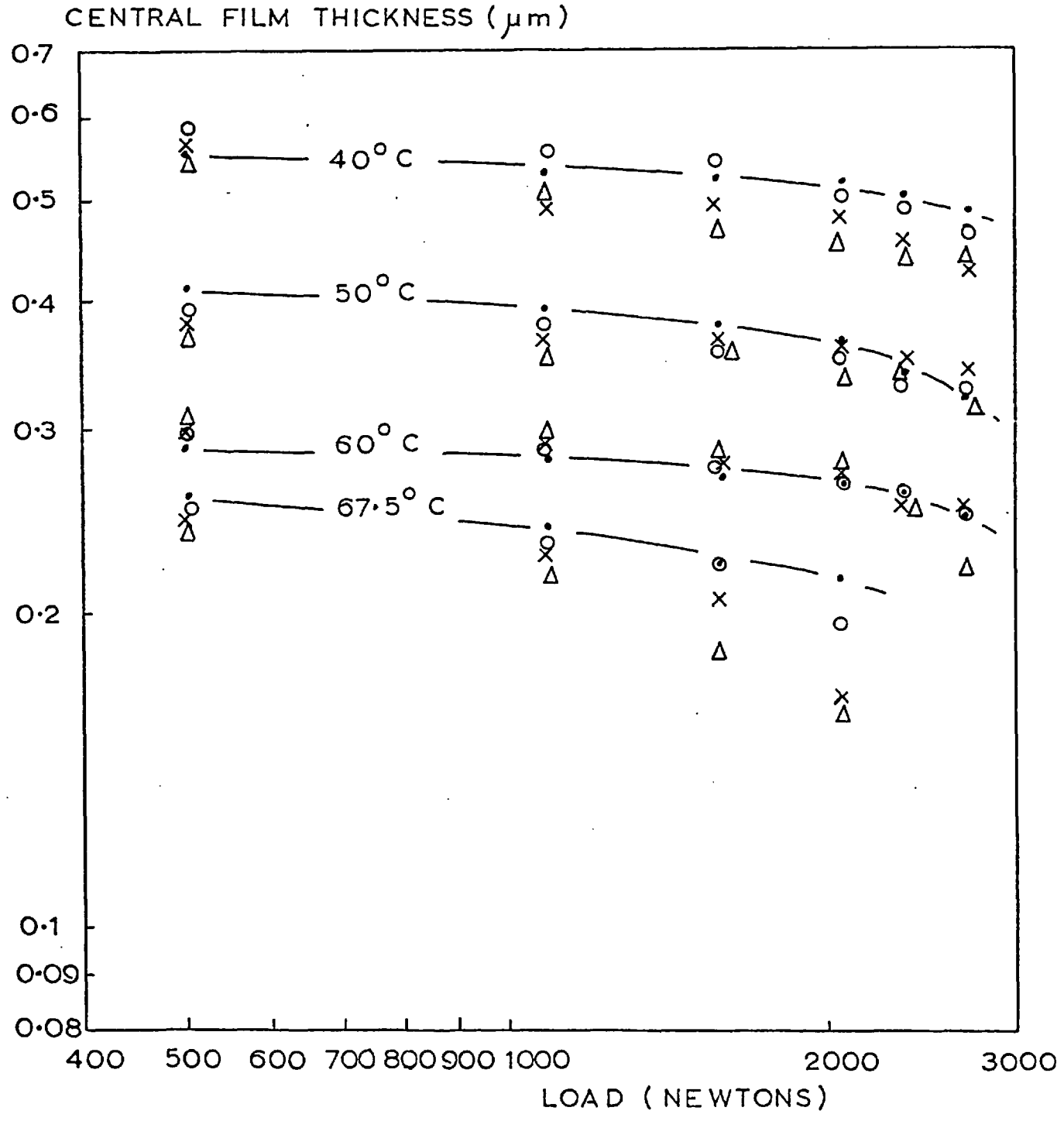

FIG. 6.23. FILM THICKNESS AGAINST LOAD FOR ROLLING AND ROLLING PLUS SLIDING

MEAN SPEED = 0·665 m / sec

LOAD = 2046 N (MAX p_{HZ} = 1·110 GN/m^2)

• ≡ PURE ROLLING ; O ≡ Σ = 0·2

Δ ≡ Σ = 0·6

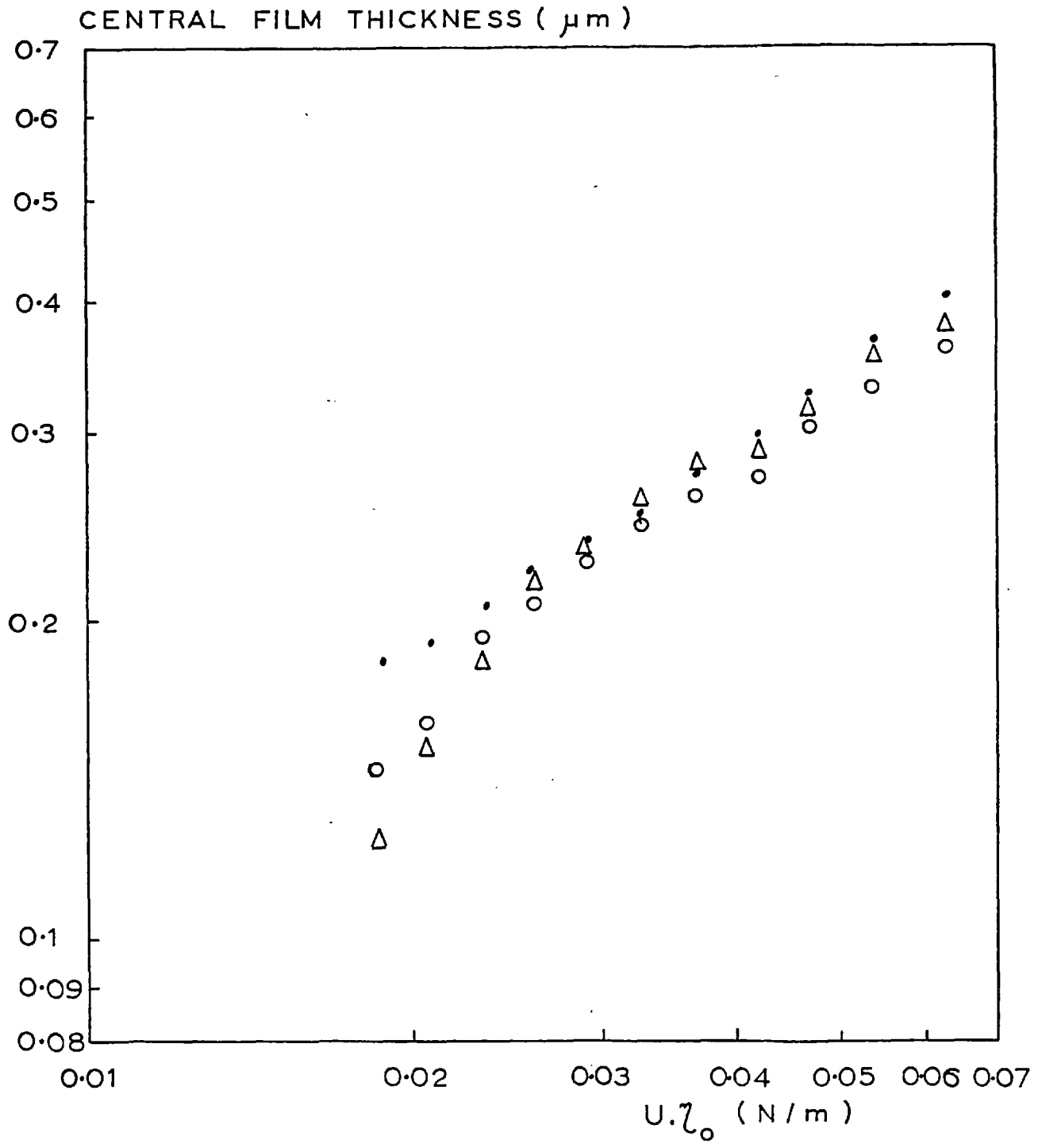

FIG. 6.24 . FILM THICKNESS AGAINST U.η_o FOR ROLLING AND ROLLING PLUS SLIDING

MEAN SPEED = 0·399 m / sec

LOAD = 2402 N (MAX p_{HZ} = 1·203 GN/m^2)

• ≡ PURE ROLLING ; O ≡ Σ = 0·2

Δ ≡ Σ = 0·6

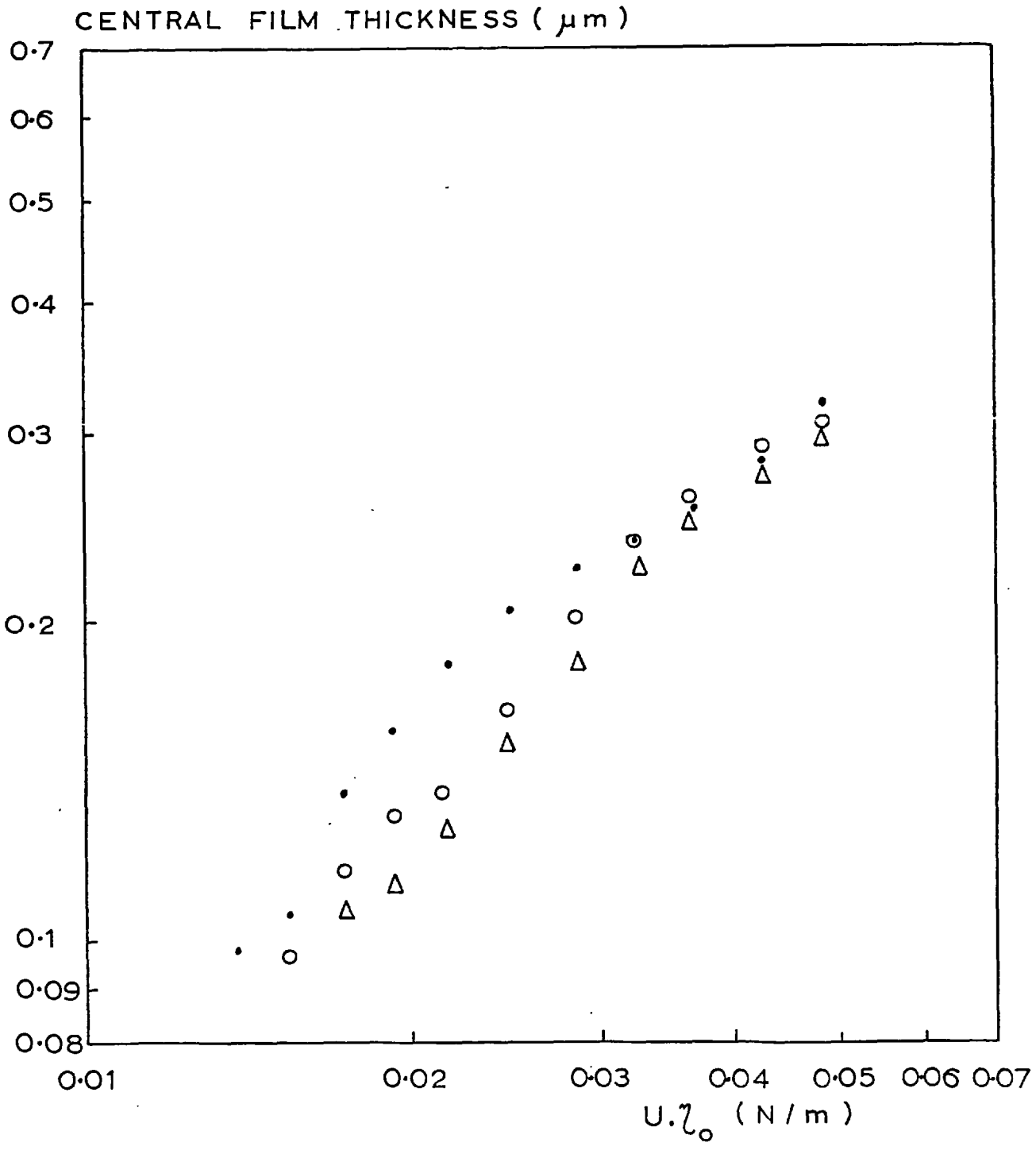

FIG. 6.25. FILM THICKNESS AGAINST U.η_o FOR ROLLING AND ROLLING PLUS SLIDING

CHAPTER 6: REFERENCES

1. KANNEL J.W. and BELL J.C. - "Interpretations of the Thickness of Lubricant Films in Rolling Contact. 1 Examination of Measurements obtained by X-rays", Trans. ASME, Oct. 1971, pp. 478 - 484.

2. PARKER R.J. and KANNEL J.W. - "Elastohydrodynamic Film Thickness Between Rolling Disks with a Synthetic Paraffinic Oil to 589 K", NASA, Technical Note, TND-6411.

3. WYMER D.G. - Ph.D. Thesis, Univ. of London, 1972, and "Elastohydrodynamic Lubrication of a Line Contact", Proc. Inst. Mech. Eng., 1974, Vol. 188, Paper 19/74, pp. 221 - 238.

CHAPTER 7

DISCUSSION

7.1 TRACTION MEASUREMENTS

The behaviour of lubricants under traction conditions has been well documented by several workers (1, 2, 3, 4, 5) and certain behaviour patterns have been found to be true in most cases. Usually the coefficients of traction are higher for the lower temperatures, lower speeds, and higher loads. The measured results appear to agree with this pattern although in general the temperature effect is not very pronounced especially at the higher values of load (Hertzian pressure). Moreover there appears to be little variance of coefficient of traction with mean rolling speed. However the speed range was very narrow and hence any effect would probably be small and consequently not easily detectable.

The most striking feature of these results is the lack of a traction peak, especially as the Hertzian pressures are quite high (up to 1.117 GN/m^2). The rate of increase of traction does fall off rapidly with increasing sliding but the coefficient of traction does not show a drop, instead a steady plateau region is reached. This type of behaviour is usually associated with the lower Hertzian pressures and not the higher ones. Moreover the absolute value of coefficient of traction is slightly lower than might have been expected; previous workers have experienced values in the range 0.05 to 0.09.

It was decided to check these results by testing the oil used in the experiment on other traction machines. This was thought to be important as these initial traction tests were considered part of the commissioning procedure for

the apparatus; consequently any apparent abnormality in behaviour had to be investigated to ensure that the major part of the experiment (measurement of EHD film thickness) was not invalidated.

Two other machines were used. The first was a two disc machine at Reading University; these tests were carried out by A.D. MOORE (6). The second was a point contact (ball on plate) apparatus at Imperial College, London; these results were provided by R.R. DUCKWORTH (7). A comparison of these two sets of results against some of the experimental results is given in Fig. 7.1 and the respective operating conditions are given in Table 7.1.

The results from Reading University (A.D. Moore) were taken for operating conditions quite close to those for the present experimental results. It can be seen that, although the traction values are very similar, Moore's results show a slight peak. On closer inspection it would appear that, rather than considering the present results to show a lack of a traction peak, the possible explanation may be found by considering the alternate approach i.e. no fall off in traction at large slide/roll ratios.

The traction machine at Reading University was completely open with a small oil feed to the EHD contact, whereas the present traction machine was enclosed, with the whole working area completely flooded with oil. It would seem reasonable to assume that the completely flooded EHD contact is able to convect away the heat generated by sliding more easily than a non-flooded contact. This would tend to reduce the thermal effects, which are generally considered to dominate the traction response at high slide/roll ratios, and hence

the fall off in traction. This could explain the difference in behaviour especially as Moore's results do fall to a fairly low traction value.

An extension of this thermal argument can be applied to the point contact traction case. There the heat generating source is small and yet there is a relatively large thermal sink in the plate and the ball to conduct away the heat. Again this would probably tend to moderate the thermal effect on traction.

Unfortunately the traction results from Imperial College (R.R. Duckworth) did not go to high enough slide/roll ratios to test this hypothesis. However the few results available do seem to suggest that any traction peak, if present at all, would not be large.

It can be seen that the absolute values of coefficient of traction are higher for the point contact case. This can be attributed to the fact that the speeds, but perhaps more important, the temperatures were lower. As mentioned previously this generally leads to higher tractions.

Thus it would appear that the present four disc machine was functioning properly as the agreement between the various sources of traction data is good.

From the comparison of traction behaviour for the steel/steel and sapphire/steel disc configurations given in Fig. 6.10, it can be seen that by replacing the central steel disc by one made of sapphire there is no discernible difference in response, even though this gives rise to Hertzian pressures which are approximately 15% higher for the same load and involved the use of a slightly different test procedure. (The outer discs were now speeded up as the central

disc was slowed down). This confirms the relative insensitivity of traction to speed, but more important it suggests that the coefficient of traction is not so much dependent on Hertzian pressure but on the load itself.

This latter suggestion is partially confirmed by Fig. 6.11 which shows traction values similar to those in Fig. 6.5, the slightly higher values in Fig. 6.11 are attributed to the much lower speed. For these measurements it was possible to use lower speeds as the film thickness was now being monitored and the risk of surface damage could be minimised by ensuring that the film thickness did not go too low. Also in Fig. 6.11 can be seen the continuing lack of suggestion of a traction peak, as was found for the other traction results.

7.2 ROLLING FILM THICKNESS MEASUREMENTS

The relationship between film thickness and the other varying parameters in EHD lubrication can be expressed in the form

$$\frac{h}{R} = h^* = A\ (U^*)^b\ .\ (W^*)^c\ .\ (G^*)^d \qquad (7.1)$$

where A, b, c, d are constants

$$U^* = \frac{U.\eta_o}{E'.R}$$

$$W^* = \frac{W}{L.E'.R}$$

$$G^* = E'.\alpha$$

U = rolling speed

η_o = inlet viscosity

W = load

L = contact length

α = pressure/viscosity coefficient

R = reduced radius $\equiv \dfrac{R_1 \cdot R_2}{R_1 + R_2}$

$R_{1,2}$ = radius of curvature of contacting surface

E' = reduced Young's Modulus $\equiv \pi \left(\dfrac{\dot{E}_1 \cdot \dot{E}_2}{\dot{E}_1 + \dot{E}_2} \right)$ for Grubin's analysis

$\equiv 2 \left(\dfrac{\dot{E}_1 \cdot \dot{E}_2}{\dot{E}_1 + \dot{E}_2} \right)$ for other analyses.

$$\dot{E}_{1,2} \equiv \frac{E_{1,2}}{(1 - \nu_{1,2}^2)}$$

$\nu_{1,2}$ = Poisson's ratio

$E_{1,2}$ = Young's Modulus

(The subscripts 1 and 2 refer to the two different surfaces).

The first theoretical analysis of EHD lubrication in these terms was performed by GRUBIN (8). This work gives the following expression for film thickness

$$h_o^* = 1.95\ U^{*8/11} \cdot W^{*-1/11} \cdot G^{*8/11} \qquad (7.2)$$

For Grubin's work the assumption of a parallel film for the whole contact was made, thus this film thickness would be more representative of the central film thickness in a real EHD contact.

Later work by Dowson, Higginson, and co-workers led to the classical expression for dimensionless minimum film thickness (DOWSON, HIGGINSON and WHITAKER (9))

$$h_{min}^* = 1.6\ U^{*0.7}\ W^{*-0.13}\ G^{*0.6} \qquad (7.3)$$

Finally an experimental investigation into EHD line contact by WYMER (10), who used optical interferometry to measure film thickness, has produced the following relation for dimensionless central film thickness

$$h^*_c = 0.44\ U^{*0.64}\ W^{*-0.17}\ G^{*0.58} \qquad (7.4)$$

The rolling film thickness results obtained in the present set of experiments will be analysed so that comparison may be drawn against each of these three relations. However, before doing so it is worthwhile noting some general points about the experimental results first.

7.2.1 General Comments on the Results

Looking at Figs. 6.13 to 6.16 it can be seen that, as expected, the film thickness is higher for higher speeds, drops with increasing load, and also with increasing temperature (this is due to the fact that both viscosity and the pressure/viscosity coefficient fall as temperature rises).

However on closer examination of the results for 0.399 m/sec (Fig. 6.13) it can be seen that the reasonably consistent pattern of the film thickness plots is disturbed in the region of 0.1 μm to 0.2 μm. This effect does not appear to be related to temperature as the same temperatures at different speeds do not produce the same response; similarly it does not appear to be a load effect. As the film thickness drops even further this anomalous behaviour seems to disappear and the plots tend to revert to their previous pattern.

This discrepancy in behaviour can be seen more clearly in the plots of film thickness against $U.\eta_o$ and $U.\alpha.\eta_o$ in Figs. 6.17 to 6.19. The majority of the results all

seem to lie on a common line until the film thickness drops below 0.2 μm. At this point a change in response is apparent, the film thickness now falls more rapidly with $U.\eta_o$ and $U.\alpha.\eta_o$ than previously. However, as the film thickness falls even further its response to changes in the parameters $U.\eta_o$ and $U.\alpha.\eta_o$ reverts to one similar to that noted before. The nett result is that there seems to have been a permanent "loss" in film thickness as it passes through the range 0.1 μm to 0.2 μm., but that on either side of this range the response to $U.\eta_o$ and $U.\alpha.\eta_o$ is consistent and the same.

Another point of interest is the response of film thickness to changes in load. It can be seen from Figs. 6.13 to 6.16 that, at higher loads, the film thickness appears to fall more rapidly with load than at lower loads. This behaviour is confirmed when power coefficients for the response of film thickness against load are calculated for (a) loads up to 2046 N (b) all loads. The response at all times is greater for case (b) than case (a), (see next section).

Thus it would appear that the film thickness is beginning to show a behaviour similar to that noted by PARKER and KANNEL (11) and at approximately the same Hertzian pressure. Unfortunately the limitations of the experimental apparatus precluded tests at higher Hertzian pressures; this was due to the hydraulic system being unable to supply a higher oil pressure (as discussed in Chapter 2), but even if this were possible there would still be the danger of cracking the sapphire from too high compressive stresses.

Although these rolling results do seem to suggest the same behaviour as that observed by Parker and Kannel, this is by no means conclusive as the experimental response can

still be adequately approximated by a straight line drawn on a double logarithmic plot. Thus it is not possible to refute the work of GENTLE, DUCKWORTH and CAMERON (12) for EHD point contact which showed no unusual response of film thickness to changes in load for Hertzian pressures up to 2.0 GN/m^2.

7.2.2 Comparison Against Other Workers' Predictions

As has been pointed out, there appears to be some anomalous behaviour for film thickness in the range 0.1 μm to 0.2 μm. For this reason, in the comparison against other workers' predictions, the film thickness results below 0.2 μm will be ignored for the present time. However they will be considered later in this chapter.

The first comparison will be the predicted power coefficients for the U* term against the ones deduced from the experimental measurements i.e. "b" where

$$h^* \propto (U^*)^b \qquad (7.5)$$

for $h^* = h/R$ and $U^* = U.\eta_o/E'.R$. As R and E' are constant for this experimental apparatus, "b" can be obtained by calculating the response of h to $U.\eta_o$.

Considering Figs. 6.17 and 6.18, the best fit straight line in each case gives values of "b" of 0.648 and 0.669 respectively. However for these results the viscosity, η_o, was varied by varying temperature. Unfortunately the temperature also affects the pressure/viscosity coefficient, α, which in turn also affects film thickness. Thus these calculated values for "b" will contain some error due to neglecting this effect.

An allowance for the effect of α can be approximated

by taking the power coefficient of the response of h against $U.\alpha.\eta_o$ to represent the response of h against $U.\eta_o$. This is based on the fact that the values of power coefficients for U* and G* are close (both 8/11 for Grubin; 0.7 and 0.6 for Dowson, Higginson and Whitaker; and 0.64 and 0.58 for Wymer). Making this approximation and using the results in Fig. 6.19 gives a value for "b" of 0.606.

However the only way to eliminate the influence of α is to keep the temperature constant (and hence the viscosity) and to vary only the speed. As only four speeds were used throughout these experiments, the accuracy of the calculations for the coefficient "b" must be somewhat suspect for each individual group due to the small number of points. However it is thought that the arithmetic mean of these many values of "b" should represent the response well.

Using a least squares regression method to obtain the best fit, all the rolling results were analysed in this manner (except those with a film thickness below 0.2 μm). The results are given in Table 7.2 for the six loads. The mean value of "b" for all the results is 0.615 with a standard deviation of 0.049.

This value compares reasonably well with Grubin's value of 0.72 for a parallel film and Dowson, Higginson, and Whitaker's value of 0.7 for the minimum film thickness. It agrees very well with Wymer's experimental value of 0.64 for central film thickness which is the film thickness measured in the present experiments.

Thus it would appear that, for film thickness above 0.2 μm the calculated values for "b" show no unusual trends.

Comparison with predicted values will now be made

for the power coefficients of the W* term i.e. "c" where

$$h^* \propto (W^*)^c \qquad (7.6)$$

Similarly to before, this is obtained from the response of h to W. This can be seen in Figs. 6.13 to 6.16.

The coefficient "c" was calculated for the four different rolling speeds. For each of these speeds a number of different values of "c" were obtained for each temperature using (a) the four loads up to and including 2046 N (b) all six loads used in the experiments. For all combinations of speed and load range the simple arithmetic mean of these values was calculated. These results, together with the standard deviations, are presented in Table 7.3.

It can be seen that at all speeds the response for the first four loads is less severe than for all six loads; it is this behaviour that suggests agreement with the work of Parker and Kannel as discussed previously.

It is also interesting to note that the response of film thickness to load appears to be more sensitive at the lower rolling speeds, this effect is very apparent for 0.399 m/sec. The reason for this is not clear but it may be due to the same effect that causes the erratic response of film thickness below 0.2 μm. (The film thickness values are lower at lower speeds).

The values of "c" obtained by Grubin; Dowson, Higginson and Whitaker; and Wymer are -0.09, -0.13, and -0.17 respectively. It can be seen that the values of "c" deduced from the present experimental results are of the right order of magnitude, but that the good agreement with Wymer's work found for the coefficient "b" has not been repeated (except

for the 0.399 m/sec and all six loads result which is itself different from the rest). The experimental results show the best comparison against Grubin's load prediction for parallel film thickness in most cases, especially for lower loads. Nevertheless in general there does not appear to be any grossly different behaviour of film thickness to changes in load from that found or predicted by these other workers, and the values certainly do not approach 0.5 as suggested by the results of KANNEL and BELL (14).

As only one oil was used in the experiment it was not feasible to test for the power coefficient of G* as the only way of altering α (E' being fixed) was to alter temperature. As mentioned before this also alters viscosity which in turn affects film thickness.

Of the three predictions for film thickness only Wymer's directly relates to central film thickness, the value measured in the present experiments. It was decided to compare the absolute values predicted by Wymer's relation against the experimental results. These are presented in Table 7.4 for a load of 2046 N and (as the results at 0.399 m/sec are subject to some doubt) only for the higher rolling speeds.

It can be seen that the predicted values are slightly higher than the experimental values. This was also found by PEMBERTON (13) who reported that Wymer's empirical relationship over-predicted his observed values consistently. Although it is possible that Wymer's relationship may contain some error, these inconsistencies can be accounted for by alternative reasoning. The first reason lies in the value of the pressure/viscosity coefficient α. For the oil used in the experiments this was deduced from viscosity data at various pressures sup-

plied by The British Petroleum Company Ltd. It was assumed that α was the mean value for the range 0 to 69 MN/m^2 (10,000 p.s.i.). This choice was fairly arbitrary and differing values of α could be obtained by choosing alternative pressure ranges, nevertheless this range was thought to be representative. The deviation of Wymer's value of pressure/viscosity coefficient may not have corresponded to this choice and so would not be strictly applicable, thus giving subsequent differences in film thickness predictions.

Secondly, the suggested values of power coefficients in Wymer's experimental relationship are quoted with an error band. This error band can give variations in predicted film thickness between approximately one-fifth and five times the mean value.

7.2.3 Summary

For the rolling film thickness measurements there are five main comments on their behaviour:-

(a) For the most part the film thickness responds in a regular and consistent manner to changes in load, temperature, and speed until its value falls below approximately 0.2 μm. At this point the film thickness drops more rapidly with a change in parameters than for higher film thicknesses. As the film thickness falls even further its response appears to revert to one similar to that observed at values above 0.2 μm, but with a permanent "additional" fall. As the film thickness rises again, this "additional" fall is recovered.

(b) In general the response of film thickness to changes

in load can be adequately represented by a straight line on a double logarithmic plot. However at the higher Hertzian pressures there is a tendency for the film thickness to be more sensitive to load changes than at lower values. This would tend to support the observations of PARKER and KANNEL (11) who show a rapid decline in EHD film thickness at high Hertzian pressures.

(c) The absolute values of power coefficient for load response are nowhere near as high as those observed by KANNEL and BELL (14).

(d) For the lowest rolling speed the load dependence of film thickness appears greater than at higher speeds. This may be linked to the anomalous behaviour of film thickness below 0.2 μm.

(e) Otherwise the film thickness behaves more or less as expected and gives power coefficients for the non-dimensional groups W* and U* similar to those obtained by most other workers.

It is interesting to note that both WYMER (10) and WESTLAKE and CAMERON (15) also detected unusual behaviour of film thickness at its lower values, and in a similar manner to that observed here. However they did not show the apparent recovery in response, albeit with a permanent film thickness loss, as the film thickness drops even further. These authors offered no explanation of the behaviour but commented that the values of film thickness at which this effect was first apparent were of the same order as the surface roughness. It will be proposed later in this chapter that it is in fact a surface

roughness mechanism which causes the anomalous behaviour in rolling film thickness below 0.2 μm , and that this mechanism also explains the fall in film thickness which is sometimes noted when sliding is introduced. This latter behaviour is commented on in the next section.

7.3 ROLLING PLUS SLIDING FILM THICKNESS MEASUREMENTS

Classical elastohydrodynamic theory does not differentiate between rolling and sliding. If the mean surface speed is the same for each case then, as long as the load, temperature and other variables do not alter, the film thicknesses should be the same. Thus the rolling and rolling plus sliding film thickness results should coincide with their respective alternates.

7.3.1 General Comments on the Results

It can be seen from Figs. 6.20 to 6.23 that the rolling and rolling plus sliding results coincide quite reasonably for most cases, but at certain times there are differences. The first of these, and the minor of the two, occurs at film thicknesses above approximately 0.5 μm. This region also corresponds to the lower temperatures and in this range the effect of a small temperature change on film thickness is significant. It will be shown later that temperature "mismeasurements" of less than $4^{o}C$ in general can account for this difference. It is thought therefore that this behaviour can be attributed to thermal effects. This will be discussed briefly later in the chapter.

A more significant discrepancy is noted at the lower film thicknesses. By comparing the results for dif-

ferent speeds it is found that this does not seem to be linked to temperature as the effect is first noticed at $\sim 35^{o}C$ for 0.399 m/sec., $\sim 50^{o}C$ for 0.665 m/sec , $\sim 60^{o}C$ for 0.998 m/sec , and $\sim 67.5^{o}C$ for 1.330 m/sec. Similarly neither rolling speed nor load appear to control the phenomenon directly.

On closer inspection it can be seen that this effect is only noticed for film thicknesses below approximately 0.25 μm. Thus it appears that this anomalous behaviour is linked to the film thickness itself, in a similar manner to the anomalous behaviour noted for rolling film thicknesses below 0.2 μm.

A further important trend is that once this discrepancy has become apparent the amount of sliding does not seem to have a large effect. This can be seen by reference to Figs. 6.20 to 6.23 where increases in sliding of two and three times produce only a small further fall in film thickness. This latter statement must be qualified however as an increase in sliding can occasionally precipitate a fall. Comparison of the various degrees of sliding for the $60^{o}C$ case in Fig. 6.22 where the film thickness seems to be at a particularly sensitive value demonstrates this fact very well.

The load has a large effect on the fall in film thickness. Again reference to Figs. 6.20 to 6.23 shows that for even the very low film thicknesses no fall is apparent until the load starts to increase (see the $45^{o}C$ and $55^{o}C$ cases in Fig. 6.20). Moreover as for sliding, if the film thickness is at a particularly sensitive value, an increase in load can precipitate a fall. For the $60^{o}C$ case in Fig. 6.22 the higher loads cause a fall first for a slide/roll

ratio of 0.6 and later for a slide/roll ratio of 0.4 as well.

The relative effects of pure rolling and rolling plus sliding are shown very clearly in Figs. 6.24 and 6.25. For the former it can be seen that the pure rolling film thickness falls quite uniformly with $U.\eta_o$ but that the rolling plus sliding film thickness shows an anomalous behaviour at approximately 0.25 μm. and begins to fall more rapidly. However, when Fig. 6.25 is examined, it can be seen that at even lower values of $U.\eta_o$ (or film thickness itself) that the pure rolling film thickness also begins to fall. The most interesting point is that the two sets of results begin to approach each other again. This suggests that the same mechanism is controlling the film thickness fall for pure rolling and rolling plus sliding but that the introduction of sliding causes the onset of the fall much sooner.

To test the apparent misbehaviour of rolling plus sliding film thickness below approximately 0.25 μm the discrepancy (defined as the measured pure rolling film thickness minus the film thickness for whichever one of the three corresponding rolling plus sliding cases is being considered) and percentage discrepancy (defined as discrepancy divided by the pure rolling film thickness x 100%) are both plotted against pure rolling and rolling plus sliding film thickness respectively. The corresponding cases were defined to be those cases which had the same temperature, load, and mean speed. For these plots all the available results were used instead of just a selection as in Figs. 6.20 - 6.23.

For this reason a computer plotting program was used to save time; the results are shown in Figs. 7.2 to 7.17.

It should be mentioned that this method of plotting

only gives an indication of which film thickness the anomalous behaviour is first noted at. As these discrepancies are only apparent at the higher loads, utilising all the film thickness results (including those at low loads) means that some of the plots may be well below the "critical" value but not show any unusual response; this leads to a masking of the behaviour pattern. Nevertheless the trends are still easily visible using this method.

Reference to Figs. 7.2 to 7.17 shows that, allowing for this masking effect, the rolling plus sliding film thickness does seem to fall with respect to the pure rolling value below 0.25 μm to 0.3 μm , and that this is true for all four mean rolling speeds.

For values above 0.3 μm the agreement between the rolling and rolling plus sliding cases is good at first but, as commented on earlier, this deteriorates for the higher film thicknesses. The absolute values of these latter discrepancies are similar to those for the lower film thicknesses, but when looked at in percentage terms do not appear as significant.

7.3.2 Summary

For the rolling plus sliding results there are four main comments on their behaviour:-

(a) The onset of the film thickness discrepancy between the rolling and rolling plus sliding cases that is noted at certain times for the lower film thicknesses is not directly controlled by load, temperature, rolling speed, nor amount of sliding. Instead it seems to depend on whether the film thickness is above or below a "critical" value; this

appears to be in the range 0.25 μm to 0.3 μm.

(b) Once the film thickness has fallen in the manner described in (a), a further increase in sliding seems to have only a small effect. However if the film thickness is in the "critical" region an increase in sliding might precipitate a fall.

(c) If the film thickness is above 0.3 μm the introduction of sliding does not cause a fall until larger film thicknesses are reached. This latter behaviour is possibly a thermal effect.

(d) The discrepancy noted at the lower values of film thickness decreases with decreasing load and, for the lowest load, shows an insignificant fall even though the film thickness may be well inside the "critical" region.

7.4 FURTHER DISCUSSION OF THE DISCREPANCY BETWEEN THE ROLLING AND ROLLING PLUS SLIDING RESULTS

According to classical elastohydrodynamic theory the film thickness is determined by the inlet conditions and, as mentioned earlier, may be expressed as a function of U*, W* and G*. The only variables in this relationship are h, U, η_o, W, α (the other properties remaining constant). Thus in trying to explain the film thickness discrepancy between the rolling and the rolling plus sliding cases, attention should first be turned to the behaviour of these parameters.

As U is a measured value direct from a digital counter it is unlikely that any error would be found here. Similarly W is found knowing the pressure on the hydrostatic bearings and should not vary when sliding is introduced. To

test this assumption the Hertzian width was measured for the static case, the pure rolling case and the rolling plus sliding case. The Hertz equations give

$$a \propto \sqrt{W} \tag{7.7}$$

where a = Hertzian half width.

WYMER (9) gives

$$h \propto W^{0.58} \tag{7.8}$$

therefore $$h \propto a^{1.16} \tag{7.9}$$

If the variation in film thickness is due to a variation in load when sliding is introduced then this increase in load would be detected by an increase in the Hertzian half width, a. The measurements of this parameter, a, were taken using the same technique described in Chapter 4 for the load calibration. No noticeable differences were detected for the three different operating modes previously mentioned.

It was estimated that these measurements could have a $\pm$ 5% error, this would give a $\pm$ 6% difference in film thickness. However the percentage discrepancies measured were as high as 40% and the change in Hertzian width due to the load necessary to cause this would be approximately 36%. This is far higher than the estimated possible error and would have been instantly detectable. It can be concluded therefore, that a change in load due to the operating characteristics of the system when sliding is introduced is not occurring, at least to any significant extent.

Hence any variation in film thickness must be attempted to be explained in terms of α and η_o if classical EHD

theory is applied.

7.4.1 Temperature Effects

The first approach is based on the fact that both α and η_o are dependent on temperature. From the experimental results for rolling shown in Figs. 6.13 to 6.16 an empirical relation was derived which gives

$$h \propto T^{-1.467} \qquad (7.10)$$

where T is the temperature in ^{o}C.

This was achieved by taking logarithms of the film thickness and its corresponding temperature for a given load and rolling speed. A best straight line fit of these parameters was then found by a least squares regression method. This was repeated for all combinations of load and rolling speed and from these a simple arithmetic average slope was calculated.

This expression was used to calculate the required error in measurement of inlet temperature which would be necessary to explain the film thickness discrepancy. Graphs were then plotted using the computer of the value of the temperature increase necessary to bring the rolling and rolling plus sliding cases into agreement, versus rolling film thickness (Figs. 7.18 to 7.21).

This method of plotting tends to exaggerate the "discontinuity" point where the film thickness discrepancy first becomes apparent.

A typical value of the temperature rise necessary to explain this discrepancy may be as high as $25^{o}C$, whereas for only marginally different conditions of load and temperature

(for a particular speed and slide/roll ratio) this figure drops to less than $5^{o}C$. Although such a behaviour is unlikely, the conditions for temperature mismeasurement of this magnitude to be possible will be examined.

There is a physical limit as to how close to the EHD contact the trailing thermocouple can be placed; in the experimental situation it is approximately 10 mm. However the point where the inlet conditions that control the film thickness are determined is much closer to the contact than this, a value of half a Hertzian contact width in front of the contact is a generally accepted figure.

One possible "mismeasurement" of temperature could be caused by a rise in oil film temperature after the trailing thermocouple, and the main source of such a temperature rise would be heat flowing back from the EHD contact into the inlet region. Higher temperatures are known to exist in the contact but no method of predicting them has yet been shown to be accurate. However, using a procedure outlined by CAMERON (16), theoretically expected contact temperatures are calculated and predictions made for the temperature rise in front of the contact. This procedure is also used in reverse with the contact temperatures necessary to explain the temperature "mismeasurement" in the inlet being calculated. In each case the inlet temperatures are calculated for a point one tenth of a Hertzian contact width in front of the contact, this should exaggerate any influence of contact temperature.

Treating each of the three contacts as independent of each other, the peak temperature rise which can be expected in the contact region (T_c) is given by

$$T_c = \frac{2q \cdot (\frac{\ell}{\pi})^{\frac{1}{2}} \cdot B_1}{(1 + \frac{B_1}{B_2})} \qquad (7.11)$$

where $$q = \frac{\mu \cdot W(U_1 - U_2)}{\mathfrak{J} \cdot L \cdot \ell}$$

$$B = \frac{1}{K} (\frac{\kappa}{U})^{\frac{1}{2}}$$

$$\ell \equiv 2a = 2 \times (\frac{8RW}{\pi E' L})^{\frac{1}{2}}$$

R = reduced radius

W = load

E' = reduced Young's Modulus

L = length of contact

U = speed of the surface

κ = thermal diffusivity

K = thermal conductivity

$\mathfrak{J}$ = mechanical equivalent of heat

μ = coefficient of friction (traction)

where applicable the suffix 1 will denote the sapphire surface and the suffix 2 will denote the steel surface.

The following physical values were used:-

R = 8.47 mm , W = 2780 N (equivalent to 1.294 GN/m^2 maximum Hertzian pressure and the highest load used), E' = 305 GN/m^2 , L = 9.53 mm , U_1 = .865 m/sec , U_2 = .465 m/sec , (giving a slide/roll ratio of approximately 0.6 and mean speed = 0.665 m/sec.), κ_1 = 0.12 x 10^{-4} m^2/sec , κ_2 = 0.12 x 10^{-4} m^2/sec , K_1 = 35.6 J/sec.m ^{o}C., K_2 = 46.1 J/sec.m ^{o}C, μ = 0.055.

Therefore

ℓ = 0.3409 mm

$$B_1 = 1.12 \times 10^{-4}\ m^{1.5}.sec.^{o}C/J$$

$$B_2 = 1.01 \times 10^{-4}\ m^{1.5}.sec.^{o}C/J$$

$$q = 22.36 \times 10^{8}\ J/m^{2}.sec$$

giving $T_c \simeq 20.9\ ^{o}C.$

However this analysis is only valid for the situation where both the moving surfaces are at the same initial temperature. In the experimental situation the temperatures of the two surfaces are not the same and, for the parameters used in the previous calculation have a temperature difference of approximately 14.5°C. Thus the division of heat generated in the contact cannot be expected to behave in the same manner assumed for the analysis, and so the predicted temperature has an inherent inaccuracy. However this effect, although significant, is not overwhelmingly large.

Unfortunately two other factors also cast some doubt as to the validity of this analysis. The first is that Cameron's treatment of the problem assumes a steady state has been reached, whereas transient thermal conditions are to be expected here. Secondly the oil film is considered to offer no thermal resistance to heat flow to the surfaces. ARCHARD (17) has suggested that this effect is not negligible and can in fact give higher temperature rises than previously calculated.

It would therefore appear that the temperatures in the contact region may well be higher than first expected, especially as the sapphire disc has to attain a temperature of 14.5°C higher than the steel disc (68% of the total predicted rise using Cameron's procedure).

However for the present time it will be assumed that the predicted value is representative. Later it will be shown that these temperatures are an order of magnitude too low to

explain the experimental results.

Continuing with the analysis, a speed factor $b = \frac{U\ell}{2\kappa}$ is now calculated for each surface, and the following values are obtained.

$$b_1 = 12.3$$

$$b_2 = 6.6$$

From Fig. 7.22 it can be seen that the temperature rise one tenth of a Hertzian contact width in front of the contact is approximately 0.05 of the peak temperature rise, i.e. approximately $1^{o}C$. This value is nowhere near the $25^{o}C$ that is required to explain the results.

Conversely, if it is assumed that the proportionality of temperature one tenth of a contact width in front of the contact to peak temperature still holds for other temperatures, the contact temperature rise necessary to give a $25^{o}C$ rise in the inlet region is approximately $500^{o}C$.

It is highly unlikely that contact temperatures of this magnitude could be present for the conditions used in this series of experiments, and virtually impossible that these temperatures are present for one set of conditions and not present for a marginally different set of conditions. A gain of heat to the inlet region from the contact is therefore thought to be an unlikely mechanism to explain the film thickness discrepancies that have been found to exist.

However some doubt remains as to the accuracy of the trailing thermocouple, especially for measuring skin temperatures. It is possible that a thin layer of hotter oil is carried from the exit of one contact into the inlet of another, and that the temperature of this layer is not measured.

This could arise because the bead of the thermocouple is large compared with the thickness of this hotter oil layer, and hence detects only the bulk surface temperature. On entry into the contact this thin layer of hotter oil would be the dominating influence on film thickness.

This line of reasoning can be eliminated as an explanation of the film thickness behaviour by a simple examination of the thermal situation in relation to the experimental conditions. As mentioned previously it is unlikely that small change in operating conditions could allow a thermal effect to become suddenly dominant, especially as a threefold increase in sliding (and hence heating) will not cause a fall in film thickness unless the film thickness is very close to the critical value of approximately 0.25 μm. An increase in sliding of this magnitude would cause a significant rise in the skin temperature and hence should have precipitated a fall in the EHD film thickness. The fact that the film thickness is usually insensitive to the proportion of sliding present suggests that the trailing thermocouple gives a fairly accurate measurement of the inlet temperature, and that a skin of hotter oil, which is too thin to be detected, is not the explanation for the discrepancy. It appears therefore that an attempt to explain the film thickness behaviour at low values when sliding is introduced is not feasible in terms of temperature effects. However before looking at other possible influences on α and η_o, it is worthwhile considering temperature effects as a possible reason for the discrepancies at the higher values of film thickness.

Figs. 7.18 to 7.21 show that errors in temperature measurement of $4^{o}C$ would bring most of the results back into

agreement. The previous analysis for heat flowing back out of the contact gives rises of $1^{o}C$,and as mentioned, this might actually be higher due to the fact that the transient nature of the thermal situation and the thermal resistance of the oil film (especially at the larger film thicknesses) are neglected in the analysis.

In addition it is not impossible that the trailing thermocouple may be unable to detect a very small layer of slightly hotter oil, sufficient to account for $1^{o}C$ or $2^{o}C$ difference in measurement of inlet temperature.

It can be seen that the combination of these two factors is probably sufficient to give an error in measurement of $4^{o}C$. It is therefore proposed that this is the explanation for the fall in film thickness with sliding at the higher values, but not at lower values.

Attention is now turned to analysing other conditions which may affect the pressure/viscosity coefficient, α, and the inlet viscosity, η_o.

7.4.2 Shear Effects

JONES, JOHNSON, WINER and SANBORN (18) have shown that, in general, α falls with increasing shear stress. Also ADAMS and HIRST (19) propose that viscosity has a non-Newtonian response above a critical shear stress. Nevertheless, although both α and η_o appear to be dependent on shear stress it is unlikely that this parameter controls the fall in film thickness. The shear stress levels in the inlet region are predominantly due to the film squeeze action of the two moving surfaces and the contribution to shear stress by the introduction of sliding is very small. Hence any fall in

film thickness due to shear stress effects should be apparent in the pure rolling situation and not be unduly affected by the presence of sliding.

This argument can be confirmed by an examination of the results. The film thickness drop only seems to be dependent on whether or not the actual film thickness is above or below a critical value. For the case where the film thickness is above this critical value, a fall in film thickness will not occur when sliding is first introduced, nor when sliding is increased threefold. However by decreasing the speed (and hence decreasing the shear stress) so that the film thickness is below the critical value, the introduction of sliding now causes a fall in film thickness. Thus at a higher shear stress level due to a higher rolling speed the introduction of sliding (and extra shear stress) does not cause a fall in film thickness, whereas at a lower shear stress level due to a lower rolling speed the introduction of sliding does cause a fall. This behaviour is not compatible with the effect of shear stress on α and η_o being the mechanism to explain the results.

In a similar manner a viscosity dependence on shear rate or a shear thinning effect seem an unlikely explanation. A large amount of shear comes from the rolling contribution to motion and yet by doubling the speed and hence greatly increasing the shear rate the film thickness does not fall, but <u>increases</u>. In fact where sliding is present and a film thickness discrepancy is noted, an increase in the rolling speed will increase the film thickness and eliminate the discrepancy at the same time.

7.4.3 Other Effects

All the attempted explanations of the results have so far concentrated on the rheological behaviour of the lubricant, and have assumed that classical EHD theory is valid. However classical EHD theory assumes that the two surfaces are smooth and that there are no surface irregularities. This is not true for the discs used in this experiment. (The surface profile traces are given in Fig. 7.23). It will be noted that, although the C.L.A. values for the steel discs are all approximately 0.04 μm , a typical value of peak to valley height taken from the trace is approximately 4 mm which, for the scaling factor of 20,000, represents 0.2 μm , i.e. of the same order of magnitude, and close to the value of film thickness at which anomalous effects are noticed. On closer examination of the traces it can be seen that, for a mean separation of the sapphire and steel surfaces of 0.25 μm , some of the larger peaks of the steel surface will intermesh with the (relatively) smooth sapphire surface. However this is only true if both the discs are stationary. When the discs are moving the situation is very different; high pressures are generated in the contact, high enough to deform small surface asperities significantly.

Thus, although surface roughness may possibly play some part in the mechanism of the film thickness fall, it is unlikely that actual surface to surface contact takes place. This view is supported by the fact that no noticeable increase in traction was detected when the film thickness fall was first apparent. It is assumed that any significant contact under sliding conditions would be accompanied by a rise in traction.

Unfortunately it was not possible to test this assumption of no asperity contact using an electrical method as both sapphire and the coating sputtered onto it (Cr_2O_3) are electrically non-conducting.

Thus it seems likely that some form of micro-elasto-hydrodynamic lubrication is taking place, as demonstrated by JACKSON and CAMERON (20), where the surface asperities all act as miniature EHD contacts and as such deform elastically, thus avoiding any surface to surface contact. In Jackson and Cameron's work the "asperities" were artificially formed and of large size, in the present work the areas of micro-EHD contact would be much smaller and not discernible. Hence it was not possible to view this phenomenon directly.

7.5 A POSSIBLE MECHANISM TO EXPLAIN THE ANOMALOUS BEHAVIOUR OF FILM THICKNESS

7.5.1 The Effect of EHD Conditions on Asperities

Recent work by CHOW and CHENG(21) has predicted the pressure perturbations due to a single ellipsoidal asperity in an EHD contact, this is somewhat similar to the present case in that one surface was relatively rough while the other surface was relatively smooth. Chow and Cheng's work was carried out for a rigid asperity whereas in reality there is some elasticity of the asperity. However, if it is assumed that the general behaviour pattern for a rigid asperity still holds here, some interesting comparisons can be drawn between these predictions and the experimental results.

One particularly interesting feature of Chow and Cheng's work is reproduced in Fig. 7.24(a). This plot shows the effect of slide/roll ratio on the perturbed pressure para-

meter Δs (defined as perturbed pressure/maximum Hertzian pressure) for two values of G (defined as pressure viscosity coefficient x reduced Young's Modulus). It can be seen that Δs is greatly dependent on the slide/roll ratio when Δs is small, and relatively insensitive when Δs is large. The two plots are for G = 100 and G = 500 whereas the value of G here is 6,000. Chow and Cheng propose that these lower values of G are more accurate than those calculated assuming a static configuration, although their justification for this is vague. They do admit however that, for higher values of G, the point of minimum Δs approaches s = 0. They also mention that this work agrees very well with studies by LEE and CHENG (22) which predict Δs a minimum for zero sliding (s = 0) at a value of G = 3180. If it is assumed that G does approximately equal 6,000, then it can be said that the magnitude of the perturbed pressure increases sharply at first with the introduction of sliding and then responds much more slowly for larger values of sliding.

Another prediction of this analysis is shown in Fig. 7.24(b). As the film thickness parameter h^*/R (defined as central film thickness/reduced radius) falls, the magnitude of the perturbed pressure parameter Δs increases for the rigid asperity but remains reasonably constant for an elastic asperity (predicted from work by CHENG (23)). This difference in behaviour for the elastic asperity is due to the fact that the asperity deforms and hence its influence is reduced. Chow and Cheng state that the rigid asperity analysis can only be considered valid for $h^*/R \geqslant 10^{-5}$, $p_{Hz}/E' \leqslant 0.003$, and $G < 500$ (p_{Hz} = maximum Hertzian pressure, E' = reduced Young's Modulus) whereas here typical values are $h^*/R = 3 \times 10^{-5}$, $p_{Hz}/E' = 0.005$, and

G = 6,000. For these ~~qualities~~ values this rigid asperity analysis can only predict general trends as local yield effects are then taking place.

Thus the elastic theory of Cheng indicates that the magnitude of the perturbed pressure stays constant as film thickness falls, because the asperity deforms, and the rigid asperity theory of Chow and Cheng suggests that the perturbed pressure increases as the film thickness falls; however in practice local yield effects must be taking place. Both these approaches suggest that in reality deformation of the asperity must occur under certain operating conditions.

Finally Figs. 7.24(c) and 7.24(d) show that as Hertzian pressure (i.e. load) increases, the magnitude of Δs increases for a rigid asperity, and remains roughly constant for an elastic asperity i.e. the perturbed pressure (defined as Δs x Hertzian Pressure) increase in both cases, although one case is more rapid. Some interpolation of the plot is needed as Fig. 7.24(c) represents $h^*/R = 10^{-5}$ and Fig. 7.24(d) represents $h^*/R = 10^{-6}$ whereas a typical experimental value is $h^*/R = 3 \times 10^{-5}$.

In the real case the asperities on a typical surface are not rigid but behave in an elastic manner and as such will respond to changes in pressure. Therefore it seems likely that the pressure perturbations predicted by rigid asperity theory will deform the actual asperity. However this deformation will modify the pressure perturbation itself, so in fact some sort of equilibrium situation will be reached.

Nevertheless, assuming that the general behaviour pattern predicted for a rigid asperity is still valid for the real, more elastic type of asperity and in particular, that

the pressure perturbation tends to flatten significantly the peak of the asperity, then it can be said that:-

(1) As the film thickness falls the flattening effect on the asperities increases. However under conditions of pure rolling this effect is not significant until low film thickness are reached.

(2) The flattening effect on the asperities is greatly increased by the presence of sliding (however the film thicknesses still have to be fairly low for this effect to be noticeable). Thus it is possible to have a film thickness at which the asperity deformation is low for pure rolling but much greater for rolling plus sliding.

(3) It only requires a small amount of sliding to increase the flattening effect, after this further increases in sliding have a diminishing influence.

(4) As the load is increased the flattening of the asperities increases; this is true for both rolling and rolling plus sliding.

It must be remembered that this flattening effect is not limitless; the absolute maximum deformation can only equal the original height of the asperity.

This predicted flattening effect has a similar behaviour pattern to that noted for film thickness discrepancy (see Section 7.3.2). Thus if a link can be established between the two phenomena, then a possible explanation of the anomalous behaviour of film thickness may exist.

7.5.2. The Effect of Asperity Behaviour on Film Thickness

The work of LEE and CHENG (22) and more recent work

by CHOW and CHENG (24) has predicted that surface roughnesses can give a significantly higher film thickness than for a smooth surface. This film thickness is defined as the separation of the mean lines through the surface roughnesses, and will be almost exactly the same as the measured optical film thickness which is also related to the separation of the mean lines.

An alternative way of visualising the situation is to consider that the mean line through the asperities is not the effective boundary for determining film thickness. In other words the contact can be treated the same as for a smooth surface, but now the equivalent smooth surface boundary passes much closer to the asperity peaks (more like an envelope boundary) - see Fig. 7.25(a). This means that the measured film thickness is greater than the smooth surface "operating" value by an amount which is dependent on the height of the asperities.

A mechanism to explain the observed film thickness behaviour can now be suggested, based on the fact that any flattening of the asperities will reduce the amount by which the film thickness is enhanced over the smooth surface value. Consequently if the asperities were totally flattened the measured value would equal the smooth surface value.

Assuming that this "equivalent smooth surface" film thickness behaves in a regular manner to changes in load, temperature, rolling speed etc. as predicted by EHD theory, it is still possible to detect a fall in measured film thickness. This fall is really a reduction in the enhancing effect of the surface roughness over the smooth surface value as the asperities flatten.

Combining this hypothesis with the predictions of CHOW and CHENG (21) for single asperities leads to the following description of measured film thickness behaviour:-

When the film thicknesses are large the deformations of the asperities for both the rolling and rolling plus sliding cases are very small. Consequently they are both enhanced over the smooth surface values by the same amount, and as the smooth surface values are not affected by the presence of sliding, neither are the measured values.

As the film thickness falls the deformation of the asperities under pure rolling is still small but the introduction of sliding significantly increases this flattening effect. Thus, although as before the equivalent smooth surface value is unaffected by the presence of sliding, the enhanced (measured) film thickness is reduced due to the flattening of the asperities - see Figs. 7.25(b) and 7.25(c).

If the film thickness falls even further the flattening effect now becomes significant for pure rolling as well, and so a plot of measured film thickness shows a more rapid fall off than before as it moves into the "critical" region.

However, as mentioned previously, the asperities cannot be flattened by more than their original height, and so a hypothetical curve of flattening effect against film thickness would look something like Fig. 7.26 for any given rolling/sliding combination. At high values of film thickness the flattening effect is small but rapidly increases as film thickness falls. Eventually there is an inflection in the curve and, at near zero values of film thickness, it asymptotes to a value equivalent to the asperity height.

Thus the deformation of the asperities and hence fall in measured film thickness are limited. This means that there must be some recovery in the rate of increase in film thickness discrepancy, and that this discrepancy should eventually approach a constant value.

The rolling plus sliding experiments did not proceed far enough to test this hypothesis, as there was concern that the optical coating would be damaged at low film thickness. However under pure rolling some low film thicknesses were reached and in Figs. 6.17 to 6.19 it can be seen that a recovery in response is apparent. Moreover in Fig. 6.25 it can be seen that the loss of enhancement for both pure rolling and rolling plus sliding appears to be approaching the same value.

It is clear that this mechanism describes the experimental behaviour very well in a qualitative manner, but it is much more difficult to assign any quantitative values to the effect; however one approach will be outlined in the following section.

7.5.3 Correction to Some of the Rolling Film Thickness Measurements

If the flattening effect on the asperities or conversely the enhancement in film thickness were known with respect to film thickness for any given set of conditions, then it would be possible to re-plot Figs. 6.17 to 6.19 so that they showed the response of equivalent smooth surface film thickness against the parameters $U.\eta_o$ and $U.\alpha.\eta_o$.
It is not possible to describe the shape of the film thickness enhancement/film thickness curve accurately, but an estimate can be made of the maximum value and related to asperity height.

As mentioned previously the C.L.A. values for surface roughness are all approximately 0.04 μm where typical peak to valley heights from the trace are 0.2 μm. If it is assumed that the equivalent smooth surface boundary passes close to the peaks, then the maximum enhancement will be approaching half the peak to valley height i.e. 0.1 μm. However as the film thickness drops this enhancement goes to zero. Thus the proposed curve will be very similar to the inverse of the curve in Fig. 7.26. (The greater the flattening effect, the less the film thickness enhancement).

In Fig. 7.27 a curve of film thickness enhancement versus measured film thickness has been constructed. This curve satisfies the end conditions above, although the maximum enhancement, 0.09 μm , is slightly less than half the typical peak to valley height of the asperities to allow for the equivalent smooth surface boundary not quite being an envelope boundary.

If this curve is used to correct the results of Fig. 6.18 then a plot of equivalent smooth surface film thickness is obtained which shows very little irregularity in behaviour (Fig. 7.28). Using these results it is possible to calculate the response of film thickness to $U.\eta_o$ although as before no allowance has been made for the effect of the pressure viscosity coefficient, α. Nevertheless a relationship of the form

$$h \alpha (U.\eta_o)^{0.71} \qquad (7.12)$$

is obtained compared with

$$h \alpha (U.\eta_o)^{0.66} \qquad (7.13)$$

obtained previously.

It can be seen that this value for the power coefficient of film thickness response to $U.\eta_o$, "b", is slightly higher than before. It suggests that the value for "b", obtained by the more accurate method of comparing the response of film thickness to speed only, will also be higher than its previous value of 0.615, thus improving the already good agreement with other workers' predictions.

The effect of this correction on "c", the power coefficient of film thickness response to load, is more difficult to quantify, but it appears to increase the value of this coefficient by approximately 25% on average. This improves the comparison against other workers' values but still leaves the experimental values well short of Wymer's value of -0.17.

7.6 CONCLUSIONS

It would appear therefore, that a surface asperity deformation mechanism adequately explains the behaviour pattern of film thicknesses measured under rolling and rolling plus sliding conditions. The important aspects of this type of mechanism are as summarised below:-

(1) For film thicknesses significantly above the average peak to valley height of a rough surface, the mean separation of the two surfaces (i.e. the separation measured by optical interferometry) is greater for rough surfaces than for equivalent smooth surfaces.

(2) As the film thickness falls the local pressure variations around the asperities increase in magnitude and cause significant deformation of the as-

perities themselves. As this happens the film thickness enhancement of rough surfaces over smooth surfaces decreases. This appears to occur at values close to the typical peak to valley height of the asperities.

(3) Although significant pressure variations with consequent flattening of the asperities can occur under conditions of pure rolling only, the introduction of sliding greatly magnifies this effect.

(4) Only relatively small amounts of sliding are necessary to increase this flattening effect, further increases have a reduced influence.

(5) The local pressure variations (and hence flattening effect) increase in magnitude with increasing load.

Support for this projected behaviour of gross deformation has recently been found at Imperial College, London (25). Experiments have been carried out using a transparent disc onto which are sputtered controlled asperities. Optical measurements of the film thickness between these asperities and a rolling or sliding ball have shown large deformations, these deformations were greater for sliding than for rolling. Unfortunately this work is only preliminary and the results have not been published as yet, however the trends agree very well with the proposed mechanism for explaining the present results.

Finally, although further work is needed to more fully understand this behaviour and be able to predict the film thickness enhancement for different surface roughnesses, the following is suggested from the results obtained here:-

For a given peak to valley height of surface rough-

ness, δ, the central film thickness, h_o is enhanced over the equivalent smooth surface value by up to 0.5δ for h_o greater than 2δ. As lower film thicknesses are encountered this enhancement falls but is still significant above $h_o \simeq \delta$ for pure rolling, and $h_o \simeq 1.25\delta$ for slide/roll ratios greater than about 0.05. For values of h_o below 0.5δ this enhancement has almost completely disappeared in both cases.

7.7 SUGGESTIONS FOR FURTHER WORK

Two sections of further experimental work must be carried out. The first is to repeat the present series of tests using different oils - at least two oils. One should have a similar viscosity to the present test oil but different pressure/viscosity coefficient, the other should have a similar pressure/viscosity coefficient but different viscosity. In this way it will be possible to study the effects of viscosity and pressure/viscosity coefficient independently. For a single oil this was not possible as the only way of altering either of these parameters was by changing temperature and hence both were affected simultaneously. From this it will be possible to discern the effect of lubricant properties on the film thickness behaviour noted in these experiments.

The second section, and perhaps the most important, is to change the surface roughness of the steel discs. If the steel discs were made rougher the quality of the optical interferometric pattern would deteriorate, and so the only possibility is to make them smoother. This requires an improvement in the polishing technique and may well necessitate specialist work as a good finish from continual polishing in the same (circumferential) direction is difficult to achieve.

Two things should be apparent from the use of smoother steel discs; the magnitude of the observed film thickness drop should be reduced as the asperity heights will be smaller and hence cannot be physically flattened by the same amount as before, and secondly the onset of the film thickness drop should occur at a lower value of film thickness. Unfortunately this lower value of film thickness may be too low to be measured by the present optical system. This could possibly be remedied by utilising optical spacer layers as used by WESTLAKE and CAMERON (15) which enables ultra-thin EHD films to be measured.

An improvement could be made in temperature measurement. Ideally it would be preferable to get a direct read-out of mean temperature under rolling plus sliding conditions. It may be possible to do this by linearising the output from the thermocouples, and then simply averaging the signals. Manufacturers of electronic systems to read directly temperature using thermocouples (similar to those used in this series of experiments) have achieved this and it would seem likely that this circuitry could be utilised. If this did not prove feasible the problem could possibly be circumvented by altering the experimental procedure. The outputs from the thermocouples on the steel and sapphire discs could be fed into a pen recorder with an event marker. This marker would be operated when the reading of film thickness was taken. Knowing the two instantaneous temperatures, the mean temperature could be calculated. (It is assumed that the mean temperature is the simple arithmetic mean). The corresponding rolling film thickness could then be measured at this mean temperature. This could easily be done as both the thermo-

couples would read exactly the same, thus making it possible to decide when the test temperature had been reached. This latter method has the disadvantage of making it very difficult to arrange for a set of rolling plus sliding results at the same mean temperature but different slide/roll ratios and/or loads, and in fact may still necessitate some form of temperature correction term.

Finally the use of infra-red techniques for measuring contact and inlet temperatures would enable the effect of temperature to be studied much more intensively than has been possible here.

Table 7.1 OPERATING CONDITIONS FOR TRACTION DATA COMPARED IN FIG. 7.1

Symbol in Fig. 7.1	Source	Maximum Hertz Press. (GN/m^2)	Mean Speed (m/s)	Temperature (^0C)
O	A.D.Moore	0.775	2.20	41.5
Δ	A.D.Moore	0.940	2.20	41.5
X	R.R.Duckworth	0.960	0.20	20.0
.	R.R.Duckworth	1.120	0.20	20.0
-----	Present 4 disc machine	0.707	~1.330	30.0
———	Present 4 disc machine	1.117	~1.330	30.0

Table 7.2 ARITHMETIC MEANS AND STANDARD DEVIATIONS FOR THE POWER COEFFICIENTS OF FILM THICKNESS RESPONSE TO SPEED

Load (N)	Mean	Standard Deviation
512	0.587	0.030
1112	0.607	0.031
1601	0.646	0.053
2046	0.637	0.032
2402	0.608	0.058
2780	0.614	0.072

Table 7.3 ARITHMETIC MEANS AND STANDARD DEVIATIONS FOR THE POWER COEFFICIENTS OF FILM THICKNESS RESPONSE TO LOAD

Speed (m/sec)	First Four Loads		All Loads	
	Mean	S. Dev.	Mean	S. Dev.
0.399	0.102	0.010	0.155	0.014
0.665	0.070	0.019	0.124	0.031
0.977	0.067	0.016	0.109	0.019
1.330	0.061	0.018	0.097	0.034

Table 7.4 COMPARISON OF EXPERIMENTAL RESULTS AGAINST THOSE PREDICTED USING WYMER'S RELATIONSHIP

Rolling Speed (m/sec)	Temperature (^{o}C)	Experimental Film Thickness (μm)	Predicted Film Thickness (μm)
0.665	30	0.50	0.59
0.665	40	0.33	0.40
0.665	50	0.23	0.29
0.665	60	0.19	0.21
0.998	30	0.62	0.76
0.998	40	0.41	0.52
0.998	50	0.29	0.37
0.998	60	0.23	0.27
1.330	40	0.55	0.63
1.330	50	0.38	0.45
1.330	60	0.28	0.33

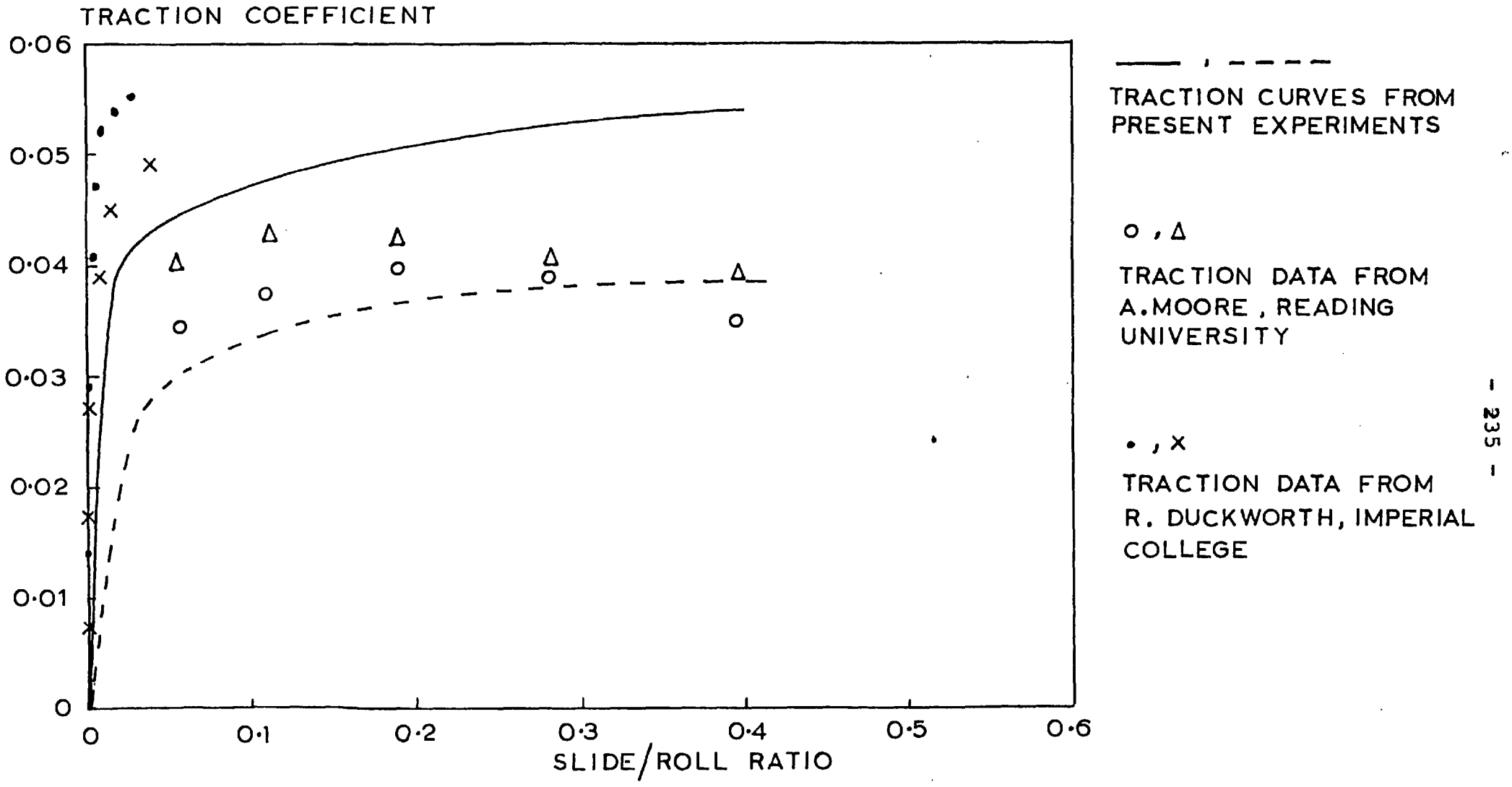

FIG. 7.1. COMPARISON OF PRESENT TRACTION DATA WITH THAT OBTAINED BY OTHER WORKERS FOR THE TEST OIL L74/1113

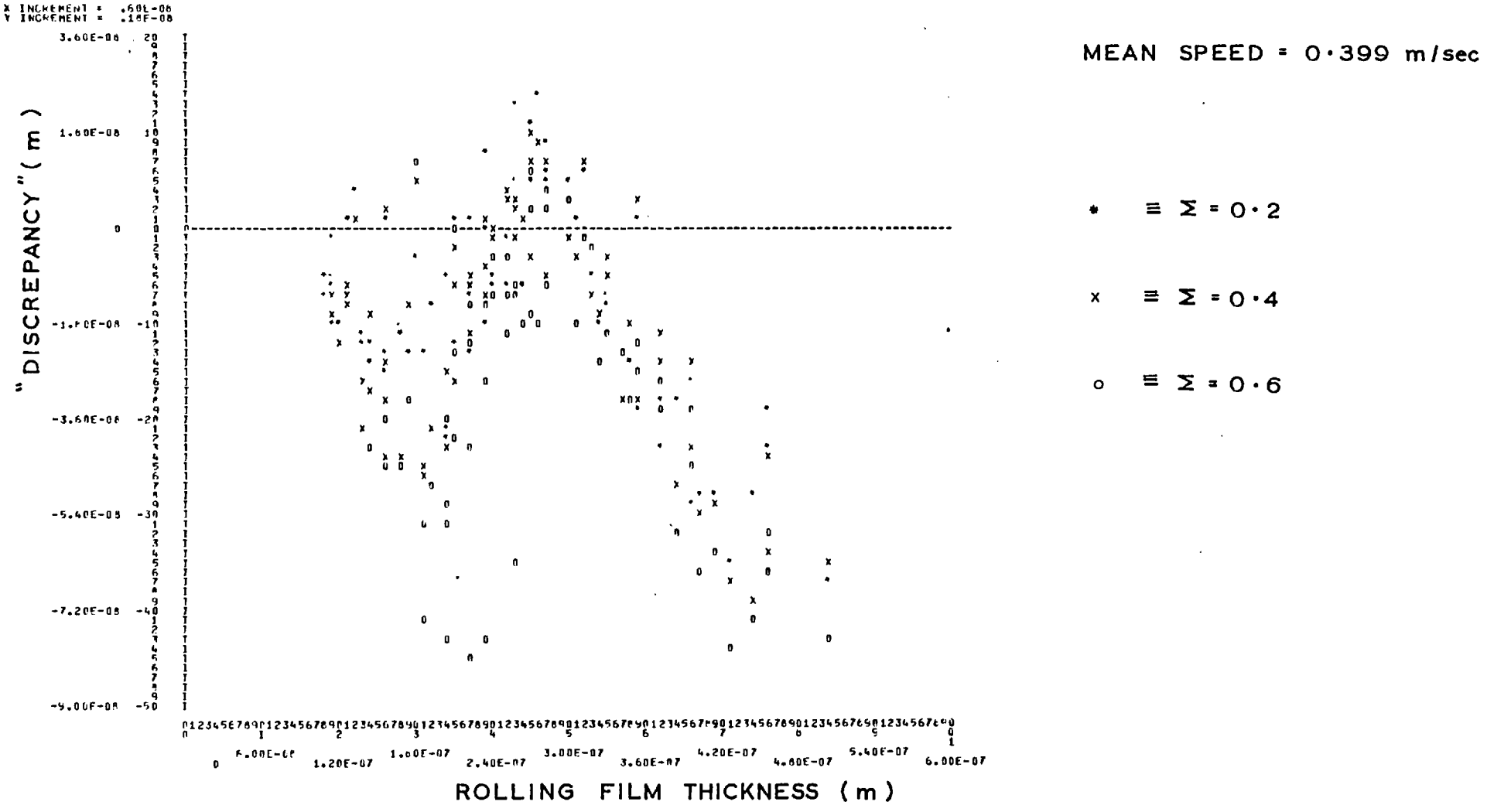

FIG. 7.2. "DISCREPANCY" AGAINST PURE ROLLING FILM THICKNESS

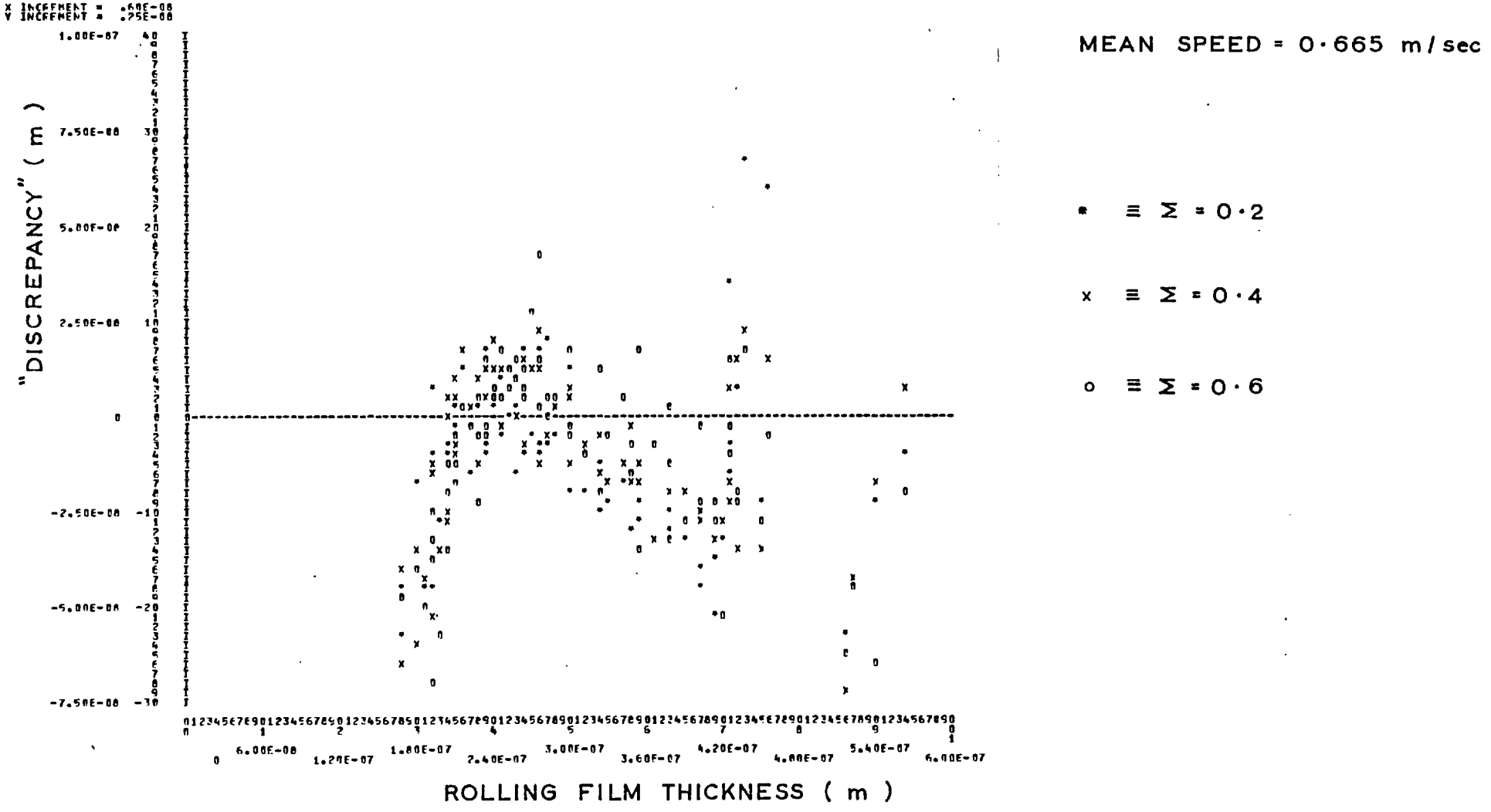

FIG. 7. 3. "DISCREPANCY" AGAINST PURE ROLLING FILM THICKNESS

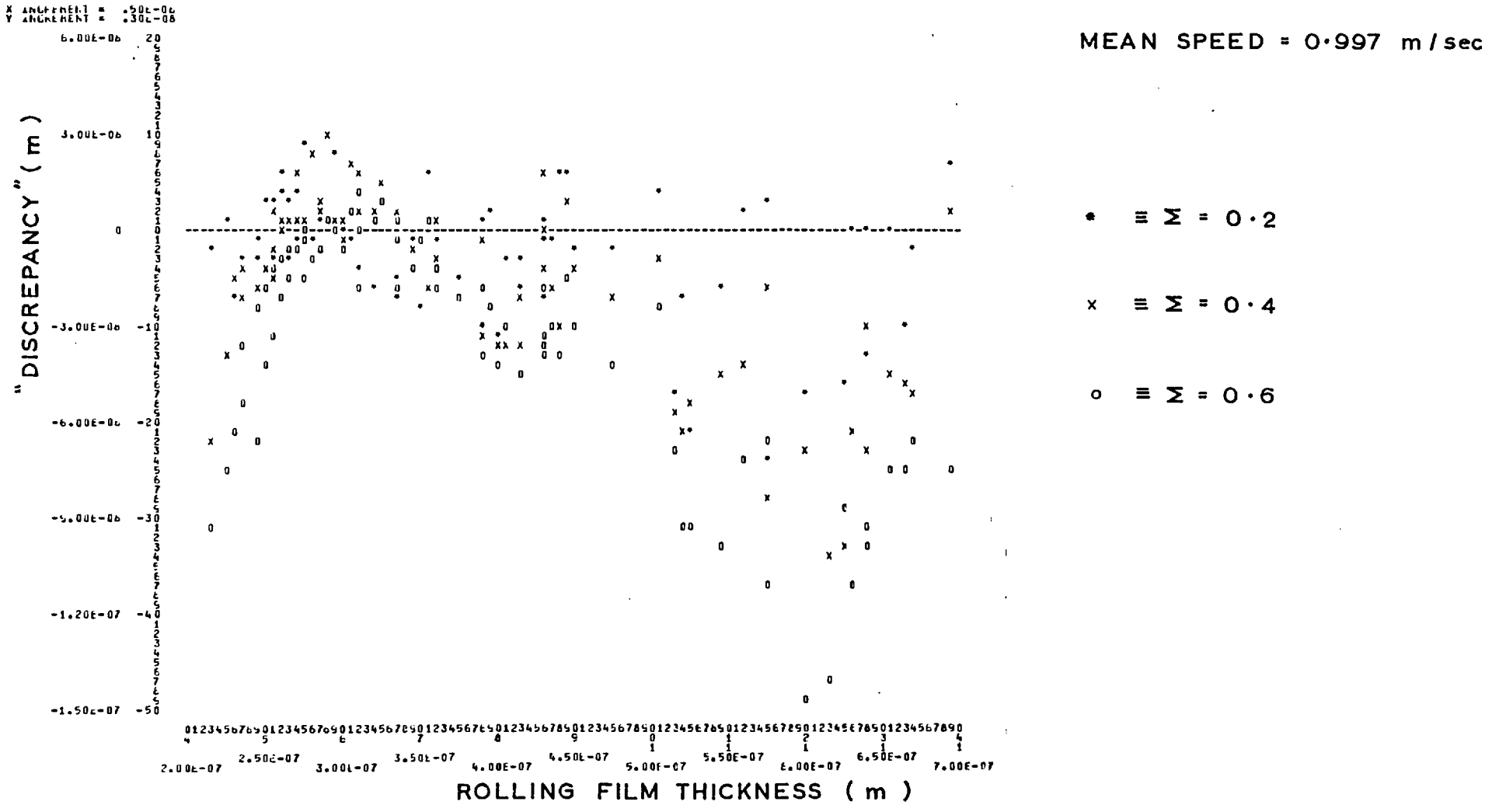

FIG. 7.4. "DISCREPANCY" AGAINST PURE ROLLING FILM THICKNESS

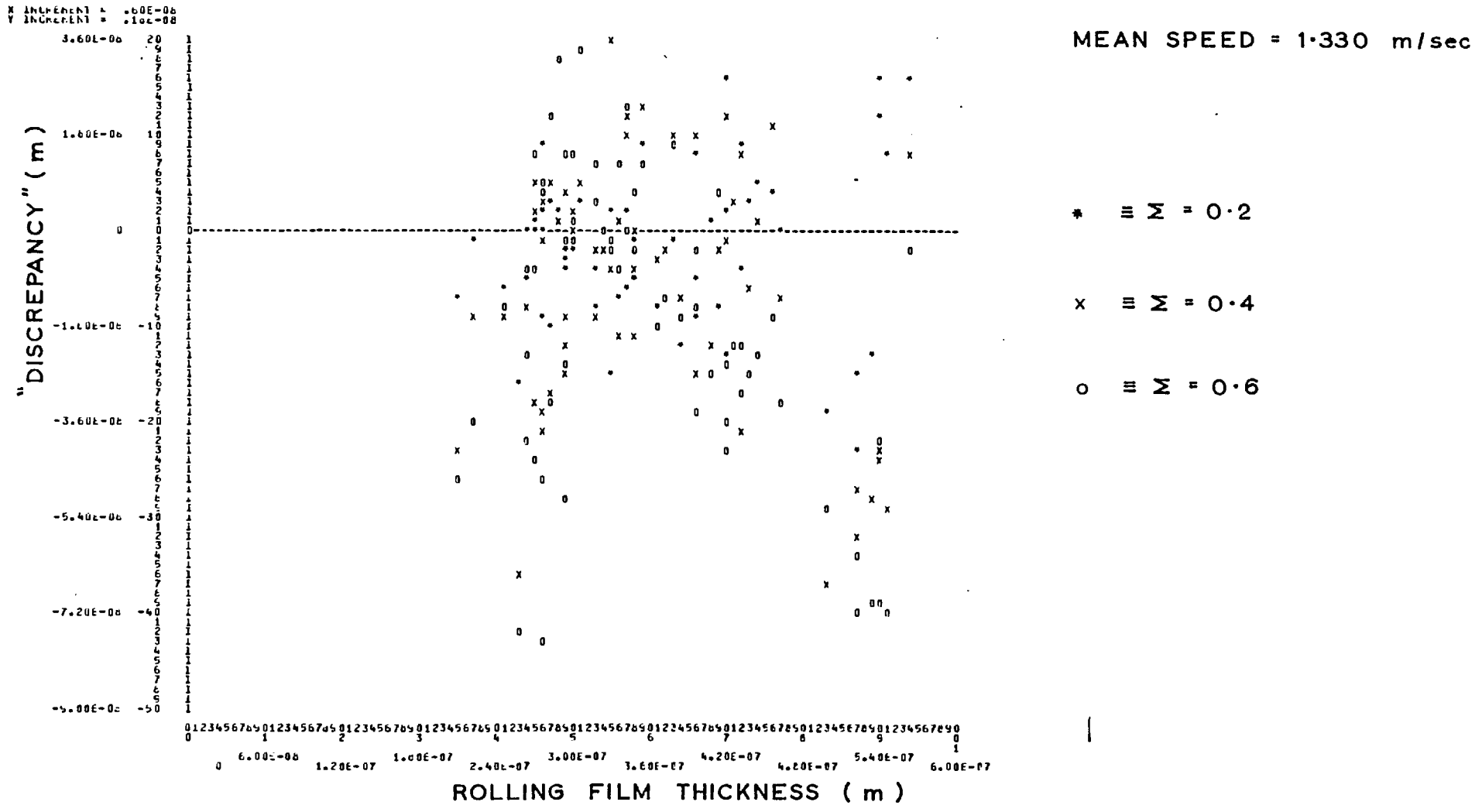

FIG. 7.5. "DISCREPANCY" AGAINST PURE ROLLING FILM THICKNESS

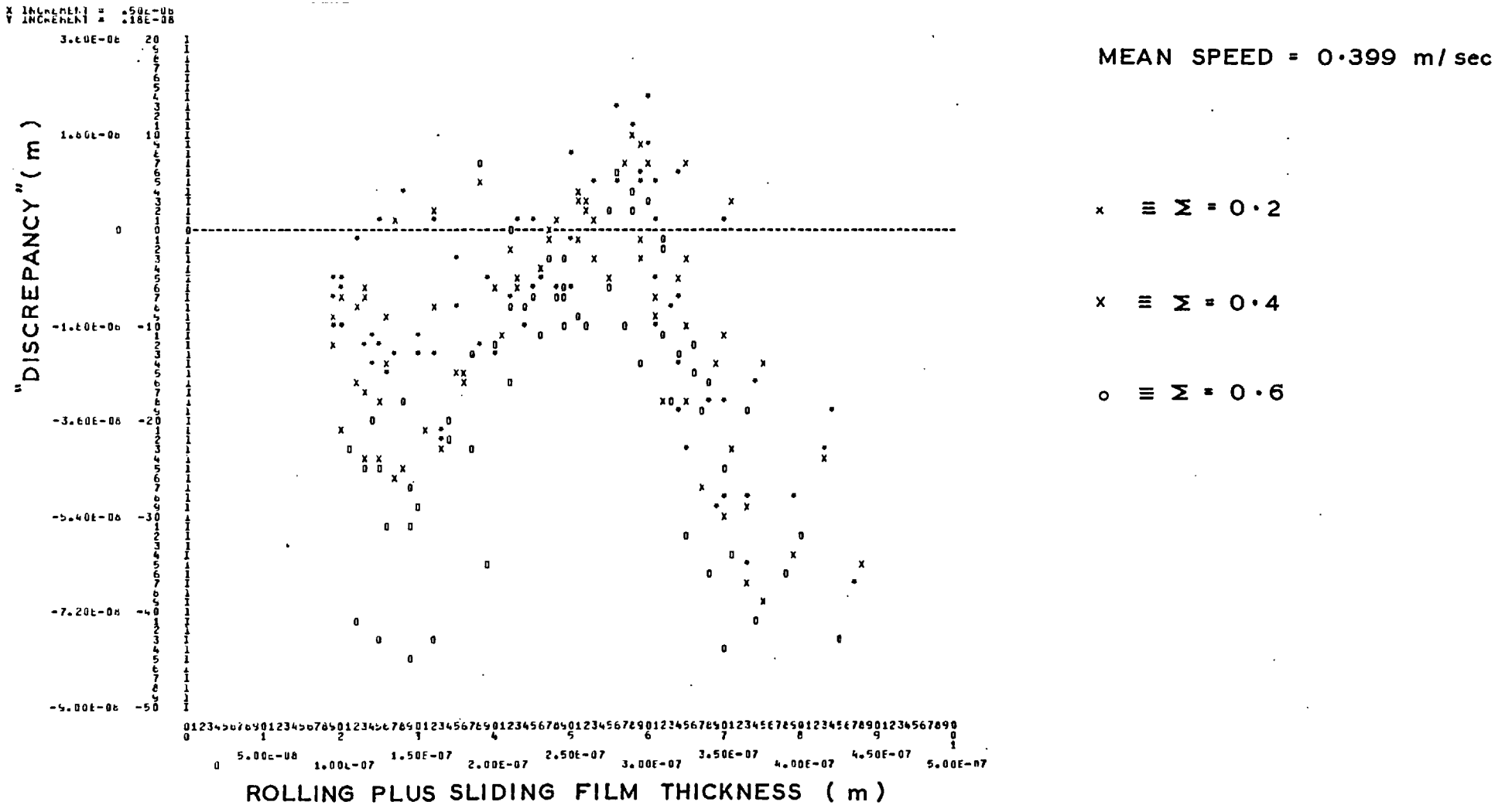

FIG. 7.6. "DISCREPANCY" AGAINST ROLLING PLUS SLIDING FILM THICKNESS

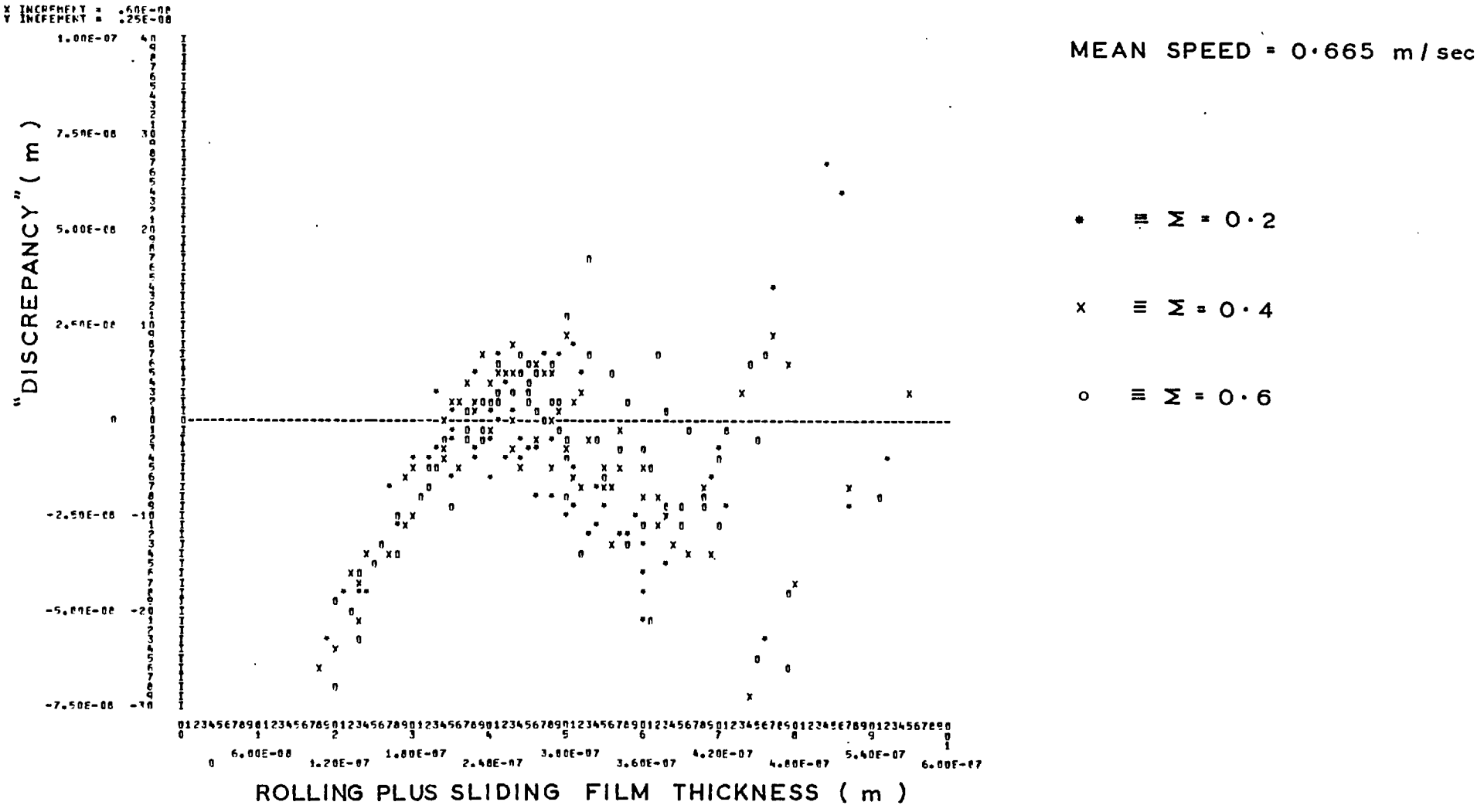

FIG. 7.7. "DISCREPANCY" AGAINST ROLLING PLUS SLIDING FILM THICKNESS

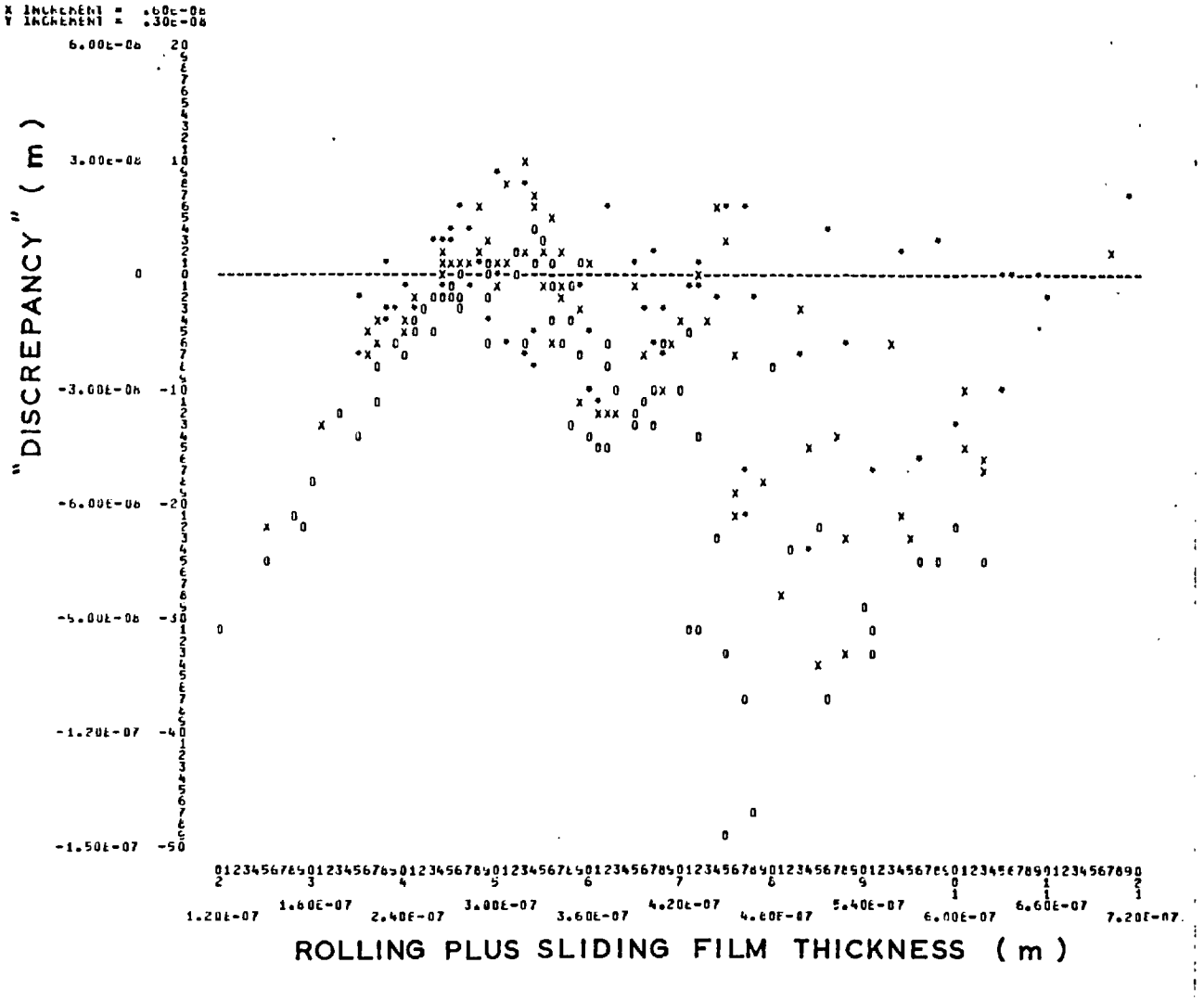

FIG. 7. 8. "DISCREPANCY" AGAINST ROLLING PLUS SLIDING FILM THICKNESS

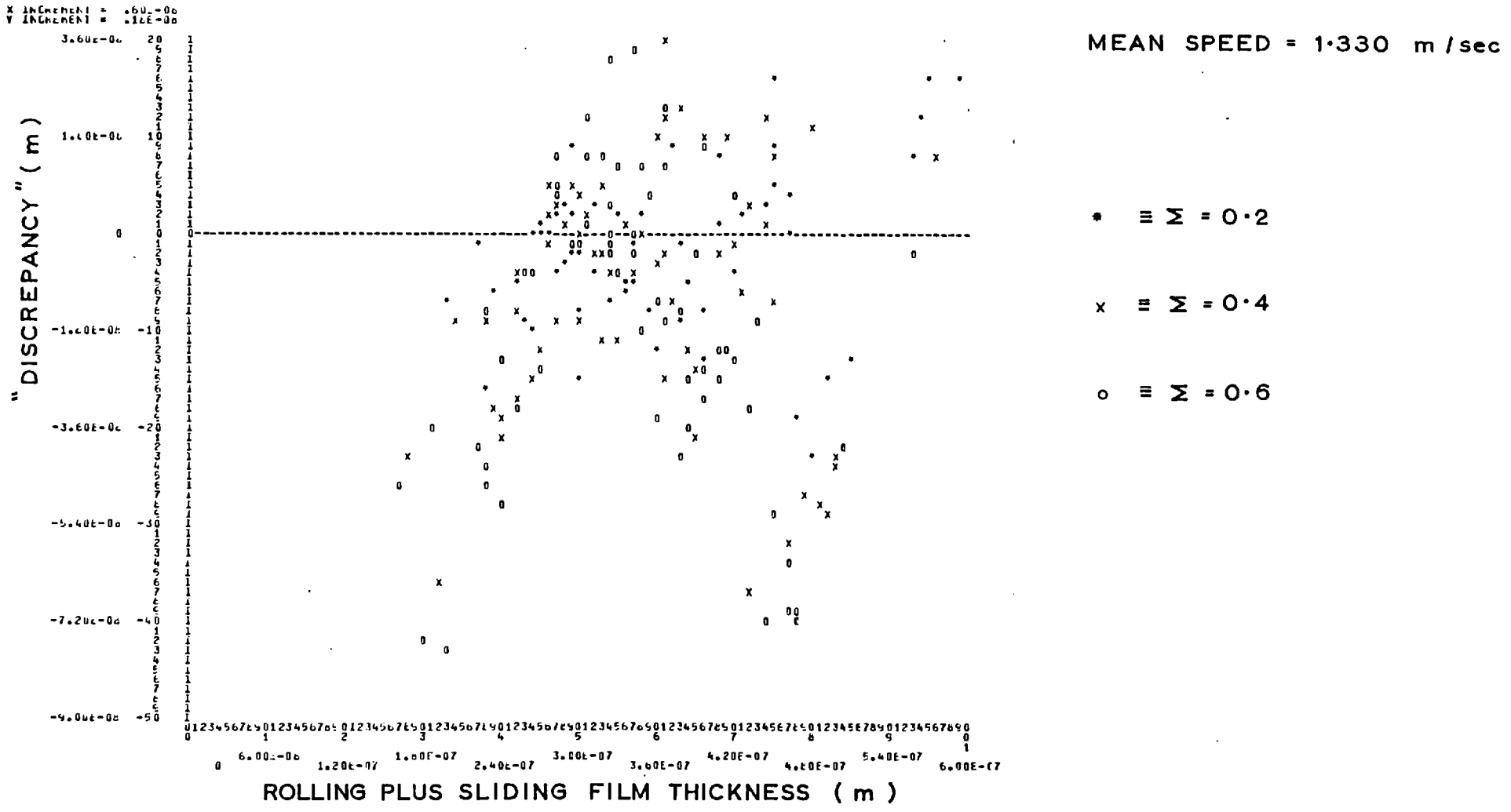

FIG. 7.9. "DISCREPANCY" AGAINST ROLLING PLUS SLIDING FILM THICKNESS

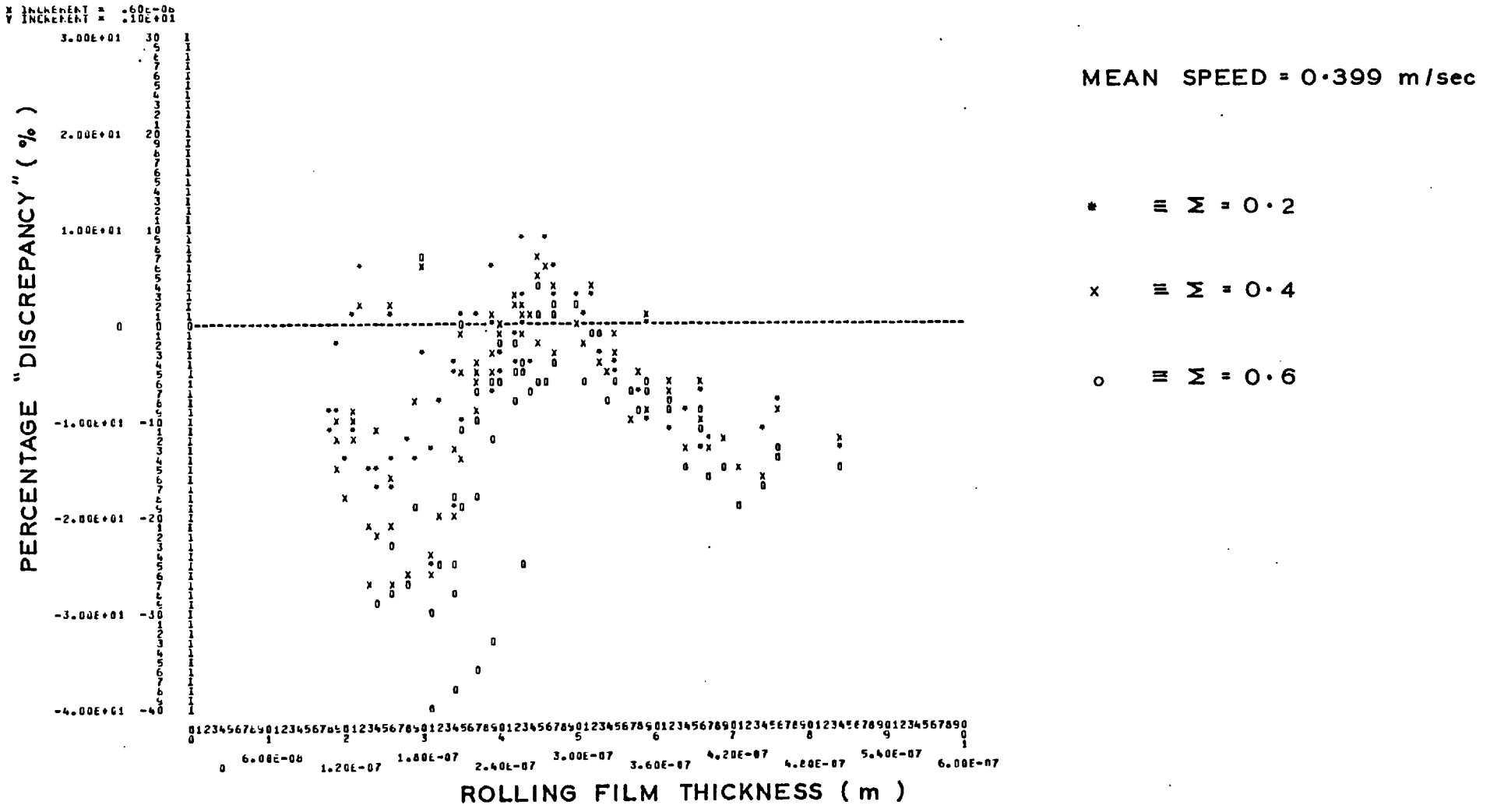

FIG. 7. 10. PERCENTAGE "DISCREPANCY" AGAINST PURE ROLLING FILM THICKNESS

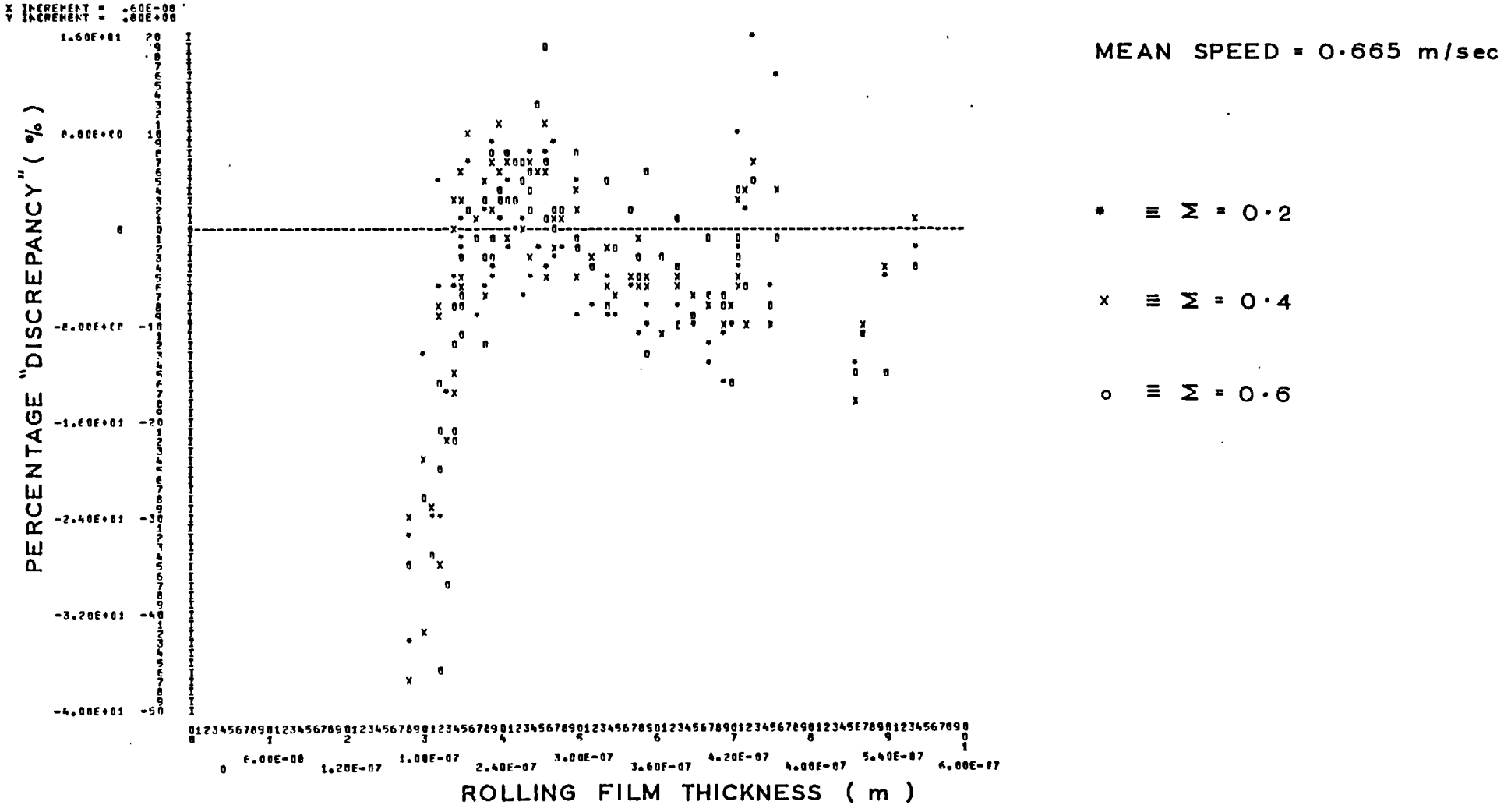

FIG. 7. 11. PERCENTAGE "DISCREPANCY" AGAINST PURE ROLLING FILM THICKNESS

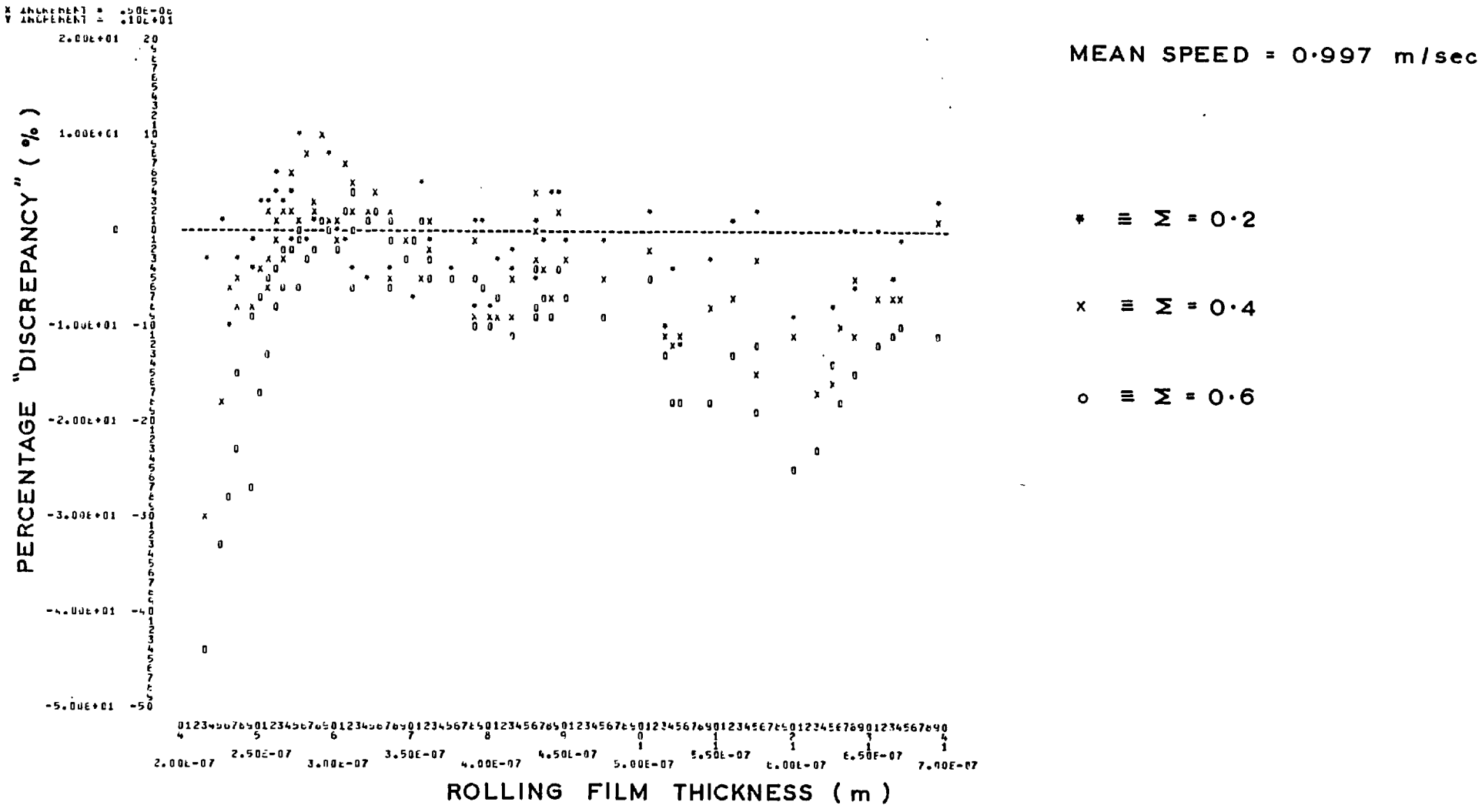

FIG. 7.12. PERCENTAGE "DISCREPANCY" AGAINST PURE ROLLING FILM THICKNESS

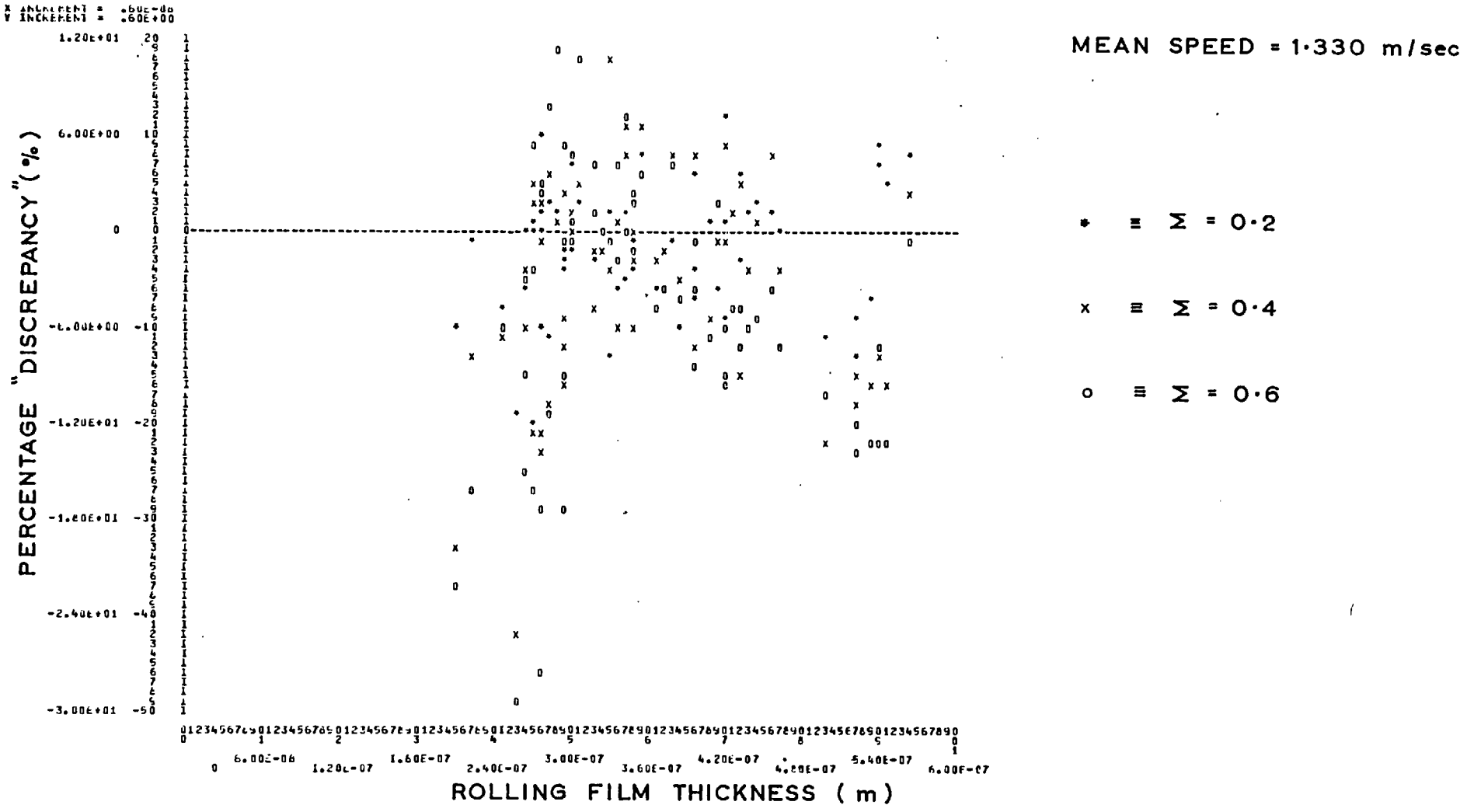

FIG. 7. 13. PERCENTAGE "DISCREPANCY" AGAINST PURE ROLLING FILM THICKNESS

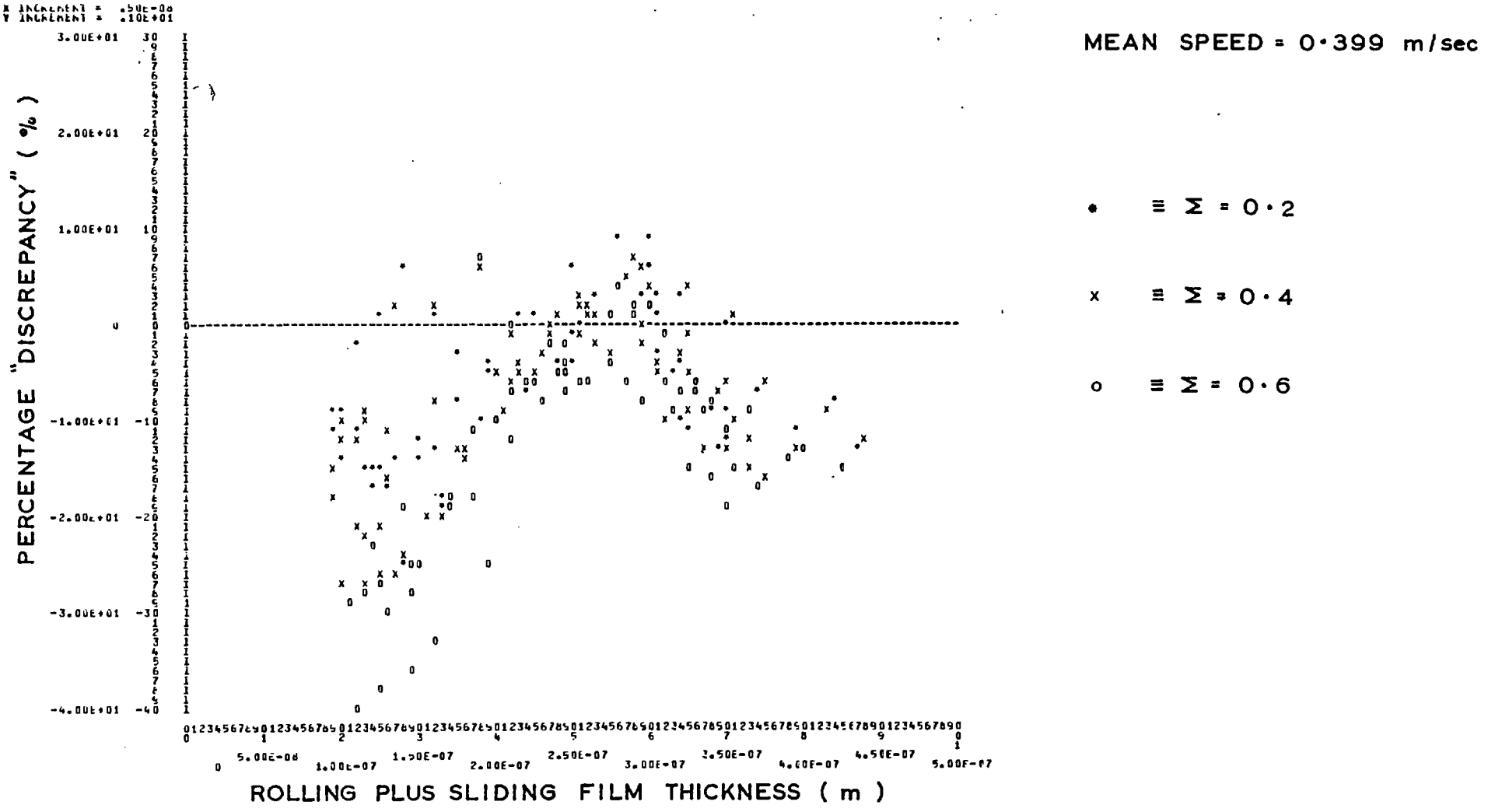

FIG. 7. 14. PERCENTAGE "DISCREPANCY" AGAINST ROLLING PLUS SLIDING FILM THICKNESS

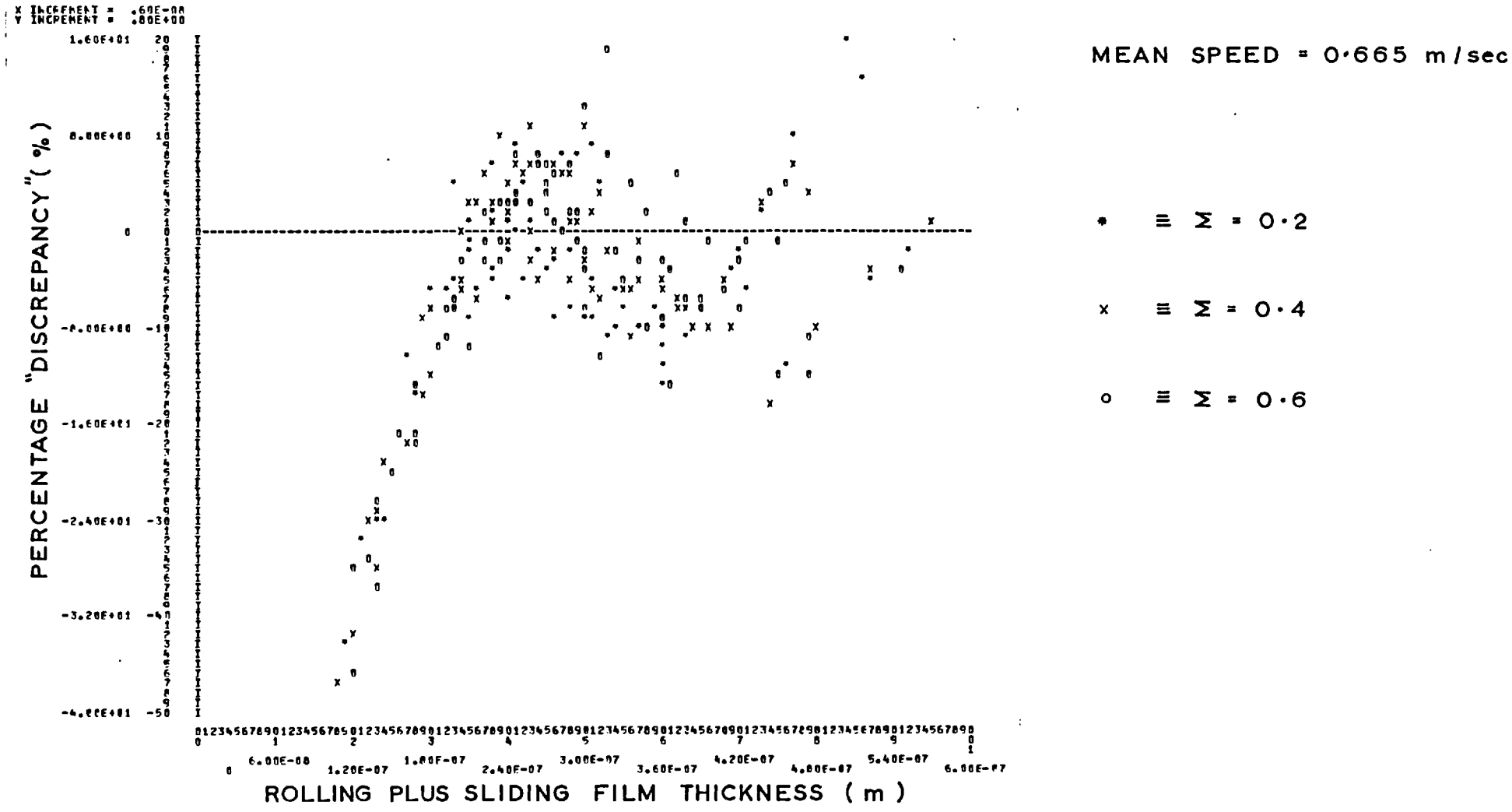

FIG. 7.15. PERCENTAGE "DISCREPANCY" AGAINST ROLLING PLUS SLIDING FILM THICKNESS

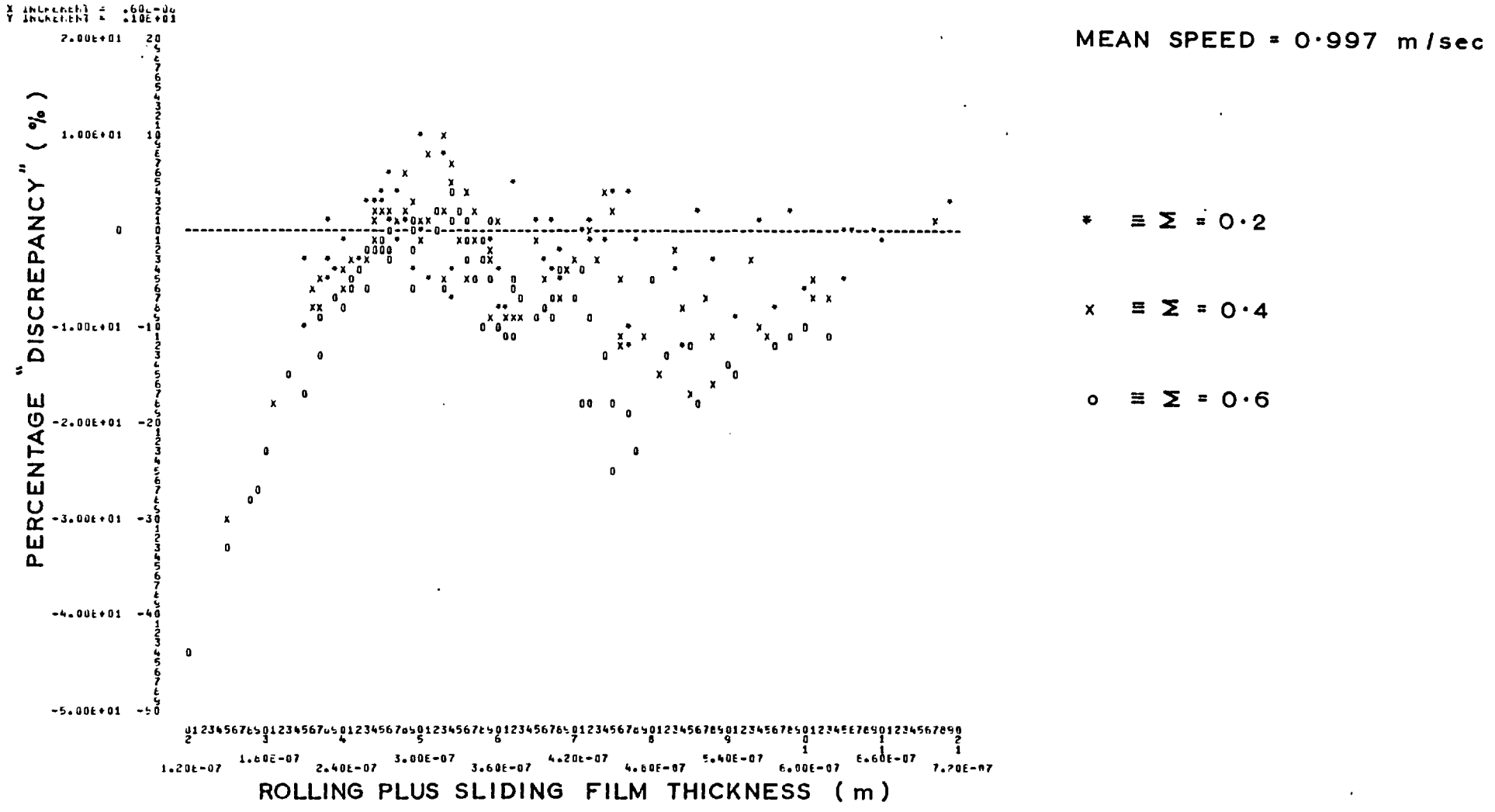

FIG. 7. 16. PERCENTAGE "DISCREPANCY" AGAINST ROLLING PLUS SLIDING FILM THICKNESS

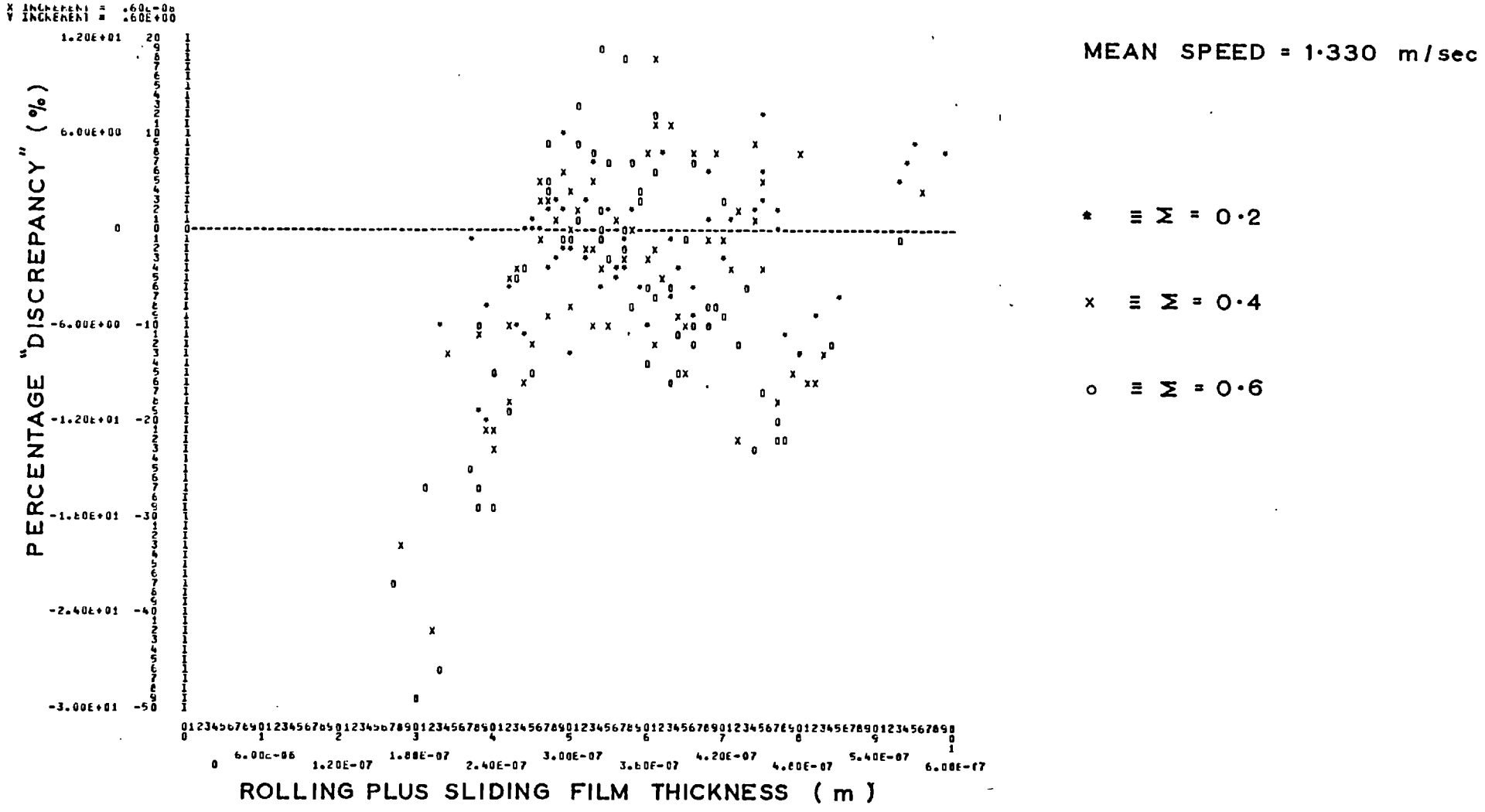

FIG. 7.17. PERCENTAGE "DISCREPANCY" AGAINST ROLLING PLUS SLIDING FILM THICKNESS

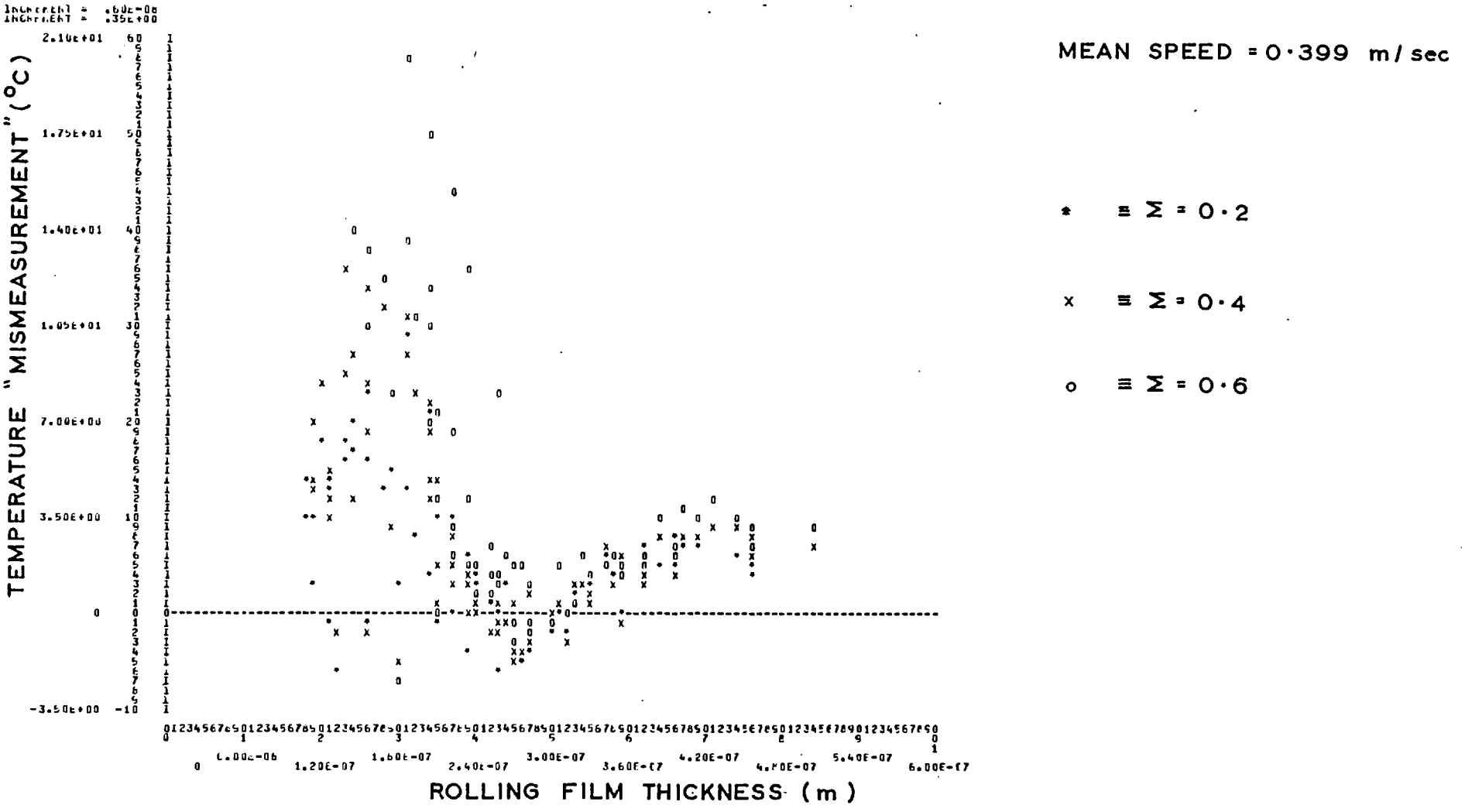

FIG. 7.18. TEMPERATURE "MISMEASUREMENT" NECESSARY TO EXPLAIN FILM THICKNESS BEHAVIOUR AGAINST PURE ROLLING FILM THICKNESS

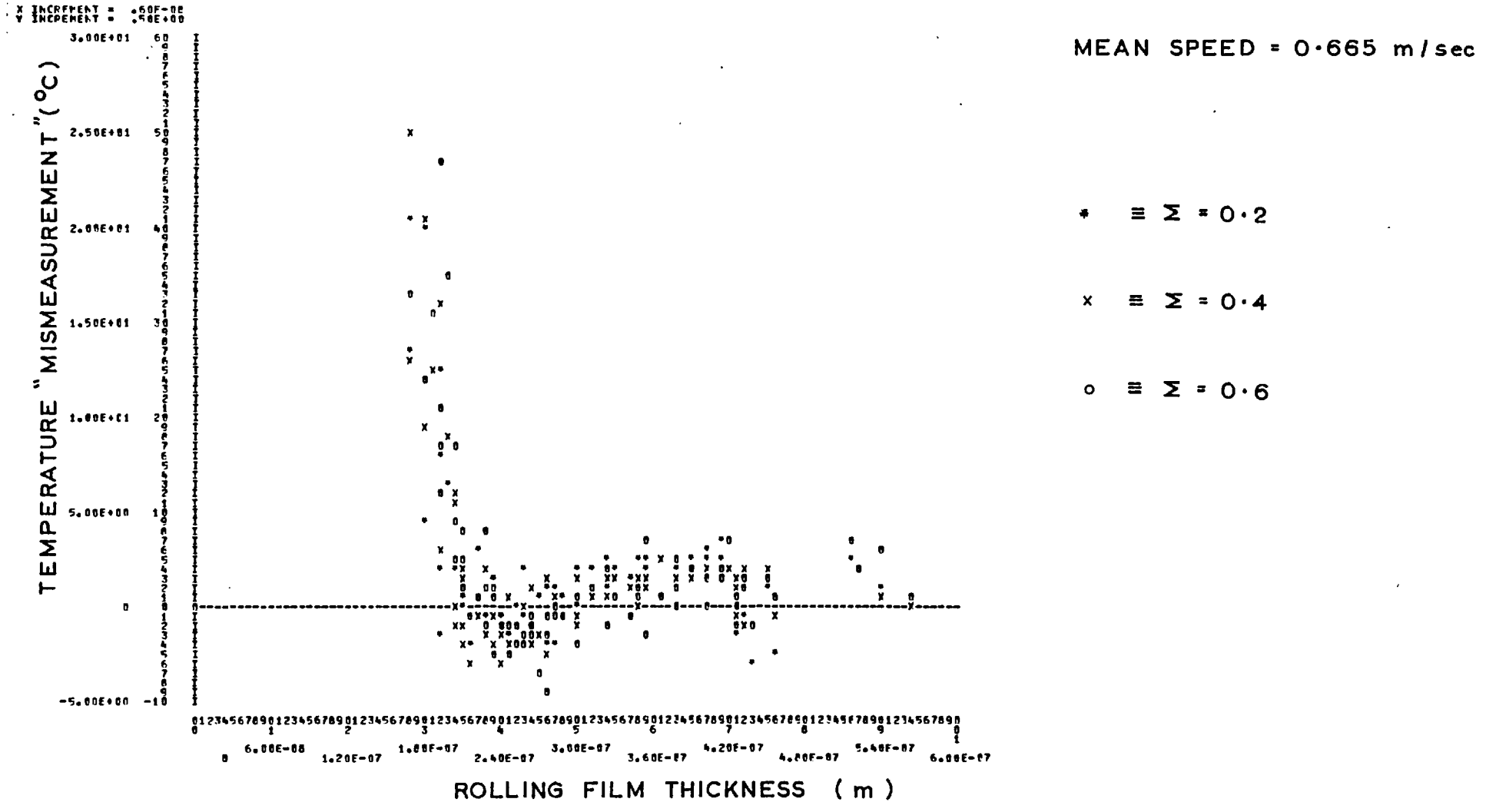

FIG. 7. 19. TEMPERATURE "MISMEASUREMENT" NECESSARY TO EXPLAIN FILM THICKNESS BEHAVIOUR AGAINST PURE ROLLING FILM THICKNESS

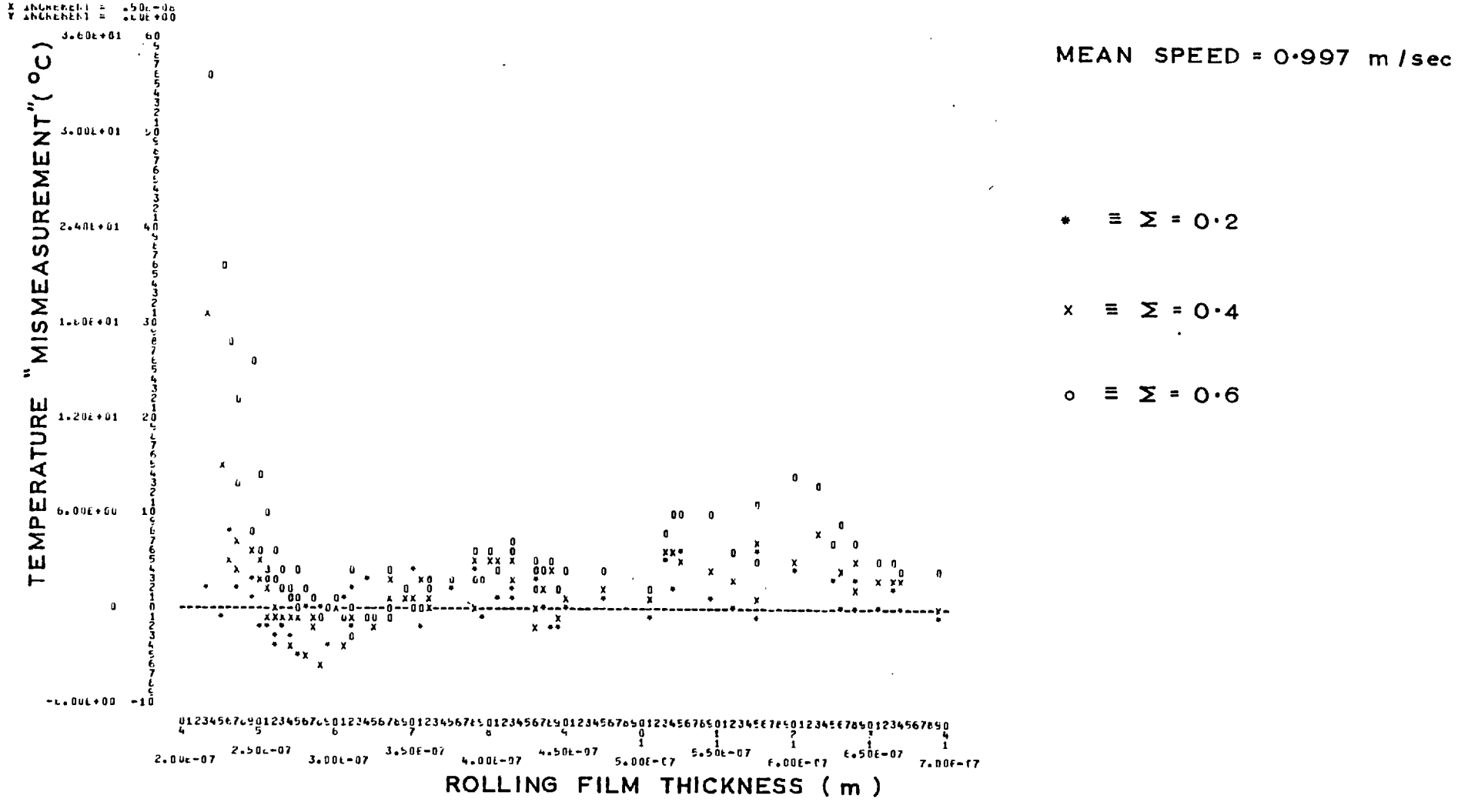

FIG. 7.20. TEMPERATURE "MISMEASUREMENT" NECESSARY TO EXPLAIN FILM THICKNESS BEHAVIOUR AGAINST PURE ROLLING FILM THICKNESS

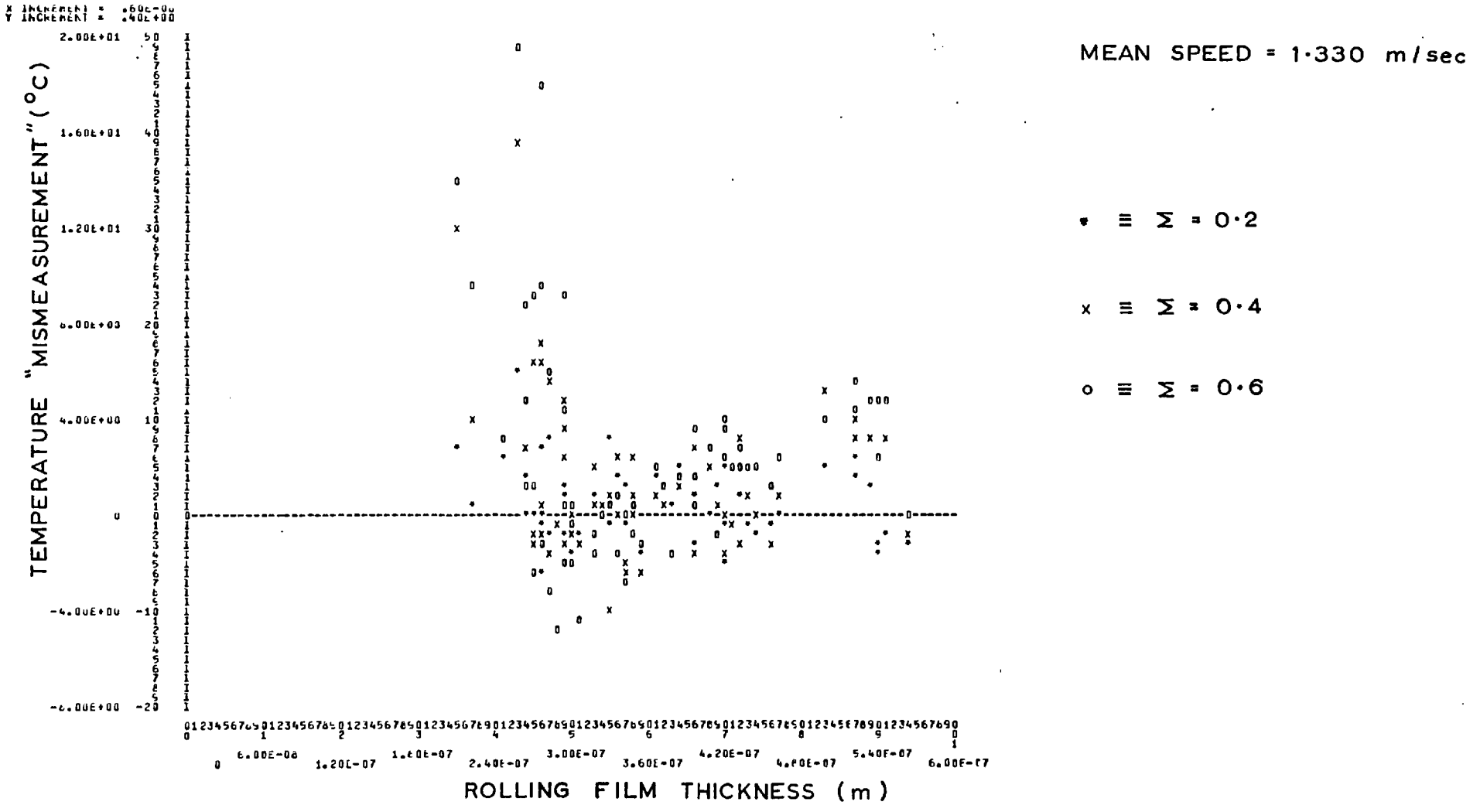

FIG. 7. 21. TEMPERATURE "MISMEASUREMENT" NECESSARY TO EXPLAIN FILM THICKNESS BEHAVIOUR AGAINST PURE ROLLING FILM THICKNESS

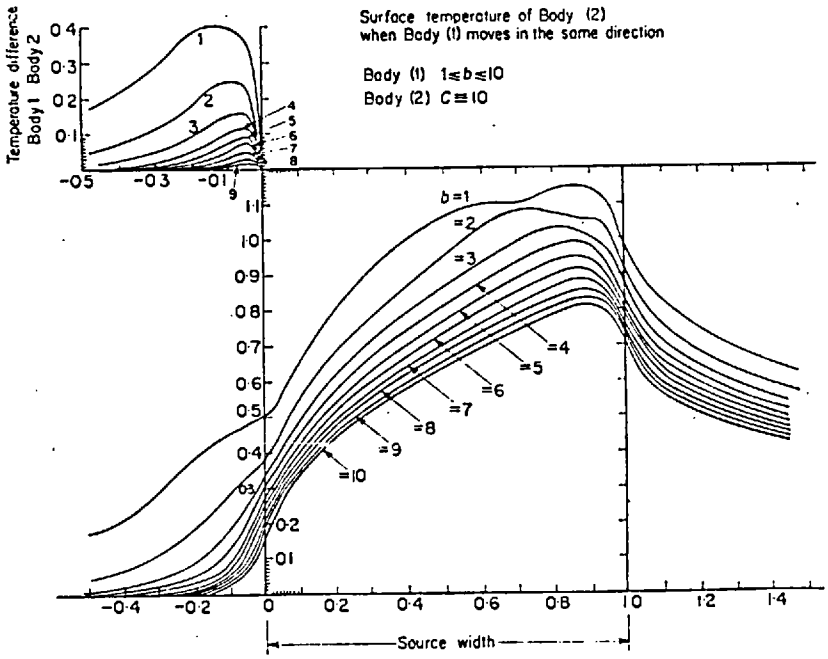

FIG. 7.22. TEMPERATURE DISTRIBUTION OVER EHD CONTACT (FROM CAMERON (16))

VERTICAL MAGNIFICATION = 20,000x

HORIZONTAL MAGNIFICATION = 100x

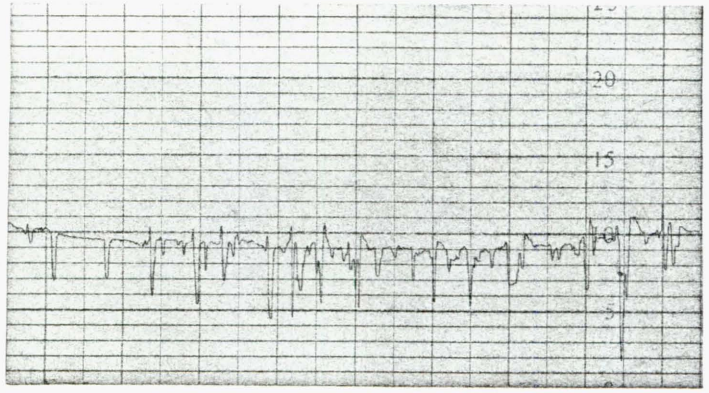

(a)

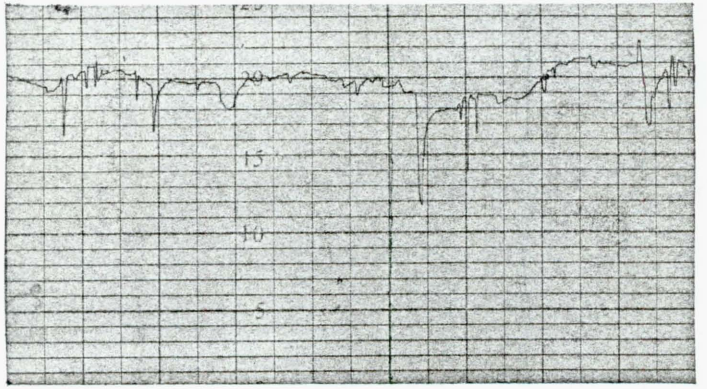

(b)

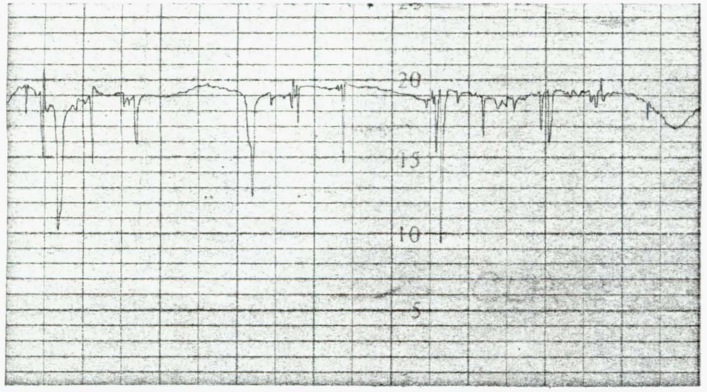

(c)

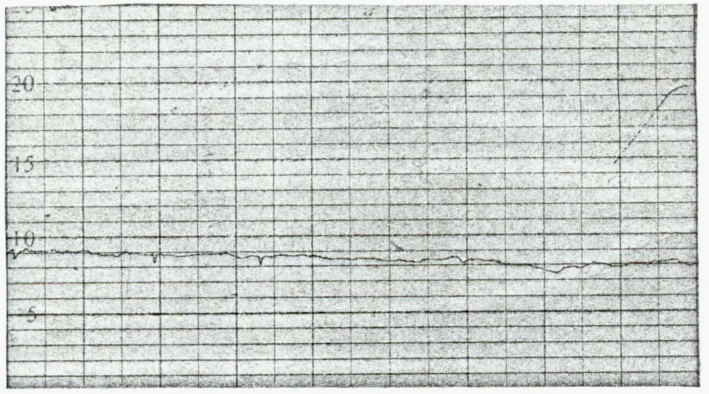

(d)

(a) 1st. STEEL DISC (THE EHD CONTACT BETWEEN THIS DISC AND THE SAPPHIRE DISC WAS VIEWED INTERFEROMETRICALLY) - C.L.A. ROUGHNESS = 0·039 μm (b) 2nd. STEEL DISC - C.L.A. ROUGHNESS = 0·042 μm (c) 3rd. STEEL DISC - C.L.A. ROUGHNESS = 0·043 μm (d) SAPPHIRE DISC - C.L.A. ROUGHNESS = 0·002 μm

FIG. 7.23. SURFACE PROFILE TRACES

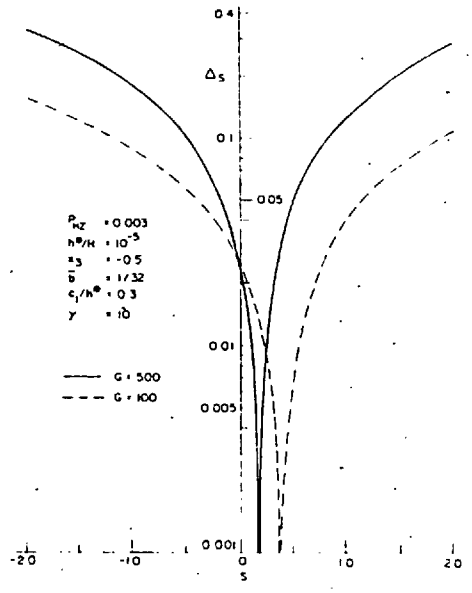

(a)

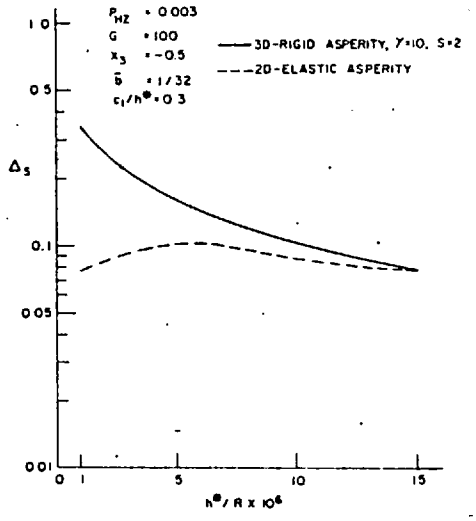

(b)

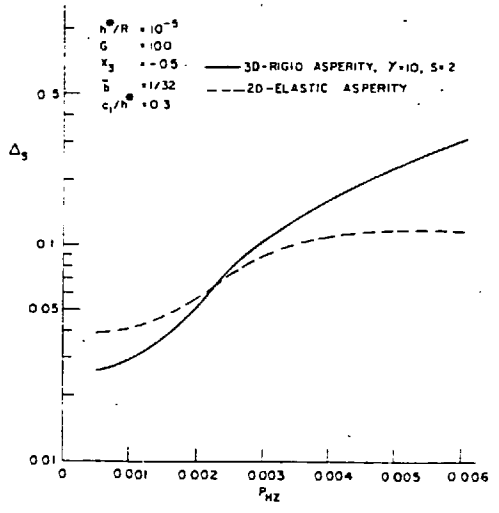

(c)

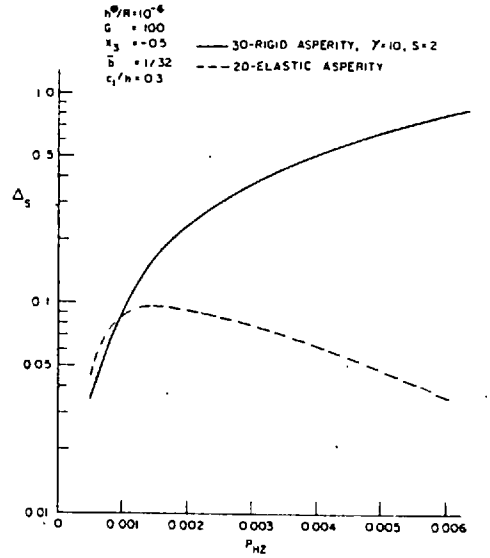

(d)

FIG. 7.24. BEHAVIOUR OF THE PRESSURE PERTURBATION PARAMETER ΔS (TAKEN FROM CHOW AND CHENG (21))

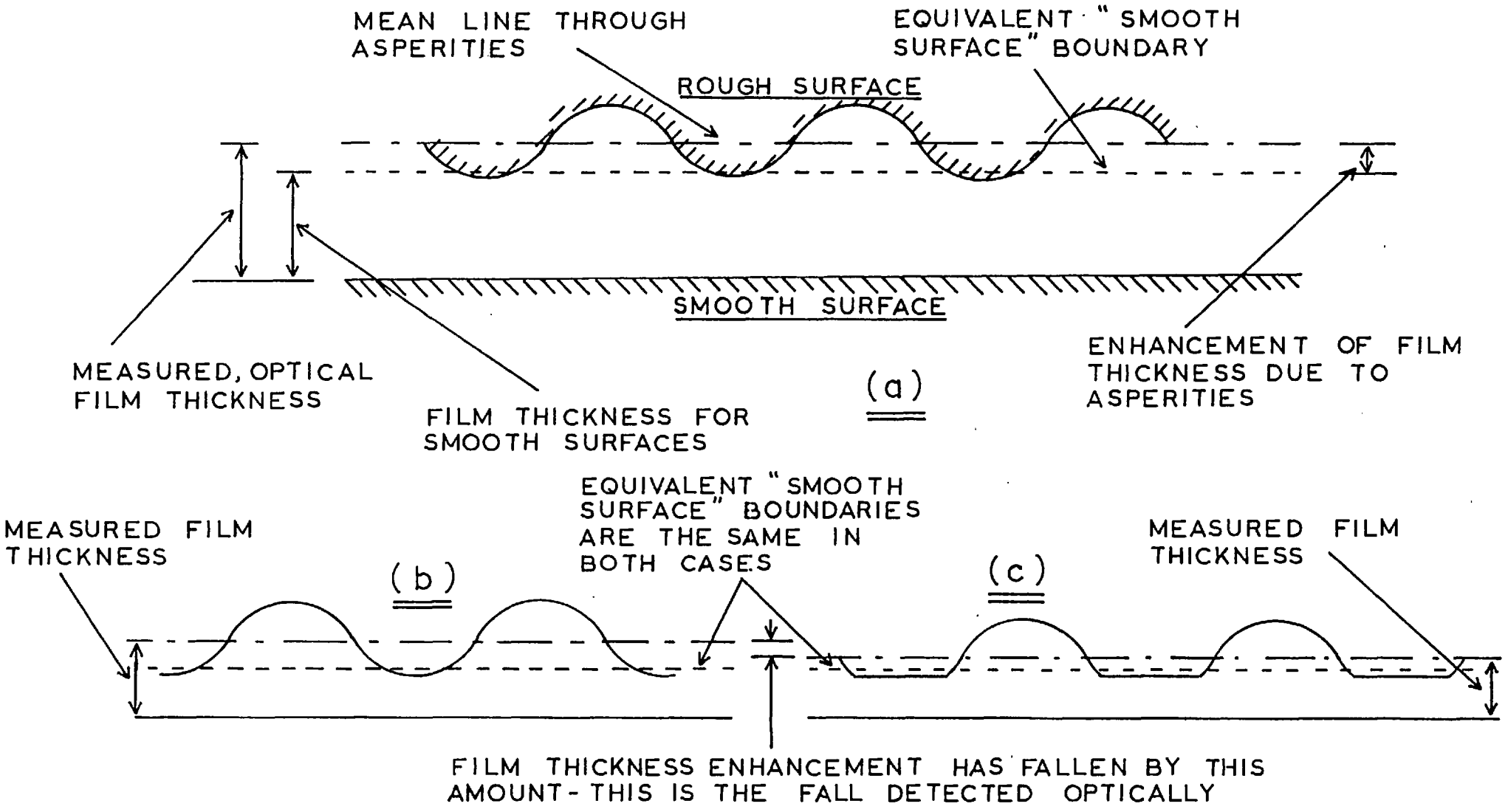

FIG. 7.25. THE EFFECT OF ASPERITIES IN AN EHD CONTACT

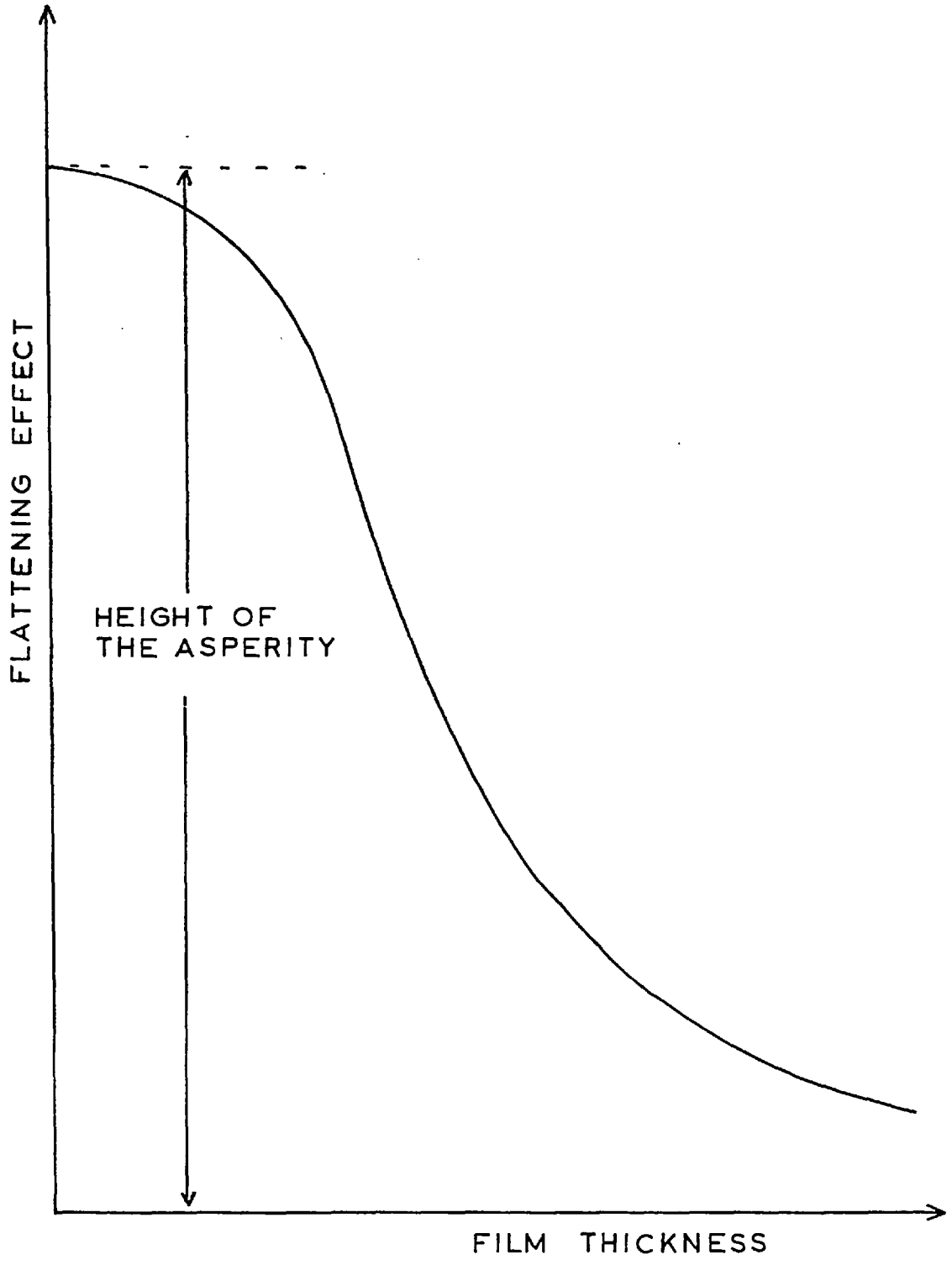

FIG. 7.26. THE PROPOSED EFFECT OF FILM THICKNESS ON THE FLATTENING EFFECT ON THE ASPERITY

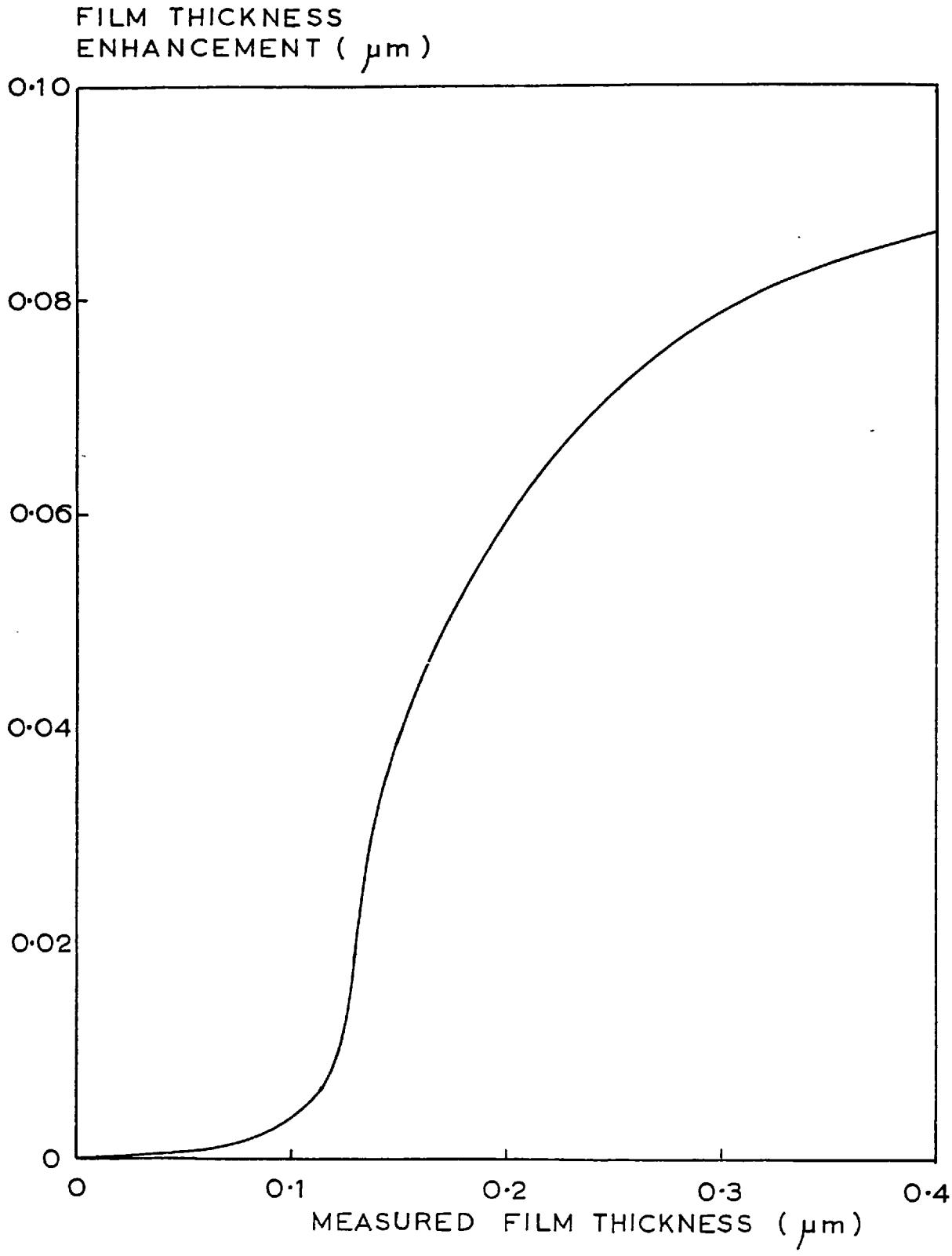

FIG. 7. 27. PROPOSED FILM THICKNESS ENHANCEMENT AS A FUNCTION OF MEASURED ROLLING FILM THICKNESS

LOAD = 2046N (MAX p_{HZ} = 1·110 GN/m^2)

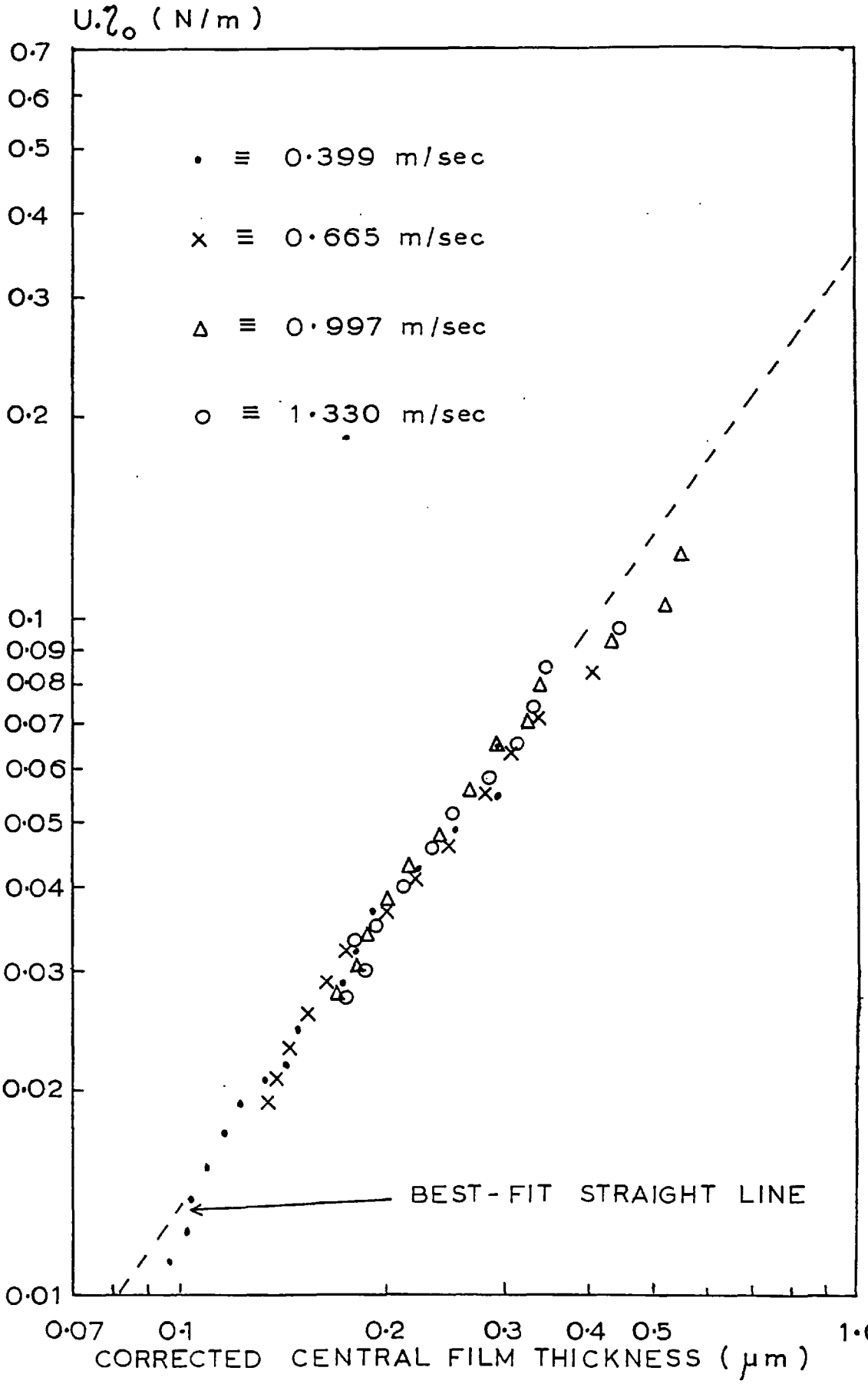

FIG. 7. 28. FILM THICKNESS AFTER REMOVAL OF ASPERITY ENHANCEMENT VALUES GIVEN BY FIG. 7.27. AGAINST Uη_o FOR PURE ROLLING

CHAPTER 7: REFERENCES

(1) CROOK A.W. - "The Lubrication of rollers IV. Measurements of Friction and Effective Viscosity", Phil. Trans. Roy. Soc., 1963, 255, Series A, Pg. 281.

(2) JOHNSON K.L. and CAMERON R. - "Shear Behaviour of EHD Oil Films at High Rolling Contact Pressures", Paper 4, Proc. Inst. Mech. Eng., Vol. 182, Part 1, No. 14, 1967-68.

(3) PLINT M.A. - "Traction in EHD Contacts", Paper 3, Proc. Inst. Mech. Eng., Vol. 182, Part 1, No. 14, 1967-68.

(4) DOWSON D. and WHOMES T.L. - "Effect of Surface Quality Upon the Traction Characteristics of Lubricated Cylindrical Contacts", Proc. Inst. Mech. Eng., Vol. 182, Part 1, No. 14, 1967-68.

(5) SMITH F.W. - "Rolling Contact Lubrication - the Application of EHD Theory", Trans. ASME, Vol. 87, Series D, Pg. 170, 1965.

(6) MOORE A.D. - Private Communication.

(7) DUCKWORTH R.R. - Private Communication.

(8) GRUBIN A.N. - "Contact stresses in toothed gears and worm gears", Cent. Sci. Res. Inst. for Tech. and Mech. Eng. (Moscow), 1949, Book No. 30, D.S.I.R. Trans. no. 337.

(9) DOWSON D., HIGGINSON G.R. and WHITAKER A.V. - "EHL, A Survey of Isothermal Solutions", J. Mech. Eng. Sci., 1962, Vol. 4, No. 2, p. 121.

(10) WYMER D.G. - Ph.D. Thesis, Univ. of London, 1972, and "Elastohydrodynamic Lubrication of a Line Contact", Proc. Inst. Mech. Eng., 1974, Vol. 188, Paper 19/74, pp. 221 - 238.

(11) PARKER R.J. and KANNEL J.W. - "Elastohydrodynamic Film Thickness Between Rolling Disks with a Synthetic Paraffinic Oil to 589 k", NASA Tech. Note, TND-6411.

(12) GENTLE C.R., DUCKWORTH R.R. and CAMERON A. - "Elastohydrodynamic Film Thicknesses at Extreme Pressures", ASME Paper, 74-Lub-27.

(13) PEMBERTON J.C. - Ph.D. Thesis, Univ. of London, 1976.

(14) KANNEL J.W. and BELL J.C. - "Interpretations of the Thickness of Lubricant Films in Rolling Contact. 1. Examination of Measurements Obtained by X-Rays", Trans. ASME, Oct. 1971, pp. 478 - 484.

(15) WESTLAKE F.J. and CAMERON A. - "Interferometric Study of Point Contact Lubrication", Inst. Mech. Eng., EHL Symposium, Leeds, 1972, Paper C39/72.

(16) CAMERON A. - Principles of Lubrication, Longmans, Pg. 229.

(17) ARCHARD J.F. - "The Temperature of Rubbing Surfaces", Wear, Vol. 2, 1958, Pg. 438.

(18) JONES W.R., JOHNSON R.L., WINER W.O. and SANBORN D.M. - "Pressure-Viscosity Measurements for Several Lubricants to 5.5 x 10^8 Newtons Per Square Meter (8 x 10^4 P.S.I.) and 149°C (300°F)",ASLE Preprint, 74LC-4C-1.

(19) ADAMS D.R. and HIRST W. - "Frictional traction in Elastohydrodynamic Lubrication", Proc. Roy. Soc. Lond., Series A, Vol. 332, 1973, pp. 505 - 525.

(20) JACKSON A. and CAMERON A. - "An Interferometric Study Of the EHL of Rough Surfaces", ASLE Preprint, 74LC-2A-1.

(21) CHOW L.S.H. and CHENG H.S. - "Pressure Perturbation in EHD Contacts Due to an Ellipsoidal Asperity", ASME Paper No. 75-Lub-2.

(22) LEE K. and CHENG H.S. - "The Effect of Surface Asperity on the Elastohydrodynamic Lubrication", NASA Report No. CR-2195, Feb. 1973.

(23) CHENG H.S. - "Isothermal Elastohydrodynamic Theory for the Full Range of Pressure-Viscosity Coefficient", Jnl. of Lub. Tech., Trans. ASME, Vol. 94, Series F, No. 1, Jan. 1972, pp. 35 - 43.

(24) CHOW L.S.H. and CHENG H.S. - "The Effect of Surface Roughness on the Average Film Thickness Between Lubricated Rollers", Jnl. Lub. Tech., Trans. ASME, Jan. 1976, Pg. 117.

(25) KANETA M. - Private Communication.